Mathematical Problems in Engineering

Human and Environmental Aspects in Logistic and Production Systems Design

Lead Guest Editor: Davide Castellano
Guest Editors: Roberto Gabbrielli, Mosè Gallo, and Dongping Song

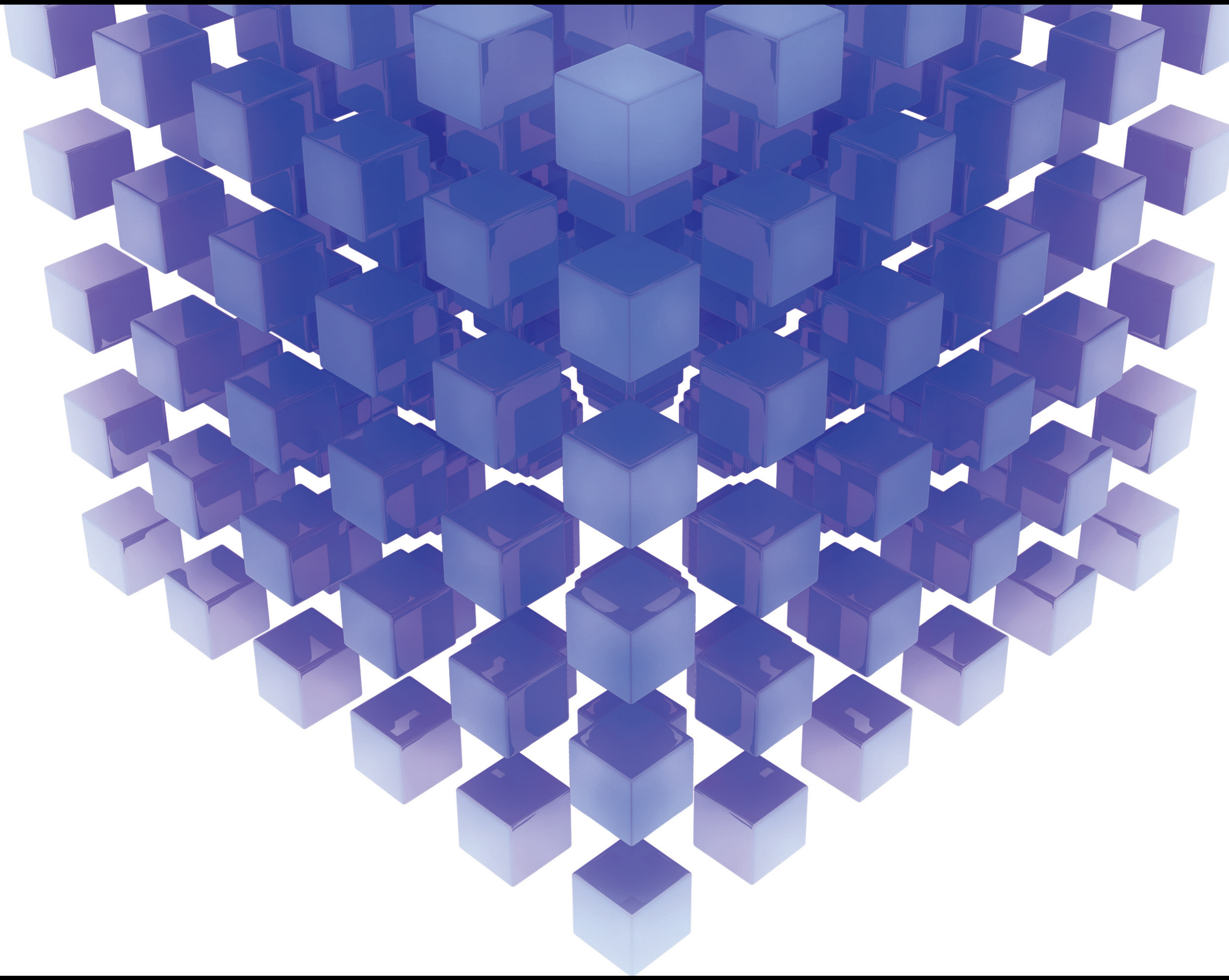

Human and Environmental Aspects in Logistic and Production Systems Design

Mathematical Problems in Engineering

Human and Environmental Aspects in Logistic and Production Systems Design

Lead Guest Editor: Davide Castellano
Guest Editors: Roberto Gabbrielli, Mosè Gallo, and Dongping Song

José António Fonseca De Oliveira Correia, Portugal
Jose Renato De Sousa, Brazil
Michael Defoort, France
Alessandro Della Corte, Italy
Laurent Dewasme, Belgium
Sanku Dey, India
Gianpaolo Di Bona, Italy
Roberta Di Pace, Italy
Francesca Di Puccio, Italy
Ramón I. Diego, Spain
Yannis Dimakopoulos, Greece
Hasan Dinçer, Turkey
José M. Domínguez, Spain
Georgios Dounias, Greece
Bo Du, China
Emil Dumic, Croatia
Madalina Dumitriu, United Kingdom
Premraj Durairaj, India
Saeed Eftekhar Azam, USA
Said El Kafhali, Morocco
Antonio Elipe, Spain
R. Emre Erkmen, Canada
John Escobar, Colombia
Leandro F. F. Miguel, Brazil
FRANCESCO FOTI, Italy
Andrea L. Facci, Italy
Shahla Faisal, Pakistan
Giovanni Falsone, Italy
Hua Fan, China
Jianguang Fang, Australia
Nicholas Fantuzzi, Italy
Muhammad Shahid Farid, Pakistan
Hamed Faroqi, Iran
Yann Favennec, France
Fiorenzo A. Fazzolari, United Kingdom
Giuseppe Fedele, Italy
Roberto Fedele, Italy
Baowei Feng, China
Mohammad Ferdows, Bangladesh
Arturo J. Fernández, Spain
Jesus M. Fernandez Oro, Spain
Francesco Ferrise, Italy
Eric Feulvarch, France
Thierry Floquet, France
Eric Florentin, France
Gerardo Flores, Mexico
Antonio Forcina, Italy
Alessandro Formisano, Italy
Francesco Franco, Italy
Elisa Francomano, Italy
Juan Frausto-Solis, Mexico
Shujun Fu, China
Juan C. G. Prada, Spain
HECTOR GOMEZ, Chile
Matteo Gaeta, Italy
Mauro Gaggero, Italy
Zoran Gajic, USA
Jaime Gallardo-Alvarado, Mexico
Mosè Gallo, Italy
Akemi Gálvez, Spain
Maria L. Gandarias, Spain
Hao Gao, Hong Kong
Xingbao Gao, China
Yan Gao, China
Zhiwei Gao, United Kingdom
Giovanni Garcea, Italy
José García, Chile
Harish Garg, India
Alessandro Gasparetto, Italy
Stylianos Georgantzinos, Greece
Fotios Georgiades, India
Parviz Ghadimi, Iran
Ştefan Cristian Gherghina, Romania
Georgios I. Giannopoulos, Greece
Agathoklis Giaralis, United Kingdom
Anna M. Gil-Lafuente, Spain
Ivan Giorgio, Italy
Gaetano Giunta, Luxembourg
Jefferson L.M.A. Gomes, United Kingdom
Emilio Gómez-Déniz, Spain
Antonio M. Gonçalves de Lima, Brazil
Qunxi Gong, China
Chris Goodrich, USA
Rama S. R. Gorla, USA
Veena Goswami, India
Xunjie Gou, Spain
Jakub Grabski, Poland

Antoine Grall, France
George A. Gravvanis, Greece
Fabrizio Greco, Italy
David Greiner, Spain
Jason Gu, Canada
Federico Guarracino, Italy
Michele Guida, Italy
Muhammet Gul, Turkey
Dong-Sheng Guo, China
Hu Guo, China
Zhaoxia Guo, China
Yusuf Gurefe, Turkey
Salim HEDDAM, Algeria
ABID HUSSANAN, China
Quang Phuc Ha, Australia
Li Haitao, China
Petr Hájek, Czech Republic
Mohamed Hamdy, Egypt
Muhammad Hamid, United Kingdom
Renke Han, United Kingdom
Weimin Han, USA
Xingsi Han, China
Zhen-Lai Han, China
Thomas Hanne, Switzerland
Xinan Hao, China
Mohammad A. Hariri-Ardebili, USA
Khalid Hattaf, Morocco
Defeng He, China
Xiao-Qiao He, China
Yanchao He, China
Yu-Ling He, China
Ramdane Hedjar, Saudi Arabia
Jude Hemanth, India
Reza Hemmati, Iran
Nicolae Herisanu, Romania
Alfredo G. Hernández-Diaz, Spain
M.I. Herreros, Spain
Eckhard Hitzer, Japan
Paul Honeine, France
Jaromir Horacek, Czech Republic
Lei Hou, China
Yingkun Hou, China
Yu-Chen Hu, Taiwan
Yunfeng Hu, China
Can Huang, China
Gordon Huang, Canada
Linsheng Huo, China
Sajid Hussain, Canada
Asier Ibeas, Spain
Orest V. Iftime, The Netherlands
Przemyslaw Ignaciuk, Poland
Giacomo Innocenti, Italy
Emilio Insfran Pelozo, Spain
Azeem Irshad, Pakistan
Alessio Ishizaka, France
Benjamin Ivorra, Spain
Breno Jacob, Brazil
Reema Jain, India
Tushar Jain, India
Amin Jajarmi, Iran
Chiranjibe Jana, India
Łukasz Jankowski, Poland
Samuel N. Jator, USA
Juan Carlos Jáuregui-Correa, Mexico
Kandasamy Jayakrishna, India
Reza Jazar, Australia
Khalide Jbilou, France
Isabel S. Jesus, Portugal
Chao Ji, China
Qing-Chao Jiang, China
Peng-fei Jiao, China
Ricardo Fabricio Escobar Jiménez, Mexico
Emilio Jiménez Macías, Spain
Maolin Jin, Republic of Korea
Zhuo Jin, Australia
Ramash Kumar K, India
BHABEN KALITA, USA
MOHAMMAD REZA KHEDMATI, Iran
Viacheslav Kalashnikov, Mexico
Mathiyalagan Kalidass, India
Tamas Kalmar-Nagy, Hungary
Rajesh Kaluri, India
Jyotheeswara Reddy Kalvakurthi, India
Zhao Kang, China
Ramani Kannan, Malaysia
Tomasz Kapitaniak, Poland
Julius Kaplunov, United Kingdom
Konstantinos Karamanos, Belgium
Michal Kawulok, Poland

Francisco J. Martos, Spain
Elio Masciari, Italy
Paolo Massioni, France
Alessandro Mauro, Italy
Jonathan Mayo-Maldonado, Mexico
Pier Luigi Mazzeo, Italy
Laura Mazzola, Italy
Driss Mehdi, France
Zahid Mehmood, Pakistan
Roderick Melnik, Canada
Xiangyu Meng, USA
Jose Merodio, Spain
Alessio Merola, Italy
Mahmoud Mesbah, Iran
Luciano Mescia, Italy
Laurent Mevel, France
Constantine Michailides, Cyprus
Mariusz Michta, Poland
Prankul Middha, Norway
Aki Mikkola, Finland
Giovanni Minafò, Italy
Edmondo Minisci, United Kingdom
Hiroyuki Mino, Japan
Dimitrios Mitsotakis, New Zealand
Ardashir Mohammadzadeh, Iran
Francisco J. Montáns, Spain
Francesco Montefusco, Italy
Gisele Mophou, France
Rafael Morales, Spain
Marco Morandini, Italy
Javier Moreno-Valenzuela, Mexico
Simone Morganti, Italy
Caroline Mota, Brazil
Aziz Moukrim, France
Shen Mouquan, China
Dimitris Mourtzis, Greece
Emiliano Mucchi, Italy
Taseer Muhammad, Saudi Arabia
Ghulam Muhiuddin, Saudi Arabia
Amitava Mukherjee, India
Josefa Mula, Spain
Jose J. Muñoz, Spain
Giuseppe Muscolino, Italy
Marco Mussetta, Italy
Hariharan Muthusamy, India
Alessandro Naddeo, Italy
Raj Nandkeolyar, India
Keivan Navaie, United Kingdom
Soumya Nayak, India
Adrian Neagu, USA
Erivelton Geraldo Nepomuceno, Brazil
AMA Neves, Portugal
Ha Quang Thinh Ngo, Vietnam
Nhon Nguyen-Thanh, Singapore
Papakostas Nikolaos, Ireland
Jelena Nikolic, Serbia
Tatsushi Nishi, Japan
Shanzhou Niu, China
Ben T. Nohara, Japan
Mohammed Nouari, France
Mustapha Nourelfath, Canada
Kazem Nouri, Iran
Ciro Núñez-Gutiérrez, Mexico
Wlodzimierz Ogryczak, Poland
Roger Ohayon, France
Krzysztof Okarma, Poland
Mitsuhiro Okayasu, Japan
Murat Olgun, Turkey
Diego Oliva, Mexico
Alberto Olivares, Spain
Enrique Onieva, Spain
Calogero Orlando, Italy
Susana Ortega-Cisneros, Mexico
Sergio Ortobelli, Italy
Naohisa Otsuka, Japan
Sid Ahmed Ould Ahmed Mahmoud, Saudi Arabia
Taoreed Owolabi, Nigeria
EUGENIA PETROPOULOU, Greece
Arturo Pagano, Italy
Madhumangal Pal, India
Pasquale Palumbo, Italy
Dragan Pamučar, Serbia
Weifeng Pan, China
Chandan Pandey, India
Rui Pang, United Kingdom
Jürgen Pannek, Germany
Elena Panteley, France
Achille Paolone, Italy

George A. Papakostas, Greece
Xosé M. Pardo, Spain
You-Jin Park, Taiwan
Manuel Pastor, Spain
Pubudu N. Pathirana, Australia
Surajit Kumar Paul, India
Luis Payá, Spain
Igor Pažanin, Croatia
Libor Pekař, Czech Republic
Francesco Pellicano, Italy
Marcello Pellicciari, Italy
Jian Peng, China
Mingshu Peng, China
Xiang Peng, China
Xindong Peng, China
Yuexing Peng, China
Marzio Pennisi, Italy
Maria Patrizia Pera, Italy
Matjaz Perc, Slovenia
A. M. Bastos Pereira, Portugal
Wesley Peres, Brazil
F. Javier Pérez-Pinal, Mexico
Michele Perrella, Italy
Francesco Pesavento, Italy
Francesco Petrini, Italy
Hoang Vu Phan, Republic of Korea
Lukasz Pieczonka, Poland
Dario Piga, Switzerland
Marco Pizzarelli, Italy
Javier Plaza, Spain
Goutam Pohit, India
Dragan Poljak, Croatia
Jorge Pomares, Spain
Hiram Ponce, Mexico
Sébastien Poncet, Canada
Volodymyr Ponomaryov, Mexico
Jean-Christophe Ponsart, France
Mauro Pontani, Italy
Sivakumar Poruran, India
Francesc Pozo, Spain
Aditya Rio Prabowo, Indonesia
Anchasa Pramuanjaroenkij, Thailand
Leonardo Primavera, Italy
B Rajanarayan Prusty, India
Krzysztof Puszynski, Poland
Chuan Qin, China
Dongdong Qin, China
Jianlong Qiu, China
Giuseppe Quaranta, Italy
DR. RITU RAJ, India
Vitomir Racic, Italy
Carlo Rainieri, Italy
Kumbakonam Ramamani Rajagopal, USA
Ali Ramazani, USA
Angel Manuel Ramos, Spain
Higinio Ramos, Spain
Muhammad Afzal Rana, Pakistan
Muhammad Rashid, Saudi Arabia
Manoj Rastogi, India
Alessandro Rasulo, Italy
S.S. Ravindran, USA
Abdolrahman Razani, Iran
Alessandro Reali, Italy
Jose A. Reinoso, Spain
Oscar Reinoso, Spain
Haijun Ren, China
Carlo Renno, Italy
Fabrizio Renno, Italy
Shahram Rezapour, Iran
Ricardo Riaza, Spain
Francesco Riganti-Fulginei, Italy
Gerasimos Rigatos, Greece
Francesco Ripamonti, Italy
Jorge Rivera, Mexico
Eugenio Roanes-Lozano, Spain
Ana Maria A. C. Rocha, Portugal
Luigi Rodino, Italy
Francisco Rodríguez, Spain
Rosana Rodríguez López, Spain
Francisco Rossomando, Argentina
Jose de Jesus Rubio, Mexico
Weiguo Rui, China
Rubén Ruiz, Spain
Ivan D. Rukhlenko, Australia
Dr. Eswaramoorthi S., India
Weichao SHI, United Kingdom
Chaman Lal Sabharwal, USA
Andrés Sáez, Spain

Bekir Sahin, Turkey
Laxminarayan Sahoo, India
John S. Sakellariou, Greece
Michael Sakellariou, Greece
Salvatore Salamone, USA
Jose Vicente Salcedo, Spain
Alejandro Salcido, Mexico
Alejandro Salcido, Mexico
Nunzio Salerno, Italy
Rohit Salgotra, India
Miguel A. Salido, Spain
Sinan Salih, Iraq
Alessandro Salvini, Italy
Abdus Samad, India
Sovan Samanta, India
Nikolaos Samaras, Greece
Ramon Sancibrian, Spain
Giuseppe Sanfilippo, Italy
Omar-Jacobo Santos, Mexico
J Santos-Reyes, Mexico
José A. Sanz-Herrera, Spain
Musavarah Sarwar, Pakistan
Shahzad Sarwar, Saudi Arabia
Marcelo A. Savi, Brazil
Andrey V. Savkin, Australia
Tadeusz Sawik, Poland
Roberta Sburlati, Italy
Gustavo Scaglia, Argentina
Thomas Schuster, Germany
Hamid M. Sedighi, Iran
Mijanur Rahaman Seikh, India
Tapan Senapati, China
Lotfi Senhadji, France
Junwon Seo, USA
Michele Serpilli, Italy
Silvestar Šesnić, Croatia
Gerardo Severino, Italy
Ruben Sevilla, United Kingdom
Stefano Sfarra, Italy
Dr. Ismail Shah, Pakistan
Leonid Shaikhet, Israel
Vimal Shanmuganathan, India
Prayas Sharma, India
Bo Shen, Germany
Hang Shen, China
Xin Pu Shen, China
Dimitri O. Shepelsky, Ukraine
Jian Shi, China
Amin Shokrollahi, Australia
Suzanne M. Shontz, USA
Babak Shotorban, USA
Zhan Shu, Canada
Angelo Sifaleras, Greece
Nuno Simões, Portugal
Mehakpreet Singh, Ireland
Piyush Pratap Singh, India
Rajiv Singh, India
Seralathan Sivamani, India
S. Sivasankaran, Malaysia
Christos H. Skiadas, Greece
Konstantina Skouri, Greece
Neale R. Smith, Mexico
Bogdan Smolka, Poland
Delfim Soares Jr., Brazil
Alba Sofi, Italy
Francesco Soldovieri, Italy
Raffaele Solimene, Italy
Yang Song, Norway
Jussi Sopanen, Finland
Marco Spadini, Italy
Paolo Spagnolo, Italy
Ruben Specogna, Italy
Vasilios Spitas, Greece
Ivanka Stamova, USA
Rafał Stanisławski, Poland
Miladin Stefanović, Serbia
Salvatore Strano, Italy
Yakov Strelniker, Israel
Kangkang Sun, China
Qiuqin Sun, China
Shuaishuai Sun, Australia
Yanchao Sun, China
Zong-Yao Sun, China
Kumarasamy Suresh, India
Sergey A. Suslov, Australia
D.L. Suthar, Ethiopia
D.L. Suthar, Ethiopia
Andrzej Swierniak, Poland
Andras Szekrenyes, Hungary
Kumar K. Tamma, USA

Yong (Aaron) Tan, United Kingdom
Marco Antonio Taneco-Hernández, Mexico
Lu Tang, China
Tianyou Tao, China
Hafez Tari, USA
Alessandro Tasora, Italy
Sergio Teggi, Italy
Adriana del Carmen Téllez-Anguiano, Mexico
Ana C. Teodoro, Portugal
Efstathios E. Theotokoglou, Greece
Jing-Feng Tian, China
Alexander Timokha, Norway
Stefania Tomasiello, Italy
Gisella Tomasini, Italy
Isabella Torcicollo, Italy
Francesco Tornabene, Italy
Mariano Torrisi, Italy
Thang nguyen Trung, Vietnam
George Tsiatas, Greece
Le Anh Tuan, Vietnam
Nerio Tullini, Italy
Emilio Turco, Italy
Ilhan Tuzcu, USA
Efstratios Tzirtzilakis, Greece
FRANCISCO UREÑA, Spain
Filippo Ubertini, Italy
Mohammad Uddin, Australia
Mohammad Safi Ullah, Bangladesh
Serdar Ulubeyli, Turkey
Mati Ur Rahman, Pakistan
Panayiotis Vafeas, Greece
Giuseppe Vairo, Italy
Jesus Valdez-Resendiz, Mexico
Eusebio Valero, Spain
Stefano Valvano, Italy
Carlos-Renato Vázquez, Mexico
Martin Velasco Villa, Mexico
Franck J. Vernerey, USA
Georgios Veronis, USA
Vincenzo Vespri, Italy
Renato Vidoni, Italy
Venkatesh Vijayaraghavan, Australia
Anna Vila, Spain
Francisco R. Villatoro, Spain
Francesca Vipiana, Italy
Stanislav Vítek, Czech Republic
Jan Vorel, Czech Republic
Michael Vynnycky, Sweden
Mohammad W. Alomari, Jordan
Roman Wan-Wendner, Austria
Bingchang Wang, China
C. H. Wang, Taiwan
Dagang Wang, China
Guoqiang Wang, China
Huaiyu Wang, China
Hui Wang, China
J.G. Wang, China
Ji Wang, China
Kang-Jia Wang, China
Lei Wang, China
Qiang Wang, China
Qingling Wang, China
Weiwei Wang, China
Xinyu Wang, China
Yong Wang, China
Yung-Chung Wang, Taiwan
Zhenbo Wang, USA
Zhibo Wang, China
Waldemar T. Wójcik, Poland
Chi Wu, Australia
Qiuhong Wu, China
Yuqiang Wu, China
Zhibin Wu, China
Zhizheng Wu, China
Michalis Xenos, Greece
Hao Xiao, China
Xiao Ping Xie, China
Qingzheng Xu, China
Binghan Xue, China
Yi Xue, China
Joseph J. Yame, France
Chuanliang Yan, China
Xinggang Yan, United Kingdom
Hongtai Yang, China
Jixiang Yang, China
Mijia Yang, USA
Ray-Yeng Yang, Taiwan

Contents

Hindawi
Mathematical Problems in Engineering
Volume 2020, Article ID 8686371, 18 pages
https://doi.org/10.1155/2020/8686371

Research Article

Optimal Supply Diversification Strategy under Supply Disruption

Xiaomeng Luo and Jia Ren

School of Business Administration, Southwestern University of Finance and Economics, Chengdu, Sichuan 611130, China

Correspondence should be addressed to Xiaomeng Luo; luoxm@swufe.edu.cn

Received 9 January 2020; Revised 16 April 2020; Accepted 18 April 2020; Published 13 August 2020

Guest Editor: Davide Castellano

When a disruption caused by human or environmental accident occurs in production systems, it may cause a shortage of the supply, and thus the buyers' procurement behaviors will be influenced. This paper studies a supply chain comprised of a buyer and two types of suppliers: one is cheap but unreliable and the other is reliable but expensive. If there is a major disruption, the unreliable supplier may not be able to fully satisfy the buyer's order, despite the fact that it exerts additional effort to rebuild capacity; at the same time, the reliable supplier cannot fulfill extra orders from the buyer due to capacity constraints. In this way, the buyer should strategically allocate its order between the two types of suppliers by offering different contracts at the very beginning, and then the unreliable supplier chooses its optimal restoration effort according to the contract if a disruption occurs. The model is built based on the real-life cases such as Walmart and Apple such that it is the buyer who determines the wholesale price of the unreliable supplier's products. The results show the optimal contracts provided by the buyer under different circumstances, which aims to help managers design their contracts under disruption risks to maximize the company's profit.

1. Introduction

It is common to observe a variety of disruptions occurring in global supply chain, and thus firms are exposed to risks and uncertainties [1]. The disruption can be attributed to various factors such as natural disasters, financial bankruptcy, government policy, and human factors. When a disruption happens, firms would be quite passive if they did not prepare backup plans. For example, two deadly earthquakes that happened in Southern Japan halted Sony's production of image sensors in 2016. This affected the procurement of its major customers, and, thus, for instance, Apple had to postpone the supply of its new iPhone while Samsung shifted to alternative suppliers at a much higher price although its production process is not affected ("Japan Quakes Close Sony Factory Making Key iPhone Part," Fortune, 16 April, 2016, https://fortune.com/2016/04/16/japan-quakes-disrupt-sony-image-sensors-apple-iphones/, accessed on January 2020). More recently, a series of actions have been taken by Apple to mitigate the effects of possible disruptions: execs from Apple, together with representatives from Google, Microsoft, and Amazon, visited Korea to ensure consistent supplies of critical chips, which might be affected by the trade war between Japan and Korea; and, considering the disruption risk caused by the US-China trade war, Apple has planned to shift 15% to 30% production out of China to reduce its dependence on Chinese suppliers ("Apple Execs Rush to Samsung in Korea Fearing Disruption in iPhone Chip Supplies," iGeeksBlog, 20 July, 2019, https://www.igeeksblog.com/apple-execs-rush-samsung-iphone-chip-supplies-135428/, accessed on January 2020).

Although it is more efficient to procure from a single supplier aiming at developing long-term relationship, firms tend to diversify their sources to prevent supply disruption in practice. A classic case regarding two famous mobile communication producers shows the benefits brought by diversifying procurement sources. In March 2000, a Philips Semiconductor plant has been shut down due to a sudden fire caused by lightning in Albuquerque, New Mexico, for six weeks. This leads to a shortage of components for both Ericsson and Nokia, but the situations of the two companies are very different. Although Nokia has lost all of the supply from the Philips plant, it was able to source from alternative suppliers by temporarily increasing their production and thus suffered little financial loss at last. However, Ericsson did not have backup suppliers to shift supply, so it eventually lost at least 400 million dollars in potential revenue [2]. To adopt multisource strategy, some critical decisions need to be determined by firms at the very beginning, such as how many suppliers to choose and how many quantities to procure from each of them. The common practice is to source the majority of products from one or two major suppliers which provide favorable terms and the minority from other small suppliers, just as Samsung and Nokia do.

The fact is if firms are sufficiently powerful, they can procure products at the prices they are pleased of. For example, more than 450 US companies competed to provide 750 products in the stores of Walmart nationwide in 2016, and only some of them won the chance to get into the stores. The unequal power in the supply and demand relationship between Walmart and its suppliers adds bargaining power to Walmart. Thus, it is Walmart's decision to set the final wholesale price based on the cost structure of the product, which requires the suppliers to eliminate excess costs ("Amy Feldman, "What It Takes To Sell To Walmart: A Senior Buyer Tells All," Forbes, 11 May, https://www.forbes.com/sites/amyfeldman/2017/05/11/what-it-takes-to-sell-to-walmart-a-senior-buyer-tells-all/#25ef71e5352b, accessed on January 2020). Other large companies such as Costco, Amazon, and Apple are similar to Walmart when bargaining with their suppliers on price. The suppliers can choose to accept the prices offered by those big names or they can leave. Most suppliers will choose to stay considering the large volume and reputation provided by big companies. Thus, the procurement decisions of those companies become how many suppliers to choose and which wholesale price and order quantity to provide to each of the suppliers.

Based on the above background, this paper aims to study the optimal procurement strategy of a powerful firm (referred to as "buyer"). Basically, the buyer can source from two types of suppliers, reliable but expensive ones and unreliable ones which may suffer production disruptions. The buyer has to decide which type of suppliers to partner with and how many quantities to procure at what wholesale price. In all, there are three possible strategies: procuring from the reliable suppliers only, sourcing from the unreliable ones only, and ordering from both types of suppliers. The buyer chooses the best answer by making a tradeoff between the profit and the risk. We are interested in which strategy would be the optimal choice for the buyer when the risk of production disruption exists. The remainder of this paper is organized as follows: Section 2 summarizes the relevant literature, Section 2 provides the model description, and optimal results are given in Section 4. Section 5 provides a numerical study. Conclusion is presented in Section 6.

2. Literature Review

The management of supply disruption has long been an interesting topic for both researchers and practitioners in the Operations Management field. We may refer to Vakharia and Yenipazarli [3] for an excellent review of relevant literature, Snyder et al. [4] for a summary for OR/MS models used in the study of supply chain disruption, and Ivanov et al. [5] for quantitative tools used in supply chain disruption recovery.

To fight against supply disruption, which is modeled as an all-or-nothing yield model, supply diversification is a useful strategy [6, 7]. Other operational tools include multiple sourcing [6, 8], improvement in reliability and process (Liu et al. [9] and Wang et al. [10]), and cost-sharing mechanism [11]. Iyer et al. (2005) studied the supplier's optimal contract structure and explored the impact of an alternate supplier in a supply chain consisting of a monopolist supplier and multiple buyers. By conducting a detailed study, Tomlin [12] considers firm characteristics such as risk tolerance and supplier characteristics such as percentage uptime, disruption length, capacity, and flexibility to study the supply disruption management problem. They provide various strategies adopted by buyers to manage supply disruption risk, including investment in inventory, cooperation with multiple suppliers, and preparation for backup orders to alternative suppliers. Hu et al. [13] study how a buyer can use incentive mechanisms to motivate a supplier's investment in capacity restoration and compare this approach with the traditional approach of diversifying part of the order to an expensive but reliable supplier. Chen et al. [14] compare two incentive mechanisms, i.e., providing financial subsidy and adjusting the wholesale price(namely, direct and indirect contract, respectively) and study their effects on the supplier's investment behavior.

A lot of factors are involved in the study for supply disruption. Gupta et al. [15] consider competition in the buyer level and find that both supply disruption and procurement times will affect the buyers' procurement decisions. Ray and Jenamani [16] analyze the uncertainty from both the supply side and the demand side, providing the optimal order allocation to hedge against supply disruption risk. Besides all-or-nothing supply, Tang et al. [17] involve partial disruption and find that subsidy is preferred in all-or-nothing setting, while both subsidy and order inflation are optimal in partial disruption setting. Tsai [18] proposes a dynamic sourcing strategy that helps managers determine the optimal number of suppliers required in different scenarios. Based on a multitier supply chain structure, Ang et al. [19] explore the interactions between the manufacturer and suppliers and show that the degree of overlap in the supply chain may impact the optimal strategies of both manufacturer and tier 1 supplier. A series of articles analyze the supply chain coordination under supply disruption risks [20–22]. Specifically, Sawik [23] provides the stochastic and deterministic approaches to coordinate the supply chain and finds that the stochastic approach offers a more diversified supply portfolio which helps deal with a variety of scenarios.

Although managers know clearly the impact of supply chain disruptions, they actually have done little to prevent the incidents and corresponding effects [24]. Chopra and Sodhi [25] thus remind managers to notice the disruption risk when they pursue cost efficiency by providing feasible advices on real actions. Based on the real situation of the Chinese dairy market, He et al. [26] explore the optimal ordering strategy for a retailer who can source from a local supplier and an oversea supplier under supply disruption.

With the help of real-option pricing methodology and actuarial techniques, they help managers to make decisions on procurement. Our model studies a supply chain composed of one buyer and two suppliers, and there are three options for buyer to choose: the first one is ordering from the reliable supplier only, the second one is ordering from the unreliable supplier only, and the third one is ordering from both of them. It is obvious that the first one is more expensive and the second one is more risky, and thus the intermediate choice not only avoids some risk but also reduces cost. The main features of our proposed model are the focus on supplier's restoration effort after disruption and buyer's order allocation strategy and pricing strategy.

3. Model Description

We consider a supply chain that consists of a buyer and two suppliers: one is reliable supplier and the other one is unreliable supplier. For simplicity, we assume that the market demand d and retail price p are fixed and given. We further assume that the original capacity of either supplier is enough to cover the market demand. Specifically, the reliable supplier can fully satisfy the buyer's order, and the unreliable supplier also can if there is no disruption. Note that once the order has been offered to the reliable supplier, no replenishment order can be placed later if the unreliable supplier suffers disruption. To better model the practice in the real world, we assume that the wholesale price of the reliable supplier's product is deterministic, which is determined by the market, while the wholesale price of the unreliable supplier's product is decided by the buyer since the buyer has power towards the unreliable supplier. Thus, the buyer has to decide an order allocation between the two suppliers and the wholesale price from the unreliable supplier to maximize its own profit.

For the unreliable supplier, we use (q_u, w_u) to denote the contract offered by the buyer. Following Anupindi and Akella [6] and Gurnani et al. [10], we assume that the risk of disruption is dichotomous (all or nothing), which means that the unreliable supplier may lose all of its capacity if there is an unexpected disruption. There is no disruption with probability β and disruption occurs with probability $1-\beta$. When disruption happens, the unreliable supplier has to decide whether and how much costly effort to exert to rebuild capacity. The amount of restored capacity is proportional to the supplier's effort level e; that is, with effort e, the restored capacity is αe, where α is a deterministic factor and we further assume that $\alpha = 1$. Restoration effort incurs a cost determined by a convex and increasing function $C_R(e)$, representing the diminishing return of effort on capacity recovery [27]. The production cost of either supplier is normalized to 0, and the unit production cost of the unreliable supplier after disruption is assumed to be c_d.

For the reliable supplier, we use (q_r, w_r) to represent the long-term contract provided by the buyer, where w_r is deterministic and is exogenously given. We assume that the reliable supplier has unlimited capacity of satisfying the order but cannot afford any more orders if the unreliable supplier is not able to meet the order. To ignore the trivial case, we assume $w_r > w_u$.

The buyer can source from two suppliers to reduce the risk of the disruption and save cost through two contracts: one is a long-term contract (q_r, w_r) for the reliable supplier and the other one is (q_u, w_u) for the unreliable supplier. The buyer's problem is whether to source from two suppliers and how many to order from either. Note that the buyer does not offer any extra incentive to the unreliable supplier for restoring capacity if a disruption occurs. This is because the buyer can still receive a part of the order from the reliable supplier even if the unreliable supplier suffers disruption and does not exert any restoration effort. If there is a disruption, the sequence of the events is shown in Figure 1.

4. Equilibrium Analysis

Our goal is to find the optimal restoration effort exerted by the unreliable supplier, e^*, the optimal order quantities, q_u^* and q_r^*, and the optimal wholesale price offered by the buyer to the unreliable supplier, w_u^*.

4.1. Optimal Strategy of Unreliable Supplier. If a disruption occurs, the unreliable supplier exerts restoration effort e based on the contract (q_u, w_u). For analytical tractability, we assume a quadratic restoration cost function $C_R(e) = ke^2/2$, where e is the effort that unreliable supplier exerts and k is a coefficient related to the rebuild cost. Similar cost functions have been widely used in the operation and marketing literature to model the diminishing impact of effort [28–30]. With the restoration effort e, we can formulate the unreliable supplier's profit function if there is a disruption for given values of q_u as follows:

$$\Pi_s(e) = -\frac{ke^2}{2} + (w_u - c_d)\min(q_u, e). \tag{1}$$

If the wholesale price w_u is less than the postdisruption unit production cost (i.e., $w_u \le c_d$), the unreliable supplier will not exert effort to restore capacity. Note that our assumption about the restoration cost $C_R(e) = ke^2/2$ implies that the marginal effort cost increases with the amount of effort. The unreliable supplier's optimal effort is summarized as follows.

Proposition 1. *If $w_u \le c_d$, the unreliable supplier will not exert any effort to restore capacity for order fulfillment; otherwise, the supplier's optimal restoration effort level $e^*(q_u)$ is increasing in q_u and*

$$e^*(q_u) = \min\left\{\frac{w_u - c_d}{k}, q_u\right\}. \tag{2}$$

Obviously, if the unreliable supplier decides to exert effort to rebuild capacity after disruption, the amount of restored capacity will not be more than the order quantity (i.e., $e^* \le q_u$). As shown in Figure 2, if q_u falls in $0 \le q_u \le ((w_u - c_d)/k)$, the supplier's restoration effort level e increases with q_u , which means that the supplier can fully meet the order even if there is a disruption without any additional incentive from the buyer. While q_u is falls in $q_u > ((w_u - c_d)/k)$, the supplier's restoration effort level e is

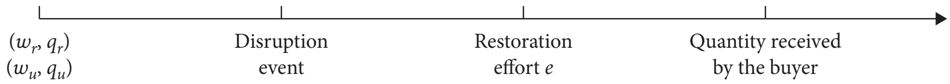

FIGURE 1: Sequence of the events.

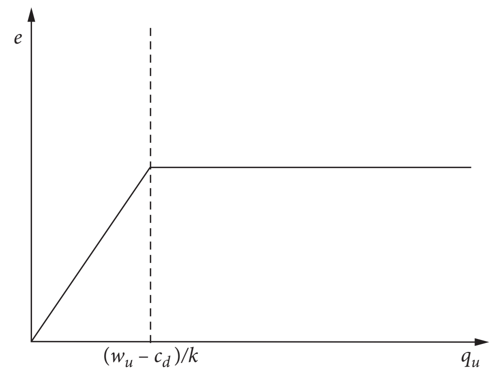

FIGURE 2: The relationship between restoration effort and order quantity.

fixed and is independent with q_u, and thus the order is not fully satisfied.

4.2. Optimal Procurement Strategy. In all, the buyer can choose among three strategies. The first strategy is ordering from the reliable supplier only (strategy R), the second one is ordering from the unreliable supplier only (strategy U), and the last one is ordering from both of the suppliers, also referred to as supply diversification strategy (strategy D).

4.2.1. Ordering Only from Reliable Supplier. The buyer orders only from the reliable supplier with fixed wholesale price w_r. We use q_r to denote the order quantity under this strategy. The profit function of the buyer is as follows:

$$\Pi_b^R(q_r) = (p - w_r)\min(q_r, d). \quad (3)$$

Under the wholesale contract, it is easy to obtain $q_r^* = d$.

4.2.2. Ordering Only from Unreliable Supplier. The buyer orders only from the unreliable supplier through a wholesale contract (q_u, w_u). If the disruption occurs with the possibility of $1-\beta$, the unreliable supplier will lose all the capacity and decide whether to exert restoration effort e to rebuild capacity. We assume that the unreliable supplier will get the restoration capacity e through the restoration effort e. From Proposition 1, we know that the restoration capacity depends on the values of q_u and w_u, and the profit function of the buyer is formulated as follows:

$$\Pi_b^U(q_u, w_u) = (p - w_u)[\beta\min(q_u, d) + (1-\beta)\min(e^*, d)]. \quad (4)$$

Taking (2) into (4), we have $\Pi_b^U(q_u, w_u) = (p - w_u)[\beta\min(q_u, d) + (1-\beta)\min(((w_u - c_d)/k), q_u, d)]$. We consider two cases: when $q_u < d$, we have $\Pi_b^U(q_u, w_u) = (p - w_u)[\beta\, q_u + (1-\beta)\min(((w_u - c_d)/k), q_u)]$, which increases with q_u; when $q_u \geq d$, we have $\Pi_b^U(q_u, w_u) = (p - w_u)[\beta d + (1-\beta)\min(((w_u - c_d)/k), d)]$, which is unrelated to q_u. We summarize the above results in Lemma 1.

Lemma 1. *If the seller orders from the unreliable supplier only, then $q_u^* = d$.*

From Lemma 1, we rewrite equation (4) as follows:

$$\Pi_b^U(w_u) = (p - w_u)\left[\beta d + (1-\beta)\min\left(\frac{w_u - c_d}{k}, d\right)\right], \quad (5)$$

where $0 \leq w_u \leq p$.

To solve the optimal wholesale price provided to the unreliable supplier, we conduct our analysis based on two cases $c_d + kd \leq p$ and $c_d + kd > p$ as follows.

When $c_d + kd \leq p$, we consider two subcases $((w_u - c_d)/k) \geq d$ and $((w_u - c_d)/k) < d$ as follows:

(1) If $((w_u - c_d)/k) \geq d$, then the profit function is

$$\Pi_b^U(w_u) = (p - w_u)d. \quad (6)$$

Since $\Pi_b^U(w_u)$ decreases with w_u, we obtain the local maximizer that $\widehat{w}_u = kd + c_d$ and $\Pi_b^U(\widehat{w}_u) = (p - kd - c_d)d$.

(2) If $((w_u - c_d)/k) < d$, we have $c_d \leq w_u < kd + c_d$; then, the profit function is

$$\Pi_b^U(w_u) = -\frac{(1-\beta)w_u^2}{k} + \left[\frac{(1-\beta)(p + c_d)}{k} - \beta d\right] \cdot w_u - \frac{(1-\beta)pc_d}{k} + \beta p d. \quad (7)$$

Since the axis of symmetry of equation (7) is $((p + c_d)/2) - (\beta k d/(2(1-\beta)))$, we have the following scenarios:

(a) When $((p + c_d)/2) - \beta k d/(2(1-\beta)) \leq c_d$, we have the local maximizer $\widehat{w}_u = c_d$ and $\Pi_b^U(\widehat{w}_u) = \beta d(p - c_d)$.

(b) When $c_d < ((p + c_d)/2) - (\beta k d/(2(1-\beta))) < c_d + kd$, we have $\widehat{w}_u = ((p + c_d)/2) - (\beta k d/(2(1-\beta)))$ and $\Pi_b^U(\widehat{w}_u) = [((p - c_d)/2) + (\beta k d/(2(1-\beta)))][(\beta d/2) + ((1-\beta)(p - c_d)/2k)]$.

(c) When $((p + c_d)/2) - (\beta k d/(2(1-\beta))) \geq c_d + kd$, we have $\widehat{w}_u = c_d + kd$ and $\Pi_b^U(\widehat{w}_u) = d[p - kd - c_d]$.

Thus, we conclude the equilibrium outcomes when $c_d + kd \leq p$ as follows:

(1) If $c_d + kd \leq p$, $((p + c_d)/2) - (\beta k d/2(1-\beta)) \leq c_d$, and $kd - (1-\beta)(p - c_d) \leq 0$ or $c_d < ((p + c_d)/2) - (\beta k d/(2(1-\beta))) < c_d + kd$ and $\Pi_b^U(c_d + kb) > \Pi_b^U$

$((p+c_d)/2)-(\beta k d/(2(1-\beta)))$ or (3) $((p+c_d)/2)-(\beta k d/(2(1-\beta)))\geq c_d+kd$, then $\widehat{w}_u=c_d+kd$ and $\Pi_b^U=(p-c_d-kd)b$.

(2) If $c_d+kd\leq p$, $((p+c_d)/2)-(\beta k d/(2(1-\beta)))\leq c_d$, and $kd-(1-\beta)(p-c_d)\geq 0$, then $\widehat{w}_u=c_d$ and $\Pi_b^U=\beta b(p-c_d)$.

(3) If $c_d+kb\leq p$, $c_d<((p+c_d)/2)-(\beta k d/(2(1-\beta)))<c_d+kb$, and $\Pi_b^U(c_d+kb)\leq\Pi_b^U(((p+c_d)/2)-(\beta k d/(2(1-\beta))))$, then $\widehat{w}_u=((p+c_d)/2)-(\beta k d/(2(1-\beta)))$ and $\Pi_b^U=[((p-c_d)/2)+(\beta k d/(2(1-\beta)))]\ \{\beta b+((1-\beta)/k)[((p-c_d)/2)-(\beta k d/(2(1-\beta)))]\}$.

When $c_d+kb>p$, we know that $((w_u-c_d)/k)<b$, i.e., $c_d<w_u<p$; thus, the profit function is as follows:

$$\Pi_b^U=\max_{w_u}\left\{-\frac{(1-\beta)w_u^2}{k}+\left[\frac{(1-\beta)(p+c_d)}{k}-\beta b\right]w_u-\frac{(1-\beta)pc_d}{k}+\beta pb\right\}. \tag{8}$$

Since the axis of symmetry of Function (8) is $((p+c_d)/2)-(\beta k d/(2(1-\beta)))$, we have the following scenarios:

(a) If $((p+c_d)/2)-(\beta k d/(2(1-\beta)))\leq c_d$, we have the local maximizer $\widehat{w}_u=c_d$ and $\Pi_b^U=\beta b(p-c_d)$.

(b) If $c_d<((p+c_d)/2)-(\beta k d/(2(1-\beta)))<p$, we have $\widehat{w}_u=((p+c_d)/2)-(\beta k d/(2(1-\beta)))$ and $\Pi_b^U=[((p-c_d)/2)+(\beta k d/(2(1-\beta)))]\{\beta b+((1-\beta)/k)[((p-c_d)/2)-(\beta k d/(2(1-\beta)))]\}$.

(c) If $((p+c_d)/2)-(\beta k d/(2(1-\beta)))\geq p$, we have $\widehat{w}_u=p$ and $\Pi_b^U=0$.

According to the above analysis, we summarize our equilibrium results in Proposition 2.

Proposition 2. *If the buyer only procures from the unreliable supplier, the equilibrium decision and profit of the buyer are summarized as follows:*

(i) If $c_d+kb\leq p$, (1) $((p+c_d)/2)-(\beta k d/(2(1-\beta)))\leq c_d$, and $kb-(1-\beta)(p-c_d)\leq 0$ or (2) $c_d<((p+c_d)/2)-(\beta k d/(2(1-\beta)))<c_d+kb$ and $\Pi_b^U(c_d+kb)>\Pi_b^U(((p+c_d)/2)-(\beta k d/(2(1-\beta))))$ or (3) $((p+c_d)/2)-(\beta k d/(2(1-\beta)))\geq c_d+kb$, then $w_u^*=c_d+kb$ and $\Pi_b^U=(p-c_d-kb)b$.

(ii) If (1) $c_d+kb\leq p$, $c_d<((p+c_d)/2)-(\beta k d/(2(1-\beta)))<c_d+kb$, and $\Pi_b^U(c_d+kb)\leq\Pi_b^U(((p+c_d)/2)-(\beta k d/(2(1-\beta))))$ or (2) $c_d+kb>p$ and $c_d<((p+c_d)/2)-(\beta k d/(2(1-\beta)))<p$, then $w_u^*=((p+c_d)/2)-(\beta k d/(2(1-\beta)))$ and $\Pi_b^U=[((p-c_d)/2)+(\beta k d/(2(1-\beta)))]\ \{\beta b+((1-\beta)/k)[((p-c_d)/2)-(\beta k d/(2(1-\beta)))]\}$.

(iii) If (1) $c_d+kb\leq p$, $((p+c_d)/2)-(\beta k d/(2(1-\beta)))\leq c_d$, and $kb-(1-\beta)(p-c_d)\geq 0$ or (2) $c_d+kb>p$ and $((p+c_d)/2)-(\beta k d/(2(1-\beta)))\leq c_d$, then $w_u^*=c_d$ and $\Pi_b^U=\beta b(p-c_d)$.

(iv) If $c_d+kb>p$ and $((p+c_d)/2)-(\beta k d/(2(1-\beta)))\geq p$, then $w_u^*=p$ and $\Pi_b^U=0$.

4.2.3. Supply Diversification Strategy. In this part, we discuss the optimal strategy of the buyer when ordering from both suppliers. We assume that $q_u+q_r=b$ and the buyer's profit is

$$\Pi_b^D(w_u,q_u)=\beta(pb-w_uq_u-w_rq_r)+(1-\beta)[p(e^*+q_r)-w_ue^*-w_rq_r], \tag{9}$$

where $e^*=\min\{(w_u-c_d)/k,q_u\}$ and $q_r=b-q_u$. We further consider two cases $q_u\leq(w_u-c_d)/k$ and $q_u>(w_u-c_d)/k$ as follows.

When $q_u\leq(w_u-c_d)/k$, we have

$$\begin{aligned}\Pi_b^D(w_u,q_u)&=pb-q_uw_u-(b-q_u)w_r\\&=(p-w_r)b+(w_r-w_u)q_u.\end{aligned} \tag{10}$$

Since $\Pi_b^D(w_u,q_u)$ is decreasing in w_u, we have $w_u=kq_u+c_d$. Taking it back into equation (10), we have

$$\Pi_b^D(q_u)=-kq_u^2+(w_r-c_d)q_u+(p-w_r)b. \tag{11}$$

Since the axis of symmetry of the function is $q_u=((w_r-c_d)/2k)$, for $0\leq q_u\leq b$, we have the following two subcases $0\leq((w_r-c_d)/2k)\leq b$ and $((w_r-c_d)/2k)>b$:

(1) If $0\leq((w_r-c_d)/2k)\leq b$, then $\widehat{q}_u=((w_r-c_d)/2k)$, $\widehat{w}_u=((w_r+c_d)/2)$, and $\Pi_b^D(\widehat{q}_u,\widehat{w}_u)=((w_r-c_d)^2/4k)+(p-w_r)b$.

(2) If $((w_r-c_d)/2k)>b$, then $\widehat{q}_u=b$, $\widehat{w}_u=kb+c_d$ and $\Pi_b^D(\widehat{q}_u,\widehat{w}_u)=(p-c_d)b-kb^2$.

When $q_u>((w_r-c_d)/2k)$, we have

$$\Pi_b^D(w_u,q_u)=[w_r-\beta w_u-(1-\beta)p]q_u+(p-w_r)b+\frac{1-\beta}{k}\left[-w^2+(p+c_d)w-pc_d\right]. \tag{12}$$

We can easily obtain that $c_d\leq w_u\leq kb+c_d$; then we consider three subcases $((w_r-(1-\beta)p)/\beta)<c_d$, $c_d\leq((w_r-(1-\beta)p)/\beta)<kb+c_d$, and $((w_r-(1-\beta)p)/\beta)\geq kb+c_d$ as follows:

(1) If $((w_r-(1-\beta)p)/\beta)<c_d$, we have the coefficient of q_u in (13) which is $w_r-\beta w_u-(1-\beta)p<0$, so $\Pi_b^D(w_u,q_u)$ is decreasing in q_u; then $\widehat{q}_u=((w_u-c_d)/k)$. Then, we can rewrite equation (12) as follows:

$$\Pi_b^D(w_u)=-\frac{w_u^2}{k}+\frac{(w_r+c_d)w_u}{k}-\frac{w_rc_d}{k}+(p-w_r)b. \tag{13}$$

Since the axis of symmetry of equation (13) is $w_u=((w_r+c_d)/2)$, for $c_d\leq w_u\leq kb+c_d$, then we have the following two scenarios:

(a) If $((w_r + c_d)/2) \leq kb + c_d$, we have $\widehat{w}_u = ((w_r + c_d)/2)$, $\widehat{q_u} = ((w_r - c_d)/2k)$, and $\Pi_b^D(\widehat{w}_u, \widehat{q_u}) = ((w_r - c_d)^2/4k) + (p - w_r)b$.

(b) If $((w_r + c_d)/2) > kb + c_d$, we have $\widehat{w}_u = kb + c_d$, $\widehat{q_u} = b$ and $\Pi_b^D(\widehat{w}_u, \widehat{q_u}) = (p - c_d)b - kb^2$.

(2) If $c_d \leq ((w_r - (1-\beta)p)/\beta) < kb + c_d$, we have the following two scenarios:

(a) If $c_d \leq w_u \leq (w_r - (1-\beta)p/\beta)$, then $w_r - \beta w_u - (1-\beta)p \geq 0$, so $\Pi_b^D(w_u, q_u)$ is increasing in q_u, for $0 \leq q_u \leq b$; we obtain $\widehat{q_u} = b$. Taking it into equation (12), we have

$$\Pi_b^D(w_u) = -\frac{1-\beta}{k}\left[w_u^2 - \left(p + c_d - \frac{\beta kb}{1-\beta}\right)w_u + pc_d\right] + \beta pb. \tag{14}$$

Since the axis of symmetry of equation (14) is $w_u = ((p + c_d)/2) - (\beta kd/(2(1-\beta)))$, we thus conduct the following discussion:

If $((p + c_d)/2) - (\beta k d/(2(1-\beta))) < c_d$, then $\widehat{w}_u = c_d$, $\widehat{q_u} = b$, and $\Pi_b^D(\widehat{w}_u, \widehat{q_u}) = \beta(p - c_d)b$.

If $c_d \leq ((p + c_d)/2) - (\beta kd/(2(1-\beta))) < ((w_r - (1-\beta)p)/\beta)$, then $\widehat{w}_u = ((p + c_d)/2) - (\beta kd/(2(1-\beta)))$, $\widehat{q_u} = b$, and $\Pi_b^D(\widehat{w}_u, \widehat{q_u}) = ((1-\beta)/k)[\widehat{w}_u = ((p + c_d)/2) - (\beta kd/(2(1-\beta)))]^2 - (((1-\beta)pc_d)/k) + \beta pb$.

If $((p + c_d)/2) - (\beta kd/(2(1-\beta))) \geq ((w_r - (1-\beta)p)/\beta)$, then $\widehat{w}_u = ((w_r - (1-\beta)p)/\beta)$, $\widehat{q_u} = b$, and $\Pi_b^D(\widehat{w}_u, \widehat{q_u}) = p(w_r + c_d) - (1-\beta)(p^2 + w_r c_d)$.

(b) If $((w_r - (1-\beta)p)/\beta) < w_u \leq kb + c_d$, then $w_r - \beta w_u - (1-\beta)p < 0$, so $\Pi_b^D(w_u, q_u)$ is decreasing in q_u, for $((w_u - c_d)/k) \leq q_u \leq b$; we obtain $\widehat{q_u} = ((w_u - c_d)/k)$. Taking it into (13), we have

Since the axis of symmetry of (16) is $w_u = ((w_r + c_d)/2k)$, we thus conduct the following discussion:

If $((w_r + c_d)/2k) < ((w_r - (1-\beta)p)/\beta)$, then $\widehat{w}_u = ((w_r - (1-\beta)p)/\beta)$, $\widehat{q_u} = ((p - c_d)/k) - ((p - w_r)/\beta k)$, and $\Pi_b^D(\widehat{w}_u, \widehat{q_u}) = -((1-\beta)(p - w_r)^2/k\beta^2) + (((1-\beta)(p^2 + w_r c_d - pw_r - pc_d))/k\beta) + (p - w_r)b$.

If $((w_r - (1-\beta)p)/\beta) \leq ((w_r + c_d)/2k) < kb + c_d$, then $\widehat{w}_u = ((w_r + c_d)/2k)$, $\widehat{q_u} = ((w_r - c_d)/2k)$, and $\Pi_b^D(\widehat{w}_u, \widehat{q_u}) = ((w_r - c_d)^2/4k) + (p - w_r)b$.

If $((w_r + c_d)/2k) \geq kb + c_d$, then $\widehat{w}_u = kb + c_d$, $\widehat{q_u} = b$, and $\Pi_b^D(\widehat{w}_u, \widehat{q_u}) = (p - c_d)b - kb^2$.

(3) If $((w_r - (1-\beta)p)/\beta) \geq kb + c_d$, we have $w_r - \beta w_u - (1-\beta)p > 0$, so $\widehat{q_u} = b$. Taking it into equation (12), we have

$$\Pi_b^D(w_u) = -\frac{1}{k}\left[w_u^2 - (w_r + c_d)w_u + w_r c_d\right] + (p - w_r)b. \tag{15}$$

Since the axis of symmetry of equation (16) is $\widehat{w}_u = ((p + c_d)/2) - (\beta kd/(2(1-\beta)))$, for $c_d \leq w_u \leq kb + c_d$, we thus conduct the following discussion:

$$\Pi_b^D(w_u) = -\frac{1-\beta}{k}\left[w_u^2 - \left(p + c_d - \frac{\beta kb}{1-\beta}\right)w_u + pc_d\right] + \beta pb. \tag{16}$$

If $((p + c_d)/2) - (\beta kd/(2(1-\beta))) < c_d$, then $\widehat{w}_u = c_d$, $\widehat{q_u} = b$, and $\Pi_b^D(\widehat{w}_u, \widehat{q_u}) = \beta(p - c_d)b$.

If $c_d \leq ((p + c_d)/2) - (\beta kd/(2(1-\beta))) < kb + c_d$, then $\widehat{w}_u = ((p + c_d)/2) - (\beta kd/(2(1-\beta)))$, $\widehat{q_u} = b$, and $\Pi_b^D(\widehat{w}_u, \widehat{q_u}) = ((1-\beta)/k)$ $[((p + c_d)/2) - (\beta kd/(2(1-\beta)))]^2 - ((1-\beta)pc_d/k) + \beta pb$.

If $((p + c_d)/2) - (\beta kd/(2(1-\beta))) \geq kb + c_d$, then $\widehat{w}_u = kb + c_d$, $\widehat{q_u} = b$, and $\Pi_b^D(\widehat{w}_u, \widehat{q_u}) = (p - c_d)b - kb^2$.

According to the above analysis, we have the following discussions to obtain our equilibrium results when the buyer adopts supply diversification strategy.

Case 1. If $((w_r - (1-\beta)p)/\beta) < c_d$ and $((w_r + c_d)/2k) \leq kd + c_d$, the analysis is shown in Figure 3.

As we can see, for $0 \leq q_u \leq b$ and $c_d \leq w_u \leq kb + c_d$, the feasible region is a rectangle with an oblique line cut into two parts, where the solution becomes better along the direction of the arrow. So under this circumstance, we obtain the global optimal solutions $w_u^* = ((w_r + c_d)/2)$ and $q_u^* = ((w_r - c_d)/2k)$, and the optimal profit is $\Pi_b^D(w_u^*, q_u^*) = ((w_r - c_d)^2/4k) + (p - w_r)b$.

Case 2. If $((w_r - (1-\beta)p)/\beta) < c_d \leq kd + c_d < ((w_r + c_d)/2)$, we have our analysis as shown in Figure 4.

It is easy to obtain the global optimal solution which is $w_u^* = kb + c_d$ and $q_u^* = b$, which is the intersection of the lines $q_u = b$ and $q_u = (w_u - c_d)/k$, and the optimal profit is $\Pi_b^D(w_u^*, q_u^*) = (p - c_d)b - kb^2$.

Case 3. If $((p + c_d)/2) - (\beta kd/(2(1-\beta))) < c_d < ((w_r + c_d)/2) < ((w_r - (1-\beta)p)/\beta) < kb + c_d$, the analysis is shown in Figure 5.

We can see that the feasible region is cut into three parts with a local optimal solution in each part. We can easily find the global optimums $w_u^* = c_d$ and $q_u^* = b$, and the optimal profit is $\Pi_b^D(w_u^*, q_u^*) = \beta(p - c_d)b$.

Case 4. If $((p + c_d)/2) - (\beta k d/(2(1-\beta))) < c_d \leq ((w_r - (1-\beta)p)/\beta) < ((w_r + c_d)/2) < kb + c_d$, the analysis is shown in Figure 6.

As we can see, the feasible region is divided into three parts which is the same as in Figure 5, but the difference is that there are two similar local optimums and we cannot intuitively obtain the global optimum. Thus, we need to compare the profit of the two points (c_d, b) and $(((w_r + c_d)/2), ((w_r - c_d)/2k))$, and the optimal profit is $\max\{\Pi_b^D(c_d, b), \Pi_b^D(((w_r + c_d)/2), ((w_r - c_d)/2k))\}$.

Case 5. If $((p + c_d)/2) - (\beta kd/(2(1-\beta))) < c_d \leq ((w_r - (1-\beta)p)/\beta) < kb + c_d < ((w_r + c_d)/2)$, the analysis is shown in Figure 7.

As we can see, there are two local optimums. Since $((p + c_d)/2) - (\beta kd/(2(1-\beta))) < c_d$, we compare the profits

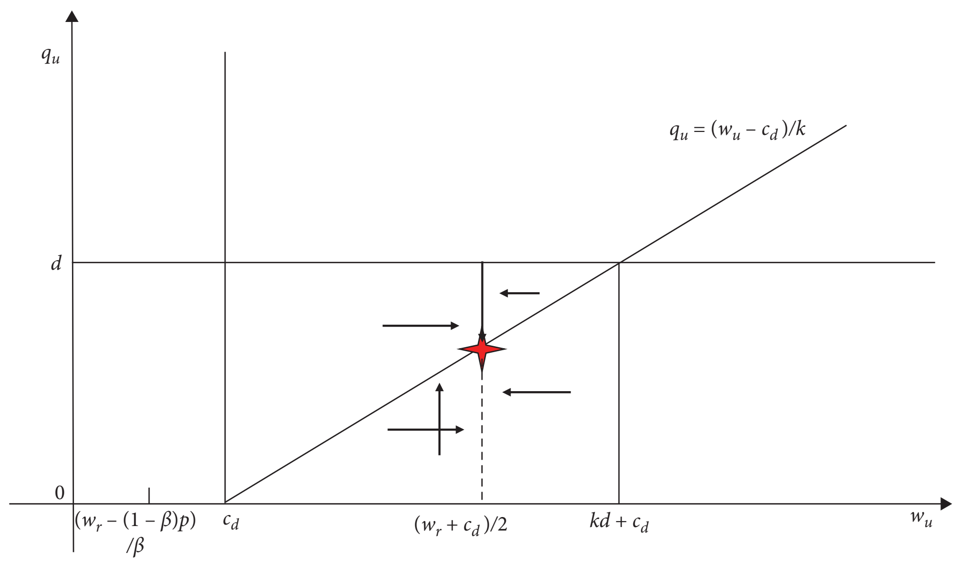

FIGURE 3: Case 1: $((w_r - (1-\beta)p)/\beta) < c_d$ and $((w_r + c_d)/2) \le kd + c_d$.

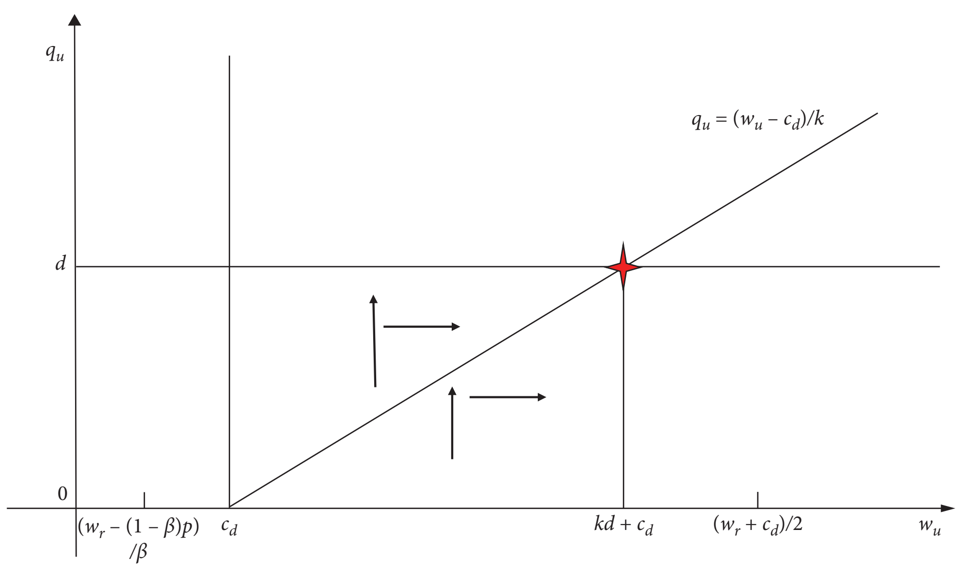

FIGURE 4: Case 2: $((w_r - (1-\beta)p)/\beta) < c_d \le kd + c_d < ((w_r + c_d)/2)$.

of the two points (c_d, b) and (kb, b) and find that $\Pi_b^D(c_d, b) \ge \Pi_b^D(kb, b)$, so the global optimum is $w_u^* = c_d$ and $q_u^* = b$, and the optimal profit is $\Pi_b^D(w_u^*, q_u^*) = \beta(p - c_d)b$.

Case 6. If $c_d \le ((p + c_d)/2) - \beta kb/2(1-\beta) < ((w_r - (1-\beta)p)/\beta)$ and $((w_r + c_d)/2) \le ((w_r - (1-\beta)p)/\beta) < kb + c_d$, the analysis is shown in Figure 8.

Similarly, there are three local optimums, but we can easily obtain that the global optimal solution is $w_u^* = ((p + c_d)/2) - (\beta kd/(2(1-\beta)))$ and $q_u^* = b$.

Case 7. If $c_d \le ((p + c_d)/2) - (\beta kb/2(1-\beta)) < ((w_r - (1-\beta)p)/\beta) < ((w_r + c_d)/2) \le kb + c_d$, the analysis is shown in Figure 9.

We can obtain that the local optimums are $(((p + c_d)/2) - (\beta kb/(2(1-\beta))), b)$ and $(w_r + c_d/2, (w_r - c_d)/2k)$. The optimal profit is $\max\{\Pi_b^D(((p + c_d)/2) - (\beta kd/(2(1-\beta))), b), \Pi_b^D((w_r + c_d)/2, (w_r - c_d)/2k)\}$.

Case 8. If $c_d \le ((p + c_d)/2) - (\beta kd/(2(1-\beta))) < ((w_r - (1-\beta)p)/\beta) < kb + c_d \le ((w_r + c_d)/2)$, the analysis is shown in Figure 10.

We can obtain the two local optimums $(((p + c_d)/2) - (\beta k d/(2(1-\beta))), b)$ and $(kb + c_d, b)$. The optimal profit is $\max\{\Pi_b^D(((p + c_d)/2) - (\beta k d/(2(1-\beta))), b), \Pi_b^D(kb + c_d, b)\}$.

Case 9. If $c_d < ((w_r + c_d)/2) < ((w_r - (1-\beta)p)/\beta) \le ((p + c_d)/2) - (\beta k d/(2(1-\beta)))$ and $(w_r - (1-\beta)p/\beta) < kb + c_d$, the analysis is shown in Figure 11.

We can see that $(((w_r + c_d)/2), ((w_r - c_d)/2k))$ is the worst solution, so the best solution is either $(((w_r - (1-$

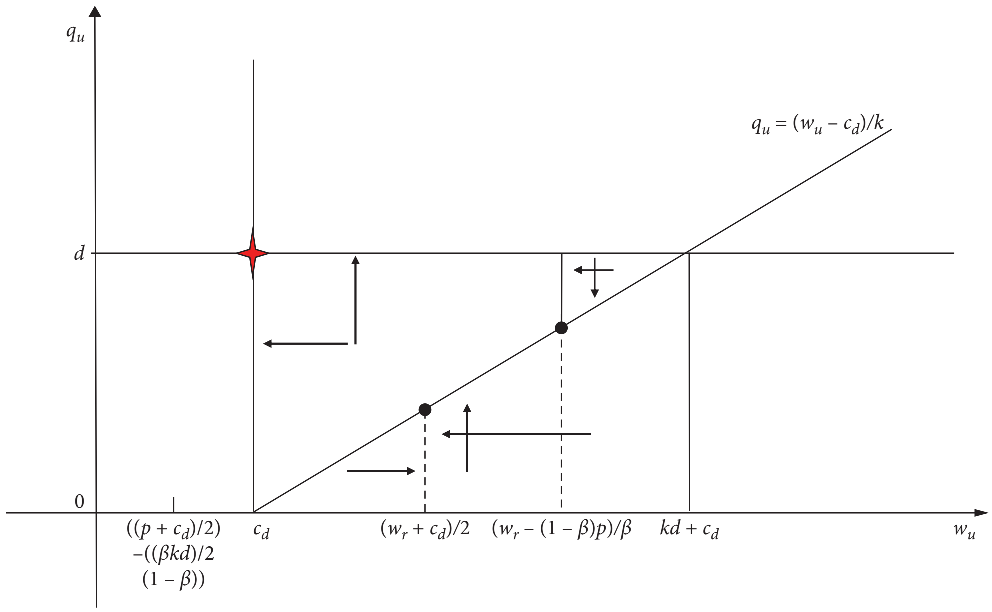

FIGURE 5: Case 3: $((p + c_d)/2) - (\beta k d/(2(1-\beta))) < c_d < ((w_r + c_d)/2) < ((w_r - (1-\beta)p)/\beta) < kb + c_d$.

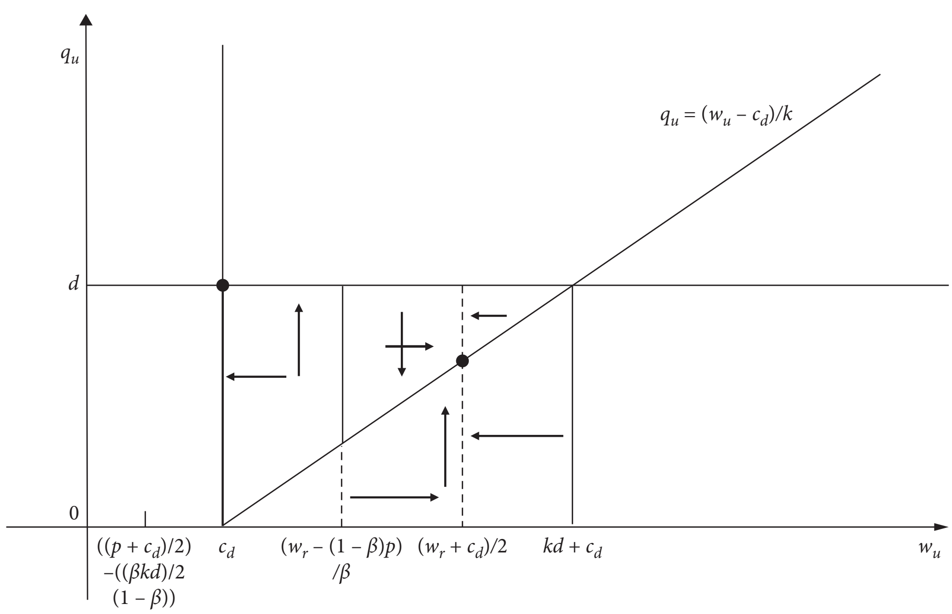

FIGURE 6: Case 4: $((p + c_d)/2) - (\beta kd/(2(1-\beta))) < c_d \le ((w_r - (1-\beta)p)/\beta) < ((w_r + c_d)/2) < kb + c_d$.

$\beta)p)/\beta), b)$ or $(((w_r - (1-\beta)p)/\beta), ((p + c_d)/2) - (\beta kb/2(1-\beta)))$. The profit of the points is $\Pi_b^D(((w_r - (1-\beta)p)/\beta), b) = p(w_r + c_d) - (1-\beta)(p^2 + w_r c_d)$ and $\Pi_b^D(((w_r - (1-\beta)p)/\beta), ((p + c_d)/2) - (\beta kd/(2(1-\beta)))) = -((1-\beta)(p - w_r)^2/k\beta^2) + ((1-\beta)(p^2 + w_r c_d - pw_r - pc_d)/k\beta) + (p - w_r)b$, and the optimal profit is the bigger one.

Case 10. If $c_d \le ((w_r - (1-\beta)p)/\beta) \le ((w_r + c_d)/2) < kb + c_d$ and $((p + c_d)/2) - (\beta kd/(2(1-\beta))) \ge ((w_r - (1-\beta)p)/\beta)$, the analysis is shown in Figure 12.

We can easily obtain the optimal solutions $w_u^* = ((w_r + c_d)/2)$ and $q_u^* = ((w_r - c_d)/2k)$, and the optimal profit is $\Pi_b^D(w_u^*, q_u^*) = ((w_r - c_d)^2/4k) + (p - w_r)b$.

Case 11. If $c_d \le ((w_r - (1-\beta)p)/\beta) \le ((p + c_d)/2) - (\beta k d/(2(1-\beta)))$ and $((w_r + c_d)/2) \ge kb + c_d$, the analysis is shown in Figure 13.

It is easy to find that the optimal solution is $w_u^* = b + c_d$ and $q_u^* = b$, and the optimal profit is $\Pi_b^D(w_u^*, q_u^*) = (p - c_d)b - kb^2$.

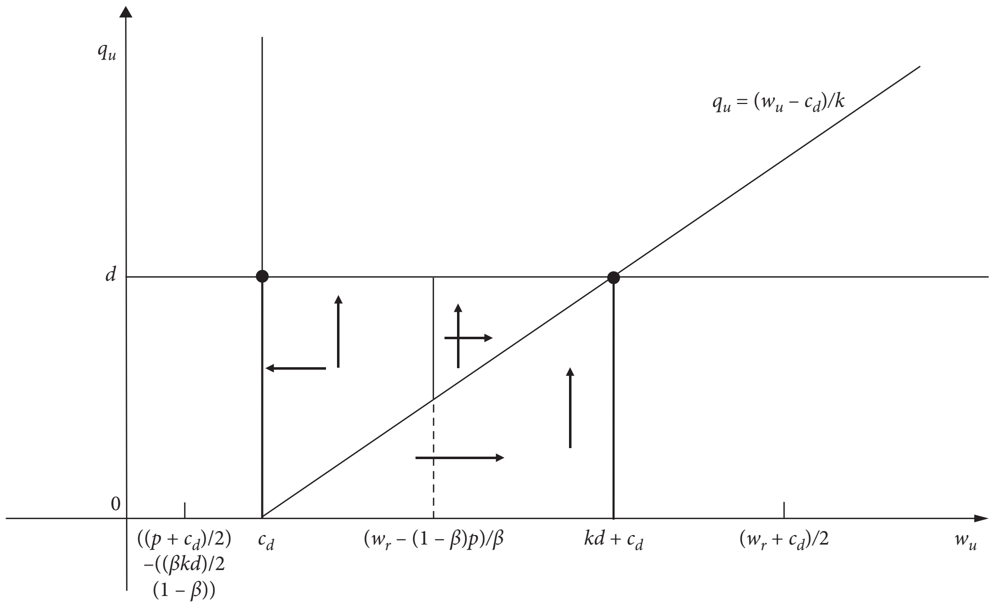

Figure 7: Case 5: $((p + c_d)/2) - (\beta kd/(2(1 - \beta))) < c_d \leq ((w_r - (1 - \beta)p)/\beta) < kb + c_d < ((w_r + c_d)/2)$.

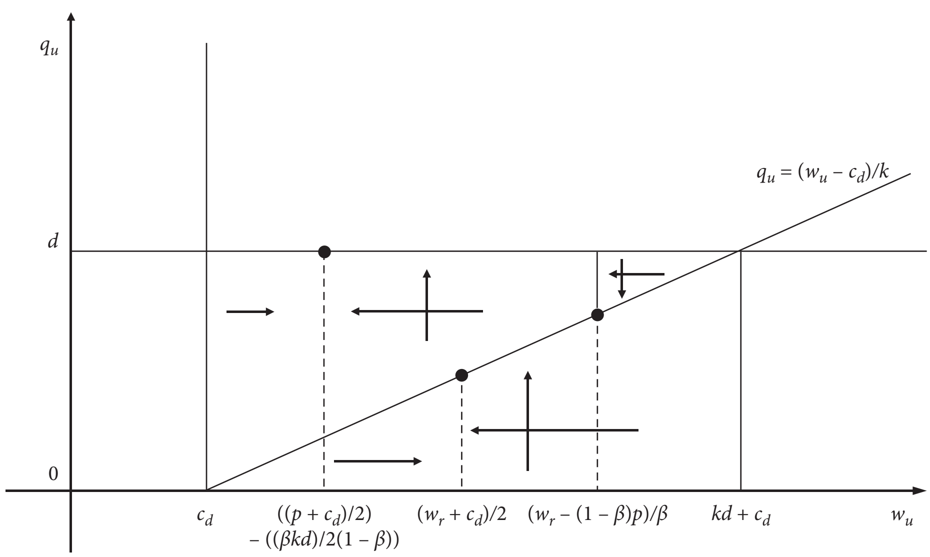

Figure 8: Case 6: $c_d \leq ((p + c_d)/2) - (\beta kb/2(1 - \beta)) < ((w_r - (1 - \beta)p)/\beta)$ and $((w_r + c_d)/2) \leq ((w_r - (1 - \beta)p)/\beta) < kb + c_d$.

Case 12. If $((p + c_d)/2) - (\beta kd/(2(1 - \beta))) < c_d < ((w_r + c_d)/2) < kb + c_d < ((w_r - (1 - \beta)p)/\beta)$, the analysis is shown in Figure 14.

As we can see, the global optimum is $w_u^* = c_d$ and $q_u^* = b$, and the optimal profit is $\Pi_b^D(w_u^*, q_u^*) = \beta(p - c_d)b$.

Case 13. If $((p + c_d)/2) - (\beta kd/(2(1 - \beta))) < c_d < kb + c_d < ((w_r + c_d)/2)$ and $((w_r - (1 - \beta)p)/\beta) \geq kb + c_d$, the analysis is shown in Figure 15.

At this circumstance, the global optimum is the same as the one above.

Case 14. If $c_d < ((p + c_d)/2) - (\beta kd/(2(1 - \beta))) < kb + c_d$ and $((w_r + c_d)/2) < kb + c_d < ((w_r - (1 - \beta)p)/\beta)$, the analysis is shown in Figure 16.

We can see that the global optimum is $w_u^* = ((p + c_d)/2) - (\beta kd/(2(1 - \beta)))$ and $q_u^* = b$, and the optimal profit is $\Pi_b^D(w_u^*, q_u^*) = (1 - \beta)/k(((p + c_d)/2) - (\beta kd/(2(1 - \beta))))^2 - ((1 - \beta)pc_d/k) + \beta pb$.

Case 15. If $c_d < ((p + c_d)/2) - (\beta kd/(2(1 - \beta))) < kb + c_d < ((w_r + c_d)/2)$ and $((w_r - (1 - \beta)p)/\beta) \geq kb + c_d$, the analysis is shown in Figure 17.

The solution is the same as the one above.

Case 16. If $c_d < ((w_r + c_d)/2) < kb + c_d \leq ((p + c_d)/2) - (\beta kd/(2(1 - \beta)))$ and $((w_r - (1 - \beta)p)/\beta) \geq kb + c_d$, the analysis is shown in Figure 18.

As we can see, the global optimum is $w_u^* = kb + c_d$ and $q_u^* = b$, and the optimal profit is $\Pi_b^D(w_u^*, q_u^*) = (p - c_d)b - kb^2$.

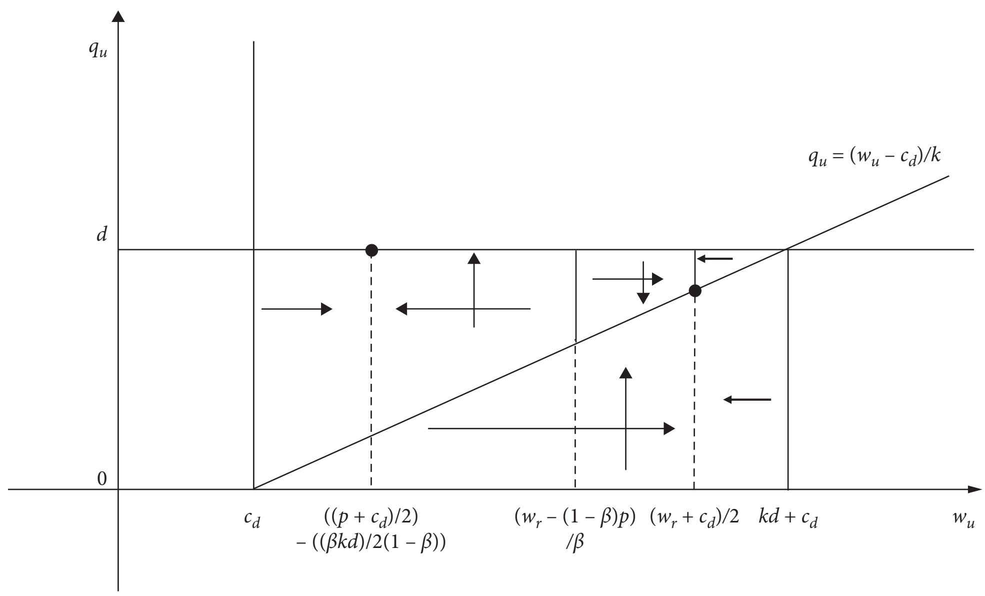

Figure 9: Case 7: $c_d \leq ((p + c_d)/2) - (\beta kd/(2(1 - \beta))) < ((w_r - (1 - \beta)p)/\beta) < ((w_r + c_d)/2) \leq kb + c_d$.

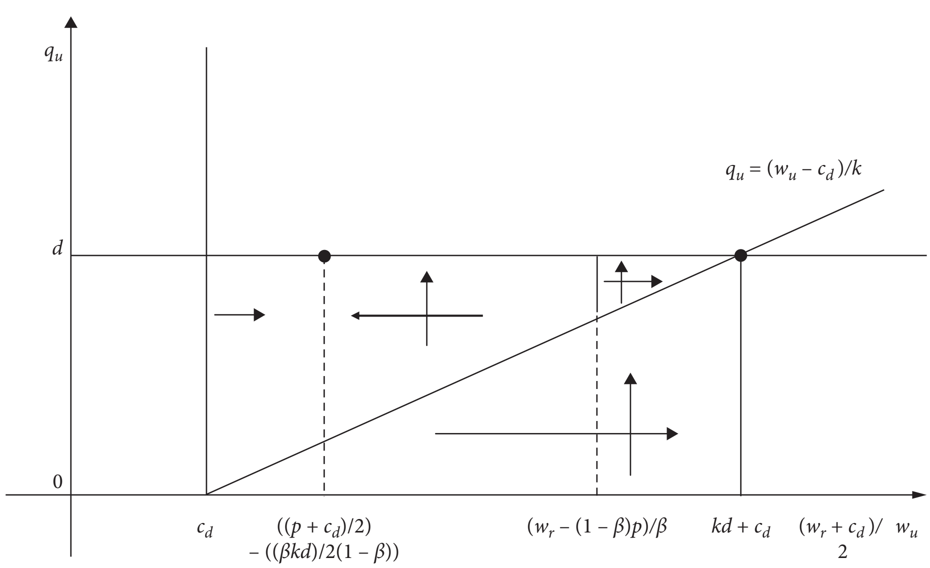

Figure 10: Case 8: $c_d \leq ((p + c_d)/2) - (\beta kd/(2(1 - \beta))) < ((w_r - (1 - \beta)p)/\beta) < kb + c_d \leq ((w_r + c_d)/2)$.

Case 17. If $((w_r + c_d)/2) \geq kb + c_d$, $((p + c_d)/2) - (\beta k d/(2(1 - \beta))) \geq kb + c_d$, and $((w_r - (1 - \beta)p)/\beta) \geq kb + c_d$, the analysis is shown in Figure 19.

The solution is the same with the one above.

According to our analysis, we come to the conclusions which are summarized in Proposition 3.

Proposition 3. *In all, the optimal strategy of the buyer might be divided into six different scenarios as follows:*

(i) $w_u^* = ((w_r + c_d)/2)$ *and* $q_u^* = ((w_r - c_d)/2k)$ *if*

(1) $((w_r - (1-\beta)p)/\beta) < c_d$ *and* $((w_r + c_d)/2) \leq kb + c_d$ *or (2)* $((p + c_d)/2) - (\beta kd/(2(1-\beta))) < c_d \leq ((w_r - (1-\beta)p)/\beta) < ((w_r + c_d)/2) < kb + c_d$ *and* $\prod_b^D ((w_r + c_d)/2, (w_r - c_d)/2k) \geq \prod_b^D (c_d, b)$ *or (3)* $c_d \leq ((p + c_d)/2) - (\beta kd/(2(1-\beta))) < ((w_r - (1-\beta)p)/\beta)$, $((w_r - (1-\beta)p)/\beta) < ((w_r + c_d)/2) < kb + c_d$, $\prod_b^D ((w_r + c_d)/2, (w_r - c_d)/2k) \geq \prod_b^D ((p + c_d)/2 - (\beta kb/2(1-\beta)), b)$, *or (4)* $c_d \leq (w_r - (1-\beta)p)/\beta \leq (w_r + c_d)/2 < kb + c_d$ *and* $(p + c_d)/2 - (\beta kb/2(1-\beta)) \geq (w_r - (1-\beta)p)/\beta$.

(ii) $w_u^* = kb + c_d$ *and* $q_u^* = b$ *if*

(1) $((w_r - (1-\beta)p)/\beta) < c_d < kb + c_d < ((w_r + c_d)/2)$ *or (2)* $c_d \leq ((p + c_d)/2) - (\beta kd/(2(1-\beta))) < ((w_r - (1-\beta)p)/\beta) < kb + c_d \leq ((w_r + c_d)/2)$ *and* $\Pi_b^D (kb + c_d, b) \geq \Pi_b^D (((p + c_d)/2) - (\beta kd/(2(1-\beta))), b)$ *or (3)* $c_d \leq ((w_r - (1-\beta)p)/\beta) \leq ((p + c_d)/2) - (\beta k d/(2(1-\beta)))$ *and* $((w_r + c_d)/2) \geq kb + c_d$, *or (4)* $((w_r - (1-\beta)p)/\beta) \geq kb + c_d$ *and* $((p + c_d)/2) - (\beta k d/(2(1-\beta))) \geq kb + c_d$.

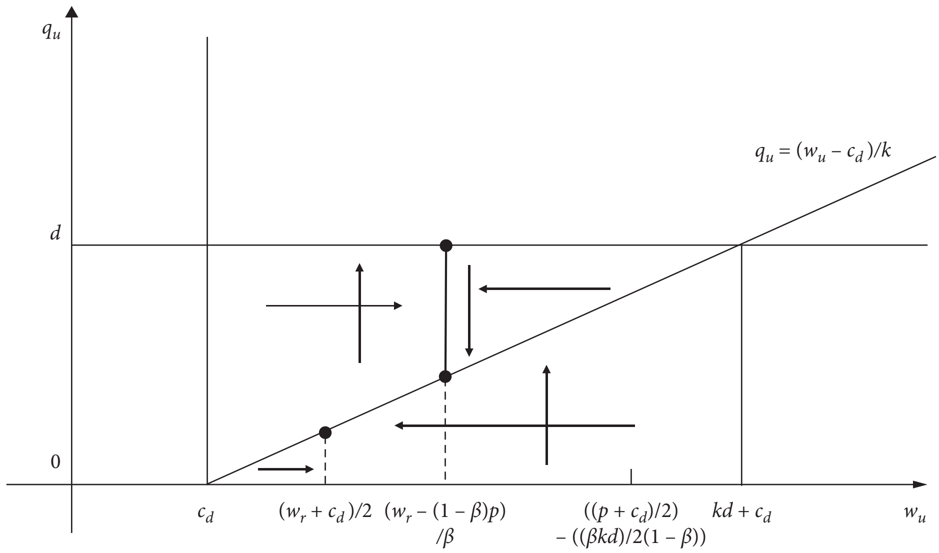

FIGURE 11: Case 9: $c_d < ((w_r + c_d)/2) < ((w_r - (1-\beta)p)/\beta) \leq ((p + c_d)/2) - (\beta kd/(2(1-\beta)))$ and $((w_r - (1-\beta)p)/\beta) < kb + c_d$.

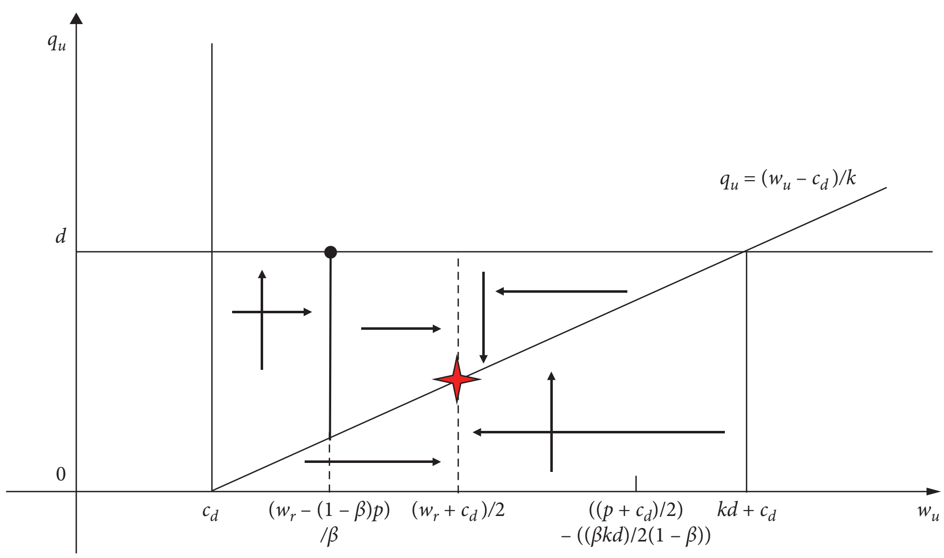

FIGURE 12: Case 10: $c_d \leq ((w_r - (1-\beta)p)/\beta) \leq ((w_r + c_d)/2) < kb + c_d$ and $((p + c_d)/2) - (\beta kd/(2(1-\beta))) \geq ((w_r - (1-\beta)p)/\beta)$.

(iii) $w_u^* = c_d$ and $q_u^* = b$ if

(1) $((p + c_d)/2) - (\beta kd/(2(1-\beta))) < c_d < ((w_r + c_d)/2) < ((w_r - (1-\beta)p)/\beta) < kb + c_d$ or (2) $((p + c_d)/2) - (\beta kd/(2(1-\beta))) < c_d \leq ((w_r - (1-\beta)p)/\beta) < ((w_r + c_d)/2) < kb + c_d$ and $\Pi_b^D(((w_r + c_d)/2), ((w_r - c_d)/2k)) < \Pi_b^D(c_d, b)$ or (3) $((p + c_d)/2) - (\beta kd/(2(1-\beta))) < c_d < ((w_r - (1-\beta)p)/\beta) < kb + c_d < ((w_r + c_d)/2)$, or (4) $((p + c_d)/2) - (\beta kd/(2(1-\beta))) < c_d < kb + c_d < ((w_r - (1-\beta)p)/\beta)$.

(iv) $w_u^* = ((p + c_d)/2) - (\beta kd/(2(1-\beta)))$ and $q_u^* = b$ if

(1) $c_d \leq ((p + c_d)/2) - (\beta kd/(2(1-\beta))) < ((w_r - (1-\beta)p)/\beta)$ and $((w_r + c_d)/2) \leq ((w_r - (1-\beta)p)/\beta) < kb + c_d$ or (2) $c_d \leq ((p + c_d)/2) - (\beta kd/(2(1-\beta))) < ((w_r - (1-\beta)p)/\beta)$, $((w_r - (1-\beta)p)/\beta) < ((w_r + c_d)/2) < kb + c_d$, and $\Pi_b^D(((w_r + c_d)/2), ((w_r - c_d)/2k)) < \Pi_b^D(((p + c_d)/2) - (\beta kd/(2(1-\beta))), b)$ or (3) $c_d \leq ((p + c_d)/2) - (\beta kd/(2(1-\beta))) < ((w_r - (1-\beta)p)/\beta) < kb + c_d \leq ((w_r + c_d)/2)$ and $\Pi_b^D(kb + c_d, b) < \Pi_b^D(((p + c_d)/2) - (\beta kd/(2(1-\beta))), b)$, or (4) $c_d \leq ((p + c_d)/2) - (\beta kd/(2(1-\beta))) < kb + c_d \leq ((w_r - (1-\beta)p)/\beta)$.

(v) $w_u^* = ((w_r - (1-\beta)p)/\beta)$ and $q_u^* = b$ if

$c_d < ((w_r + c_d)/2) < ((w_r - (1-\beta)p)/\beta) \leq ((p + c_d)/2) - (\beta kd/(2(1-\beta)))$, $((w_r - (1-\beta)p)/\beta) < kb + c_d$, and $\Pi_b^D((w_r - (1-\beta)p)/\beta, b) \geq \Pi_b^D(((w_r - (1-\beta)p)/\beta), (p - c_d)/k - (p - w_r)/\beta k)$.

(vi) $w_u^* = ((w_r - (1-\beta)p)/\beta)$ and $q_u^* = ((p - c_d)/k) - (p - w_r)/\beta k$ if

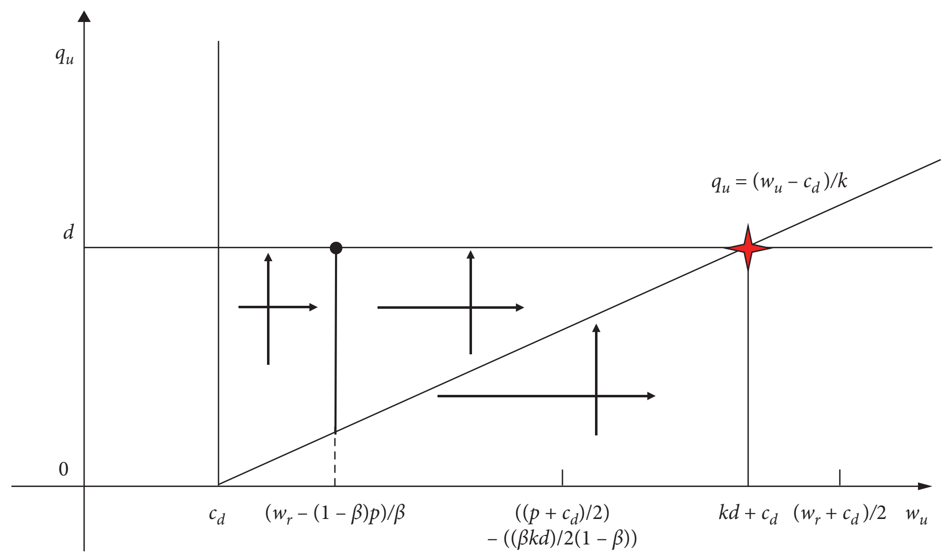

Figure 13: Case 11: $c_d \le ((w_r - (1-\beta)p)/\beta) \le ((p + c_d)/2) - (\beta k d/(2(1-\beta)))$ and $((w_r + c_d)/2) \ge kb + c_d$.

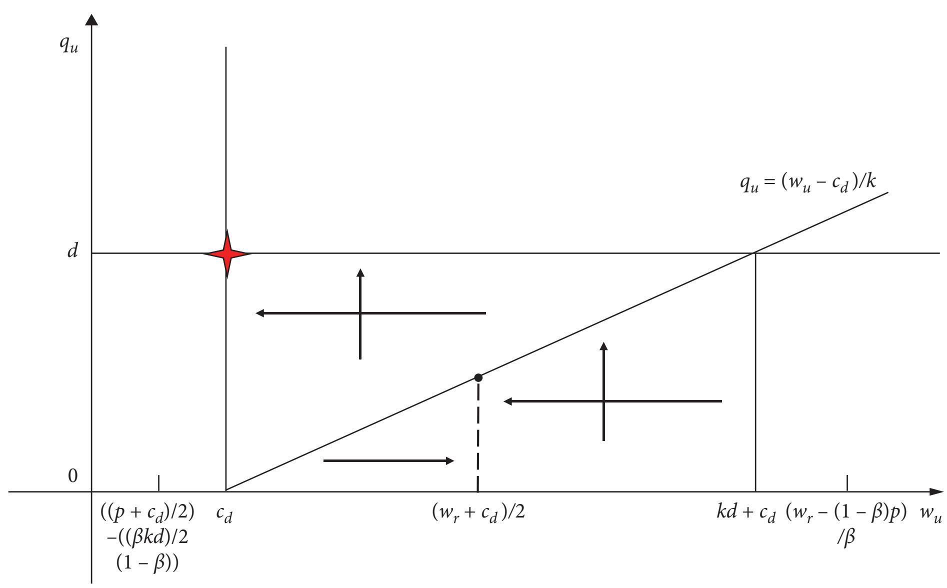

Figure 14: Case 12: $((p + c_d)/2) - (\beta k d/(2(1-\beta))) < c_d < ((w_r + c_d)/2) < kb + c_d < ((w_r - (1-\beta)p)/\beta)$.

$c_d < ((w_r + c_d)/2) < ((w_r - (1-\beta)p)/\beta) \le ((p + c_d)/2) - (\beta k d/(2(1-\beta)))$, $((w_r - (1-\beta)p)/\beta) < kb + c_d$, *and* $\Pi_b^D((w_r - (1-\beta)p)/\beta, b) < \Pi_b^D(((w_r - (1-\beta)p)/\beta), (p - c_d)/k - (p - w_r)/\beta k)$.

Furthermore, from Proposition 3, we can obtain the optimal restoration effort of the unreliable supplier as shown in Proposition 4.

Proposition 4. *Given the optimal contract provided by the buyer* (w_u^*, q_u^*), *the optimal restoration effort exerted by the unreliable supplier is* $e^*(w_u^*, q_u^*) = \min\{((w_u^* - c_d)/k), q_u^*\}$.

5. Numerical Study

Since it is hard to obtain the closed forms of our decision variables, we conduct the following numerical analysis to generate some managerial insights. When the buyer orders only from the reliable supplier, the case would be easy to understand. In this way, we conduct numerical analyses for the case when the buyer orders only from the unreliable supplier and the case when the buyer adopts supply diversification strategy. Among all parameters, the probability without disruption β and the unit production cost after disruption c_d would be the two most important factors that affect the buyer's ordering strategy. Thus, we first assign the

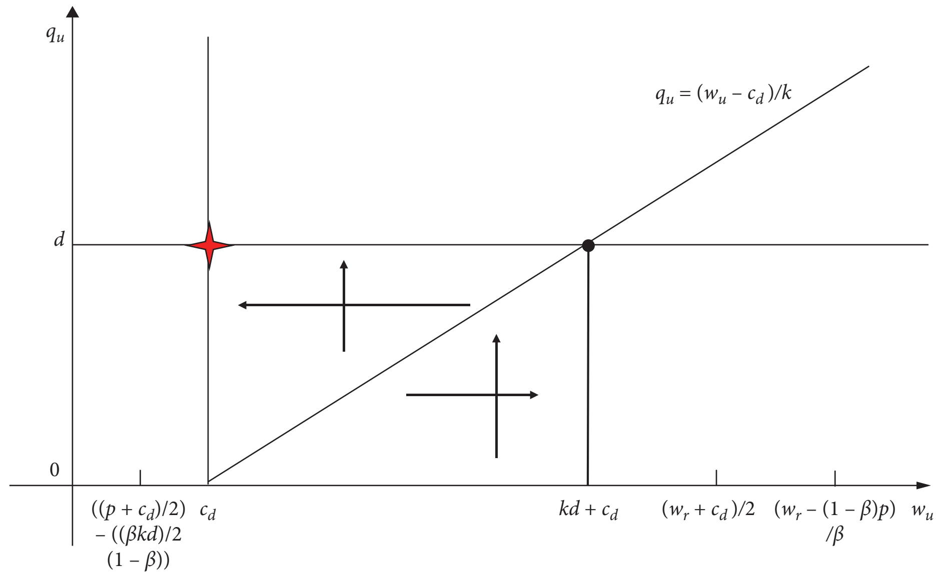

Figure 15: Case 13: $((p + c_d)/2) - (\beta k d/(2(1-\beta))) < c_d < kb + c_d < ((w_r + c_d)/2)$ and $((w_r - (1-\beta)p)/\beta) \geq kb + c_d$.

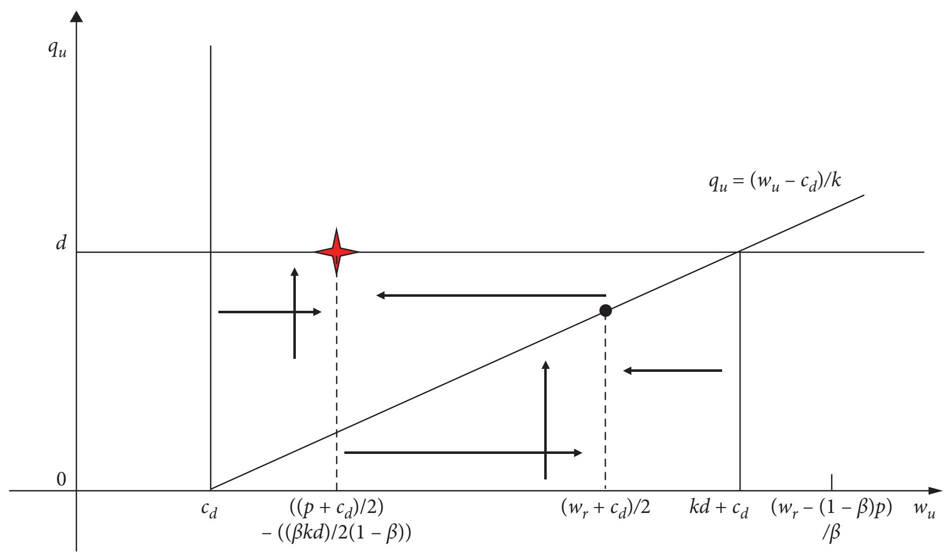

Figure 16: Case 14: $c_d < ((p + c_d)/2) - (\beta k d/(2(1-\beta))) < kb + c_d$ and $((w_r + c_d)/2) < kb + c_d < ((w_r - (1-\beta)p)/\beta)$.

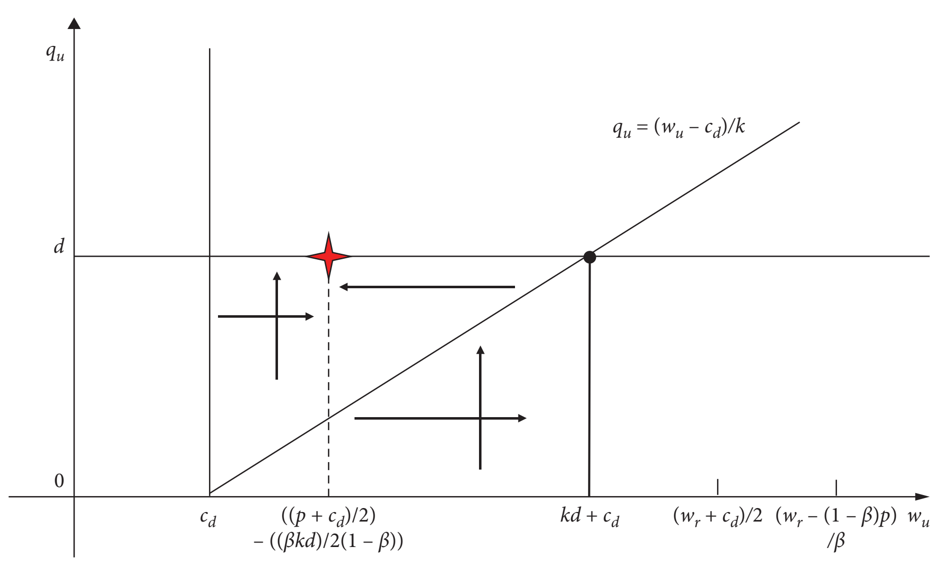

Figure 17: Case 15: $c_d < ((p + c_d)/2) - (\beta k d/(2(1-\beta))) < kb + c_d < ((w_r + c_d)/2)$ and $((w_r - (1-\beta)p)/\beta) \geq kb + c_d$.

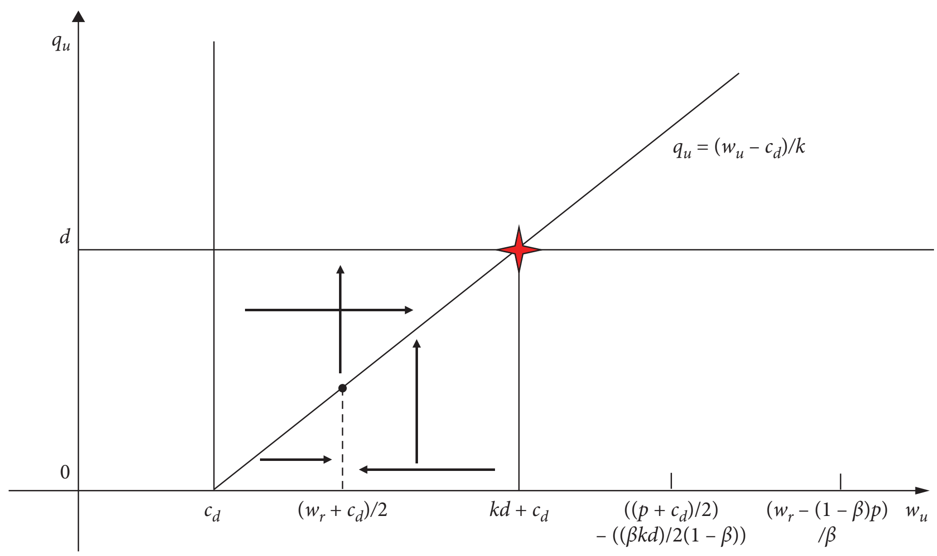

FIGURE 18: Case 16: $c_d < ((w_r + c_d)/2) < kb + c_d \leq ((p + c_d)/2) - (\beta k d/(2(1-\beta)))$ and $(w_r - (1-\beta)p)/\beta \geq kb + c_d$.

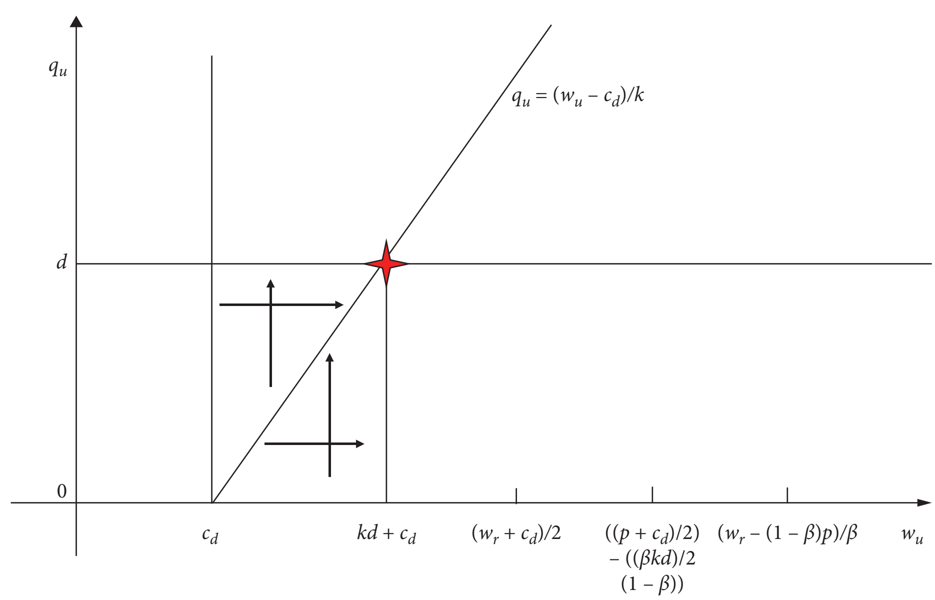

FIGURE 19: Case 17: $((w_r + c_d)/2) \geq kb + c_d$, $((p + c_d)/2) - (\beta k d/(2(1-\beta))) \geq kb + c_d$, and $((w_r - (1-\beta)p)/\beta) \geq kb + c_d$.

following values to other parameters: $d = 1, k = 1/2, p = 1, w_r = 1/2$.

5.1. Ordering Only from Unreliable Supplier. When ordering only from the unreliable supplier, the buyer has to offer a contract (q_u, w_u) to the unreliable supplier. Through equilibrium analysis, it is easy to obtain $q_u^* = d$. Here, we conduct a numerical study on w_u^* to show its property based on Proposition 2. The results are shown in Figure 20.

From Figure 20, we find that the wholesale price for the unreliable supplier (w_u^*) increases with the unit production cost after disruption (c_d) and decreases with the probability without disruption (β). The interesting observation is that, if β is high enough, w_u^* would always be equal to c_d (see Figure 20(c)); otherwise, there exists a threshold of c_d where w_u^* would be higher when β is relatively low below this threshold (see Figures 20(a) and 20(b)). This reflects the fact that when the disruption is easy to occur, the buyer would provide a more favorable contract with a higher wholesale price to encourage the unreliable supplier to exert effort on restoring capacity.

5.2. Supply Diversification Strategy. In this part, we conduct a numerical study when the buyer adopts supply diversification strategy. From equilibrium analysis, we know that the buyer would always order the quantity that equals the deterministic demand from both retailers. Thus, the order quantity from the reliable supplier q_r would be equal to $d - q_u$. Here, we concentrate on the contract (q_u, w_u) provided to the unreliable supplier. The results are shown in Figures 21 and 22.

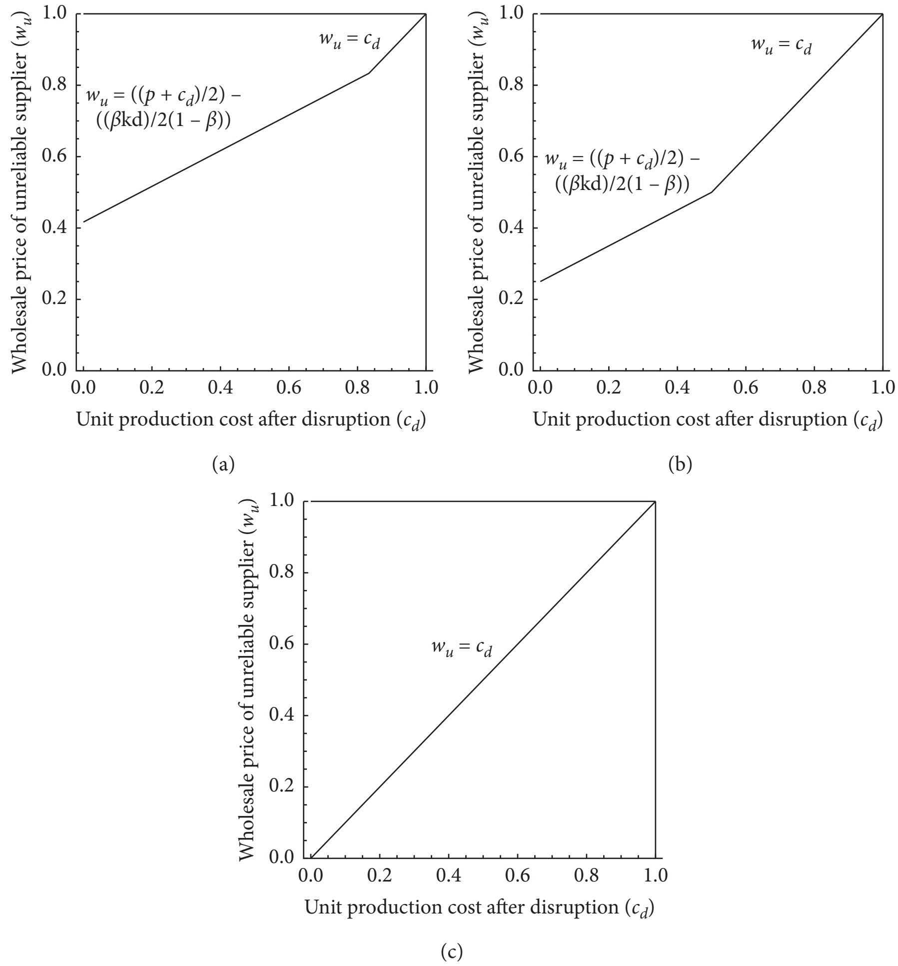

FIGURE 20: Optimal wholesale price w_u^* for unreliable supplier in the case of ordering only from the unreliable supplier.

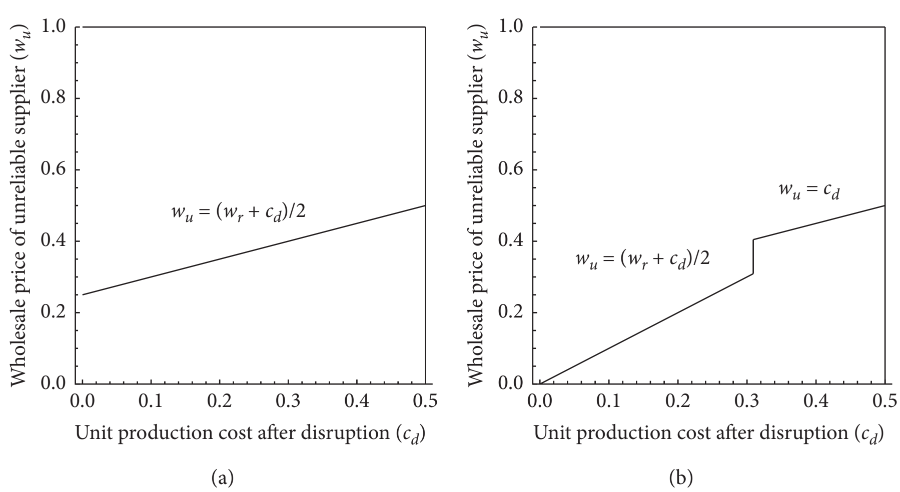

FIGURE 21: Continued.

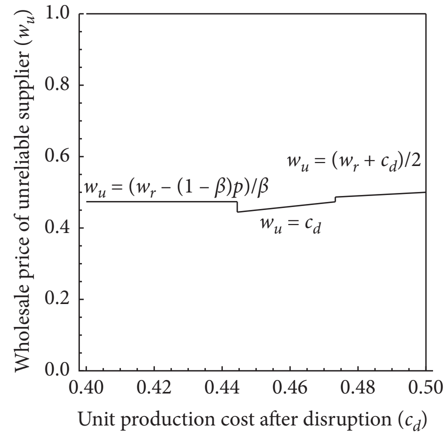

(c)

Figure 21: Optimal wholesale price w_u^* for unreliable supplier in the case of supply diversification strategy.

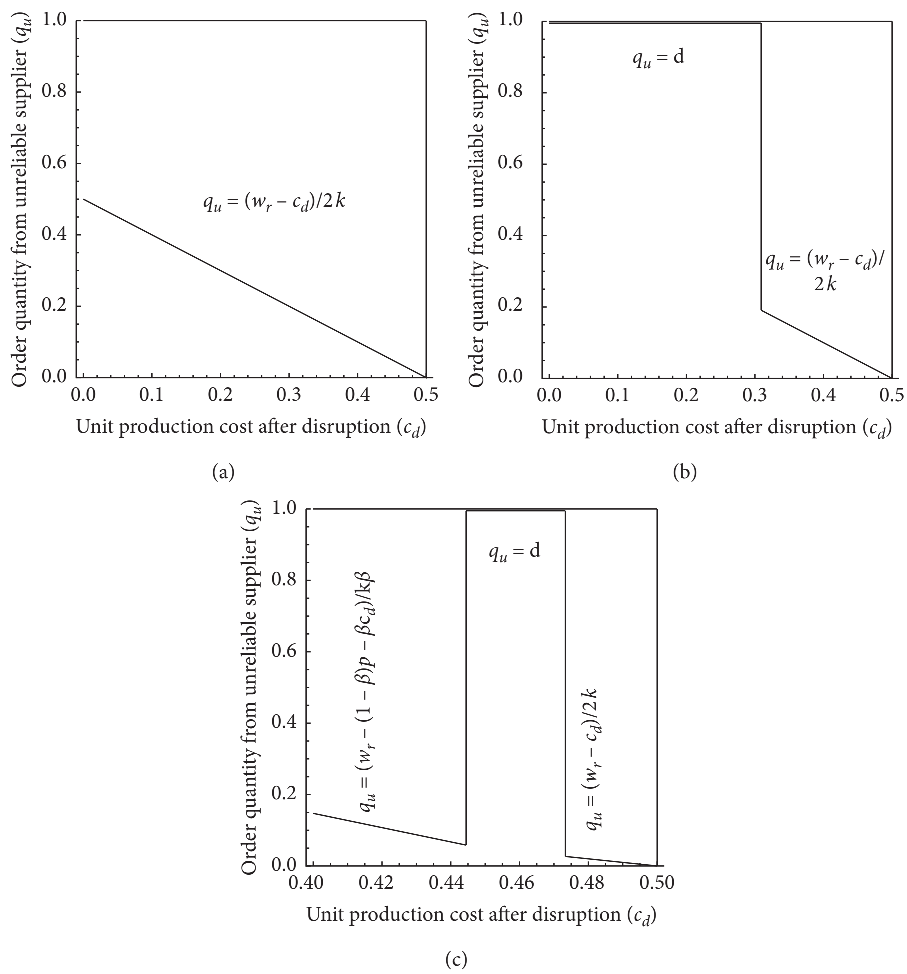

Figure 22: Optimal order quantity q_u^* for unreliable supplier in the case of supply diversification strategy.

From Figure 21, we find that the wholesale price for the unreliable supplier (w_u^*) is a nondecreasing function of the unit production cost after disruption (c_d), while the effect of the probability without disruption (β) on the wholesale price for the unreliable supplier (w_u^*) is not consistent. Specifically, if β is relatively low, w_u^* increases with c_d at a constant rate (see Figure 21(a)). If β is intermediate, there would be a sudden increase in w_u^* when c_d reaches a certain threshold, but the increase rate would be lower since then (see Figure 21(b)). If β is high enough, c_d has no effect on w_u^* when c_d is relatively low and would have a larger effect on w_u^* when c_d is intermediate than when c_d is high enough (see Figure 21(c)).

This shows that if the disruption is easy to happen, the buyer would trade off between the wholesale price from the reliable supplier (w_r) and the unit production cost after disruption (c_d) to offer a good wholesale price to the unreliable supplier, encouraging it to restore capacity when the disruption happens. However, with the increase of the unit production cost after disruption (c_d), the buyer would rely more on the reliable supplier than on the unreliable one by reducing the order quantity from the unreliable supplier (q_u^*) (see Figure 22(a)). If the probability without disruption is neither too low nor too high, the buyer would tend to encourage the unreliable supplier to guarantee supply and source all the demand from the unreliable one when c_d is below a threshold but would only offer a w_u^* that just equals c_d when c_d is very high (see Figure 22(b)). If the disruption seldom happens, sourcing from the unreliable supplier would be the best choice for the buyer especially when c_d is relatively low. Under this circumstance, the buyer would choose a wholesale price that jointly considered the retail price (p), the probability without disruption (β), and the wholesale price from the reliable supplier (w_r). However, when c_d is intermediate, the buyer would offer a contract that sources all the demand from the unreliable supplier with a wholesale price that equals the unit production cost after disruption.

6. Conclusion

Various human or environmental factors such as natural disasters and political disputes can cause production disruption, which negatively affects the buyer's procurement process and thus causes financial loss. This paper studies a noncooperative model that consists of two suppliers and one buyer. Since the buyer is a large-scale company with widespread reputation like Walmart and Apple, it chooses between the two types of suppliers: one is cheap but unreliable and the other is expensive but reliable and it offers contracts to them. Jointly considering the contract provided by the buyer and the cost of restoring capacity, the unreliable supplier may make efforts to rebuilt its capacity when a disruption occurs. The optimal procurement strategy is supply diversification strategy that is ordering from both suppliers with different proportions. This paper provides the contract offered by the buyer with optimal wholesale price and order quantity to the unreliable supplier in different scenarios. The main contributions to the literature are twofold. On the one hand, the proposed model characterizes the real situation of big retailers who have the power towards pricing when wholesale products from small suppliers and the contract offered by the buyer can affect the unreliable supplier's optimal strategy on its restoration effort when a disruption occurs. On the other hand, the results generate the optimal contract containing the wholesale price and order quantity provided by the buyer to the unreliable supplier under different circumstances, which can be used by managers to design the procurement contract facing different types of suppliers and different environment. There are some possible ways to extend this research. First, the proposed model assumes that the market demand is deterministic, which might be extended to stochastic demand. Second, the restoration cost of the unreliable supplier is assumed to be deterministic, which is proportional to the restoration effort, and it is worthwhile to define the cost as other distribution functions of the restoration effort. At last, by assuming that the wholesale price for the reliable supplier is exogenously given and the total order quantity equals the demand, the proposed model mainly designs the contract for the unreliable supplier; it might be interesting to codetermine the contracts offered to both suppliers by relaxing the above assumptions.

Data Availability

No data were used to support this study.

Conflicts of Interest

The authors declare that there are no conflicts of interest regarding the publication of this paper.

Acknowledgments

This research was supported by the Fundamental Research Funds for the Central Universities (Grant no. JBK2001067).

References

[1] Y. Zhou, J. Feng, J. Wei, and X. Sun, "Pricing decisions of a dual-channel supply chain considering supply disruption risk," *Mathematical Problems in Engineering*, vol. 2018, Article ID 6841519, 16 pages, 2017.
[2] A. Latour, "A fire in Albuquerque sparks crisis for European cell-phone giants," *The Wall Street Journal*, 2001.
[3] A. J. Vakharia and A. Yenipazarli, "Managing supply chain disruptions," *Foundations and Trends in Technology, Information and Operations Management*, vol. 2, no. 4, pp. 243–325, 2008.
[4] L. V. Snyder, Z. Atan, P. Peng, Y. Rong, A. J. Schmitt, and B. Sinsoysal, "OR/MS models for supply chain disruptions: a review," *IIE Transactions*, vol. 48, no. 2, pp. 89–109, 2016.
[5] D. Ivanov, A. Dolgui, B. Sokolov, and M. Ivanova, "Literature review on disruption recovery in the supply chain," *International Journal of Production Research*, vol. 55, no. 20, pp. 6158–6174, 2017.
[6] R. Anupindi and R. Akella, "Diversification under supply uncertainty," *Management Science*, vol. 39, no. 8, pp. 944–963, 1993.

[7] M. Dada, N. C. Petruzzi, and L. B. Schwarz, *A Nesvendor Model with Unreliable Suppliers*, University of Illinois at Urbana-Champaign, Champaign, IL, USA, 2003.

[8] H. Gurnani, R. Akella, and J. Lehoczky, "Optimal order policies in assembly systems with random demand and random supplier delivery," *IIE Transactions*, vol. 28, no. 11, pp. 865–878, 1996.

[9] S. Liu, K. C. So, and F. Zhang, "Effect of supply reliability in a retail setting with joint marketing and inventory decisions," *Manufacturing & Service Operations Management*, vol. 12, no. 1, pp. 19–32, 2010.

[10] Y. Wang, W. Gilland, and B. Tomlin, "Mitigating supply risk: Dual sourcing or process improvement?" *Manufacturing & Service Operations Management*, vol. 12, no. 3, pp. 489–510, 2010.

[11] W. Wang, K. Xue, and X. Sun, "Cost sharing in the prevention of supply chain disruption," *Mathematical Problems in Engineering*, vol. 2017, Article ID 7843465, 8 pages, 2017.

[12] B. Tomlin, "On the value of mitigation and contingency strategies for managing supply chain disruption risks," *Management Science*, vol. 52, no. 5, pp. 639–657, 2006.

[13] X. Hu, H. Gurnani, and L. Wang, "Managing risk of supply disruptions: incentives for capacity restoration," *Production and Operations Management*, vol. 22, no. 1, pp. 137–150, 2013.

[14] Z. Chen, J. Li, Z. Liu, and Z. Zheng, "Incentive contracts for capacity restoration under risk of supply disruption," *IEEE Transactions on Engineering Management*, vol. 66, no. 4, pp. 746–762, 2019.

[15] V. Gupta, B. He, and S. P. Sethi, "Contingent sourcing under supply disruption and competition," *International Journal of Production Research*, vol. 53, no. 10, pp. 3006–3027, 2015.

[16] P. Ray and M. Jenamani, "Sourcing decision under disruption risk with supply and demand uncertainty: a newsvendor approach," *Annual Operation Research*, vol. 237, no. 1-2, pp. 237–262, 2016.

[17] S. Y. Tang, H. Gurnani, and D. Gupta, "Managing disruptions in decentralized supply chains with endogenous supply process reliability," *Production and Operations Management*, vol. 23, no. 7, pp. 1198–1211, 2014.

[18] W. C. Tsai, "A dynamic sourcing strategy considering supply disruption risks," *International Journal of Production Research*, vol. 54, no. 7, pp. 2170–2184, 2016.

[19] E. Ang, D. A. Iancu, and R. Swinney, "Disruption risk and optimal sourcing in multitier supply networks," *Management Science*, vol. 63, no. 8, pp. 2397–2419, 2016.

[20] J. Li, X. Liu, J. Wu, and F. Yang, "Coordination of supply chain with a dominant retailer under demand disruptions," *Mathematical Problems in Engineering*, vol. 2014, Article ID 854681, 10 pages, 2014.

[21] T. Shu, F. Yang, S. Chen, S. Wang, K. K. Lai, and L. Gan, "Contract coordination in dual sourcing supply chain under supply disruption risk," *Mathematical Problems in Engineering*, vol. 2015, no. 10, Article ID 473212, 2015.

[22] H. Zhang, Y. Liu, and J. Huang, "Supply chain coordination contracts under double sided disruptions simultaneously," *Mathematical Problems in Engineering*, vol. 2015, Article ID 812043, 9 pages, 2015.

[23] T. Sawik, "Stochastic versus deterministic approach to coordinated supply chain scheduling," *Mathematical Problems in Engineering*, vol. 2017, Article ID 3460721, 15 pages, 2017.

[24] C. S. Tang, "Robust strategies for mitigating supply chain disruptions," *International Journal of Logistics Research and Applications*, vol. 9, no. 1, pp. 33–45, 2006.

[25] S. Chopra and M. Sodhi, "Reducing the risk of supply chain disruptions," *MIT Sloan Management Review*, vol. 55, no. 3, pp. 72–80, 2014.

[26] J. He, F. Alavifard, D. Ivanov, and H. Jahani, "A real-option approach to mitigate disruption risk in the supply chain," *Omega*, vol. 88, pp. 133–149, 2019.

[27] T. A. Roemer and R. Ahmadi, "Concurrent crashing and overlapping in product development," *Operations Research*, vol. 52, no. 4, pp. 606–622, 2004.

[28] C. J. Corbeet, D. Zhou, and C. S. Tang, "Deigning supply contracts: contract type and information asymmetry," *Management Science*, vol. 51, no. 1, pp. 30–44, 2004.

[29] P. S. Desai and K. Srinivasan, "Demand signalling under unobservable effort in franchising: linear and nonlinear price contracts," *Management Science*, vol. 41, no. 10, pp. 1608–1623, 1995.

[30] H. S. Heese and J. M. Swaminathan, "Product line design with component commonality and cost-reduction effort," *Manufacturing & Service Operations Management*, vol. 8, no. 2, pp. 206–219, 2006.

Hindawi
Mathematical Problems in Engineering
Volume 2020, Article ID 9437605, 15 pages
https://doi.org/10.1155/2020/9437605

Research Article

Impact of UAV Delivery on Sustainability and Costs under Traffic Restrictions

Yuyu Li[1] **, Wei Yang,**[2] **and Bo Huang**[3]

[1]*School of Economics and Management, Chongqing Normal University, Chongqing 400047, China*
[2]*College of Computer and Information Science, Chongqing Normal University, Chongqing 400047, China*
[3]*School of Economics and Business Administration, Chongqing University, Chongqing 400044, China*

Correspondence should be addressed to Bo Huang; huangbo@cqu.edu.cn

Received 5 January 2020; Revised 9 June 2020; Accepted 7 July 2020; Published 8 August 2020

Academic Editor: Mosè Gallo

Compared with traditional vehicles delivery, unmanned aerial vehicle (UAV) delivery can reduce energy consumption and greenhouse gas emissions, which benefits environmental sustainability. Besides, UAVs can overcome traffic restrictions, which are the big obstacle in parcel delivery. In reality, there are two kinds of most popular traffic restrictions, vehicle-type restriction, and half-side traffic. We propose a mixed-integer (0-1 linear) green routing model with these two kinds of traffic restrictions for UAVs to exploit the environmental aspects of the use of UAVs in logistics. A genetic algorithm is proposed to efficiently solve the complex routing problem, and an experimental analysis is made to illustrate and validate our model and the algorithm. We found that, under both these two traffic restrictions, UAV delivery can accomplish deliveries that cannot be carried out or are carried out at much higher costs by vehicles only and can always effectively save costs and cut CO_2 emissions, which is environmentally friendly. Furthermore, UAV delivery saves more cost and cuts more CO_2 emission under the first kind of traffic restriction than that under the second.

1. Introduction

Brick-and-mortar retail stores being gradually replaced by e-commerce saves energy consumption for heating and lighting in stores and warehouses. However, the rapid development of e-commerce dramatically increases the demands on logistics or parcel delivery, which is mainly carried out by traditional vehicles. As a result, energy consumption and CO_2 emission are increased [1].

With the development of unmanned aerial vehicles (UAVs), they become one of the best choices improving the "last-mile" delivery of products to consumers, both economically and environmentally, due to their significant performances in saving costs and energy. Unfortunately, current UAVs have two big shortcomings: both delivery range (distance and flight time) and capacity (weight and size) are limited. Therefore, they often cannot deliver all packages themselves in a single trip, and the most reasonable way to use a UAV is to pair it with a traditional vehicle. In this "UVA-vehicle mode," a UAV is loaded on the roof of the vehicle, and the driver guides the UAV to carry the package to the destination. At the same time of UAV delivery, the vehicle serves other customers. Although the UAV only serves part of customers, this mode of package delivery makes a best use of the advantages of UAVs and avoids their disadvantages. In other words, this mode normally delivers all packages in one signal trip with much lower time, cost, and energy consumption.

Besides, in many big cities, because of heavy traffic jam or severe air pollution from vehicle exhaust, vehicle-type restriction is implemented on vehicles. Delivery vehicles are forbidden to run on some roads during some periods. Besides, during the maintenance of some roads, only one lane is available, and vehicles traveling in opposite directions have to take turns on the road with a much lower speed. This is half-side traffic, which is other most popular traffic restriction. Traffic restrictions bring big troubles to package delivery service and even some "impossible missions" to delivery by vehicles only, which can be normally overcome through UAV delivery.

In order to make the most use of the advantages of this "UAV-vehicle mode" and better understand the economic and environmental impact of using UAVs on packages delivery, we should optimize the routing plan of "UVA-vehicle mode." To this end, we propose a mixed-integer (0-1 linear) green routing model with traffic restrictions for UAVs and design a genetic algorithm (GA) to effectively solve the routing plan model. Finally, we make an experimental analysis to illustrate and validate our model and algorithm, as well as better understand the environmental benefits of delivering with UAVs.

The rest of this paper is organized as follows: we review the literature on "green routing" and routing problem with UAVs in Section 2; we propose a UAV-vehicle routing model with traffic restrictions and design a genetic algorithm to effectively solve the model in Sections 3 and 4, respectively; an experimental analysis is made in Section 5; and conclusions are drawn in Section 6.

2. Literature Review

Since the emergence of "truck dispatching problem," vehicle routing problem (VRP) has been a hot research field [2]. And many heuristic algorithms were developed to solve VRP [3]. Our paper is mainly relevant to two topics: green vehicle routing problem and routing with UAVs, which are reviewed below.

2.1. Green Vehicle Routing Problem. A series of studies show that, for the logistics, transportation accounts for about 90% of the energy consumption of the whole logistics. Therefore, reducing CO_2 emissions is the core of the green vehicle routing problem (GVRP). As early as 1985, Cermak and Takeda [4] outlined criteria for simulating atmospheric boundary layer and physical simulation of source characteristics in boundary layer wind tunnels and studied the air problem in urban environment. Their work led subsequent scholars to study logistics and carbon emissions.

Pradenas et al. [5] studied the vehicle path problem for the energy required for each path from the perspective of vehicle distance and estimated the load and distance between customers to achieve the goal of reducing fuel consumption and carbon emission. Qian [6] developed routing and scheduling model for fleets of transport vehicles to minimize fuel emissions in the speed-dependent road network from the perspective of vehicle speed. In this paper, the route of each vehicle needs to be clarified, the speed of vehicles on different roads on their respective paths is regarded as a decision variable, and the time insertion algorithm is given for a single path. Finally, a tabu search algorithm based on column generation is proposed to solve this problem. Kwon et al. [7] built a vehicle path model that minimizes energy consumption and pollution emissions with time windows from the perspective of vehicle load. Their simulation process is based on the actual route of motor vehicles, and their method can save more than 6.9% of fuel compared with the existing method. Although these papers only studied GVRP without UAVs, we can refer to their methods of calculating delivery cost and fuel consumption in establishing our model.

2.2. Routing with UAVs. The "last kilometer problem" is always the bottleneck of logistics distribution due to traffic conditions, distribution personnel, customer acceptance location, and other factors. In recent years, UAVs were introduced into logistics to reduce costs and solve the "last kilometer problem."

In 2013, Jeff Bezos, CEO and founder of Amazon.com, announced on "60 minutes" that UAVs could be used to speed up the delivery of packages to consumers. Subsequently, routing with UAVs became a hot topic in VRP field [8]. D'Andrea [9] calculated the energy consumption and the cost of high-end lithium ion batteries in the high-performance mobile delivery of UAVs based on the principle of first computability and systematically analyzed the economy of UAV technology and future applications. Zhi [10] designed a two-stage hitch-matching algorithm to serve the UAV driving equipment, which greatly reduced the logistics cost and improved the efficiency. Weng [11] made a systematic evaluation of UAV logistics from the aspects of laws and regulations, technical safety, audience preference, operation safety, and use cost. Ma et al. [12] established a model of UAV flight stability index and various factors and analyzed and studied the main factors influencing the flight stability of UAVs through Matlab.

The feature of our "UVA-vehicle mode" is that UAV departures from the roof of the vehicle to deliver package; meanwhile, the vehicle serves other customers, which improves logistics efficiency and reduces energy consumption. Chiang et al. [2] proposed a UAV-vehicle model and a GA to study the economic and environmental impact of using UAVs on package delivery. Murray and Chu [13] conducted relevant research, proposing two mixed-integer linear programming formulas for unmanned delivery problems, as well as two simple but effective heuristic solutions to satisfy the scheduling of UAVs and delivery trucks. Ha et al. [14] considered a new variant of TSP-D in which the objective is to minimize operational costs including total transportation cost and one created by waste time a vehicle has to wait for the other. They formulated problem and proposed two algorithms, TSP-LS and GRASP, to solve the problem. Wang et al. [15] pose a number of questions in order to study the maximum savings that can be obtained from using drones and derived a number of worst-case results. Poikonen et al. [16] studied the UAV-vehicle delivery routing with the aim of minimizing the total operation time. Pugliese and Guerriero [17] analyzed the delivery process with drones, by taking into account the total transportation cost, under the assumption that all customers should be served within their time window.

Although the above papers studied UAV-vehicle routing problems under different circumstances, they failed to research the use of UAVs and its effect on relieving one of the greatest constraints in parcel delivery and traffic restrictions [18]. In fact, there are two kinds of traffic restrictions, which allow the implementation of our UAV-vehicle mode but greatly affect the cost, energy consumption, and efficiency of parcel delivery. The first is vehicle-type restriction, mainly on delivery vehicles. For example, during the maintenance, all vehicles except public transportation were banned to run across Shimen Bridge, located in Chongqing, China. Under this circumstance, the delivery vehicle has to choose other way or use a UAV. The second is half-side traffic, under which the delivery vehicle can choose this road but may have to wait to pass through it. During its waiting, the engine is still operating and consuming gasoline, causing a higher cost and CO_2 emission [19].

2.3. Algorithms for VRP. To solve VRP, we should design an algorithm. Generally, there are two categories of algorithms: exact algorithm and approximation algorithm [20]. The advantage of exact algorithm is that it can find the accurately optimal solution of VRP, but it is only suitable for VRP of small scale [21]. When the scale is large, it is mainly applied to obtain the initial solution for the approximation algorithm [22].

Approximation algorithm can be roughly divided into two categories: heuristic algorithm, which consists of constructive heuristic algorithm and improved heuristic algorithm, as well as meta-heuristic algorithm [23]. The advantage of constructive heuristic algorithm is that it is simple and easy to understand, but the solutions found may be far from the optimal solutions. Therefore, it is no longer used for solving VRP alone but combined with the improved heuristic algorithm, being used to generate initial solutions [24]. Improved heuristic algorithm can obtain better solutions from initial solutions generated by constructive heuristic algorithm through neighborhood search. Its advantage is that the probability of obtaining the optimal solution is high, but the operation time may be very long [25].

The biggest disadvantage of heuristic algorithm is that it is easy to fall into local optimal. In order to overcome it, there appeared a variety of meta-heuristic algorithms with the advantage of jumping out of the local optimal and seek the global optimal, such as genetic algorithm, simulated annealing algorithm, and tabu search algorithm [26, 27]. Among meta-heuristic algorithms, the genetic algorithm is popularly applied for solving VRP, including VRP with UAVs [28, 29]. However, the mode of UAV delivery in these studies is that the truck is just used as a mobile base, which is very different with ours. Therefore, these genetic algorithms cannot solve the key issue in our mode, that is, which customer is served by the UAV and how many and which customers should be served by the vehicle.

The main contributions of this paper are as follows. Firstly, taking into account two kinds of traffic restrictions which affect parcel delivery, we propose a mixed-integer (0-1 linear) UAV-vehicle routing model with traffic restrictions to incorporate environment aspects to study the impacts of using UAVs for package delivery under these two circumstances and analyze the efficiency of UAV delivery to reduce cost and energy consumption by comparing the results under these two circumstances and that without UAVs. Secondly, we develop a genetic algorithm to effectively solve the model and analyze the impact of UAV delivery. In our GA, we make improvement and contribution in the generation of initial solution and grouping customers to determine which customer is served by the UVA and which customer(s) should be served by the vehicle during UAV delivery.

3. Problem Description and the Model

3.1. Problem Description. In an urban area, a delivery company uses vehicles equipped with UAVs to deliver parcels from a warehouse to customers in its delivery area. Each customer has only one parcel waiting to be delivered. This UVA-vehicle mode is as follows. Every vehicle is equipped with a UAV. As both delivery range (distance and flight time) and capacity (weight and size) of the UAV are limited, it only delivers parts of the parcels, but the vehicle can deliver all the parcels. Each UAV may depart from its vehicle at a location of a customer or the warehouse and carry a parcel to one and only one customer. Then, the UAV returns to its vehicle to reload a parcel and recharge or swap batteries, which is instantaneous. While the UAV delivers the parcel, the vehicle carries out its delivery to one or several customers. Therefore, the UAV returns to its vehicle at a different customer location. As a matter of course, if the vehicle arrives at the customer location, where the UAV is retrieved, it waits for the UAV, and vice versa. For the sake of the safety of the UAV, if the UAV arrives before the vehicle, it hovers in the air waiting for the vehicle.

In the delivery area of the warehouse, there may be traffic restrictions on the vehicles. Generally, there are two kinds of traffic restrictions, under which this UAV-vehicle mode is practicable but greatly affected. The first is vehicle-type restriction, under which delivery vehicles are forbidden to run through some paths and have to choose other way or use a UAV. The second is half-side traffic, under which only one lane of a road is available, and vehicles traveling in opposite directions can only take turns on this road. Under this circumstance, the delivery vehicle can run on this road but may have to wait for its turn with the operating engine and raise the variable cost and CO_2 emission.

According to the regulation on working hours, the service time of every pair of UAV and vehicle is 8 hours. Therefore, it is probable that more than one pair of UAV and vehicle are needed.

There are two goals of routing the UAV-vehicle. The first is minimizing the total cost, and the alternative is minimizing the energy consumption (or CO_2 emission). The total cost consists of fixed cost whenever a pair of UAV-vehicle is used, as well as variable cost, which is the function of unit route cost, travel distance, and gross weight (empty weight of the vehicle or UAV plus the payload). The total CO_2 emission of a vehicle is the function of weighted average emission rate of vehicles, travel distance, and gross weight, and that of a UAV is the function of CO_2 emission rate of generating per watt-hour, average energy requirement of UAV, travel distance, and gross weight.

It should be noted that the two kinds of traffic restrictions may simultaneously exist, but as we analyze the impact of UAV delivery under every kind of traffic restriction, they are in our models separately.

3.2. The Model. According to Laporte [30], there are three ways to formulate the vehicle routing problem (VRP), including the simple set division formula of VRP first proposed by Balinski and Quandt in 1964, the commodity flow formula of Shlifer and Graves in 1979, and the two-index vehicle flow formula of Laporte and Norbert in 1983. In our study, the GVRP problem is mainly involved, and the weight of vehicles, commodities, and drones in the whole route needs to be considered. Therefore, we choose to continue to expand the commodity flow formula, which is clearly expressed and promotes the development of heuristic algorithm.

The basic GVRP problem is as follows: both the UAV and the vehicle can travel back and forth on any available path. Therefore, an undirected graph $R = (M, N)$ is given, where N is the set of edges with nonnegative routing costs, $\{i, j\} \in N$ represents the edges from node i to node j. $M = \{0, 1, \ldots, n\}$ is the set of all nodes with a total of n customers, and the warehouse is labeled as 0. Therefore, $U = M\backslash\{0\}$ is the set of customer nodes. The distance between each node is L_{ij}. Every customer has a demand for P_i units; for calculating energy consumption, we measure demand in units of weight.

In our UAV-vehicle mode, each vehicle with a payload (weight) capacity of Q^V is equipped with a UAV. Each pair of a vehicle and a UAV has a fixed cost C^F, as well as a variable route cost, which is a function of range and gross weight (see next paragraph). The unit route cost C^U of the UAV is expected to be much lower than that of the vehicle C^V. However, the payload (capacity) Q^U of the UAV and the distance L^U and the time T^U that the UAV can fly in the air are limited. Note that the time limit may include the time the UAV has to wait for the vehicle before landing. The distance between the vehicle and the UAV may be different; in fact, another potential advantage of UAVs is that they may choose more efficient routes than vehicles. For example, vehicles need to follow the Manhattan metric, while UAVs can use Euclidean distances. Therefore, we distinguish between the distance from i to j by the vehicle, L_{ij}^V, and that by the UAV, L_{ij}^U. It is assumed that the UAV will serve only one customer before returning to the vehicle but can serve other customers after returning the vehicle to reload and replace batteries.

If the vehicle starts from the node i to the node j, $\{i, j\} \in N$, let N_{ij} be 1; otherwise, let it be 0. Let M_{ij} be the vehicle payload weight for edge $\{i, j\} \in N$. Obviously, $M_{ij} = 0$, if the vehicle does not run from the node i to the node j. Finally, if the UAV leaves the vehicle at node i, serves the q_j unit required by customer j, and returns to node k and lands on the roof of the vehicle, then $Z_{ijk} = 1$ and the flight time is T_{ijk}; otherwise, $Z_{ijk} = 0$.

In the delivery area of the warehouse, there separately exist two kinds of traffic restrictions on the vehicles. Under the vehicle-type restriction (labeled as "circumstance 1"), there are some edges where vehicles are forbidden to drive. Let $\overline{N}_1$ be the set of these edges, then, for any $\{i, j\} \in \overline{N}_1$, $N_{ij} = 0$. Under half-side traffic (labeled as "circumstance 2"), the average speed, variable cost, and CO_2 emission of the vehicle on these edges are raised by R^S, R^C, and R^E times, respectively. Let $\overline{N}_2$ be the set of these edges, then $R_{ij}^S = R_{ij}^C = R_{ij}^E = 1$ for any $\{i, j\} \notin \overline{N}_2$ and $R_{ij}^S < 1$, $R_{ij}^C > 1$, and $R_{ij}^E > 1$ for any $\{i, j\} \in \overline{N}_2$.

Franzese and Davidson [31] pointed out that the increase in total vehicle weight has a certain impact on its fuel efficiency, and fuel is an important component of variable transportation costs, so they added relevant factor of fuel to GVRP. Bateman et al. [32] pointed out that the carbon footprint of transportation emissions can be estimated by transportation weight and distance traveled.

On the route from node i to j, the total vehicle weight is W_{ij}, including the empty weight of the vehicle W^V, plus the payload weigh M_{ij}, and the UAV weight W^U if the UAV is on the vehicle. The weight can be expressed as a nonlinear function:

$$W_{ij} = W^V N_{ij} + M_{ij} + W^U N_{ij}\left(1 - \sum_{h\in U} Z_{ihj}\right). \quad (1a)$$

The first term on the right hand of (1) is the vehicle empty weight when running from i to j, the second is the weight of packages on the vehicle from i to j, and the third is the weight of the UAV if it is on the vehicle from i to j. Another linear formula is

$$W_{ij} \geq W^V N_{ij} + M_{ij} + W^U\left(N_{ij} - \sum_{h\in U} Z_{ihj}\right). \quad (1b)$$

Although (1b) may generate negative values for edges that do not exist in the solution, these values will be 0 because of (21). To calculate the vehicle route cost, we use the unit cost, C^V, time distance, L_{ij}^V, and time total vehicle weight, W_{ij} (note that C^V is calculated in dollars per pound-mile and can determined by regression analysis).

On the route of the UAV flying from i to j to k, the total weights of the UAV are different. On the route of the UAV flying from i to j, the total weight of the UAV is

$$W_{ij}^U = \left(W^U + q_j\right)Z_{ijk}. \quad (2a)$$

On the route of the UAV flying from j to k, the total weight of the UAV is

$$W_{jk}^U = W^U Z_{ijk}. \quad (2b)$$

To calculate the vehicle route cost, we use the unit cost, C^U, time distance, ${L_{ij}}^U$ and ${L_{jk}}^U$, and total UAV weight, W_{ij}^U and W_{jk}^U.

There are two ways to analyze the impact of UAV delivery. The first is the benefit on total CO_2 emission. The total CO_2 emission of a vehicle can be calculated by the ways of Goodchild and Toy [33] as follows:

$$E_1^V = \text{WAER} \sum_{i \in M} \sum_{j \in M} L_{ij}^V \times W_{ij}, \tag{3a}$$

$$E_2^V = \text{WAER} \sum_{i \in M} \sum_{j \in M} R_{ij}^E \times L_{ij}^V \times W_{ij}, \tag{3b}$$

where WAER is the weighted average emission rate of vehicles. (3a) is the formulation of a vehicle's total CO_2 emission under circumstance 1, and (3b) is that under circumstance 2. Obviously, in (3a), $W_{ij} = 0$ for any $\{i, j\} \in \overline{N}_1$.

The total CO_2 emission of UAV is calculated as

$$E^U = \text{PGFER} \times \text{AER} \sum_{i \in M} \sum_{j \in M} \sum_{k \in M} \left(L_{ij}^U W_{ij}^U + L_{jk}^U W_{jk}^U \right), \tag{4}$$

where PGFER is the CO_2 emission rate per watt-hour (Wh) of the power generation facilities in the generation of electricity for using the UAV and AER is the average energy requirement of UAV in Wh per pound-mile.

Therefore, the environmental goals of minimizing total CO_2 emission under circumstances 1 and 2 are, respectively,

$$\text{minimize} \left(E_1^V + E^U \right), \tag{5a}$$

$$\text{minimize} \left(E_2^V + E^U \right). \tag{5b}$$

The alternative way is examining its impact on the traditional objective of minimizing total cost, TC, under circumstances 1 and 2, including the fixed cost of the pair of a UAV and a vehicle and the variable route cost of the vehicle and the UAV:

$$\text{TC}_1 = C^F \sum_{j \in U} N_{0,j} + C^V \sum_{i \in M} \sum_{j \in M} L_{ij}^V \times W_{ij} + C^U \sum_{i \in M} \sum_{j \in U} \sum_{k \in M} \left(L_{ij}^U W_{ij}^U + L_{jk}^U W_{jk}^U \right), \tag{6a}$$

$$\text{TC}_2 = C^F \sum_{j \in U} N_{0,j} + C^V \sum_{i \in M} \sum_{j \in M} R_{ij}^C \times L_{ij}^V \times W_{ij} + C^U \sum_{i \in M} \sum_{j \in U} \sum_{k \in M} \left(L_{ij}^U W_{ij}^U + L_{jk}^U W_{jk}^U \right). \tag{6b}$$

Therefore, the traditional goals of minimizing total cost under circumstances 1 and 2 are, respectively, as follows:

$$\text{minimize TC}_1, \tag{7a}$$

$$\text{minimize TC}_2 \tag{7b}$$

Let V_{ij}^V and V_{ij}^U, respectively, be the average speed of the vehicle and the UAV from node i to node j (mile/hour). The constraint set of the two goals can be expressed as follows. It should be noted that the same set of constraints are applied to the above two objectives and is solved twice:

$$\sum_{j \in M} N_{ij} + \sum_{h \in M} \sum_{k \in M} Z_{hik} = 1, \quad \forall j \in U, \tag{8}$$

$$\sum_{i \in M} N_{ij} + \sum_{h \in M} \sum_{k \in M} Z_{hjk} = 1, \quad \forall j \in U, \tag{9}$$

$$\sum_{j \in U} N_{0j} = \sum_{i \in U} N_{i0}, \tag{10}$$

$$\sum_{\substack{j \in M \\ j \neq i}} M_{ji} - \sum_{\substack{j \in M \\ j \neq i}} M_{ij} + \sum_{h \in M} \sum_{k \in M} q_i Z_{hij} - \sum_{j \in M} \sum_{k \in M} q_j Z_{ijk} = q_i, \quad \forall i \in U, \tag{11}$$

$$N_{ik} \geq \sum_{j \in M} Z_{ijk}, \quad \forall i, k \in M, \tag{12}$$

$$\sum_{j \in M} q_j + W^U \leq Q^V, \tag{13}$$

$$q_j \sum_{i \in M} \sum_{k \in M} Z_{ijk} \leq Q^U, \quad \forall j \in U, \tag{14}$$

$$\left(L_{ij}^U + L_{jk}^U \right) Z_{hik} \leq L^U, \quad \forall i, j, k \in M, \tag{15}$$

$$T_{ijk} \geq \left(\frac{L_{ij}^U}{V_{ij}^U} + \frac{L_{jk}^U}{V_{jk}^U}\right) Z_{hjk}, \quad \forall i, k \in M, \forall j \in U, \tag{16a}$$

$$T_{ijk} \geq \frac{L_{ik}^V}{V_{ik}^V} N_{ik}, \quad \forall i, k \in M, \forall j \in U, \tag{16b}$$

$$T_{ijk} \geq \frac{L_{ik}^V}{R_{ik}^S V_{ik}^V} N_{ik}, \quad \forall i, k \in M, \forall j \in U, \tag{16c}$$

$$T_{ijk} \leq T^U + G\left(1 - Z_{hjk}\right), \quad \forall i, k \in M, \forall j \in U, \tag{16d}$$

$$W_{ij} \geq W^V N_{ij} + M_{ij} + W^U \left(N_{ij} - \sum_{h \in U} Z_{ihj}\right), \quad \forall \{i, j\} \in N, \tag{17}$$

$$M_{ij} \geq q_j N_{ij}, \quad \forall \{i, j\} \in N, \tag{18}$$

$$N_{ij} = 0, \quad \forall \{i, j\} \in \overline{N}_1, \tag{19a}$$

$$R_{ij}^S = R_{ij}^C = R_{ij}^E = 1, \quad \forall \{i, j\} \notin \overline{N}_2, \tag{19b}$$

$$\begin{aligned} R_{ij}^S &< 1, \\ R_{ij}^C &> 1, \\ R_{ij}^E &> 1, \\ \forall \{i, j\} &\in \overline{N}_2, \end{aligned} \tag{19c}$$

$$\sum_{i \in M} \sum_{k \in M} \left[\frac{L_{ik}^V}{V_{ik}^V} N_{ik} + \sum_{j \in U} y_{ijk} \left(T_{ijk} - \frac{L_{ik}^V}{V_{ik}^V} N_{ik}\right)\right] \leq T^w, \tag{20a}$$

$$\sum_{i \in M} \sum_{k \in M} \left[\frac{L_{ik}^V}{R_{ik}^S V_{ik}^V} N_{ik} + \sum_{j \in U} y_{ijk} \left(T_{ijk} - \frac{L_{ik}^V}{R_{ik}^S V_{ik}^V} N_{ik}\right)\right] \leq T^w, \tag{20b}$$

$$T_{ijk} \geq 0, \quad \forall i, k \in M, \forall j \in U, \tag{21}$$

$$W_{ij} \geq 0, \quad \forall \{i, j\} \in N, \tag{22}$$

$$\begin{aligned} N_{ij} &= \{0, 1\}, \\ N_{00} &= 0, \\ \forall \{i, j\} &\in N, \end{aligned} \tag{23}$$

$$Z_{ijk} \in \{0, 1\}, \quad \forall i, j, k \in M. \tag{24}$$

Constraints (8) and (9) ensure that each customer is served by a vehicle or a UAV. Constraint (10) ensures that the numbers of vehicles leaving and entering the warehouse are the same. Constraint (11) ensures that each customer's demand is met. Constraint (12) synchronizes vehicle and UAV so that the vehicle picks up the UAV at node k. We will relax the restrictions (12) in Section 4 to allow vehicles to make multiple stops before receiving the UAV. Constraints (13) and (14) are constraints on vehicle and UAV payloads, respectively. The distance range limit and the time range limit of UAV are, respectively, guaranteed by constraints (15) and (16d), where is a very large value. The flight time of UAV, T_{ijk}, is the larger one in the travel time of UAV (16a) and vehicle under circumstance 1 (16b) or vehicle under circumstance 2 (16c). The constraint (17) determines the vehicle weight described in the preceding paragraph. Note that a simple lower bound (constraint (18)) can be included on the load of the vehicle at any time. Constraint (19a) ensures vehicles are forbidden to run on the edges of traffic restriction under circumstance 1, and constraints (19b) and (19c) ensure that the average speed, variable cost, and CO_2 emission of the vehicle on the edges of traffic restriction under circumstance 2 are changed. (20a) and (20b) are the constraints of working hours under circumstances 1 and 2, respectively, where T^w is the upper limit of working hours, normally 8 hours. $\sum_{j\in U} y_{ijk}(T_{ijk} - (L^V_{ik}/V^V_{ik})N_{ik})$ is the time length of the vehicle waiting for its UAV, where $y_{ijk} = 1$ if $T_{ijk} > (L^V_{ik}/V^V_{ik})N_{ik}$; otherwise, $y_{ijk} = 0$. Finally, we can avoid the use of UAVs for specific routes (perhaps near airports) or for specific customers (who cannot receive such deliveries) by setting $Z_{ijk} = Z_{hij} = 0$ for route $\{i, j\}$ or $Z_{ijk} = 0$ for customer j.

4. Solution Methodology

The application of our genetic algorithm in our routing problem with UAV is described below.

4.1. Design. In the design of our genetic algorithm, we adapt the following service strategy. The work should be completed within one day; that is, all parcels should be delivered within legal working hours, normally 8 hours. Meanwhile, fuel consumption should be minimized, or CO_2 emission should be minimized. Firstly, we can run our algorithm, where only a pair of a UAV and a vehicle is used, to calculate the total working hours. Then, the number of needed vehicles is determined by dividing the total working hours by the legal working hours. After that, the region is divided according to the number of vehicles by a line (or lines) crossing the warehouse, where the number of customers served by each vehicle and the service time of each vehicle are as close to each other as possible.

In our algorithm, we first sequence the customers (please see the methods in 4.1.2). The pair of a vehicle and a UAV serves customers according to the sequence. Then, we group customers randomly as follows. Generate a random positive integer $x \in [1, n]$, where n is the number of total customers served by a pair of a UAV and a vehicle. And the first x customers are put into the first group. Repeat it till all customers are grouped. As a matter of course, if there are more than one edge where vehicles are forbidden, and they are divided into different groups. If there is only one customer in the group, the vehicle serves the customer. Otherwise, the UAV serves a customer randomly selected from the group, except the last one, where the UAV is retrieved, and the vehicle serves the others. If there is an edge connecting two customers in the group, where vehicles are forbidden, we randomly select one from these two customers for the UAV to serve. Based on this strategy, we developed a genetic algorithm to solve the proposed minimization problem (fuel consumption and CO_2 emissions or total cost).

4.1.1. Encoding. We use natural number coding method to encode customers, warehouse, and group information. That is, we use positive integers from 1 to n to encode customers and encode the warehouse as 0. And we randomly generated positive integer(s) to encode the number of customers in a service group.

4.1.2. Initial Population Generation. In our GA, the initial population is artificially optimized to reduce iteration times and improve optimization efficiency. Specifically, we equally divide the service area into subareas of an even number. Then, we arrange the service sequence of the initial individuals as follows. The pair of a vehicle and a UAV serves customers in one of the nearest subareas from the nearest customer to the farthest customer and goes to an adjacent subarea to serve customers from the farthest to the nearest. Repeat it until all customers are served, and both the UAV and the vehicle come back into the warehouse. After that, we group the customers and obtain the initial population generation.

The following is an example to illustrate the service strategy, grouping, encoding, and initial population generation of our algorithm. There are 20 customers who should be satisfied. We encode them as {1, 2, 3, 4, 5, 6, 7, 8, 9, 10, 11, 12, 13, 14, 15, 16, 17, 18, 19, 20} and the warehouse as 0. As only 1 pair of a UAV and a vehicle is needed, they serve the whole delivery area. Then, we divide the whole delivery area into eight subareas and arrange the service sequence of the initial individuals as follows. The pair of a UAV and a vehicle serves customers in the first subarea from left to right and goes up to the second subarea to serve customers from right to left. Then, they go left to the third subarea to serve customers from right to left and go down to the fourth subarea to serve customers from left to right. After that, they go down to the fifth subarea to serve customers from right to left and go down to the sixth subarea to serve customers from left to right. Finally, they go right to the seventh subarea to serve customers from left to right and go up to the eighth to serve customers from right to left and go back to the warehouse. Now, we obtain the service sequence codes as {18,1,3,7,9,19,6,12,16,8,14,2,13,15,20,11,17,4,5,10} (Figure 1).

Then, we randomly generate the group codes as {2,5,3,4,5,1}. So, the customers are divided into 6 groups with encoding result {{18,1}, {3,7,9,19,6}, {12,16,8}, {14,2,13,15}, {20,11,17,4,5}, {10}}. As there are two customers, 18 and 1, in the first group, the UAV departs from the vehicle at the location of the warehouse to deliver parcel to customer 18 and fly to customer 1. Meanwhile, the vehicle goes to serve customer 1 and retrieve the UAV there. There are 5 customers, 3, 7, 9, 19, and 6, in the second group. As customer 6 is the last one, we randomly choose 7 from 3, 7, 9, and 19 to be the customer served by the UAV. So, the UAV departs from customer 13 to serve 7 and fly to 6, while the UAV sequentially serves customers 3, 9, 19, and 6 and retrieves the UAV at 6. There are 3 customers in the third group. We randomly choose the first customer, 12, to be served by the UAV. As a result, the UAVs fly from 6 to 12 and to 8, while the vehicle runs from 6 to 16 and to 8 and picks up the UAV here. For the fourth group, the UAV serves customer 14, and the vehicle sequentially serves 2, 13,

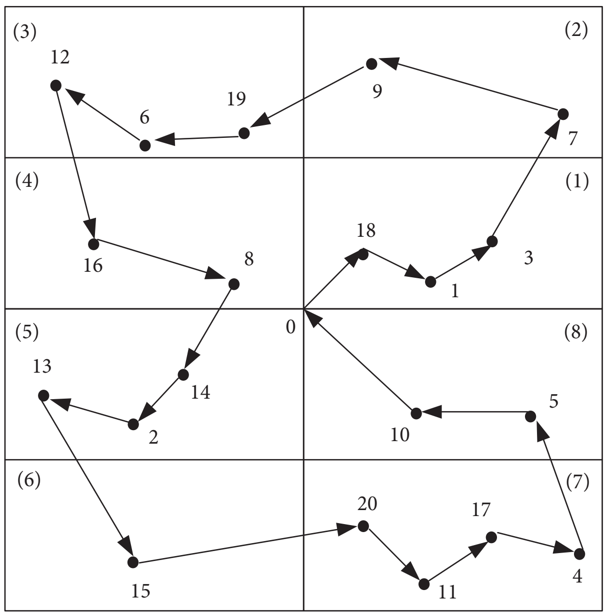

Figure 1: An example of partitioning service area and sequencing customers.

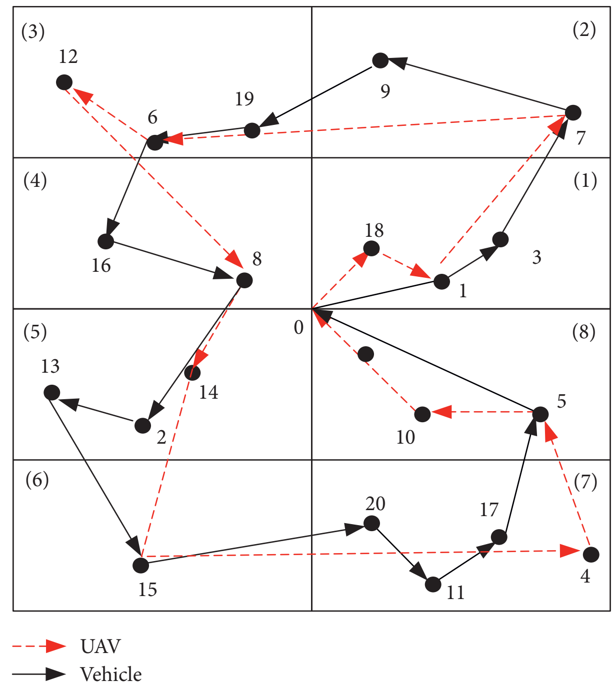

Figure 2: An example of an initial population generation.

and 15 and retrieves the UAV here. For the fifth group, the UAV serves 4, and the vehicle serves 20, 11, 17, and 5 and retrieves the UAV here. It should be noticed that although there is only customer 10 in the last group, the UAV should depart from customer 5 to serve customer 10 and fly back to the warehouse, and the vehicle should directly run from customer 10 back to the warehouse. The initial population generation is shown in Figure 2.

4.1.3. *The Algorithms*

(1) Fitness Function. In Section 3, we explained the design of the model in detail, in which the objective function mentioned mainly includes the load of the vehicle and the UAV, the distance between customers and the corresponding energy consumption function and cost function. Accordingly, the fitness function can be defined as $\text{fitness}(X) = (1/T(X))$, where X is the combination of service sequence and grouping and $T(X)$ is the target function.

(2) Selection, Crossover, and Variation. In the process of optimal individual selection, the greater the fitness of an individual, the greater the probability of being selected as the parent of the next generation, and the method is similar to roulette. As long as the fitness of an individual is large enough, the same individual in the genetic algorithm can exist in different generations. In the specific selection, select the elite individual retention strategy and copy the individuals with the highest fitness to the alternative parent group of cross-matching, then cross match all the individuals in the parent group, select the individuals with the highest fitness, and repeat this process, so as to gradually eliminate the individuals with poor fitness, leaving the elite individuals. At the same time, the method of double point crossing and real-value variation is adopted.

(3) Termination Conditions. After several iterations, when the output iteration results meet the following conditions, the convergence value is reached and the algorithm is terminated:

(1) There was no significant change in the fitness value after continuous iteration; in other words, the change is less than 1‰ of the fitness value

(2) The population no longer evolves and the number of iterations reaches the set value

4.2. *Algorithm Steps.*

In this paper, the algorithm steps are as follows:

(1) Determine the coding mechanism, generate the initial population, and set the probability of cross variation and the maximum number of iterations.

(2) Evaluate the fitness of the current population and find the chromosome with the minimum objective function value and corresponding function value.

(3) Determine whether the termination conditions are met. Output the optimal chromosome and corresponding solutions if satisfied; otherwise, select the current population again.

(4) Repeated crossover and mutation in the newly obtained generation.

(5) Evaluate the fitness of the results and move to (3).

5. Experimentation

In this section, we use the software Matlab R2017a to carry out the experiment and test our model and GA. The computer was used in the experiment is ASUS Rock 5

Generation, whose configuration is Inter(R) Core(TM) i7-8550u processor (1.8 GHz base, 1.99 GHz Max Turbo), 128 GB SSD, 8 GB RAM.

5.1. Data Parameters. The range of customer demand, q_j, is 1~10 pounds, among which 80% is no more than 5 pounds, and the position of each customer (x, y) coordinate values x and y randomly evenly generated in the interval [−10, +10]. The distance of the vehicle from customer i to j is L_{ij}^V, following the Manhattan metric; the distance of the UAV from customer i to j is L_{ij}^U, following the Euclidean metric; in addition, the warehouse is located at the center of the region (0,0).

Referring to Chiang et al. [2], we set the other parameters as follows.

The empty weight of the UAV, W^U, is 55 pounds; the payload of the UAV, M^U, is 5 pounds; the maximum flight distance of the UAV, L^U, is 10 miles; and the average flight speed of the UAV from customer i to j, V_{ij}^U, is 25 miles per hour. For roads with the second kind of traffic restriction, $R_{ij}^C = R_{ij}^E = 1.2$ and $R_{ij}^S = 0.8333$.

The empty weight of the vehicle (truck), W^V, is 6100 pounds, its payload, M^V, is 6000 pounds, and the average speed of the vehicle from customer i to j, V_{ij}^V, is 25 miles per hour.

The fixed cost of a pair of a vehicle and a UAV, C^F, is \$500, the unit route cost of a vehicle, C^V, is \$0.00016/pound-mile, and the unit route cost of a UAV, C^U, is \$0.00036364/pound-mile.

Referring to Goodchild and Toy [33], the weighted average emission of vehicles, WAER, is 1.2603 Kg/pound-mile, the CO_2 emission from the power generation facilities in the generation of electricity, PGFER, is 3.773×10^{-4} Kg/Wh, and the average energy requirement of UAV, AER, is 3.3333 Wh/pound-mile.

5.2. The Examples. Firstly, we present an example of 20 customers under the two separate kinds of traffic restrictions, in order to analyze the efficiency of UAV delivery overcoming traffic restrictions. When there are 20 customers, only one vehicle or a pair of a vehicle and a UAV is needed. Figure 3(a) shows the routing of a vehicle under no traffic restriction, and Figures 3(b)–3(d) separately show the routings of a vehicle and a pair of a vehicle and a UAV under two kinds of traffic restrictions. From Figure 3(d), we can find that the routings under two kinds of traffic restrictions are the same.

The results of costs and emissions under different circumstances are as follows. When a vehicle is under no traffic restriction, the CO_2 emission is 161.3032 kg, and the variable cost is \$134.09. When a vehicle is under the first kind of traffic restriction, the CO_2 emission is 167.4327 Kg, and the variable cost is \$139.19. When a vehicle is under the second kind of traffic restriction, the CO_2 emission is 166.3727 Kg, and the variable cost is \$138.30. When a pair of a vehicle is under both the first and the second kinds of traffic restriction, the CO_2 emissions are the same, which is 151.6250 kg, and the variable cost is the same too, which is \$113.97.

From Figure 3(d) and the result of costs and emissions, we can find that the routing as well as cost and emission under the first kind of traffic restriction are the same as those under the second. The main reason is no matter which kind of the traffic restriction is, we always use a UAV instead of a vehicle to deliver a parcel when facing a traffic restriction.

Comparing Figures 3(a)–3(d), as well as the corresponding result of costs and emissions, we can obtain the following conclusions.

Firstly, traffic restrictions raise the cost and emission, and first kind of traffic restriction raises them further higher. The main reason is that when a road in the routing is blocked for the delivery vehicle, it has to choose other road, while if there is only one lane available, the vehicle could still run through the road if the cost and emission are lower than those running through other roads. Therefore, the cost and emission under the second kinds of traffic restriction are higher than those under no traffic restriction but lower than those under the first kind of traffic restriction.

Secondly, UAV delivery can always reduce the cost and emission no matter if there is traffic restriction and which kind of traffic restriction is. Furthermore, UAV delivery saves more cost and cuts more emission under the first kind of traffic restriction than that under the second, as the cost and emission under the first kind of traffic restriction are the highest and those under two kinds of traffic restrictions are the same.

In the following section, firstly, we present the result of 200 customers under the first kind of traffic restriction. The location of the 200 customers and the weight of their demand of were randomly generated and shown in Table 1. 2 cars are needed for customer service within 8 hours per day. The service times of each vehicle are 6.65 hours and 6.94 hours, respectively. The routing of the two pairs of vehicles and drones is shown in Figure 4, and the results of costs and emissions are as follows.

The CO_2 emission of the first vehicle is 209.5249 Kg, and that of the corresponding UAV is 0.1277 Kg. The CO_2 emission of the second vehicle is 218.6621 kg and that of the corresponding UAV is 0.1636 kg. Therefore, the total CO_2 emission from the package delivery is 428.4783 kg. If no UAV is used, the total CO_2 emission will be 467.8864 kg.

The variable costs of the first pair of a vehicle and a UAV are \$145.52 and \$2.03, respectively, and the variable costs of the second pair of a vehicle and a UAV are \$152.21 and \$2.60. Therefore, the total cost of serving the 200 customers is \$1302.36. The total cost will be \$1388.95, if no UAV is used.

5.3. Extended Examples. In the section, we extend our example to 300 and 400 customers.

5.3.1. The Impact of UAVs on CO_2 Emissions. Table 2 shows the CO_2 emissions without the use of UAVs, and Table 3 shows the CO_2 emissions with the use of UAVs. Table 4

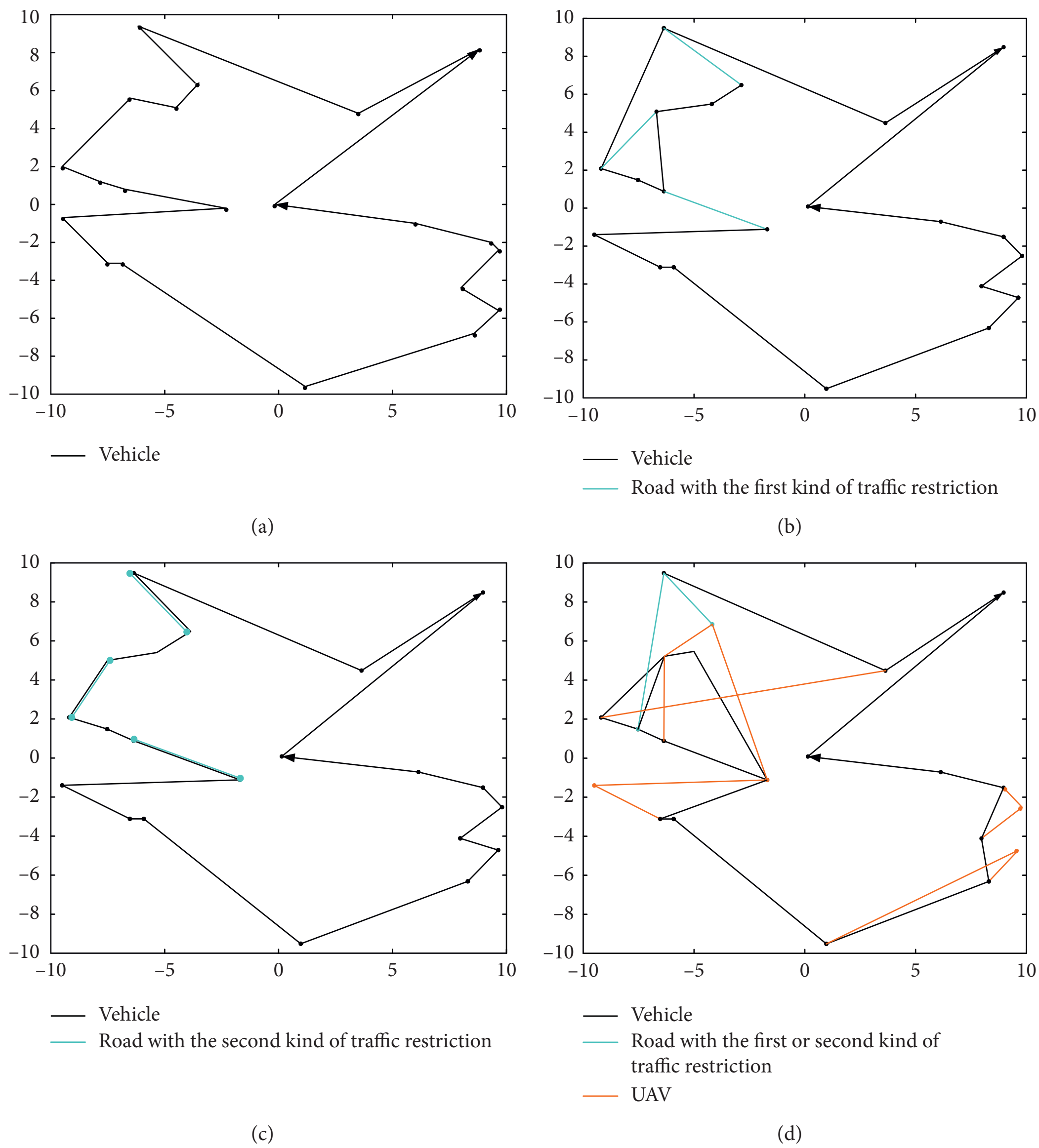

Figure 3: Routings under different circumstances: (a) routing of only vehicle under no traffic restriction; (b) routing of only vehicle under the first kind of traffic restriction; (c) routing of only vehicle under the second kind of traffic restriction; (d) routing of vehicle with UAV under two kinds of traffic restrictions.

shows the intuitive comparison between the results without UAVs and those with UAVs.

It can be seen from Tables 2–4 that, in the case of traffic restrictions, with the increase in the number of customers, the number of vehicles and CO_2 emissions are also rising. From Table 4, we can find that when there are 300 or 400 customers, 3 and 4 vehicles are needed, respectively, when no UAVs are being used, while only 2 and 3 vehicles are needed, respectively, when UAVs are being used. We also found that using UAVs can effectively reduce CO_2 emission even when there are 200 customers and the number of vehicles is not reduced.

5.3.2. The Impact of UAVs on Costs. Now, we analyze the impact of using UAVs on delivery costs. Table 5 shows the delivery costs without UAV, Table 6 shows the delivery costs with UAV, and Table 7 shows the comparison between the costs without UAVs and that with UAVs.

From Tables 5–7, we found that the variable cost, fixed cost, and total cost rise with the increase in the number of customers. And as per our expectation, we found from Table 7 that using UAVs can always effectively reduce variable cost and total cost, as well as fixed cost when there are 300 and 400 customers because the number of required vehicles is reduced. Our expectation is that using UAVs greatly reduces the variable cost by at least 28.64% and up to 43.47%.

Tables 4 and 7 show that using UAVs in package delivery reduces not only the variable cost and total costs but also CO_2 emission. In other words, UAV delivery is environmentally and economically beneficial.

Table 1: Location of the 200 customers and the weight of their demand.

Customer	Location	Weight of demand (pound)	Customer	Location	Weight of demand (pound)
1	(3.5985, 3.6248)	2.6464	101	(6.6985, −7.8311)	2.4695
2	(1.6070, 2.0104)	2.0035	102	(−1.9531, −3.3253)	4.6376
3	(6.7836, 3.9658)	4.9405	103	(−7.8722, −1.6863)	5.3956
4	(2.7794, 2.7118)	0.4074	104	(5.0983, −0.4058)	5.5206
5	(5.4746, −1.4383)	5.5835	105	(−7.3811, −9.4588)	2.7891
6	(3.7286, −5.7173)	2.6218	106	(−9.7011, −9.1042)	0.6035
7	(−3.9446, −0.7422)	0.9957	107	(−8.0567, 4.1457)	5.7241
8	(−6.6992, 6.3058)	0.8271	108	(−6.8909, −9.5609)	2.0171
9	(−8.7527, −4.0516)	0.7294	109	(−5.7863, 4.4279)	6.1105
10	(−4.4899, −5.3138)	1.3197	110	(7.3203, 5.0068)	2.3235
11	(4.4820, −3.0529)	6.0178	111	(8.0247, −7.8543)	4.213
12	(1.4923, −1.8090)	4.5951	112	(−5.0841, 1.2691)	5.5378
13	(−8.3485, 2.9984)	3.7066	113	(3.0984, −5.5088)	4.0103
14	(3.5833, −0.3746)	4.2485	114	(−8.4013, −2.8959)	3.9066
15	(−8.8362, 3.5809)	4.8984	115	(−1.5125, 3.4101)	4.5946
16	(−3.4012, 2.5994)	2.6331	116	(4.7787, 8.0351)	2.5481
17	(−3.2365, 0.3061)	5.1189	117	(0.5036, −1.8153)	4.4859
18	(−9.3533, 3.8708)	2.3671	118	(9.2231, −5.6816)	6.1265
19	(5.7948, 3.0688)	1.6931	119	(−0.7709, −0.2432)	0.8386
20	(−9.3260, 2.3723)	6.0346	120	(0.1749, 0.4201)	2.5176
21	(5.5314, −8.4922)	3.9256	121	(6.5870, −5.7042)	3.4506
22	(−5.3389, −1.8910)	4.0786	122	(5.1065, −4.8937)	5.6184
23	(5.0150, 1.0702)	0.5409	123	(−6.5286, −4.1542)	4.5411
24	(5.3291, 8.8109)	0.726	124	(4.8201, 0.3814)	1.8215
25	(5.1424, 2.8790)	3.9069	125	(−8.0454, 2.6018)	3.8553
26	(−8.5682, −4.6079)	0.2204	126	(5.8765, 0.1324)	0.413
27	(2.4282, −7.1526)	5.7625	127	(−8.9043, 2.6839)	2.5147
28	(5.3858, 3.9510)	5.8148	128	(3.2194, 4.7627)	3.5148
29	(−3.1541, −4.4266)	6.0896	129	(−3.9258, 0.0123)	4.7808
30	(6.9408, 0.1415)	1.0124	130	(0.0193, 9.3367)	4.6436
31	(6.9864, 6.0812)	2.2663	131	(−1.7297, −2.4018)	5.7673
32	(−2.2162, −7.0139)	2.0512	132	(7.9912, 3.1555)	4.0447
33	(1.7152, 6.3001)	1.4065	133	(−1.3450, 1.1250)	2.9504
34	(7.2730, 1.6194)	0.4455	134	(4.6406, 2.6336)	6.0704
35	(−9.0451, −1.9021)	5.6629	135	(−1.8672, −3.1354)	3.7547
36	(3.9235, 3.1469)	5.9208	136	(4.4430, 7.4150)	0.8491
37	(−4.1134, 9.0178)	0.7815	137	(−7.3532, 3.6512)	0.8283
38	(4.1405, 0.6544)	5.1735	138	(6.8433, 5.5395)	2.5081
39	(−9.0047, 2.8633)	5.2433	139	(8.1880, 8.9098)	2.8487
40	(3.9065, −5.4808)	3.8613	140	(−8.6609, −7.1078)	4.798
41	(6.8066, 6.7106)	1.008	141	(6.5072, 1.6621)	4.9815
42	(1.4364, −6.4336)	4.315	142	(−1.7420, 8.7680)	1.4472
43	(−8.9608, −7.4226)	5.8182	143	(−8.7449, −4.7519)	3.4111
44	(0.6380, 1.0638)	5.9632	144	(2.5800, 9.5467)	5.5106
45	(−5.3386, −5.5256)	1.804	145	(−6.2282, 2.4928)	3.4125
46	(−2.7935, 0.2916)	3.8737	146	(9.7491, 2.2369)	3.6908
47	(−3.2275, −7.6894)	6.1055	147	(5.0762, −8.1123)	3.9738
48	(6.0844, 5.0847)	6.0703	148	(−2.1303, 7.2874)	2.6361
49	(−5.1356, −5.9556)	3.0152	149	(−6.2300, −6.5167)	2.699
50	(2.6515, 7.7721)	0.0072	150	(6.2027, −0.4723)	4.6166
51	(−0.0056, −0.1799)	3.3836	151	(2.0571, 3.5960)	5.8956
52	(2.7594, −4.9004)	5.8689	152	(9.7581, 5.6005)	1.1632
53	(6.6679, 7.1263)	5.246	153	(5.2829, 1.7994)	2.5925
54	(9.8432, 3.9686)	1.3284	154	(−2.2265, 6.9336)	2.3741
55	(−5.3313, 6.4587)	1.3662	155	(−8.9635, 6.1876)	3.3864
56	(−7.3582, 2.8845)	5.5513	156	(7.3399, −1.8563)	2.5694
57	(0.1812, 2.1129)	3.2123	157	(−3.4740, −8.4158)	5.951
58	(−7.1705, 7.0471)	2.6717	158	(−0.1858, 1.4740)	0.9742
59	(8.5137, 5.5096)	4.5286	159	(−0.3142, −5.9115)	2.0432
60	(−1.5415, −7.7999)	3.7548	160	(−8.6928, 3.0577)	4.5069

Table 1: Continued.

Customer	Location	Weight of demand (pound)	Customer	Location	Weight of demand (pound)
61	(6.4396, 6.4118)	3.0396	161	(−8.9804, 1.7362)	3.4904
62	(8.1804, −3.8801)	5.6087	162	(0.8940, 8.4429)	1.8262
63	(−9.6267, 6.2938)	1.5951	163	(−1.6117, −7.0373)	2.0569
64	(9.7571, 7.7541)	5.2335	164	(−6.0486, −4.1884)	0.8061
65	(−7.4305, −1.9970)	6.0315	165	(0.5796, −2.2476)	4.9394
66	(−4.1666, 9.7131)	4.442	166	(−3.0904, −9.0519)	1.6785
67	(8.6054, −5.4922)	5.3479	167	(8.5203, −7.3574)	2.4377
68	(−9.7305, 1.9685)	3.6987	168	(9.3078, −5.7472)	2.9458
69	(4.0727, −8.2039)	3.3089	169	(−1.0789, −5.0646)	6.195
70	(−3.8506, 8.7982)	3.216	170	(3.4054, −9.4300)	0.0608
71	(−7.1437, 7.1571)	2.9886	171	(−8.1767, −0.5804)	2.5696
72	(8.6707, 3.3893)	4.1855	172	(1.0544, −1.7339)	4.0753
73	(−6.2558, −1.5341)	3.2457	173	(−8.5217, −1.5462)	0.9069
74	(−4.9621, −2.4825)	1.0398	174	(7.3960, 5.3860)	2.8008
75	(6.5565, −1.0670)	1.6786	175	(7.8358, −1.8235)	4.3691
76	(−9.1507, −8.5815)	2.1336	176	(0.7854, −0.1814)	2.1629
77	(2.3058, 3.3969)	3.1581	177	(7.3398, 4.4719)	4.8862
78	(−6.1230, 1.4946)	1.635	178	(3.6908, 0.0740)	5.8748
79	(−6.8841, 5.0681)	2.3038	179	(−1.7045, 5.2675)	3.5177
80	(3.1371, −3.3084)	5.5688	180	(−4.3713, −5.1950)	3.6966
81	(1.7032, −5.9946)	0.4024	181	(8.7083, −8.4181)	2.1445
82	(−1.5590, 5.8996)	4.9225	182	(3.5814, 9.0920)	4.3845
83	(−5.1026, 7.0859)	3.2166	183	(4.9116, −6.6143)	2.1252
84	(−2.3133, −0.0468)	1.2746	184	(−9.3055, −6.6730)	5.3135
85	(−1.9291, −8.8507)	5.5929	185	(1.1326, 9.1880)	2.7653
86	(4.6261, −7.2169)	0.2662	186	(2.4269, 9.3005)	3.8122
87	(7.3182, 2.3801)	0.2147	187	(−8.2876, 9.1493)	4.9769
88	(6.0759, −3.9352)	5.8295	188	(−9.5075, 5.6753)	2.5376
89	(8.0556, −4.2223)	2.5624	189	(8.3507, −0.2268)	6.1962
90	(−5.7516, 8.0645)	5.6345	190	(6.5826, 3.3623)	3.7944
91	(8.1302, 8.2009)	3.6932	191	(7.2440, −6.8963)	3.5641
92	(3.9469, 4.9619)	1.1317	192	(−1.3492, −6.6058)	4.005
93	(2.0032, −8.4006)	1.2813	193	(1.2460, −5.5328)	0.036
94	(7.8395, 7.5786)	1.4329	194	(−1.1003, 0.0472)	5.9488
95	(−7.5101, −8.0132)	0.9963	195	(−2.2261, −3.0986)	1.1039
96	(8.9171, 7.1257)	5.1115	196	(2.2383, −1.0874)	1.6342
97	(−0.0308, −6.0585)	2.2	197	(0.0418, −8.8158)	5.8702
98	(4.7966, 9.9410)	4.871	198	(3.8139, 2.0351)	4.0963
99	(−9.4510, −7.4800)	0.9984	199	(5.2971, −5.0442)	4.8425
100	(6.4788, −0.9906)	1.6839	200	(5.0138, −0.5799)	4.0817

6. Discussion

In this paper, we classified traffic restrictions into two circumstances and studied the environmental and economic impact of UAV delivery under traffic restriction, and we found that UAV delivery can effectively save energy and cost. In other words, UAV delivery economically benefits not only logistics firms but also the sustainability of environmental development, which is supported by Chiang et al. [2]. We also found that, under the two kinds of traffic restrictions, UAV delivery can accomplish deliveries that cannot be carried out or are carried out at much higher costs by vehicles only, and it is more effective under the first kind of traffic restriction, which has not been studied.

We would like to point out that, with the development of UAV technology, UAV delivery is more and more popularly accepted as the best resolution of "last-mile" delivery problem. Amazon, UPS, Walmart, Google, JD.com, and Alibaba started to apply UAVs in package delivery. In this paper, we proposed managers an effective model to create competitiveness by optimally coordinating vehicles and UAVs. Shifting small package delivery from trucks to UAVs greatly reduces energy consumption and costs in package delivery. As a matter of course, to realize the environmental and economic benefits of UAV delivery, firms should carefully plan and control the routing and cooperation of vehicles and UAVs. Operational decisions can effectively reduce delivery costs and CO_2 emission, as well as improve the environment [34].

Absolutely, the current power technology of UAVs limits the range and payload capacity of UAVs. At present, the battery used in UAVs is lithium ion battery with an energy density of around 300 Wh/kg, while the fluorinated battery can reach 2585 Wh/kg, which can greatly improve the performance of UAVs [35]. This means future developments in emerging energy sources will ease current restrictions on

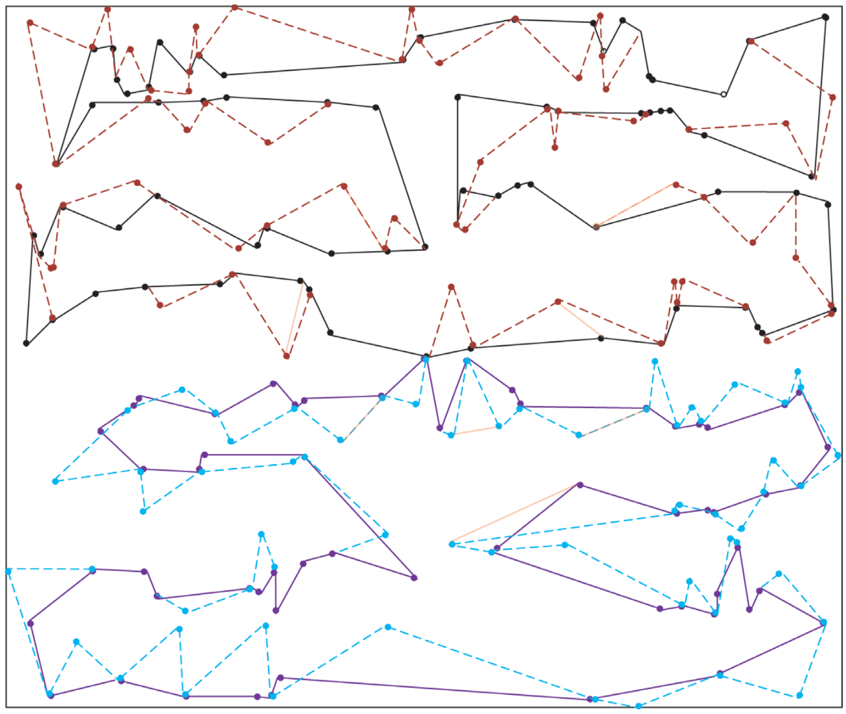

FIGURE 4: Routing of the 2 pairs of vehicles and UAVs.

TABLE 2: CO_2 emissions without UAVs.

Number of customers	Number of vehicles	Service time of each vehicle (hours)				CO_2 emission of each vehicle (kg)				Total emission (kg)	CPU time (s)
200	2	7.17	7.68			225.9088	241.9776			467.8864	26.58
300	3	5.65	5.79	7.29		178.0174	182.4284	229.6897		590.1355	75.32
400	4	4.94	5.41	6.41	5.06	155.6471	170.4556	201.9631	159.4279	687.4937	156.24

TABLE 3: CO_2 emissions with UAVs.

Number of customers	Number of vehicles	Service time of each vehicle (hours)			CO_2 emission of each vehicle (kg)			CO_2 emission of each UAV (kg)			Total emission (kg)	CPU time (s)
200	2	6.65	6.94		209.5249	218.6621		0.1277	0.1636		428.4783	29.11
300	2	7.75	7.89		244.1831	248.5942		0.1900	0.1623		493.1296	87.19
400	3	6.31	6.32	7.08	198.8123	199.1274	223.0731	0.1485	0.1472	0.1604	621.4689	179.21

TABLE 4: Comparison of CO_2 emissions of using UAVs and not using UAVs.

Number of customers	Number of vehicles		Number of reduced vehicles	CO_2 emission (kg)				CO_2 emission reduction	
	Without UAV	With UAV		Without UAV	With UAV			(kg)	(%)
					Vehicle	UAV	Total		
200	2	2	0	467.8864	428.1870	0.2913	428.4783	39.4081	9.20
300	3	2	1	590.1355	492.7773	0.3523	493.1296	97.0059	19.67
400	4	3	1	687.4937	621.0128	0.4561	621.4689	66.0248	10.62

Table 5: Variable costs without UAVs.

Number of customers	Number of vehicles	Service time of each vehicle (hours)	Cost per vehicle ($)	Total variable cost ($)	CPU time (s)
200	2	7.17 7.68	188.32 200.63	388.95	26.58
300	3	5.65 5.79 7.29	154.96 158.05 198.55	511.56	75.32
400	4	4.94 5.41 6.41 5.06	142.15 155.39 182.69 145.72	625.95	156.24

Table 6: Variable costs with UAVs.

Number of customers	Number of vehicles	Service time of each vehicle (hours)	Cost per vehicle ($)	Cost per UAV ($)	Total variable cost ($)	CPU time (s)
200	2	6.65 6.94	145.52 152.21	2.03 2.60	302.36	29.11
300	2	7.75 7.89	173.42 177.54	3.02 2.58	356.56	87.19
400	3	6.31 6.32 7.08	131.74 135.09 182.26	2.36 2.34 2.55	456.34	179.21

Table 7: Comparison of the costs of using UAV and not using UAV.

Number of customers	Number of reduced vehicles		Number of reduced vehicles	Number of reduced vehicles		Percentage of variable cost reduction by using UAV (%)	Number of reduced vehicles		Percentage of total cost reduction by using UAV (%)
	Without UAV	With UAV		Without UAV	With UAV		Without UAV	With UAV	
200	2	2	0	388.95	302.36	28.64	1388.95	1302.36	6.65
300	3	2	1	511.56	356.56	43.47	2011.56	1356.56	48.28
400	4	3	1	625.95	456.34	43.01	2625.95	1956.34	34.23

drone use and may provide additional cost savings that will allow UAV-vehicle delivery of last-mile packages to be further improved.

7. Conclusions

In this paper, we classified traffic restrictions into two circumstances and proposed a mixed-integer (0-1 linear) UAV-vehicle routing model with these two kinds of traffic restrictions to exploit the environmental aspects of the use of UAVs in logistics. A genetic algorithm was proposed to solve the model, and an experimental analysis was made to illustrate and validate our model and the algorithm. We found that, under the two kinds of traffic restrictions, delivering with UAVs can accomplish deliveries that cannot be carried out or are carried out at much higher prices by vehicles only and can effectively save costs and reduce CO_2 emissions, which is environmentally friendly. Furthermore, UAV delivery saves more cost and cuts more CO_2 emission under the first kind of traffic restriction than that under the second.

Data Availability

The data used to support the findings of this study are included within the article.

Conflicts of Interest

The authors declare that there are no conflicts of interest.

Acknowledgments

This research was supported by the Natural Science Foundation of Chongqing (no. cstc2019jcyj-msxmX1363) and Fundamental Research Funds for the Central Universities (no. 2018CDXYJG0040).

References

[1] D. Weideli, *Environmental Analysis of US Online Shopping*, MIT Center for Transportation and Logistics, Cambridge, MA, USA, 2013.

[2] W.-C. Chiang, Y. Li, J. Shang, and T. L. Urban, "Impact of drone delivery on sustainability and cost: realizing the UAV potential through vehicle routing optimization," *Applied Energy*, vol. 242, no. 5, pp. 1164–1175, 2019.

[3] A. A. R. Hosseinabadi, N. S. H. Rostami, M. Kardgar, S. Mirkamali, and A. Abraham, "A new efficient approach for solving the capacitated vehicle routing problem using the gravitational emulation local search algorithm," *Applied Mathematical Modelling*, vol. 49, no. 9, pp. 663–679, 2017.

[4] J. E. Cermak and K. Takeda, "Physical modeling of urban air-pollutant transport," *Journal of Wind Engineering and Industrial Aerodynamics*, vol. 21, no. 1, pp. 51–67, 1985.

[5] L. Pradenas, B. Oportus, and V. Parada, "Mitigation of greenhouse gas emissions in vehicle routing problems with backhauling," *Expert Systems with Applications*, vol. 40, no. 8, pp. 2985–2991, 2013.

[6] J. Qian, *Fuel Emission Optimization in Vehicle Routing Problems with Time-Varying Speeds*, Lancaster University, Lancashire, UK, 2011.

[7] Y.-J. Kwon, Y.-J. Choi, and D.-H. Lee, "Heterogeneous fixed fleet vehicle routing considering carbon emission," *Transportation Research Part D: Transport and Environment*, vol. 23, no. 8, pp. 81–89, 2013.

[8] L. Zhou, *Research on the Route Optimization of Rural E-Commercial Distribution Based on "Vehicle- Unmanned Aircraft"*, Wuhan University of Technology, Wuhan, China, 2017.

[9] R. D'Andrea, "Guest editorial can drones deliver?" *IEEE Transactions on Automation Science and Engineering*, vol. 11, no. 3, pp. 647-648, 2014.

[10] Q. Y. Zhi, *Research on Scheduling Mechanism of Unmanned Device in Logistics*, University of Electronic Science and Technology of China, Chengdu, China, 2015.

[11] D. N. Weng, "Analysis of the main influencing factors of drone logistics distribution," *Enterprise Reform and Management*, vol. 23, no. 8, pp. 179–218, 2015.

[12] B. Ma, D. D. Dai, and J. R. Pan, "Regression analysis and research on influencing factors of UAVs flight stability based on MATLAB," *Precise Manufacturing & Automation*, vol. 53, no. 2, pp. 32–34, 2017.

[13] C. C. Murray and A. G. Chu, "The flying sidekick traveling salesman problem: optimization of drone-assisted parcel delivery," *Transportation Research Part C: Emerging Technologies*, vol. 54, no. 5, pp. 86–109, 2015.

[14] Q. M. Ha, Y. Deville, Q. D. Pham, and M. H. Hà, "On the min-cost traveling salesman problem with drone," *Transportation Research Part C: Emerging Technologies*, vol. 86, no. 1, pp. 597–621, 2018.

[15] X. Wang, S. Poikonen, and B. Golden, "The vehicle routing problem with drones: several worst-case results," *Optimization Letters*, vol. 11, no. 4, pp. 679–697, 2017.

[16] S. Poikonen, X. Wang, and B. Golden, "The vehicle routing problem with drones: extended models and connections," *Networks*, vol. 70, no. 1, pp. 34–43, 2017.

[17] L. D. P. Pugliese and F. Guerriero, "Last-mile deliveries by using drones and classical vehicles," in *Proceedings of the International Conference on Optimization and Decision Science*, Sorrento, Italy, September 2017.

[18] M. Pereyra and A. G. Farji-Brener, "Traffic restrictions for heavy vehicles: leaf-cutting ants avoid extra-large loads when the foraging flow is high," *Behavioural Processes*, vol. 170, no. 1, Article ID 104014, 2020.

[19] H. Hu, X. Li, Y. Zhang, C. Shang, and S. Zhang, "Multi-objective location-routing model for hazardous material logistics with traffic restriction constraint in inter-city roads," *Computers & Industrial Engineering*, vol. 128, no. 2, pp. 861–876, 2019.

[20] B. Sureshkumar, "Review of routing algorithm for manet based on optimization techniques," *Journal of the Gujarat Research Society*, vol. 21, no. 17, pp. 280–285, 2019.

[21] C. Lee, "An exact algorithm for the electric-vehicle routing problem with nonlinear charging time," *Journal of the Operational Research Society*, vol. 71, no. 3, pp. 1–24, 2020.

[22] O. Bräysy and M. Gendreau, "Vehicle routing problem with time windows, part I: route construction and local search algorithms," *Transportation Science*, vol. 39, no. 1, pp. 104–118, 2005.

[23] M. Yu, V. Nagarajan, and S. Shen, "An approximation algorithm for vehicle routing with compatibility constraints," *Operations Research Letters*, vol. 46, no. 6, pp. 579–584, 2018.

[24] S. I. Suliman, I. Musirin, R. Dzulkifli, and R. Rifin, "The implementation of constructive heuristic algorithm for frequency assignment task in wireless communications," *Advanced Science Letters*, vol. 23, no. 6, pp. 5318–5323, 2017.

[25] T. Vidal, T. G. Crainic, M. Gendreau, and C. Prins, "Heuristics for multi-attribute vehicle routing problems: a survey and synthesis," *European Journal of Operational Research*, vol. 231, no. 1, pp. 1–21, 2013.

[26] E. Jabir, V. V. Panicker, and R. Sridharan, "Design and development of a hybrid ant colony-variable neighbourhood search algorithm for a multi-depot green vehicle routing problem," *Transportation Research Part D: Transport and Environment*, vol. 57, no. 12, pp. 422–457, 2017.

[27] Y. Xia, Z. Fu, S.-B. Tsai, and J. Wang, "A new TS algorithm for solving low-carbon logistics vehicle routing problem with split deliveries by backpack-from a green operation perspective," *International Journal of Environmental Research and Public Health*, vol. 15, no. 5, pp. 949–960, 2018.

[28] K. Peng, J. Du, F. Lu et al., "A hybrid genetic algorithm on routing and scheduling for vehicle-assisted multi-drone parcel delivery," *IEEE Access*, vol. 7, pp. 49191–49200, 2019.

[29] M. Moeini and H. Salewski, "A genetic algorithm for solving the truck-drone-ATV routing problem," in *Proceedings of the 2019 World Congress on Global Optimization*, Metz, France, July 2019.

[30] G. Laporte, "Fifty years of vehicle routing," *Transportation Science*, vol. 43, no. 4, pp. 408–416, 2009.

[31] O. Franzese and D. Davidson, *Effect of Weight and Roadway Grade on the Fuel Economy of Class-8 Freight Trucks*, Oak Ridge National Laboratory, Oak Ridge, TN, USA, 2011.

[32] A. H. Bateman, E. E. Blanco, and Y. Sheffi, "Disclosing and reporting environmental sustainability of supply chains," in *Sustainable Supply Chains*, pp. 119–144, Springer, Cham, Switzerland, 2017.

[33] A. Goodchild and J. Toy, "Delivery by drone: an evaluation of unmanned aerial vehicle technology in reducing CO_2 emissions in the delivery service industry," *Transportation Research Part D: Transport and Environment*, vol. 61, no. 6, pp. 58–67, 2018.

[34] H. Duan, G. Zhang, S. Wang, and Y. Fan, "Integrated benefit-cost analysis of China's optimal adaptation and targeted mitigation," *Ecological Economics*, vol. 160, no. 6, pp. 76–86, 2019.

[35] C. Peng, Y. Li, F. Yao et al., "Ultrahigh-energy-density fluorinated calcinated macadamia nut shell cathodes for lithium/fluorinated carbon batteries," *Carbon*, vol. 153, no. 11, pp. 783–791, 2019.

Hindawi
Mathematical Problems in Engineering
Volume 2020, Article ID 1904790, 13 pages
https://doi.org/10.1155/2020/1904790

Research Article

How Does Bilateral Preference Affect Shared Parking in Sharing Economy?

Yuxue Zhang,[1] Haoyu Wen ,[1] Ming Zhao,[2] and Zhaojun Yang[1]

[1]*School of Economics and Management, Xidian University, Xi'an 710071, China*
[2]*Department of Information, Xi'an Vehicle Parking Service Center, Xi' an 710000, China*

Correspondence should be addressed to Haoyu Wen; hywen@xidian.edu.cn

Received 24 December 2019; Revised 5 March 2020; Accepted 13 April 2020; Published 28 July 2020

Guest Editor: Davide Castellano

Sharing economy is seen as an essential building block for sustainability. Yet, inefficient utilizing of parking spaces needs more attention, by which both direct and indirect traffic congestions may be caused, jeopardizing the economic potential of sustainable development. Conventional parking service may gradually lose favour in analogy to its counterpart, of which a novel approach solving shortage of urban parking resources is offered by shared parking. Hence, in this paper, problems of how to redistribute the available private-owned parking slots that be shared are focused due to the parking slot location properties that can be labelled as random, disordered, unstable, widely distributed, etc. Specifically, shared parking greatly enhances reasonability by considering satisfaction. Based on the mechanism of time matching between supply and demand, this paper thoroughly takes the bilateral preference of both parking demanders and parking space suppliers into account in terms of maximization of the utilization rate of shared parking spaces as well as the satisfaction of parking demanders, in which a multiobjective optimization model is established and the weighted sum method combined with the Hungarian method is adopted. Compared with the first-come-first-served (FCFS) strategy, the performance of the proposed method enjoys more advantages in utilizing shared parking spaces and in satisfying parking demanders. The model established and algorithm conducted in this paper meet the requirements induced by parking space redistribution in which inequalities exist between supply and demand, facilitating automobile parking and realizing higher efficiencies in using public resources regarding shortage of parking spaces in urban areas.

1. Introduction

Transportation is a representative of energy-dependent industry which results in excessive energy consumption and environmental pollution. Under energy and environment pressures, how to alleviate shortage of parking resources without occupying too much space poses a serious challenge for transportation [1]. At present, the number of registered automobiles in China skyrocket as the economy develops [2]. Statistics of the Traffic Management Bureau [3] showed that, in China, there are 66 cities with the number of cars exceeding 1 million until June 2019. However, the rapid increasing of cars has brought too much inconvenience due to most cities' inability to supply adequate parking spaces. Taking Beijing as a typical example, according to the 2019 Beijing Traffic Development Annual Report [4], the shortage of the parking lots was up to 1.37 million. The public and private belonging property of the parking space, together with the imbalance between parking space supply and demand, determines the scarcity of the available parking slots; hence, underutilization of existing parking spaces [5, 6] should be restored to its expected level, which helps alleviate the serious shortage of parking resources [7].

Owing to the severe imbalance between supply and demand of parking spaces, to which the major component is composed of private-owned ones, urban residents have to face great inconveniences and even difficulties when parking cars. For many cities, contradiction between creating more parking spaces and finite resources has become the inescapable problem, to which enormous increase in financial expenditure may not help within a short period of time. Under such circumstances, improving the utilization rate of public- and private-owned parking spaces seems a better alternative regarding the scarcity of parking resources [8, 9], of which can be summarized as the motivations of this research.

Therefore, the scheme of shared parking is rendered as acceptable to alleviate inconveniences and difficulties of parking [10]. However, despite some public-owned parking spaces which cannot be taken into consideration by the scheme at present, redistributing and matching the available private-owned shared parking spaces which locate in residential communities may encounter complicated situations due to the parking spaces' position and distribution, to which more attention should be paid. Hence, the sharing and redistributing of private-owned parking spaces is prioritized in accordance with their properties. In this study, problems regarding how to redistribute private parking slots in terms of bilateral preference under shared parking management are incorporated accordingly, thereby approaching this problem by an optimization algorithm.

The rest of the paper is organized as follows. An overview of the related issues is performed in Section 2, followed by problem description (including the shared parking scene and notations) in Section 3. Section 4 will present the parking time matching model considering bilateral preference with an algorithm designed to solve it. Numerical experiments are conducted in Section 5. Conclusions and further research directions are given in Section 6.

2. Related Work

Some scholars, foreign and domestic, have verified the feasibility and effectiveness of shared parking from multiple perspectives [11, 12]. Stin and Resha [13] analyzed the potential of shared parking for different purposes of building facilities and explored the feasibility of building shared parking lots. Liu et al. [14] found out that it is efficient for traffic management to reserve parking through parking permits distribution and trading. What's more, appropriate combination of reserved and unreserved parking spots can temporally relieve traffic congestion at the bottleneck and reduce the total system cost. Xiao and Xu [15] proposed a fair recurrent double auction mechanism and thought it plays an important role in promoting shared parking. Therefore, not only can the quantity of car trips be curbed by promoting appropriate parking spaces [16] but also the congestions be alleviated from road traffic networks by adopting the scheme of shared parking, not to mention the reduction in carbon emissions.

In researching shared parking matching strategy, Shao et al. [17] studied parking models of parking lots adopting both same and different available time and proposed a simple model for residents and public users to share parking spaces in residential areas. Cai et al. [18] researched the shared parking strategy of public-owned parking lots and proposed a network-based parking space allocation method. Kong et al. [19] proposed a parking matching method for intelligent parking space sharing, distribution, and pricing, which is based on IoT/cloud technology architecture and on the auction perspective. Hao et al. [20] studied the floating charging method of shared parking.

Most of the existing researches concerning shared parking focused on the following three factors, namely, the analysis of the feasibility of shared parking, the construction of shared parking allocation model, the design of third-party shared parking platform [21]. Yet, few matching research literatures brought to light the exclusive scarcity of shared parking spaces and the distinctive characteristics of parking demanders, which can be specifically classified as the bilateral preference (including demanders' and supplies' preferences), the matching and redistributing of shared parking in residential communities, the time that shared parking spaces cost in the same period, and the number of parking demanders.

The research objects are therefore sketched as residential area-located parking demanders who are featured with multiple parking demands and sharable parking spaces in multiple sharable periods. This paper considers shared parking space preference (parking space utilization) and parking demanders preferences (such as walking distance after parking, parking fees, and safety) in terms of redistributing and matching time of both shared private parking space and parking demanders. Accordingly, the preference is divided into three terms by the shared parking platform with regard to the different expressions of the parking preference, including clear numbers, interval numbers, and language term preference, which maximizes the utilization of shared parking spaces and the satisfaction degree of parking demanders. The key contributions of this paper can be recapitulated as constructing a multiobjective optimization model for shared parking in terms of bilateral preference, to which a relevant algorithm is designed. Shared parking is formulating its tendency throughout the developing process of the sharing economy. Our work will be reasonable for policymakers and business supervisors who wish to satisfy users' experience of parking.

3. Problem Description

In this section, the shared parking scene for matching parking demanders with parking suppliers is sketched. Related notations are therefore defined to denote the sets and variables included.

3.1. Description for Shared Parking Scenario. In specific cases with finite parking spaces in public parking areas, there is a partial overflow parking seeker. Parking spaces located in residential areas within a certain distance around the public parking area can provide shared parking spaces due to the tidal effect. Such parking spaces are identified as shareable parking spaces. According to the different use of the land properties, the shared parking with maximum satisfaction refers to the parking space allocation that maximizes the preference of the supply and demand by implementing the different time sharing [13]. The satisfaction degree is calculated according to the bilateral preference. The parking space allocation is assumed to be within walking distance of the public parking area (studies showed that 95% of users can accept a maximum walking distance of 350 m after parking) [22]. The residential area provides n shared parking space. Among the parking demanders in the public parking area, there are m drivers who reserve the use of shared parking spaces.

In the study of the simulated shared parking scenario, we set the following definitions with explanations: an owner of the shared parking space is identified as a "supplier," whilst a parking demander is regarded as a "demander" and two types of participants are connected through a "shared parking platform." Therefore, the shared parking scenario can be identified as follows (as shown in Figure 1): the shared parking platform connects two types of participants together, including suppliers and demanders. The suppliers would like to submit the information of the shared parking space to the platform, including shareable time and location, whilst the demanders are also submitting their information (parking time and the expected value of the parking space attributes) to the parking platform, wishing to obtain slots for parking. The parking platform returns the corresponding feedbacks (matched participants and priority attributes) to participants. It is emphasized that each round of allocation is closely connected with the former allocations, since the previous records (participants' participation times, compliance, and matched result) are combined with allocation result before the final feedbacks in each round can be concluded.

3.2. Notations. In order to describe the matching problem between the shared parking space and the parking demanders, the following symbols are used in this paper:

$D = \{D_1, D_2, \ldots, D_m\}$: a set of m parking demanders, where D_i denotes the i_{th} parking demanders, $i = 1, 2, \ldots, m$.

$P = \{P_1, P_2, \ldots, P_n\}$: a set of n shared parking spaces, where P_j denotes the j_{th} shared parking spaces, $j = 1, 2, \ldots, n$.

t_i^a, t_i^b represent the expected arriving and leaving time of the i_{th} owner at the parking space, respectively.

a_j^s, a_j^e are the starting and ending moments at which the j_{th} parking space can be shared.

b_s, b_e represent the start and end time of a shared parking space during a certain time period (such as 0–24 as the time period involved in the model). $b_s \le \forall a_j^s, b_e \ge \forall a_j^e$ are set to discretize the time segment.

$C = \{C_1, C_2, \ldots, C_q\}$: a set of q attributes for evaluating the parking space, where C_g denotes the g_{th} attribute, $g = 1, 2, \ldots, q$. Here, the attributes are considered in three formats, crisp number (such as parking fee), interval number (such as walking distance after parking), and linguistic terms (such as parking safety). The crisp number can be regarded as a special interval number with the same upper and lower limits. Let $C = \{C^C, C^I, C^L\}$ be a set of attribute subsets, where C^C, C^I, C^L denote the attribute values in the formats of crisp number, interval number, and linguistic term, respectively, $C^C \cap C^I = \varnothing, C^C \cap C^L = \varnothing, C^I \cap C^L = \varnothing$.

$E = [e_{ig}]_{m\times q}$: a decision matrix for the aspiration level of parking demanders, where e_{ig} denotes the aspiration level provided by parking demanders D_i to shared parking spaces concerning attribute C_g, $i = 1, 2, \ldots, m, g = 1, 2, \ldots, q$.

$A = [a_{jg}]_{n\times q}$: a decision matrix for the evaluation level of shared parking spaces, where a_{jg} denotes the evaluation level of shared parking spaces P_j concerning attribute C_g, $j = 1, 2, \ldots, n; g = 1, 2, \ldots, q$.

$W = \{w_1, w_2, \ldots, w_q\}$: a vector of attribute weights, where w_g denotes the weight of attribute C_g, $\sum_{g=1}^{q} w_g = 1, 0 \le w_g \le 1, g = 1, 2, \ldots, q$.

4. Model Construction

In this section, a model-based method is proposed to solve the abovementioned problem regarding private parking slot sharing. An optimization model of parking time matching is established in terms of satisfaction, under which an algorithm is designed accordingly.

4.1. Model for Matching Parking Demanders and Suppliers. The parking time is discretized during the time period involved in the model. The time interval ranging from b_s to b_e is divided into $T = (b_e - b_s)/\Delta T$ equal time periods (such as 0.5 hours) and each time interval is ΔT. The period of the shared parking spaces can be expressed as $b_s + (t-1)\cdot \Delta T$ to $b_s + t\cdot \Delta T$, where $t = 1, 2, \ldots, T$.

Depending on the shareable parking period and the parking demanders period provided by the shared parking space, d_{ij} is used to indicate the relationship between the rental period of shared parking space and the parking demanders period:

$$d_{ij} = \begin{cases} 0, & \left(t_i^a, t_i^d\right) \in \left(a_j^s, a_j^e\right), \\ 1, & \left(t_i^a, t_i^b\right) \notin \left(a_j^s, a_j^e\right), \\ & i = 1, 2, \ldots, m,\ j = 1, 2, \ldots, n. \end{cases} \tag{1}$$

By analyzing whether there is an intersection of the parking time windows for different vehicles, it can be judged whether different vehicles can be allocated to the same parking space within the available time provided by the shared spaces so that p_{ir} represents the relationship of different vehicle reservation time:

$$p_{ir} = \begin{cases} 1, & \left(t_i^a, t_i^d\right) \cap \left(t_r^a, t_r^d\right) \neq \varnothing, \\ 0, & \left(t_i^a, t_i^d\right) \cap \left(t_r^a, t_r^d\right) = \varnothing, \\ & i, r \in 1, 2, \ldots, m. \end{cases} \tag{2}$$

By judging whether there is an intersection between the time of parking demanders and the time of the shared parking space, the demand column vector can be constructed as

$$q_i = \left(q_{1i}, q_{2i}, \ldots, q_{ti}, \ldots, q_{Ti}\right)^T, \quad i \in 1, 2, \ldots, m; t = 1, 2, \ldots, T, \tag{3}$$

where

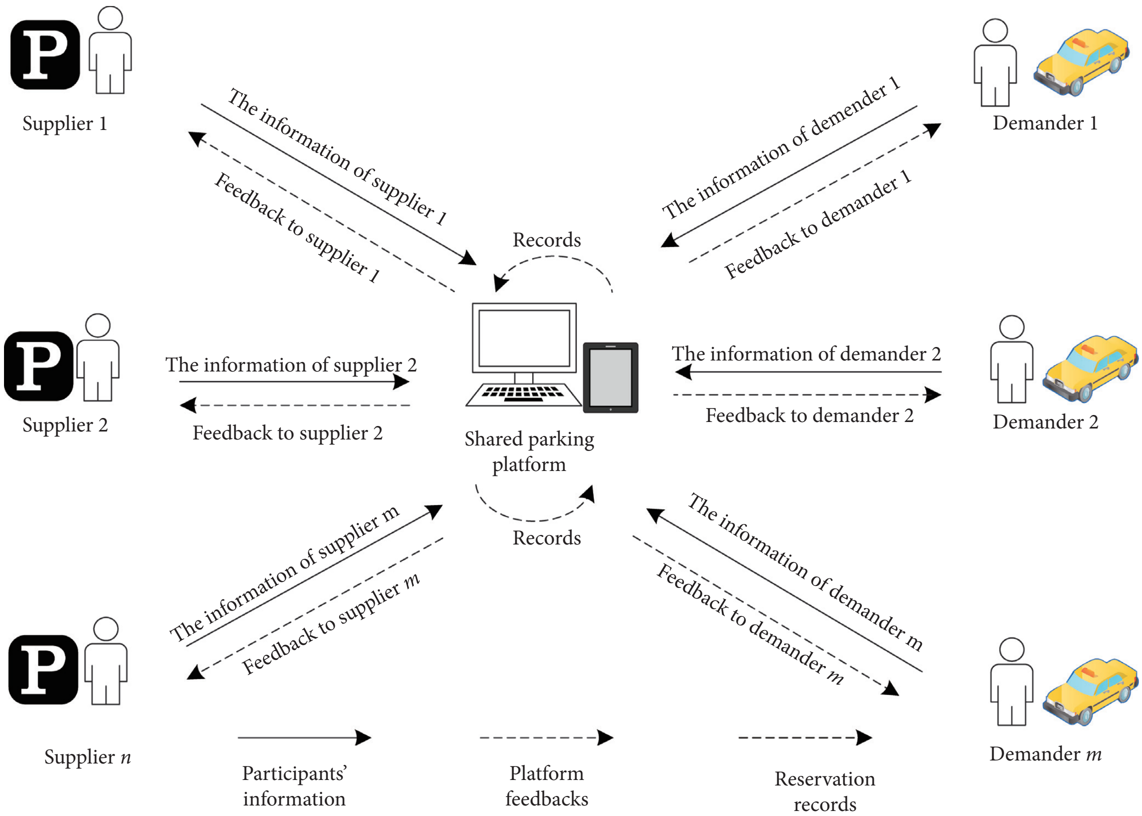

FIGURE 1: The shared parking scenario.

$$q_{ti} = \begin{cases} 1, & (t_i^a, t_i^d) \cap [b_0 + (t-1)\cdot\Delta T, b_0 + t\cdot\Delta T] = \varnothing, \\ 0, & (t_i^a, t_i^d) \cap [b_0 + (t-1)\cdot\Delta T, b_0 + t\cdot\Delta T] = \varnothing, \\ & i \in 1, 2, \ldots, m,\ t = 1, 2, \ldots, T. \end{cases} \tag{4}$$

For example, $q_i = (0, 0, 1, 1, 0, \ldots, 1, 1)^T$ indicates the 3rd to 4th time and the last two periods of the i parking demanders reservation.

The decision variable x_{ijt} indicates the matching between the i_{th} owner and the j_{th} parking space during the t period,where

$$x_{ijt} = \begin{cases} 1, & At, \text{ the owner is assigned to } j \text{parking space}, \\ 0, & At, \text{ the owner is not assigned to } j \text{parking space}. \end{cases} \tag{5}$$

The target model $M1$ can be built and expressed as

$$\max z_1 = \sum_{i=1}^{m}\sum_{j=1}^{n}\sum_{t=1}^{T}\left(q_{ti}x_{ijt}\right), \tag{6}$$

$$\text{s.t.} \quad \sum_{j=1}^{n} x_{ijt} \leq 1, \quad i = 1, 2, \ldots, m,\ t = 1, 2, \ldots, T, \tag{7}$$

$$d_{ij} + x_{ijt} \leq 1, \quad i = 1, 2, \ldots, m;\ j = 1, 2, \ldots, n;\ t = 1, 2, \ldots, T, \tag{8}$$

$$x_{ijt} + p_{ir}x_{rjt} \leq 1, \quad i, r = 1, 2, \ldots, m,\ j = 1, 2, \ldots, n,\ t = 1, 2, \ldots, T, \tag{9}$$

$$x_{ijt} \in \{0, 1\}, \quad i = 1, 2, \ldots, m;\ j = 1, 2, \ldots, n;\ t = 1, 2, \ldots, T. \tag{10}$$

In the scene of shared parking, the shared parking spaces prefer the allocation scheme with high utilization rate. Therefore, the objective function is to maximize the efficiency of the shared parking spaces during the time period involved in the model, where q_{ti} indicates whether the parking demanders i and the shareable parking spaces have an intersection at the time t. In formulas (6) and (7), the value of x_{ijt} is fixed by 0 or 1, which means each parking request is assigned only one parking space at the time of t, where 0 means that i is not allocated to the parking space j at the time of t, and 1 means that the owner i is allocated to the parking space at j parking. Constraint (8) denotes the sharing time window, such as $d_{ij} = 1$, meaning that the time of the vehicle does not match the parking space,$x_{ijt} = 1$ means the owner i is assigned to the parking space j, which does not match the former j parking space time. Hence, the abovementioned two parameters i and j cannot be fixed at 1 simultaneously. Constraint (9) means that the same parking space cannot allow parking of two cars simultaneously, of which the same time period conflicts with each other.

5. Measuring Satisfaction Degrees of Parking Demanders and Suppliers

The shared parking platform analyzes the previous parking data and counts the key factors affecting the parking space selection. The platform is divided into three forms, clear numbers, interval numbers, and language term preference, in terms of the different expression forms of the parking factors [23]. $C = \{C^C, C^I, C^L\}$ is the classified attribute set, C^C, C^I, C^L represent clear numbers, interval numbers, and attribute set of language term preference, respectively. Firstly, the matching of the parking time period should be prioritized throughout the process of matching between parking demanders and parking spaces [24]. Secondly, an optimization model considering satisfaction is therefore established to complete the matching of parking demanders and shared parking spaces in accordance with the preference of the parking demanders for the parking space.

When the platform provides parking spaces to the parking demanders, whether the real evaluation level of each shared parking space reaches the aspiration level of parking demanders should be taken into serious consideration. Inasmuch as measuring the degree of the aspiration level, it is necessary to calculate the parking demanders satisfaction of each attribute, thereby obtaining the overall satisfaction degree regarding the weight of each attribute.

The following process of calculation describes the satisfaction degree with three formats of attribute values.

5.1. Calculation of Satisfaction Degree for the Attribute Value Type C^C. When $C_g \in C_c$, the attribute value C_g including the expectation and evaluation level attributes is a clear number. Then, $e_{ig} = e_{ig}'$ and $a_{jg} = a_{jg}'$ indicate the expectation level of parking demanders and the evaluation level of parking spaces on shared parking platforms, respectively, where $e_{ig}' \geq 0, a_{jg}' \geq 0$. Hence, with regard to the attribute C_g, the satisfaction u_{ij}^g of parking demanders D_i to the shared parking space P_j is calculated as follows:

For benefit attribute,

$$u_{ij}^g = \begin{cases} \dfrac{a_{jg}' - a_g^{'\min}}{e_{ig}' - a_g^{'\min}}, & a_g^{'\min} \leq a_{jg}' \leq e_{ig}', \\ 1, & e_{ig}' \leq a_{jg}' \leq a_g^{'\max}, \\ & i = 1, 2, \ldots, m,\ j = 1, 2, \ldots, n,\ g = 1, 2, \ldots, q, \end{cases} \tag{11}$$

for cost attribute,

$$u_{ij}^g = \begin{cases} 1, & a_g^{'\min} \leq a_{jg}' \leq e_{ig}', \\ \dfrac{a_g^{'\max} - a_{jg}'}{a_g^{'\max} - e_{ig}'}, & e_{ig}' \leq a_{jg}' \leq a_g^{'\max}, \\ & i = 1, 2, \ldots, m,\ j = 1, 2, \ldots, n,\ g = 1, 2, \ldots, q, \end{cases} \tag{12}$$

where $a_g^{'\min} = \min_g \{a_{jg}'\}, a_g^{'\max} = \max_g \{a_{jg}'\}, \quad j = 1, 2, \ldots, n.$.

5.2. Calculation of Satisfaction Degree for the Attribute Value Type C^I. When the attribute value type including the expectation level and the evaluation level attribute C_g is an interval number. Then, $e_{ig} = (e_{ig}^L, e_{ig}^R)$ and $a_{jg} = (a_{jg}^L, a_{jg}^R)$ indicate the expectation level of parking demanders and the evaluation level of parking spaces on shared parking platforms, respectively, where $e_{ig}^R \geq e_{ig}^L, a_{jg}^R \geq a_{jg}^L$ and $e_{ig}^L \geq 0, a_{jg}^L \geq 0$. Hence, with regard to the attribute C_g, the satisfaction u_{ij}^g of parking demanders D_i to the shared parking space P_j is calculated as follows:

$$u_{ij}^g = \begin{cases} \dfrac{a_{jg} - a_g^{\min}}{e_{ig}^L - a_g^{\min}}, & a_g^{\min} \leq a_{jg} \leq e_{ig}^L, \\ 1, & e_{ig}^L \leq a_{jg} \leq e_{ig}^R, \\ \dfrac{a_g^{\max} - a_{jg}}{a_g^{\max} - e_{ig}^R}, & e_{ig}^R \leq a_{jg} \leq a_g^{\max}, \\ & i = 1, 2, \ldots, m,\ j = 1, 2, \ldots, n,\ g = 1, 2, \ldots, q, \end{cases} \tag{13}$$

where $a_g^{\min} = \min_g \{a_{jg}\}, a_g^{\max} = \max_g \{a_{jg}\}, \quad j = 1, 2, \ldots, n.$.

5.3. Calculation of Satisfaction Degree for the Attribute Value Type C^L. If $C_g \in C^L$, the attribute value type including the expectation level and the evaluation level attribute is a language term. We suppose $O = \{O_1, O_2, \ldots O_k\}$ is a fully ordered set of language terms with an odd base, where O_k is the k language term in the collection O and $k+1$ is the cardinality of the attribute set O. We assume α_{ig} is the subscript value of the linguistic term corresponding to the parking demanders' aspiration level e_{ig} and presume β_{jg} is the subscript value of the linguistic term corresponding to the shared parking platform evaluation level. Hence, with regard to the attribute C_g, the satisfaction u_{ij}^g of parking demanders D_i to the shared parking space P_j is calculated as follows:

for benefit attribute,

$$u_{ij}^g = \begin{cases} \dfrac{\beta_{jg} - \beta_g^{\min}}{\alpha_{ig} - \beta_g^{\min}}, & \beta_g^{\min} \le \beta_{jg} \le \alpha_{ig}, \\ 1, & \alpha_{ig} \le \beta_{jg} \le \beta_g^{\max}, \\ & i = 1, 2, \ldots, m, \; j = 1, 2, \ldots, n, \; g = 1, 2, \ldots, q, \end{cases} \tag{14}$$

for cost attribute,

$$u_{ij}^g = \begin{cases} 1, & \beta_g^{\min} \le \beta_{jg} \le \alpha_{ig}, \\ \dfrac{\beta_g^{\max} - \beta_{jg}}{\beta_g^{\max} - \alpha_{ig}}, & \alpha_{ig} \le \beta_{jg} \le \beta_g^{\max}, \\ & i = 1, 2, \ldots, m, \; j = 1, 2, \ldots, n, \; g = 1, 2, \ldots, q, \end{cases} \tag{15}$$

where $\beta_g^{\min} = \min_g \{\beta_{jg}\}, \beta_g^{\max} = \max_g \{\beta_{jg}\}, \quad j = 1, 2, \ldots, n.$

The overall satisfaction of the parking demanders to the shared parking space regarding satisfaction degree of each attribute u_{ij} and the corresponding attribute weight w_g is calculated as follows:

$$u_{ij} = \sum_{g=1}^{q} w_g u_{ij}^g. \tag{16}$$

6. Constructing the Optimization Matching Model

Based on the principle of time matching and the satisfaction degree u_{ij}, the multiobjective optimization model $M2$ for matching parking demanders and shared parking spaces is established as follows:

$$\max z_1 = \sum_{i=1}^{m} \sum_{j=1}^{n} \sum_{t=1}^{T} \left(q_{ti} x_{ijt}\right), \tag{17}$$

$$\max z_2 = \sum_{i=1}^{m} \sum_{j=1}^{n} \sum_{t=1}^{T} \left(u_{ij} x_{ijt}\right), \tag{18}$$

$$\text{s.t.} \quad \sum_{j=1}^{n} x_{ijt} \le 1 \quad i = 1, 2, \ldots, m, t = 1, 2, \ldots, T. \tag{19}$$

$$d_{ij} + x_{ijt} \le 1, \quad i = 1, 2, \ldots, m; \; j = 1, 2, \ldots, n; \; t = 1, 2, \ldots, T, \tag{20}$$

$$x_{ijt} + p_{ir} x_{rjt} \le 1, \quad i, r = 1, 2, \ldots, m; \; j = 1, 2, \ldots, n; \; t = 1, 2, \ldots, T, \tag{21}$$

$$x_{ijt} \in \{0, 1\}, \quad i = 1, 2, \ldots, m; \; j = 1, 2, \ldots, n; \; t = 1, 2, \ldots, T. \tag{22}$$

The abovementioned model consists of two objective functions. The objective function (17) is to maximize the efficiency of the shared parking space, meaning that the time of each shared parking space is used as long as possible. The objective function (18) is to maximize the satisfaction of parking demanders. Formulas (19) to (22) are constraints, where constraint (19) ensures that each parking demander can only match at most one shared parking space and constraint (20) ensures that the time matching of shared parking spaces and parking demanders does not conflict to each other despite whether it is assigned to the parking space. Constraint (21) ensures that the same parking space cannot stop two vehicles at the same time.

7. An Algorithm for Solving the Optimization Matching Model

The model $M2$ is a two-objective 0-1 integer programming problem. As participants (m and n) increase, the solution of the model $M2a$ becomes very complicated. To deal with $M2$ MODEL, this section proposes a solution algorithm based on the weighted sum method and the Hungarian algorithm, which [25] is used to convert the dual-objective optimization model $M2$ into a single-objective optimization model $M3$ by adopting the weighted sum method. Then, according to the single-objective optimization model $M3$, a standard assignment model $M4$ is built, which can be solved by the Hungarian method [26]. The result of the model $M4$ is the noninferior solution of the two-objective optimization model $M2$. The specific solution process is as follows.

Let α and $1-\alpha$ be the weights (importance degrees) of the objective functions z_1 and z_2, respectively, varying between 0 and 1. Generally, they can be assigned by the shared parking platform or be assigned in terms of core competence theory [27] as follows:

$$\begin{cases} \alpha = \dfrac{|D|}{(|D| + |P|)}, \\ \\ 1-\alpha = \dfrac{|P|}{(|D| + |P|)}, \end{cases} \tag{23}$$

where $|D|$ is the cardinality of set D. Besides, multiple values of α can be used to obtained multiple satisfied demander supply matching results, and then the shared parking platform can select one from the multiple satisfied demander supply matching results according to the practical requirements. According to the dual-target optimization model $M2$, a single-objective optimization model $M3$ that maximizes the satisfaction of parking demanders and parking spaces can be constructed:

$$\max z = \alpha \sum_{i=1}^{m} \sum_{j=1}^{n} \sum_{t=1}^{T} \left(q_{ti} x_{ijt}\right) + (1-\alpha) \sum_{i=1}^{m} \sum_{j=1}^{n} \sum_{t=1}^{T} \left(u_{ij} x_{ijt}\right), \tag{24}$$

$$\text{s.t.} \quad \sum_{j=1}^{n} x_{ijt} \leq 1, \quad i = 1, 2, \ldots, m\, t = 1, 2, \ldots, T \tag{25}$$

$$d_{ij} + x_{ijt} \leq 1, \quad i = 1, 2, \ldots, m; j = 1, 2, \ldots, n; t = 1, 2, \ldots, T, \tag{26}$$

$$x_{ijt} + p_{ir} x_{rjt} \leq 1, \quad i, r = 1, 2, \ldots, m; j = 1, 2, \ldots, n; t = 1, 2, \ldots, T, \tag{27}$$

$$x_{ijt} \in \{0, 1\}, \quad i = 1, 2, \ldots, m; j = 1, 2, \ldots, n; t = 1, 2, \ldots, T. \tag{28}$$

The parking demander can select a satisfactory parking space from the multiple matching results of the parking space-demander with regard to the difference of satisfaction between the two parties. Similarly, the shared parking space can also select a satisfactory demander from multiple matching demanders. The abovementioned analysis shows that the model $M3$ is a basic allocation model, which is transformed into a standard distribution model by adopting the Hungarian algorithm.

It is known that by the objective function of the model $M3$, $z = \alpha \sum_{i=1}^{m} \sum_{j=1}^{n} \sum_{t=1}^{T} (q_{ti} x_{ijt}) + (1-\alpha) \sum_{i=1}^{m} \sum_{j=1}^{n} \sum_{t=1}^{T} (u_{ij} x_{ijt}) = \sum_{i=1}^{m} \sum_{j=1}^{n} \sum_{t=1}^{T} [\alpha q_{ti} + (1-\alpha) u_{ij}] x_{ijt}$, where $\alpha q_{ti} + (1-\alpha) u_{ij}$ is the weighted satisfaction of the standard allocation model $M3$. Therefore, let $V = [v_{ij}]_{m \times n}$ denote the weighted satisfaction degree matrix of the model $M3$, where v_{ij} represents the weighted satisfaction of the matching demander i and the parking space j. The weighted satisfaction degree can be calculated by the following equation:

$$v_{ij} = \begin{cases} \alpha q_{ti} + (1-\alpha) u_{ij}, & x_{ijt} = 1, \\ 0, & x_{ijt} \neq 1, \\ & i = 1, 2, \ldots, m, \ j = 1, 2, \ldots, n. \end{cases} \tag{29}$$

The objective of the Hungarian algorithm is to minimize the objective function. In order to establish a standard allocation model, it is necessary to convert the maximization problem into a minimization problem. In specific cases, the parking demander has only one parking demander in the matching cycle involved in the model, the parking space can be shared only one shareable time period and the number of parking demanders equals to the number of shared parking spaces, and the adoption of the Hungarian algorithm maximizing the problem can be directly translated into an equivalent of minimization problem. However, in reality, a person who seeks for parking may have multiple parking demanders. A shareable parking space may have multiple different shareable time periods. The number of parking demanders and shareable parking spaces may not be equal, which in turn generates the following method conducted in this paper.

Inasmuch as the principle of the Hungarian method in specific cases, we know that if there is a person who seeks for parking with multiple parking demanders within the period involved in the model, the demander is transformed into multiple demanders with the same preference but different parking periods. By converting parking demanders who are featured with multiple parking needs into parking demanders with only one parking requirement, m parking demanders can therefore be converted into $m\prime$ parking demanders, so $D' = \{D_1, D_2, \ldots, D_m, \ldots, D_{m\prime}\}$. Similarly, a shareable parking space with multiple shareable time periods is converted into multiple parking spaces with the same preference value but different sharing time periods, and each parking space has only one shareable time period. Therefore, n parking spaces can be converted to $n\prime$ parking spaces, then $P' = \{P_1, P_2, \ldots, P_n, \ldots, P_{n\prime}\}$. Let $b = \max\{m', n'\}$, if the number of parking demanders and the number of shared parking spaces are different, setting virtual $b - m\prime$ parking demanders or $b - n\prime$ shareable parking spaces will turn the original matrix into a b matrix. D'_f represents the first parking demander and P'_h represents the first shareable parking space. Therefore, $L = [l_{fh}]_{b \times b}$ represents the converted comprehensive satisfaction matrix. The specific solution process for converting a complex situation into a standard allocation model is as follows:

(1) Finding the maximum value of the initial comprehensive satisfaction N, then $N = \max \{v_{ij} \mid i = 1, 2, \ldots m; \ j = 1, 2, \ldots n\}$;

(2) Judging whether there is only one parking demander for a parking seeker, whether one shared

parking space has only one shareable time period, and whether the value of these two factors equals to each other. If so, proceed to the third step. If not, convert the parking demanders and the shareable parking space to only one parking requirement and only one shareable time period, respectively. Setting $b - m\prime$ as virtual parking demanders or setting $b - n\prime$ as shareable parking spaces. The original matrix becomes a b order square matrix, and the weighted satisfaction of the virtual parking demanders or shareable parking space is 0.

(3) The maximum value N of the initial comprehensive satisfaction minus the remaining weighted satisfaction v_{ij} and the converted cost value is l_{fh}.

$Y = [y_{fh}]_{b\times b}$ denotes the decision matrix. If $y_{fh} = 1$, the equation indicates that the consumer D_j' matches the parking space P_h'. If $y_{fh} = 0$, it means other conditions. According to the cost matrix $L = [l_{fh}]_{b\times b}$ and the decision matrix $Y = [y_{fh}]_{b\times b}$, the standard allocation model $M4$ can be constructed as follows:

$$\min z' = \sum_{f=1}^{b}\sum_{h=1}^{b} l_{fh} y_{fh}, \tag{30}$$

$$\text{s.t.} \quad \sum_{h=1}^{b} y_{fh} = 1, \quad f = 1, 2, \ldots, b, \tag{31}$$

$$\sum_{f=1}^{b} y_{fh} = 1, \quad h = 1, 2, \ldots, b, \tag{32}$$

$$y_{fh} \in \{0, 1\}, \quad f, h = 1, 2, \ldots, b. \tag{33}$$

In the model $M4$, the objective function of constraint (30) minimizes the overall opportunity cost. The constraint (31) ensures that a demander only matches a shareable parking space. The constraint (32) guarantees that a parking space can only be assigned to a demander. For the standard allocation model $M4$, it can be solved by the Hungarian algorithm.

In summary, the matching problem solver proposed in this paper has 6 steps (as shown in Figure 2), which considers the maximum efficiency of shared parking spaces and maximizes the satisfaction of the owner.

1st step: matching supply and demand time. The shared parking platform receives demand information from the parking demander and the shared information from the shared parking space, respectively, thereby matching and building the model $M1$ according to the supply and demand time.

2nd step: satisfaction calculation is performed. The parking demanders will submit the expectation level of each attribute of the shareable parking space to the platform. The platform generates the evaluation level of the shareable parking space in terms of the parking space information submitted by the owner of the shared parking space whereby the satisfaction of the demander is calculated.

3rd step: construction of a dual-objective model. A dual-objective optimization model $M2$ that maximizes the utilization of the parking space and the satisfaction of the demander is constructed with the help of the supply and demand time matching model $M1$ as well as the satisfaction of the demander.

4th step: transforming into a single-objective model. By adopting the weighted sum method, the dual-objective model $M2$ is transformed into a single-objective optimization model $M3$ that maximizes the overall weighted satisfaction.

5th step: model standardization is done. Through conducting the specific cases of Hungarian algorithm, the transformation of the original model is therefore described as follows. A parking seeker has only one parking demand, a shareable parking slot has only one shareable time period, and the number of demanders and parking slots is the same.

6th step: establishing a standard allocation model. Transforming the maximization problem into a minimization problem. Establishing the standard allocation model $M4$ by adopting the Hungarian algorithm, thereby obtaining the distribution result.

8. Numerical Experiments

In this section, an example for shared parking is presented to illustrate the implementation of the proposed method. Simulations are performed to test the effectiveness and fairness of the proposed model and of the optimization algorithm, which is conducted by comparing with the first come first serve (FCFS) allocation method.

In order to verify the validity of the proposed model and the optimization algorithm (OA), the simulation experiment is designed according to the idle time characteristics of the parking space in the residential area and compared with the first come first serve (FCFS) allocation method (the result is shown in Figure 3). Taking the parking status of Xi'an for instance, we suppose $D = \{D_1, D_2, \ldots, D_{10}\}$ means 10 parking demanders (the detailed information is shown in Table 1) (this article takes 0.5 hours as an example). $P = \{P_1, P_2, P_3, P_4, P_5\}$ means 5 shared parking spaces in 5 residential areas. The specific information is shown in Table 2.

The shared parking platform provides a level of shared parking space with five attributes, including unit parking cost C_1, time required for the vehicle to reach the parking space C_2, walking distance after parking C_3 (this article in meters), the safety of the parking space C_4, and the priority attribute C_5 (calculated by the historic transaction records, including convenience, confidence, and the surroundings of parking spots). The information of five shared parking spaces is shown in Table 3:

In Table 3, C_1, C_2, and C_3 are quantitative attributes, and the satisfaction degree for C_1 and C_2 is expressed in the form of 1–10 points (1: very bad, 10: very good). Since the distance

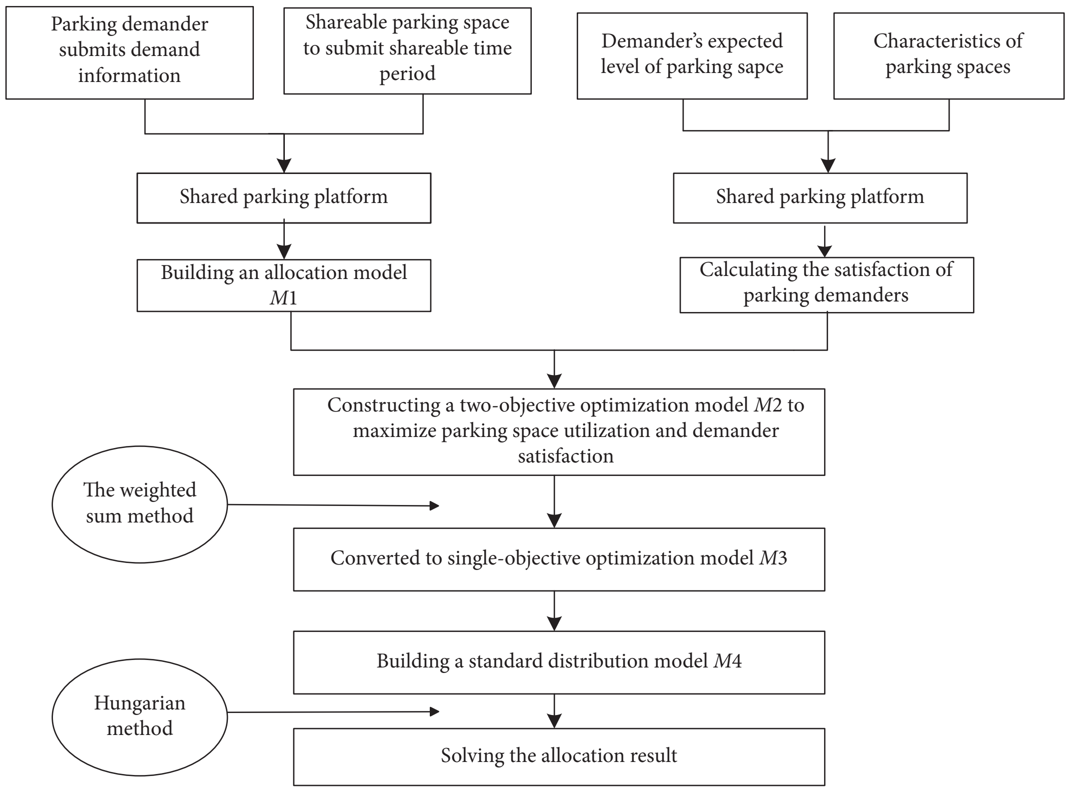

Figure 2: Matching method framework.

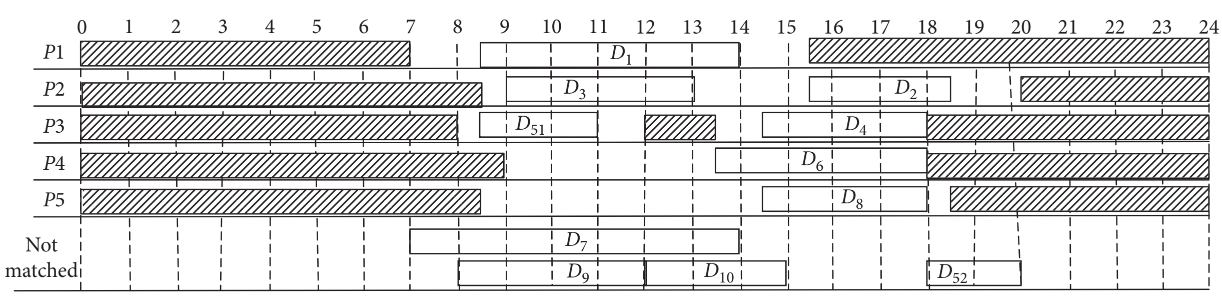

Figure 3: FCFS method assignment result.

Table 1: Parking seekers' time information.

Parking seekers	Parking seekers period	Parking seekers	Parking seekers period
D_1	[8:30, 14:00]	D_6	[13:30, 18:00]
D_2	[15:30, 18:30]	D_7	[7:00, 14:00]
D_3	[9:00, 13:00]	D_8	[14:30, 18:00]
D_4	[14:30, 18:00]	D_9	[8:00, 12:00]
D_5	[8:30, 11:00], [18:00, 20:00]	D_{10}	[12:00, 15:00]

Table 2: Shared parking space sharing time information.

Shared parking space number	Parking space sharing time
P_1	[7:00, 15:30]
P_2	[8:30, 20:00]
P_3	[8:00, 12:00], [13:30, 18:00]
P_4	[9:00, 18:00]
P_5	[8:30, 18:30]

Table 3: Evaluation level of shared parking spaces.

Parking space/attribute	C_1	C_2	C_3	C_4	C_5
P_1	8	8	150	O_3	O_4
P_2	9	8	220	O_4	O_5
P_3	10	9	180	O_3	O_3
P_4	8	10	290	O_4	O_3
P_5	8	9	270	O_4	O_2

Table 4: The demand level of parking seekers for shared parking spaces.

	C_1	C_2	C_3	C_4	C_5
D_1	7	8	[280, 300]	O_3	O_4
D_2	8	7	[300, 350]	O_4	O_3
D_3	9	8	[250, 290]	O_5	O_5
D_4	8	9	[270, 330]	O_4	O_5
D_5	8	9	[230, 300]	O_3	O_4
D_6	10	9	[300, 340]	O_3	O_3
D_7	8	8	[260, 290]	O_5	O_3
D_8	9	9	[200, 350]	O_5	O_5
D_9	5	8	[230, 290]	O_4	O_5
D_{10}	8	7	[270, 300]	O_3	O_3

Table 5: Satisfaction of parking seekers with shared parking spaces.

	P_1	P_2	P_3	P_4	P_5
D_1	1	1	0.93	0.93	0.85
D_2	0.85	1	0.85	1	0.85
D_3	0.63	0.95	0.84	0.64	0.59
D_4	0.56	0.72	0.79	0.90	0.85
D_5	0.72	0.65	1	0.93	0.85
D_6	0.51	0.62	1	0.79	0.64
D_7	0.89	0.95	0.89	0.95	0.80
D_8	0.35	0.67	0.79	0.74	0.59
D_9	0.84	1	0.79	0.90	0.85
D_{10}	1	1	1	1	0.85

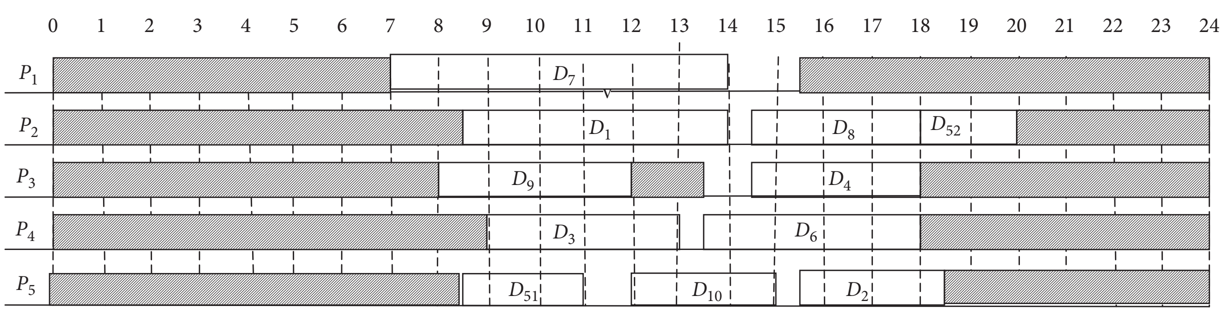

Figure 4: Optimizing the method assignment result.

of walking to the destination after parking is an estimated interval, the value of C_3 is the interval number form. C_4, C_5 attributes are qualitative attributes, where the values of C_4 and C_5 are in the format of linguistic terms in the 7-granularity linguistic terms as follows: $O = \{O_0 =$ absolutely poor, $O_1 =$ very poor, $O_2 =$ poor, $O_3 =$ medium, $O_4 =$ good, $O_5 =$ very good, $O_6 =$ absolutely good$\}$. As shown in Table 4, the parking demander displays the expectation level of the shareable parking space by five attributes of C_1, C_2, C_3, C_4, C_5. In real cases, the expectation value of the demander's walking distance after parking is C_3, which is expressed in intervals.

We assume that the shared parking platform uses AHP to determine the weight vector, where $w = (0.21, 0.28, 0.25, 0.11, 0.15)^T$. The satisfaction level of the demander to the shared parking space can be calculated in terms of the evaluation level of the shared parking spaces in Table 3 and of the expected level of the demanders in Table 4. The calculation results are shown in Table 5.

In line with the rule of equality, we settle $\alpha = 1 - \alpha = 0.5$. Considering the development stage of the shared parking platform, the weights can take different values. By adopting the weighting sum method and the Hungarian algorithm, the supply and demand data are input into the Lingo program for matching operation, thereby obtaining the optimal matching result between the demander and the parking space. The corresponding optimal allocation scheme is shown in Figure 4.

Comparing the abovementioned two results, two parking demanders are not allocated to the shareable parking space. The resource utilization rate stays low and the shared parking space does not reach its expected value in the

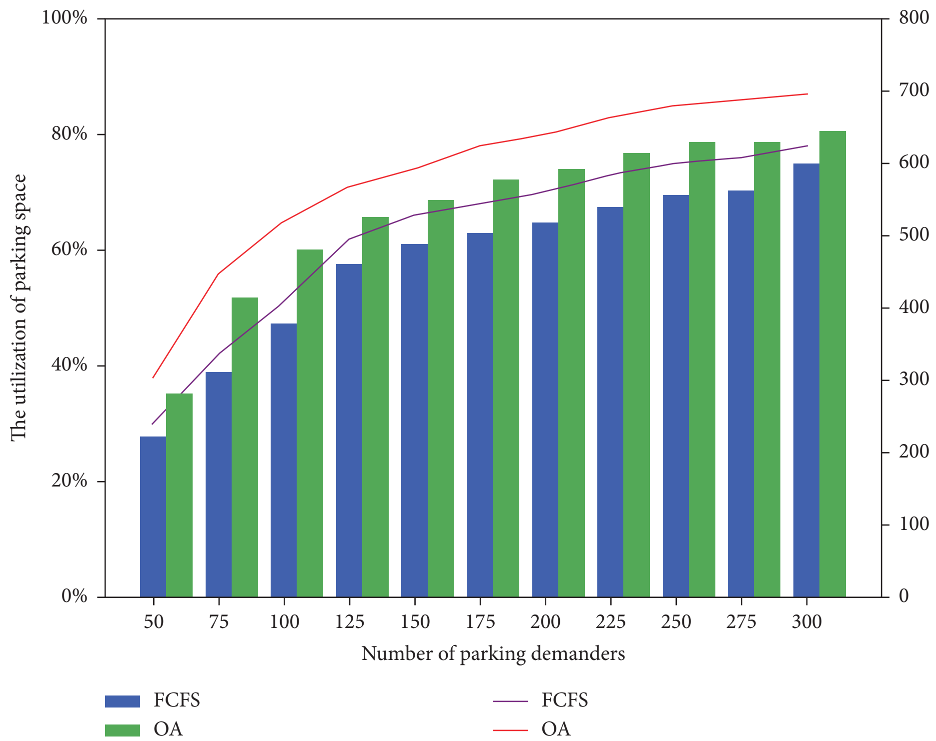

Figure 5: Comparison of parking utilization between FCFS and OA.

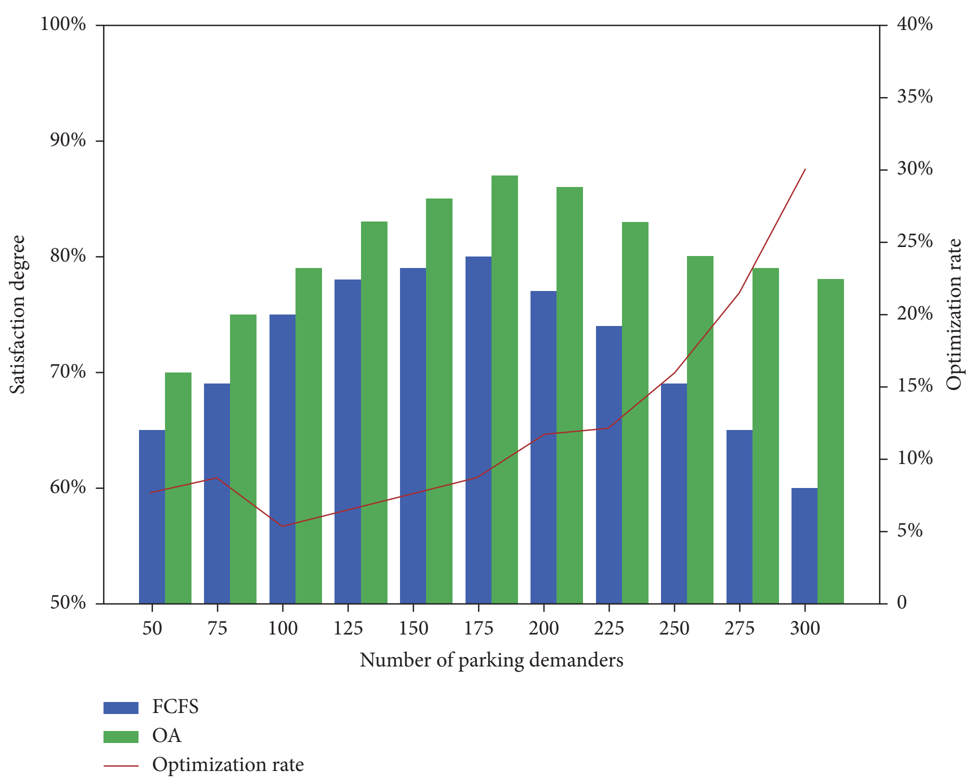

Figure 6: Comparison of parking satisfaction degree between FCFS and OA.

FCFS allocation scheme. Under the same supply and demand conditions, the shared parking space allocation scheme of the proposed paper can increase the parking space utilization time from 26 h to 42 h, and the parking space utilization rate is increased by 33.68%. The satisfaction level is increased from 55.64% to 79.73%, and the parking satisfaction is increased by 24.09%, which meet the requirements of the practical applications.

To further evaluate the feasibility and applicability of the optimization model, simulation experiments are performed between the proposed method and the FCFS allocation method. We suppose the modeling time interval is 0.5 h and the modeling period is 12 h starting from 8:00 AM and ending at 8:00 PM on a typical day. In the basic case, we suppose that a total number of shared parking lots is 100. Furthermore, we suppose that, in any minute during the whole modeling period, the arrival of the parking demander follows a Poisson distribution and parking duration follows a negative exponential distribution, as usually considered in the literature [28, 29]. The utilization efficiency of a parking lot is the ratio of the allocated total periods to the total periods provided by the parking space. The optimization rate of satisfactory degree is the ratio of difference between FCFS and the optimization algorithm (OA) to the satisfactory of FCFS. The environment is based on Python language. The test was repeated 30 times, and the experimental results are shown in Figures 5 and 6.

Simulation results showed that, under same conditions, the matching results of the shared parking space model and the algorithm adopted far outweighed the FCFS allocation method. These findings help the shared parking platform set better targeted policies to optimize indicators involving the parking utilization rate and total preference of the whole system, making breakthroughs in shared parking applications as well as in figuring out the satisfactory solution of parking allocations.

9. Conclusions

As a novel approach alleviating difficulties in car parking in terms of the scarcity of spaces amid urban environment, shared parking has proven an effective mechanism as one of the cornerstones in shared economy. To realize full use of the shared private-owned parking slots and to improve the satisfaction of both demander and supplier sides, this paper presents a novel method determining the satisfied matching between shared parking spaces and parking demanders. Firstly, a time matching model regarding supply and demand is built. Secondly, the preference is divided into three forms by the shared parking platform with regard to the different expressions of the parking preference, through which an optimization model considering the satisfaction degree is therefore constructed and an algorithm is accordingly designed. Thirdly, the superiority of the proposed model is verified and validated by comparing it with the first come first served (FCFS) strategy.

The model is ready to be applied to the shared parking system of Xi'an. The parking space allocation model of this paper is based on the known demand period of the parking demanders and the sharable time of the shared parking space. In reality, the demand of the parking demanders and the shareable time of the shared parking space are changing dynamically. The model can be further extended by considering the priority attributes of demanders and the dynamic matching between the supply and demanders considering bilateral preference, which will be the future interest of our research works.

Data Availability

The data used to support the findings of this study are available from the corresponding author upon request.

Conflicts of Interest

The authors declare no conflicts of interest.

Acknowledgments

This study was financially supported by the National Social Science Foundation of China (Grant number. 15BGL040).

References

[1] C. L. Cao, "Measuring sustainable development efficiency of urban logistics industry," *Mathematical Problems in Engineering*, vol. 2018, Article ID 9187541, 9 pages, 2018.

[2] Z. Peng, Y. Wang, and Q. Chen, "The generation and development of road rage incidents caused by aberrant overtaking: an analysis of cases in China," *Transportation Research Part F: Traffic Psychology and Behaviour*, vol. 60, pp. 606–619, 2019.

[3] C. G. Network, "The first half of 2019, the number of motor vehicles in the country reached 340 million," 2019, http://www.mot.gov.cn/guowuyuanxinxi/201907/t20190704_3221036.html.

[4] Beijing Transportation Development and Research Center, "Beijing traffic development annual report," Beijing Transportation Development and Research Center, Beijing, China, 2019, http://mini.eastday.com/a/190801063939079.html.

[5] C. Lei and Y. Ouyang, "Dynamic pricing and reservation for intelligent urban parking management," *Transportation Research Part C: Emerging Technologies*, vol. 77, pp. 226–244, 2017.

[6] A. J. Pel and E. Chaniotakis, "Stochastic user equilibrium traffic assignment with equilibrated parking search routes," *Transportation Research Part B: Methodological*, vol. 101, pp. 123–139, 2017.

[7] T. Zou, Y. K. Su, and Y. W. Wang, "Research on the hybrid ANP-FCE approach of urban community sustainable construction problem," *Mathematical Problems in Engineering*, vol. 2018, Article ID 8572498, 10 pages, 2018.

[8] Q. Chen, J. Yi, and Y. Wu, "Cellular automaton simulation of vehicles in the contraflow left-turn lane at signalised intersections," *IET Intelligent Transport Systems*, vol. 13, no. 7, pp. 1164–1172, 2019.

[9] Y. Can, C. Qun, and C. Lu, "Modeling and simulation of following behaviors of pedestrians under limited visibility," *Acta Physica Sinica*, vol. 68, no. 24, pp. 87–101, 2019.

[10] M. Yu and T. Li, "Information sharing in a supply chain under cap-and-trade regulation," *Mathematical Problems in Engineering*, vol. 2018, Article ID 4573919, 18 pages, 2018.

[11] S. X. Xu, M. Cheng, X. T. R. Kong, H. Yang, and G. Q. Huang, "Private parking slot sharing," *Transportation Research Part B: Methodological*, vol. 93, pp. 596–617, 2016.

[12] B. Yang, "The study on allocation model of shared parking slots in multi-parking lots," in *Proceedings of the 2017 5th International Conference on Mechatronics, Materials, Chemistry and Computer Engineering*, pp. 457–465, Chongqing, China, July 2017.

[13] H. Stin and J. Resha, *Shared Parking Handbook*, Stein Engineering, Beaverton, OR, USA, 1997.

[14] W. Liu, H. Yang, Y. Yin, and F. Zhang, "A novel permit scheme for managing parking competition and bottleneck congestion," *Transportation Research Part C: Emerging Technologies*, vol. 44, p. 44, 2014.
[15] H. Xiao and M. Xu, "How to restrain participants opt out in shared parking market? a fair recurrent double auction approach," *Transportation Research Part C: Emerging Technologies*, vol. 93, pp. 36–61, 2018.
[16] S. Pan, Z. Liang, and Q. Chen, "When will car owners abandon car driving? analysis based on a survey of the parking experiences of people in Changsha, China," *International Journal of Modern Physics B*, vol. 33, no. 15, p. 1950148, 2019.
[17] C. Shao, H. Yang, Y. Zhang, and J. Ke, "A simple reservation and allocation model of shared parking lots," *Transportation Research Part C: Emerging Technologies*, vol. 71, pp. 303–312, 2016.
[18] Y. Cai, J. Chen, C. Zhang, and B. Wang, "A parking space allocation method to make a shared parking strategy for appertaining parking lots of public buildings," *Sustainability*, vol. 11, no. 1, 2018.
[19] X. T. R. Kong, S. X. Xu, M. Cheng, and G. Q. Huang, "IoT-enabled parking space sharing and allocation mechanisms," *IEEE Transactions on Automation Science and Engineering*, vol. 15, no. 4, pp. 1654–1664, 2018.
[20] J. Hao, J. Chen, and Q. Chen, "Floating charge method based on shared parking," *Sustainability*, vol. 11, no. 1, 2019.
[21] W. Liu, H. Yang, and Y. Yin, "Expirable parking reservations for managing morning commute with parking space constraints," *Transportation Research Part C: Emerging Technologies*, vol. 44, pp. 185–201, 2014.
[22] M. Z. Duan, "Parking spaces allocation model of residential areas sharing parking based on personalized guidance," 2017.
[23] X. Chen, L. Zhao, H. Liang, and K. K. Lai, "Matching patients and healthcare service providers: a novel two-stage method based on knowledge rules and OWA-NSGA-II algorithm," *Journal of Combinatorial Optimization*, vol. 37, no. 1, pp. 221–247, 2019.
[24] X. Chen, Z. Li, Z.-P. Fan, X. Zhou, and X. Zhang, "Matching demanders and suppliers in knowledge service: a method based on fuzzy axiomatic design," *Information Sciences*, vol. 346-347, pp. 130–145, 2016.
[25] A. Charnes and W. W. Cooper, "Goal programming and multiple objective optimizations," *European Journal of Operational Research*, vol. 1, no. 1, pp. 39–54, 1977.
[26] H. W. Kuhn, "The Hungarian method for the assignment problem," *Naval Research Logistics Quarterly*, vol. 2, no. 1, pp. 83–97, 2015.
[27] C. Lawson, "Towards a competence theory of the region," *Cambridge Journal of Economics*, vol. 23, no. 2, pp. 151–166, 1999.
[28] D. E. Cleveland, "Accuracy of the periodic check parking study," *Traffic Engineering*, vol. 33, no. 12, pp. 14–17, 1963.
[29] A. Richardson, "An improved parking duration study method," in *Proceedings of the Australian Road Research Board (ARRB) Conference*, vol. 7, Adelaide, Australia, 1974.

Hindawi
Mathematical Problems in Engineering
Volume 2020, Article ID 5647383, 8 pages
https://doi.org/10.1155/2020/5647383

Research Article

Consumer Purchasing Intentions and Marketing Segmentation of Remanufactured New-Energy Auto Parts in China

Shibin Zhang,[1] Chuhan Zhou ,[1] and Yanran Liu [2]

[1]*School of Management Engineering, Shandong Jianzhu University, Jinan 250101, Shandong, China*
[2]*Tongji University, 1239 Siping Rd., Yangpu District, Shanghai 200092, China*

Correspondence should be addressed to Yanran Liu; yanran_liu@yahoo.com

Received 30 October 2019; Accepted 21 May 2020; Published 2 July 2020

Guest Editor: Roberto Gabbrielli

This study tests and verifies the main factors influencing consumers' intention to purchase and the marketing strategy of remanufactured new-energy automobile parts in China. The revised model of Theory of Reasoned Action is used to study the factors influencing consumers' intention to purchase. The main factors influencing consumer purchase intention of remanufactured new-energy automobile parts in China are identified through correlation analysis of factors including subjective norms, attitudes, face consciousness, brand extension, and perceived risk. Through market segmentation, consumers in China are divided into three types: passive-accepted, brand-driven, and green-consuming; the marketing strategy is developed accordingly. This study provides theory and decision-making basis for remanufactured new-energy automobile parts markets.

1. Introduction

The remanufacturing of new-energy automobile parts using various advanced technologies (for cleaning, repairing, and surface treatment) enables remanufactured products to reach or exceed the performance of the original manufactured parts. Remanufacturing also extends the parts' service life. Remanufactured automobiles are becoming a critical component of the future of the automobile industry, and remanufacturing auto parts has become a resource-saving and cost-cutting strategy for many automobile manufacturers. In 2017, the Ministry of Industry and Information Technology of China began relevant research into formulating a timetable to eliminate the production and sales of traditional-energy vehicles. In fact, many other countries have already established similar timetables for the suspension of selling fossil fuel-powered vehicles. For example, the United Kingdom plans to implement a comprehensive ban on the sale of traditional diesel and petrol vehicles by 2040, while the Netherlands and Norway will ban the sale of fossil fuel-powered vehicles by 2025. Given these clear commitments to banning traditional fuel-powered vehicles from the roads, new-energy vehicles will become the future of the auto industry. However, remanufacturing new-energy auto parts is not yet a common practice in the global markets. Introducing remanufactured new-energy auto parts into the market is a strategic move, as this practice makes the best possible use of resources and materials and helps to achieve the sustainable development of both the economy and the environment. In this study, we take the Chinese market as an example.

Remanufacturing used products is not only an important way to protect the environment and reserve resources; it is also a promising business model in the field of waste recycling. For example, Xerox offers to recycle the toner and ink cartridges used in Xerox printers and copiers, and Kodak's recycling programs include a policy of recycling and reusing postconsumer materials. In fact, both companies have achieved economic benefits through their respective recycling programs [1]. What currently sets Chinese consumers apart is that they still misunderstand and mistrust remanufactured products. For example, they see remanufactured products as defective, refurbished, and inferior, and thus, China's market acceptance of remanufactured products is low [2]. Numerous experts and scholars have been studying these existing issues in marketing remanufactured products, and many empirical research studies have been conducted. However, most of these studies focus on product strategies, pricing strategies, and sales strategies. He and Sun studied the influence of product knowledge on Chinese consumers' intentions to purchase remanufactured products [3, 4]. Liu et al. studied consumer awareness and purchasing behavior of remanufactured products in China [5, 6]. Liu researched the market segmentation of remanufactured products [2]. However, very few scholars have specifically studied consumer purchasing intentions as they relate to remanufactured auto parts.

A consumer's purchasing intention refers to that consumer's attitude toward a specific purchasing behavior and the consumer's degree of willingness to pay. This, essentially, is a signal of consumer purchasing behavior [7]. The reasonable behavior model is considered to be a representative theoretical model and is among the group of prediction models used to analyze consumer behavioral intent. In this paper, we use a modified Theory of Reasoned Action model [8] for guidance in conducting empirical research into the main factors that influence Chinese consumers' intentions to purchase remanufactured new-energy auto parts. The main influencing factors are then used as variables in a two-step clustering analysis, in order to segment the consumer market.

2. Theoretical Models and Research Hypotheses of Factors Influencing Consumers' Intention to Purchase

2.1. Theory of Reasoned Action (TRA) and the Revised Model

2.1.1. Theory of Reasoned Action Model. The Theory of Reasoned Action (TRA) states that subjective norms and attitudes determine behavioral intentions. Meanwhile, one's behavior is the result of specific behavioral intent [9]. Therefore, one's intent is a great tool for predicting individual behavior [10] (Figure 1). Many studies have been conducted on Chinese consumer purchasing intentions using the TRA model. These include the study of consumers' ethical purchasing intentions in a Chinese context [11] and the research into the revision of the TRA model under the influence of Chinese culture [12].

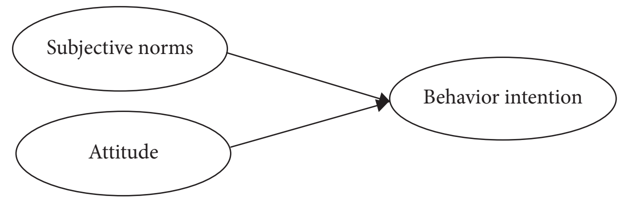

Figure 1: Model 1.

2.1.2. Theory of Reasoned Action Revised Model. Although the TRA model explains consumers' purchasing intentions very well, the model was originally established under the guidance of Western consumer behavior theories. As such, the model might not be suitable for direct use in other social and economic environments [13]. In the meantime, more variables should be taken into consideration, and modification should be made when using the TRA model to study consumers' intentions to purchase different products [2, 14].

Remanufactured auto products are made from sources including wasted and used auto products. As such, consumers' brand recognition of the original manufactured products will have a significant influence on their choice and purchase of remanufactured new-energy auto parts. In other words, the demand for remanufactured new-energy auto parts is closely and directly related to the brand extension effect of the original manufactured products. At the same time, a Chinese consumer's intention to purchase is affected by what is referred to as face consciousness. "Face" refers to one's self-sense of reputation in a social context. Being the first to purchase and use a new product will allow Chinese consumers to gain "face." Remanufactured new-energy auto parts are emerging products in China. As such, the level of social recognition is relatively low. Consumers perceive that there are high risks associated with purchasing remanufactured new-energy auto parts. Therefore, the effect of brand extension, face consciousness, and perceived risk is added to the revised TRA model (Figure 2).

2.2. Hypothesis

2.2.1. Subjective Norms and Chinese Consumer Intentions to Purchase Remanufactured New-Energy Auto Parts. A subject norm is the influence of the surrounding environment on individual behavior. A subject norm can also be described as the external pressure on individuals to perform (or not to perform) in a certain way. Generally speaking, when an individual has a positive attitude and the people around that person agree with his or her behavior, the individual will be more inclined and feel more greatly encouraged to take action. Conversely, negative attitudes and disagreements will lead to a weaker intention and inclination to act. Pollution and a scarcity of natural resources have given rise to the emergence of a special group of consumers who only purchase environment-friendly products. These consumers tend to influence the social norm through their green consumption behavior. Remanufactured products make use of used products and waste materials, which is in line with the government's stated policies regarding environmental protection and sustainable development.

H1: subjective norms are positively associated with Chinese consumer intentions to purchase remanufactured new-energy auto parts.

2.2.2. Attitudes and Chinese Consumer Intentions to Purchase Remanufactured New-Energy Auto Parts. Attitude refers to the comprehensive evaluation of an individual's positive or negative cognition of a certain behavior. Chinese consumer attitudes toward green products are strongly related to their intention to purchase such products [15]. Consumers will first consider cost when they compare original manufactured and remanufactured new-energy

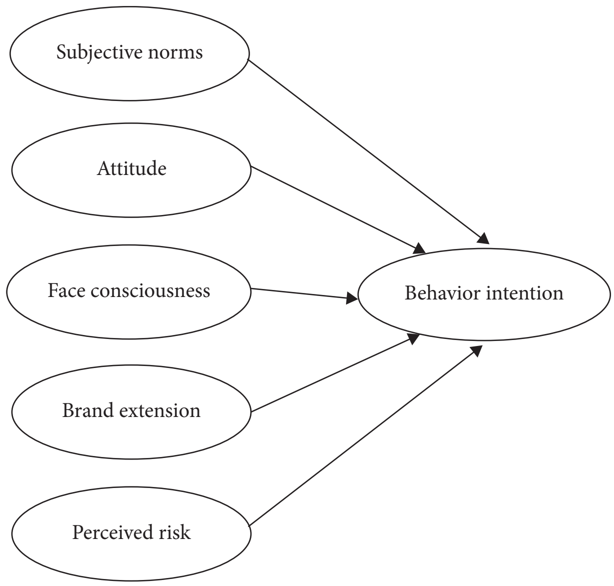

Figure 2: Model 2.

auto parts [16]. Moreover, only when consumers believe in the quality and functionality of remanufactured new-energy auto parts will they make the decision to purchase such parts [17].

H2: attitude is positively associated with Chinese consumer intentions to purchase remanufactured new-energy auto parts.

2.2.3. Face Consciousness and Chinese Consumer Intentions to Purchase Remanufactured New-Energy Auto Parts. The term "face consciousness" refers to an individual's purchasing behavior under the influence of that person's self-sense of reputation in a social context. Chinese people tend to place great value on four main relationship orientations, including respect for authorities, interdependency, group orientation, and "face." Under the influence of traditional Chinese culture, consumer relationships in marketing are categorized into face consciousness and group orientation [12]. Newly introduced products represent new technologies and new market trends. Also, users of new products will earn "face," which may lead to the decision to purchase newly introduced products.

H3: face consciousness is positively associated with Chinese consumer intentions to purchase remanufactured new-energy auto parts.

2.2.4. Brand Extension and Chinese Consumer Intentions to Purchase Remanufactured New-Energy Auto Parts. Using the brand extension strategy when introducing new products or services will help expand market shares, lower marketing costs, and avoid failure in the promotion of those new products or services. In the 1990s, 81% of new products in the United States were successfully introduced into new markets through brand extension strategies [18].

Brand extension has a significant impact on Chinese consumer intentions to purchase remanufactured new-energy auto parts. First of all, when facing a newly introduced product, a consumer will have to refer to the product's brand, merely due to the lack of any information regarding the new product, as well as information asymmetry [19]. At the current stage, remanufactured new-energy auto parts have gained neither the trust nor the recognition of Chinese consumers. Therefore, market acceptance of these new-energy auto parts is still relatively low. However, if remanufactured new-energy auto parts are introduced with brand names with which consumers are familiar, the products will become more acceptable and less concerning to consumers. Moreover, remanufactured new-energy auto parts have equivalent or higher quality than the original manufactured products. When consumers are provided with products that have the same or higher quality and brand but lower prices, they tend to make repeat purchases because of their familiarity with the brand [20].

H4: brand extension is positively associated with Chinese consumer intentions to purchase remanufactured new-energy auto parts.

2.2.5. Perceived Risk and Chinese Consumer Intentions to Purchase Remanufactured New-Energy Auto Parts. The concept of perceived risk was first put forward by Bauer, who stated that consumer-perceived risk affects not only consumers' purchasing activity but also their postpurchase processes. This is due to the asymmetry of information and for other reasons [21]. Subsequent research studies prove that perceived risk is negatively related to consumer purchasing intentions [22].

The perception of risk exists throughout the activities that occur both before and after the purchase of remanufactured new-energy auto parts. On the one hand, consumers' perception of risk before purchasing remanufactured new-energy auto parts is very high, due to the current lack of product recognition and market acceptance. On the other hand, certain differences do indeed exist between remanufactured new-energy auto parts and original manufactured auto parts [23]. Consumers perceive risk and have concerns about remanufactured new-energy auto parts due to an insufficient supply of information [24]. Consumers believe that remanufactured products are refurbished products, inferior products, defective products, products with quality defects, etc., and the market acceptance is not high [25–27].

H5: perceived risk is negatively associated with Chinese consumer intentions to purchase remanufactured new-energy auto parts.

3. Design of Consumer Market Research

3.1. Research Methods. Information and data on the subject norm, attitudes, face consciousness, brand extension, and perceived risk were collected through questionnaires. Analysis of the correlation between variables and comparisons between different theoretical models were conducted using SPSS 20.0. We used a two-step clustering algorithm by AMOS 17.0, in order to segment the target market.

3.2. Sample Selection. The questionnaire was distributed and the answers were collected using online software in this research. Of the 394 distributed questionnaires, all 394 were recovered, and 358 were deemed to be valid and effective. Among the respondents, 52.65% were male and 47.35% were female; 12.36% have obtained a three-year college degree and below, while 56.83% have obtained a Bachelor's degree, and 30.81% have obtained a Master's degree or above.

3.3. Variables Measurement. This design of this questionnaire on consumer intentions to purchase is based on the characteristics of remanufactured new-energy auto parts, combined with established theories and relevant documents. A Likert 5-point scale is used to express the degree to which respondents agree and disagree with statements on the questionnaire.

The measurement of attitude is mainly drawn from Bagozzi's research. The statements for this category include "I feel that purchasing remanufactured new-energy auto parts is a correct action" and two other items [28]. The measurement of brand extension is mainly drawn from Coulter's research. Here, the statements in the questionnaire include "I would love to purchase remanufactured new-energy auto parts that have been introduced by the brands I am familiar with" and two other items [29]. The measurement of perceived risk is mainly drawn from Dodds' research. The statements to which the respondents were asked to rank include "The quality and performance of remanufactured new-energy auto parts are more likely to cause issues, thus causing economic losses," and three other items [30]. The measurements of subjective norm and purchase intention are mainly drawn from Lee's research. The statements for subjective norm measurement include "In my opinion, my family members want me to purchase remanufactured new-energy auto parts" and two other items. The statements used for purchase intention measurement include "In my next purchase, I will choose remanufactured new-energy auto parts" and another item [31]. Finally, for face consciousness measurement, the statements used include "I will get applause from others for purchasing remanufactured new-energy auto parts" and three other items.

4. Consumer Market Survey Data Testimony and Analysis

4.1. Reliability Test. Cronbach's α is used to measure the reliability level. This test indicates the overall consistency of the measurements within each variable in the questionnaire. Six factors are formed based on the results, including subjective norm, attitude, face consciousness, brand extension, perceived risk, and purchasing intention. The accumulated variance contribution rate is 71.90%, the KMO value is 0.892, and Cronbach's α value of each factor exceeds 0.7 (subjective norm 0.909, attitude 0.775, face consciousness 0.910, brand extension 0.867, perceived risk 0.904, and purchase intention 0.927). These results show that all measurements of all the relevant variables are reliable.

4.2. Validity Test. A validity test was also conducted, because the scale items passing the reliability test may be invalid. In this research, a confirmatory factor analysis of all relevant variables is conducted through AMOS 17. The results of this analysis show that, compared to other models, the five-factor model has the best fit in this study and also indicates better discriminant validity (χ^2 $(55) = 65.19$, $p < 0.01$; $RMSEA = 0.045$, $AGFI = 0.907 > 0.80$, $CFI = 0.945 > 0.90$, and $N\text{-}N\ FI = 0.938 > 0.90$).

In terms of content validity, the questions used in this research were designed based on established theories, advice from experts and professionals, and research studies on related fields, in combination with the characteristics of remanufactured new-energy auto parts. Therefore, the scale items have high content validity.

Based on the results, the scale items used in this study have high reliability and validity.

5. Consumer Intentions to Purchase and Marketing Segmentation of Remanufactured New-Energy Auto Parts

5.1. Factors Influencing Consumer Intentions to Purchase Remanufactured New-Energy Auto Parts

5.1.1. Correlation Analysis. The following results were obtained via SPSS 20.0 correlation analysis: subjective norm is positively correlated with purchase intention ($r = 0.421^{**}$, $p < 0.01$). Attitude is positively correlated with purchase intention ($r = 0.439^{**}$, $p < 0.01$). Face consciousness is positively correlated with purchase intention ($r = 0.324^{**}$, $p < 0.01$). Brand extension is positively correlated with purchase intention ($r = 0.0.408^{**}$, $p < 0.01$). Perceived risk is negatively correlated with purchase intention ($r = -0.189^{**}$, $p < 0.01$).

5.1.2. Theoretical Model Structural Equation Analysis. Structural equations are used to compare the fit of the two theoretical models and the collected data. The results of the AMOS analysis show that both models are a good fit:

(i) Model 1: $\chi 2/df = 5.197$, $RMSEA = 0.095$, $GFI = 0.952$, and $CFI = 0.902$

(ii) Model 2: $\chi 2/df = 4.564$, $RMSEA = 0.091$, $GFI = 0.955$, and $CFI = 0.902$

When comparing the two models, it can be seen that Model 1 has higher $\chi 2/df$ value and higher RMSEA value, which indicates that Model 2 fits better. In order to clarify the correlation between the variables, path diagrams of both models are created (Figures 3 and 4).

Figure 3 shows that the path coefficient of the subjective norm is 0.32, while the path coefficient of attitude is 0.37. Figure 4 shows that the path coefficients are as follows: subjective norm is 0.23; attitude is 0.18; face consciousness is 0.08; brand extension is 0.37; and perceived risk is −0.07.

The Theory of Reasoned Action Revised model (Model 2) fits better than the Reasoned Action model (Model 1). The factors proposed in the revised model (including subjective norm, behavioral attitudes, face consciousness, brand

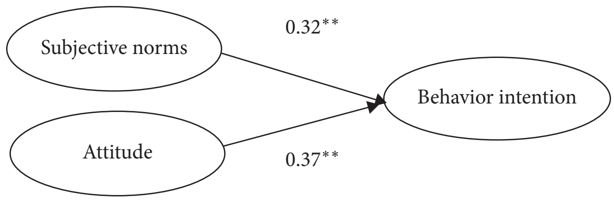

Figure 3: Path diagram of Model 1. ** indicates the significance level at 1%.

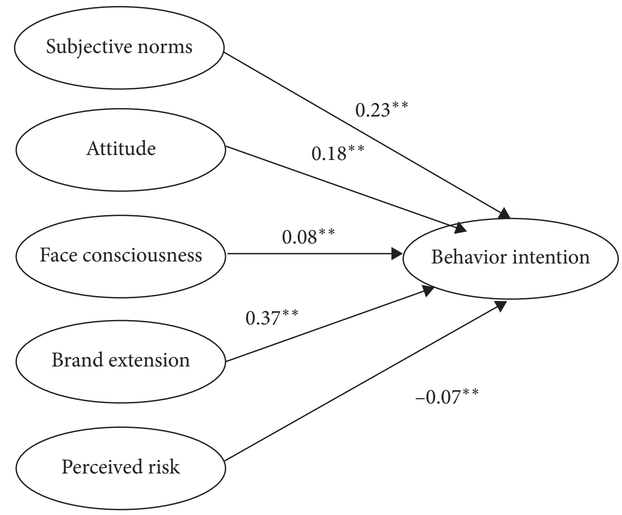

Figure 4: Path diagram of Model 2. ** indicates the significance level at 1%.

extension, and perceived risk) all have a significant influence on Chinese consumer intentions to purchase remanufactured new-energy auto parts (Table 1).

5.2. Marketing Segmentation of Remanufactured New-Energy Auto Parts. First of all, a cluster analysis is conducted, and the influencing factors, including subjective norm, attitudes, face consciousness, brand extension, and perceived risk, are segmented into discrete groups. Secondly, the two-step cluster analysis is used to segment the consumer markets. The best classification is also determined by the value change of distance between the BIC value and the AIC value. Finally, market segmentation is determined, and the results of the cluster analysis are verified. In this research, consumers are segmented into three types, with silhouette value >0.4, which suggests a good quality of clustering analysis [32].

5.2.1. Passive-Accepted. This type of consumer has a subjectively low purchasing intention and is highly influenced by social norms. This type of consumer shows relatively high scores in the areas of subjective norm and face consciousness, but they have low scores in other factors. One reason for these findings is that these consumers either do not care about or have not recognized the environmental value of remanufactured new-energy auto parts. They are also extremely sensitive to the perceived risks, and thus, they have a negative purchasing attitude. The second reason is that the consumers in this group are older, and it will probably take longer for them to accept new products. Another reason is that the consumers in this group pay special attention to their reputation and social status; they are greatly influenced by social norms and face consciousness. In this study, more than half of the consumers in this group work for private businesses.

5.2.2. Brand-Driven. This type of consumer attaches great importance to the product brand. As shown in Table 2, more than 90% of the consumers in this group are college students. The high score in subjective norm suggests that college students are more concerned with others' opinions and social norms. College students have a very positive attitude with regard to purchasing remanufactured new-energy auto parts, so the attitude score of this group is relatively high. However, no sufficient evidence exists to show that they consider such consumption behavior to be honorable. This group has a relatively high score in perceived risk and shows significant care for the quality and performance of remanufactured new-energy auto parts.

5.2.3. Green-Consuming. This group of consumers has a decent understanding of the economic, social, and environmental benefits of remanufactured new-energy auto parts. The results of the analysis of consumer perceived risk, subjective norm, and attitude all show positive numbers. Conversely, the results for brand extension and face consciousness both present negative numbers. Although green consumers know about the risks of purchasing remanufactured new-energy auto parts, their general perception is that there are in reality few risks, and they are subjectively willing to purchase the products for the greater eco-environmental value. In all, 47% of the consumers in this group work either for the government or in state-owned enterprises, and they are generally better off. The purchase potential of this group is huge, given their high level of environmental consciousness. Therefore, this group of consumers should be one of the target markets for the remanufactured new-energy auto parts industry.

6. Contribution and Implications

6.1. Contribution. The research conclusions of this paper are shown in Table 3.

6.2. Implications

(1) Establishing a social credit system will create a friendly market environment for remanufactured new-energy auto parts in China, even though the "Remanufactured Units Quality and Technical Control Regulations (TRAIL)" stipulate that remanufactured products must meet the same quality and performance standards as original manufactured products. In spite of this, many consumers still consider remanufactured products to be inferior to the original manufactured versions. This is because consumers do not trust the manufacturers enough, due to the inefficiency of the social credit system. Therefore, the establishment and implementation of

Table 1: Research hypothesis conclusion.

Number	Hypothesis	Conclusion
1	Subjective norms are positively associated with Chinese consumer intentions to purchase remanufactured new-energy auto parts.	Yes
2	Attitude is positively associated with Chinese consumer intentions to purchase remanufactured new-energy auto parts.	Yes
3	Face consciousness is positively associated with Chinese consumer intentions to purchase remanufactured new-energy auto parts.	Yes
4	Brand extension is positively associated with Chinese consumer intentions to purchase remanufactured new-energy auto parts.	Yes
5	Perceived risk is negatively associated with Chinese consumer intentions to purchase remanufactured new-energy auto parts.	Yes

Table 2: Consumer market segmentation of remanufactured new-energy auto parts.

Type		Passive-accepted					Brand-driven					Green-consuming				
Factor score		SN	A	FC	BE	PR	SN	A	FC	BE	PR	SN	A	FC	BE	PR
Avg.		1.23	−1.82	0.86	−0.53	−0.7	1.02	0.73	−0.13	1.42	−0.35	0.78	0.21	−0.47	−0.09	0.46
Stats.	%	162 people −45.20%					97 people −27%					99 people −27.80%				
	Avg. age	40					20					25				
	Avg. annual income (¥)	150,000					20,000					80,000				
	Occup.	Company employees or managers					Students					Government officers or SOE employees				
	Dist.	94 people (58.02%)					88 people (90.72%)					47 people (47.47%)				

Table 3: Analysis conclusion.

Number	Conclusion	Explanation
1	The theory of reasoned action model shows a certain degree of cross-cultural adaptability.	However, the model needs to be modified when applied to different social and economic environments and to different research objects [33]. In this study, Model 1 proves the validity of the TRA model, while Model 2 is better suited to explaining consumer intentions to purchase remanufactured new-energy auto parts in China.
2	The factors of subjective norm, attitude, face consciousness, and brand extension are positively associated with Chinese consumer intentions to purchase remanufactured new-energy auto parts.	Conversely, perceived risk is negatively associated with Chinese consumer intentions to purchase remanufactured new-energy auto parts. The one special exception is that of the green consumers, with whom the perceived risk is positively associated with purchasing intentions. This is due to the fact that this group of consumers is highly aware of the environmental benefits of remanufactured new-energy auto parts and is therefore willing to bear the perceived risks [34].
3	Brand extension is the most important factor that influences Chinese consumer intentions to purchase remanufactured new-energy auto parts. This factor has the highest coefficient (0.37) with purchase intention in the path diagram.	Remanufactured new-energy auto parts are emerging products in the Chinese market, and they have not yet been fully accepted and recognized by Chinese consumers. In the current market situation, leveraging the recognition and trust of established brands will help the providers of remanufactured products to gain consumer trust and thus increase the level of consumers' intentions to purchase remanufactured new-energy auto parts [19].
4	According to the analysis detailed above, consumers of remanufactured new-energy auto parts should be segmented into three types, namely, passive-accepting, brand-driven, and green-consuming.	Different marketing strategies should be provided and based upon different consumer needs and characteristics. Among all types of consumers, the passive-accepting consumer group is the largest. This finding indicates low consumer acceptance of remanufactured products at the current stage. On the other hand, green consumers should be the target market for suppliers of remanufactured new-energy auto parts [35]. A same conclusion is also obtained in the authors' another research on consumers' purchase intention on remanufactured products [33].

a social credit system should be speeded up, so that enterprises can operate with increasing integrity. At that stage, consumers will have proper guidance and adequate trust and belief in the manufacturers when purchasing remanufactured products.

(2) Increasing publicity will enhance market acceptance of remanufactured new-energy auto parts. On the one hand, actively carrying out a public service will increase the awareness of consumer social responsibility. Advocating green consumption will also help remanufactured new-energy auto parts to attract more attention. On the other hand, increasing the level of the promotion of remanufactured products will also encourage price-sensitive consumers to purchase remanufactured products.

(3) Relevant parties must ensure that the quality of remanufactured new-energy auto parts is as good as or better than the original parts. When that happens, the level of consumer perceived risk reduces. Not only should manufacturers provide good quality remanufactured auto parts at reasonable prices, but they should also provide after-sale services, such as maintenance and repairs. At the same time, the government should strengthen the supervision and control of the quality of remanufactured new-energy auto parts and remove any unqualified products from the remanufactured products market.

(4) Leveraging the trust and recognition of established brands to promote remanufactured new-energy auto parts is possibly the best way to market remanufactured new-energy auto parts in the Chinese market. Evidence clearly shows that brand extension is a critical factor that influences consumer purchasing intentions. Therefore, new-energy auto parts that have been remanufactured by the original parts manufacturer would make those parts more acceptable to Chinese consumers. Therefore, it is necessary to encourage more original product manufacturers to participate in the recycling, reusing, and remanufacturing of waste products. This could be done by enforcing extended producer responsibility.

(5) Different marketing strategies should be used for different market segments. Consumer needs vary and therefore, market strategies should diversify accordingly. Meanwhile, a strategy should be adopted that concentrates on green consumers, thus gradually developing consumer loyalty to remanufactured new-energy auto parts. Such a strategy would drive passive-accepting and brand-driven consumers to accept remanufactured new-energy auto parts.

Data Availability

The data used to support the findings of this study are available from the corresponding author upon request.

Conflicts of Interest

The authors declare that they have no conflicts of interest.

Acknowledgments

The authors would like to thank the National Social Science Fund of China (Grants nos. 15ZDC030 and 12AZD104), the PhD Fund of Shandong Jianzhu University (Grant no. XNBS1828), and Social Science Planning Research Project of Shandong Province (Grant no. 20CGLJ18) for their support in this research.

References

[1] L. B. Toktay, L. M. Wein, and S. A. Zenios, "Inventory management of remanufactures able products," *Management Science*, vol. 46, no. 11, pp. 1412–1426, 2000.

[2] G. Liu, S. Zhang, and S. Lu, "Top-level design mechanisms of intellectual property rights in Chinese renewable resources industry," *Science of Science And Management of S.& T*, vol. 35, no. 100, pp. 3–12, 2014, in Chinese.

[3] W. He, "Interactive relations of product knowledge on the purchase intention to remanufacturing products in China: an experiment analysis," 2013.

[4] X. Sun, "Research on the impact of product knowledge on chinese consumers' purchase intention of remanufacturing products," 2012, in Chinese.

[5] H. Liu, L. Liang, H. Zhang, and W. Li, "Study on consumers' awareness and purchases behavior of remanufactured products in China," *Operation Research and Management Science*, vol. 18, no. 11, pp. 159–163, 2009, in Chinese.

[6] H. Zhang, "Research on purchase intention of Chinese remanufactured products consumers," 2011, in chinese.

[7] A. H. John and N. S. Jagsish, *Theory of Buyer Behavior (Marketing)*, John Wiley & Sons, New York, NY, USA, 1969.

[8] M. Fishbein, *Readings in Attitude Theory and Measurement*, John Wiley & Sons, New York, NY, USA, 1967.

[9] I. Ajzen, "Perceived behaviroral control, self-efficacy, locus of control, and the theory of planned behavior," *Journal of Applied Social Psychology*, vol. 32, no. 4, pp. 665–682, 2002.

[10] M. Fishbein and I. Ajzen, *Belief, Attitude, Intention, and Behavior: An Introduction to Theory and Research*, Addison-Wesley, Reading, MA, USA, 1975.

[11] X. Deng, "Consumers' ethical purchasing intention in Chinese context: based on TPB perspective," *Nankai Business Review*, vol. 15, no. 3, pp. 22–32, 2012.

[12] D. Li, B. Wu, and R. Wu, "The model of the purchase intention of chinese consumers," *Management World*, vol. 14, no. 1, pp. 121–129, 2009, in Chinese.

[13] L. Zhang, "Applicability of fishbein model and impacts of acculturation: a study of foreign-brand mobile phone buying intentions," *Journal of Management Science*, vol. 20, no. 1, pp. 30–37, 2007, in Chinese.

[14] R. Y. K. Chan, Y. H. Wong, and T. K. P. Leung, "Applying ethical concepts to the study of "Green" consumer behavior: an analysis of Chinese Consumers' intentions to bring their own shopping bags," *Journal of Business Ethics*, vol. 79, 2007.

[15] R. Y. K. Chan, "Determinants of Chinese consumers' green purchase behavior," *Psychology and Marketing*, vol. 18, no. 4, pp. 389–413, 2001.

[16] S. P. Hutchens, *Consumer Attitudes toward Remanufactured Products as a Form of Recycling*, University Microfilms International, Fayetteville, AR, USA, 1982.

[17] J. D. Abbey, M. G. Meloy, V. D. R. Guide, and S. Atalay, “Remanufactured products in closed-loop supply chains for consumer goods,” *Production and Operations Management*, vol. 24, no. 3, pp. 488–503, 2015.

[18] Y. Yuan, D. Dong, R. Liu, and D. Yu, “Review of the mechanism of consumer evaluations on brand extensions,” *Forecasting*, vol. 28, no. 4, pp. 1–7, 2009, in Chinese.

[19] S. Wu and T. Lu, “An empirical study: effects of corporate brand and its product brand on purchase intention,” *Chinese Journal of Management*, vol. 6, no. 1, pp. 112–117, 2009, in Chinese.

[20] J. Chai and D. Wan, “Review of the advantages and disadvantages of brand extention and brand extension performance,” *Forecasting*, 2004.

[21] R. A. Bauer, “Consumer behavior as risk taking. Hancock: dynamic marketing for a changing world,” in *Proceedings of the 43rd. Conference of the American Marketing Association*, American Marketing Association, Chicago, IL, USA, 1960.

[22] S. Ye, H. Chen, X. Shen, and Y. Li, “An emperical analysis of factors influencing consumers’ online shopping,” *Forecasting*, vol. 27, no. 4, pp. 53–58, 2008, in Chinese.

[23] A. N. Atasu, M. Sarvary, and L. Van Wassenhove, “Remanufacturing as a marketing strategy,” *Management Science*, vol. 54, no. 10, pp. 1731–1746, 2008.

[24] G. R. Dowling and R. Staelin, “A model of Perceived risk and intended risk-handling activity,” *Journal of Consumer Research*, vol. 21, no. 1, p. 119, 1994.

[25] V. V. Agrawal, A. Atasu, and K. Van Ittersum, “Remanufacturing, third-party competition, and consumers’ perceived value of new products,” *Management Science*, vol. 61, no. 1, pp. 60–72, 2015.

[26] S. Ganesan, “Determinants of long-term orientation in buyer-seller relationships,” *Journal of Marketing*, vol. 58, no. 2, pp. 1–19, 1994.

[27] Y. Liu and S. Zhagn, “Research on intellectual property sharing path between original manufacturer and third party remanufacturer,” *Science & Technology Progress and Policy*, vol. 35, no. 6, pp. 122–130, 2018, in Chinese.

[28] R. P. Bagozzi, K. H. Lee, and M. F. Van Loo, “Decisions to donate bone marrow: the role of attitudes and subjective norms across cultures,” *Psychology and Health*, vol. 16, no. 1, pp. 29–56, 2001.

[29] R. Coulter and G. Zaltman, “Seeing the voice of the customer: metaphor-based advertising research,” *Journal of Advertising Research*, vol. 35, no. 4, pp. 35–51, 1995.

[30] B. W. Dodds, K. B. Monroe, and D. Grewal, “Effects of price, brand, and store information on buyers’ product evaluations,” *Journal of Marketing Research*, vol. 28, no. 3, p. 307, 1991.

[31] C. Lee and R. T. Green, “Cross-cultural examination of the Fishbein behavioral intentions model,” *Journal of International Business Studies*, vol. 22, no. 2, pp. 289–305, 1991.

[32] Z Chen, W. Gao, and P. Xie, “Green lifestyle, green attitude toward products and purchase intenton,” 2014.

[33] G. Liu, S. Zhang, and C. Men, “Research on consumers’ purchase intention on remanufactured products and marketing strategy,” *Forecasting*, vol. 34, no. 40, pp. 27–33, 2015, in Chinese.

[34] B. Jiménez-Parra, S. Rubio-Lacoba, and A. Vicente-Molina, “An approximation to the remanufactured electrical and electronic equipment consumer,” in *Proceedings of the 6th International Conference on Industrial Engineering and Industrial Management*, Springer, London, UK, pp. 433–440, 2012.

[35] R. Hammond, T. Amezquita, and B. Bras, “Issues in the automotive parts remanufacturing industry: a discussion of results from surveys performed among remanufacturers,” *Engineering Design and Automation*, vol. 4, no. 1, pp. 27–46, 1998.

Hindawi
Mathematical Problems in Engineering
Volume 2020, Article ID 4571890, 14 pages
https://doi.org/10.1155/2020/4571890

Research Article

Risk Influencing Factor Analysis of Urban Express Logistics for Public Safety: A Chinese Perspective

Mingjing Zhao[1] **Shouwen Ji**[1] **Qianru Zhao,**[1,2] **Cheng Chen,**[3] **and Zhen-Lin Wei**[1]

[1]*School of Traffic and Transportation, Beijing Jiaotong University, Beijing 100044, China*
[2]*Beijing Jiaotong University Haibin College, Cangzhou, Hebei 061199, China*
[3]*School of Mechanical-Electronic and Vehicle Engineering, Beijing University of Civil Engineering and Architecture, Beijing 100044, China*

Correspondence should be addressed to Shouwen Ji; shwji@bjtu.edu.cn

Received 10 December 2019; Revised 16 April 2020; Accepted 5 May 2020; Published 17 June 2020

Academic Editor: Mosè Gallo

Due to the uncertainty and complexity of multilinks and multifactors in urban express logistics system, it is very difficult to analyze the risk factors and the correlation among them for urban public security. In this paper, a method combining domain knowledge and data learning is proposed to construct Bayesian network, which can effectively deal with this problem. Based on the literature review and the investigation of transportation companies, this paper summarizes the risk factors to public safety caused by pick up, warehouse storage, transport, and the end distribution in the process of urban express logistics, which are divided into 5 dimensions: management, weather, human, transportation tools and facilities, and goods, including 11 risk factors. In this paper, Interpretative Structural Model is used to construct the initial hierarchical model to describe the complex relationship between factors, and then causal mapping method is used to improve the initial model to transform the structure into the final Bayesian network model. Finally, the sensitivity of one node to other nodes is analyzed based on the incident data. The results show that Bayesian network is effective in improving urban express logistics operation ability and avoiding public safety risks and has a strong generalization ability, which is simple and easy in practical application.

1. Introduction

Taniguchi et al. [1] defined urban logistics as "in the market economy, considering the urban traffic environment, traffic congestion, and energy consumption, while private enterprises to achieve the overall optimal logistics and transport activities process." Based on the national conditions of China, this paper gives the definition of urban logistics: urban logistics is an activity that takes improving the competitiveness of a city as the core, realizes the optimization of urban logistics and transportation activities through the application of advanced information technology, and tries to reduce the negative impact of logistics activities on urban traffic congestion, traffic environment, and energy consumption. The operation process of urban express logistics involves many links, such as pick up, warehouse storage, transport, and the end distribution, during which the business status is diverse and the risk factors are numerous, which can easily threaten the public security of the city. The risk of urban public security refers to the force majeure and the possibility of objective existence that threaten the basic values, norms, and interests of urban public domain [2]. The control of urban public security risks should prevent risks and potential harm caused by public security incidents from the source of risk factors.

The risks of urban logistics to public security are mainly manifested as vehicle collision and explosion, warehouse fire and explosion, contraband transportation, burglary, and assault by courier. Frequent in recent years, the Chinese express logistics accidents caused a great deal of personnel and property losses. However, there is no unified system of the research on the risk factors affecting the public security of urban express logistics. At present, most of the research studies focus on the single risk of a certain logistics link, such as the hidden danger in the process of transportation [3, 4] and fire risk in logistics storage [5] or the internal risk analysis of logistics enterprises, such as the risk cost of logistics enterprises [6], logistics outsourcing risk [7], and project logistics risk [8]. There is no systematic study on the risks and hidden dangers of the whole logistics link to public security. The analysis of risk factors is the primary part of accident prevention because it can provide operational information for logistics-related enterprises and management departments. They can focus on the potential risks and take preventive measures.

At present, risk-based research is generally concentrated in the fields of automobile collision, coal mine, transportation of dangerous goods, and aviation. Commonly used risk research methods include BP neural network [9], fuzzy comprehensive evaluation method [10], analytic hierarchy process (AHP) [11, 12], and Bayesian network (BN) [13, 14], focusing on the evaluation of risk, but lack of risk identification and control research. Other traditional risk research methods are fault tree analysis (FTA) [15], probability theory [16], Swiss cheese model, human factor analysis, and classification system (HFACS) [17]. However, the various influencing factors in these methods are independent. In reality, these factors are often related to each other.

Based on the above problems, this paper adopts the method of literature review and the survey of transportation companies to divide the factors that affect the risk of urban logistics into five dimensions: management, weather, human, transportation tools and facilities, and goods, including 11 influencing factors. The impact factors of urban logistics on public safety risk are analyzed by using Interpretative Structural Model (ISM), and the initial network model is established. Then, the initial model is transformed into BN model by using causal mapping method. The sensitivity of specific nodes to other nodes is obtained, and the relationship between risk factors of urban logistics is identified. It helps managers to enhance the scientific nature of risk management decisions, provides a new basis for improving the operational stability of urban logistics, helps to reduce the occurrence of urban public security incidents, and alleviates the potential loss of risks to society, economy, and environment.

The rest of this paper is organized as follows: Section 2 presents the historical research on risk identification and ISM. Section 3 introduces the basic theory including BN and ISM. Section 4 constructs a Bayesian network model and analyzes the sensitivity of each node. Section 5 discusses the advantages and future development of this study. Section 6 provides our conclusions.

2. Literature Review

Most of the previous research studies that analyzed the factors responsible for urban logistics accidents used a statistical method. The researchers primarily limited to the collection, analysis, and interpretation of data from accident reports or accident databases [13]. Ren [5] analyzed in a large number of fire accidents of logistics warehouses reveal four factors that affect the fire risk: warehouse building, commodity, management, and environment. Zhao et al. [13] collected 94 cases of dangerous goods transportation accidents and adopted the expectation maximization algorithm to derive three main risk factors affecting hazardous materials transportation: human factors, transportation vehicles and facilities, and packaging and loading of dangerous goods. Chen and Liu [18] analyzed the data of logistics road transportation accidents and concluded that the main risk factors include personnel factors, vehicle factors, and road factors. They used the Delphi method to make qualitative analysis of the potential accident, effectively helping the security management personnel of logistics enterprises to recognize the causes and potential problems of truck accidents and take precautions in advance.

Although statistical methods can be used to obtain the accident influencing factors, it cannot explain the connection between the different factors and the important role of key factors in accidents. In recent years, BN has been widely used in economic analysis [19], biological genetic [20], medical diagnosis [21], mechanical engineering [22], civil engineering [23], transportation [24], computer science [25], mining accidents [26], and other fields. BN is also applicable to the field of logistics. Aiming at the limitation that complex logistics service supply chain system is difficult to carry out reliability analysis in the face of a lot of uncertain fuzzy information, Cai and Liu [27] proposed a reliability analysis method of polymorphic system combining Bayesian network and fuzzy set theory. The reliability analysis efficiency of logistics system is improved and theory and data support for logistics enterprises are provided to improve the weak links. Yan and Suo [28] identified and classified the risks of logistics financial business, took the failure of enterprises as the root node, constructed a Bayesian network to measure the risk level of enterprises, and found the most critical risk factors by calculating several important indicators. Zhu and Yang [29] constructed the early warning index system of agricultural products logistics by using Bayesian network, designed the early warning model, and realized the early warning of agricultural products cold chain logistics.

As far as we know, there are few research papers on the application of BN in logistics risk factor analysis, such as Li et al. [30] based on factor analysis to determine the effect of emergency logistics risk factors. The factors are divided into human factor, equipment factor, materials factor, environment factor, and supervision factor. And the Bayesian network of emergency logistics risk is established. The prior probability and the posterior probability can be used to find the weak links of logistics and realize the rapid positioning of logistics risk. Huang and Qian [31] analyzed the main faults in the process of cold chain transportation using Bayesian network, summarized the influence of different factors on the faults, and provided an effective method for improving the fault analysis and prevention in the process of cold chain transportation.

However, these literature studies only apply BN model to logistics risk and do not discuss how to establish BN model of logistics for public security. This paper proposes a method to construct BN by means of ISM and causal mapping method and conducts sensitivity analysis on risk factors of urban logistics for public security. The relationship among the factors and the important influencing factors are obtained, and the corresponding methods for accident prevention are put forward.

3. Methodology

3.1. Bayesian Network. Bayesian network is a network combining probabilistic inference and graph. It encodes the probabilistic relationship between the variables of interest. BN can provide a rational and coherent theory under various conditions of uncertainties (e.g., uncertainty in parameters and models or uncertainty in domain knowledge) and complexity that are described by subjective belief or probability [32]. BN has several advantages for data analysis:

(1) It is easy to handle the absence of certain data items.

(2) It can be modeled in terms of causality, so it can be used to gain an understanding of the problem domain and predict the outcome of the intervention.

(3) Since the model has both causal and probabilistic semantics, it is an ideal representation of combining prior knowledge and data (usually in the form of a causal relationship). BN is particularly useful for modeling uncertainty.

Based on the advantages of BN and its wide application in the field of risk assessment, this paper proposes a hybrid method combining domain knowledge and data learning to construct a BN and realize the integration of multiple factors and quantification of uncertainty in the network model to assess the public security risks of urban logistics.

BN is represented by a series of variable nodes and a directed arc representing causality. The conditional probability table (CPTs) is used to determine the quantitative relationship between variables. BN can be represented as $N = (G, P)$, where N represents the network, G represents the graph, and P represents the joint probability of the network. G is a graph, which can be further represented by (V, E), where V represents the set of nodes $(x_1, x_2, x_3, \ldots, x_n)$ and E represents the directed edge of causal relationship between variables. In addition, the calculation method of joint probability equation P on variables is shown in equation (1). The joint probability P is obtained by multiplying the respective local conditional probability distributions:

$$P(X_1, X_2, \ldots, X_k) = P(X_k \mid X_1, X_2, \ldots, X_{k-1}) \cdots P(X_2 \mid X_1) P(X_1). \tag{1}$$

The construction of BN usually adopts three methods: data-based method, knowledge-based method, and the combination of the two methods. The data-based method uses the conditional independence semantics of BN to generalize the model from the data. The knowledge-based approach utilizes the causal knowledge of domain experts to construct BN. Knowledge-based approaches are particularly useful when domain knowledge is critical and data availability is scarce. The method modeling combining domain knowledge and data is the most commonly used method at present, which not only avoids the dependence on expert domain knowledge, but also avoids the invalid learning when given a small or noisy dataset.

3.2. Interpretative Structural Modeling. Interpretative Structural Modeling (ISM) is developed by Warfield [33] in 1973 when analyzing complex structural problems in socioeconomic systems. The basic idea is to extract the elements of the problem through various creative techniques and use directed graph, matrix, and computer technology to process the information of the elements and their mutual relations. The model is intuitive and instructive and is widely used to recognize and deal with complex system problems. Singh et al. [34] implemented knowledge management in the engineering industry and found the interdependence among the variables. Hu et al. [32] evaluated the seismic liquefaction potential by combining interpretation structure model and BN method and achieved good prediction results. Ravi and Shankar [35] adopted the ISM method to analyze the obstacles in reverse logistics activities and extract the key influencing factors.

The advantages of ISM include the following [25]:

(1) Systematic integration of expert opinions and domain knowledge

(2) Providing enough opportunities for decision modification

(3) For a system with factors between 10 and 15, the amount of calculation is small, which is convenient for practical application

The basic working principle and steps of the method are as follows:

Step 1: determine the factors of the system and relationship table. According to the field knowledge and field research, we can summarize the factors related to the problem. Establish the relationship between various factors according to relevant knowledge in the field.

Step 2: construct a structural self-interaction matrix (SSIM) and calculate the reachability matrix M. From the determination of the direct relationship between every two factors, SSIM of each factor is constructed. At this time, the matrix belongs to Boolean matrix and follows the logic operation rules.

For example, there is a system s containing n factors, $s = \{S_i \mid i = 1, 2, \ldots, n\}$. If factor S_i has no influence on factor S_j, then a_{ij} in the intersection position between the row S_i and the column S_j is represented as "0"; if there is a direct influence, it is represented as "1." The structural self-interaction matrix A is expressed as follows:

$$A = \begin{array}{c} \\ S_1 \\ S_2 \\ \cdots \\ S_n \end{array} \begin{array}{c} \begin{array}{cccc} S_1 & S_2 & \cdots & S_n \end{array} \\ \begin{bmatrix} a_{11} & a_{12} & \cdots & a_{1n} \\ a_{21} & a_{22} & \cdots & a_{2n} \\ \cdots & \cdots & \cdots & \cdots \\ a_{n1} & a_{n2} & \cdots & a_{nn} \end{bmatrix} \end{array}, \tag{2}$$

$$a_{ij} = \begin{cases} 1, & S_i \text{ is relative to } S_j, \\ 0, & \text{no relationship between } S_i \text{ and } S_j. \end{cases}$$

By adding the binary relation matrix A and the identity matrix I, the connection matrix N can be obtained, and then matrix M can be calculated through Boolean operation. The reachability matrix represents whether there is a connection path from one element to another.

Step 3: hierarchical decomposition. The reachability matrix is divided into different hierarchical structures. The reachable set $R(S_i)$ represents the factors set reachable by factor S_i in the reachable matrix and is defined in the following formula:

$$R(S_i) = \left\{ S_j \mid S_j \in S, m_{ji} = 1, j = 1, 2, \ldots, n \right\}, \quad i = 1, 2, \ldots, n. \tag{3}$$

The antecedent set $Q(S_i)$ represents the factors set of reachable factors S_i in the reachable matrix and is defined as follows:

$$Q(S_i) = \left\{ S_j \mid S_j \in S, m_{ij} = 1, j = 1, 2, \ldots, n \right\}, \quad i = 1, 2, \ldots, n. \tag{4}$$

Furthermore, an intersection set $C(S_i)$ is defined, i.e., $R(S_i) \cap Q(S_i)$, as follows:

$$C(S_i) = \left\{ S_j \mid S_j \in S, m_{ij} = 1, m_{ji} = 1, j = 1, 2, \ldots, n \right\}, \quad i = 1, 2, \ldots, n. \tag{5}$$

According to the condition of $R(S_i) \cap Q(S_i) = R(S_i)$, hierarchical extraction is carried out. Each round, one layer of elements is extracted. These elements are separated from other elements, and no iteration is carried out until the level of all elements is determined.

Step 4: draw a directed graph. According to the reachability matrix and the obtained hierarchical relationship, a multilevel hierarchical directed graph is drawn.

Step 5: evaluate and modify. Evaluate the points in the model that are inconsistent with the concept and make necessary corrections.

4. Building Bayesian Network Model

4.1. Building the Initial Model

4.1.1. Defining Variables and Structures. There are many risk factors caused by urban logistics. Our research mainly focuses on the impact of urban logistics on public security, so we focus on the risk factors that are likely to cause hidden dangers to public security. According to literature review [18, 30, 36], survey of transportation companies and combine the actual cases collected, follows the principle of (1) the main factors, (2) the factors available for most logistics accident data, and (3) the factors that are easy to obtain and identify, human factor (H), transportation tools and facilities factor (F), and goods factor (G) are identified as the direct factors of the accidents, and management factor (M) and weather factor (W) are identified as indirect factors. Generally, the research on logistics risk focuses on four aspects: people, machinery, environment, and management. We refine the indicators of these four aspects and creatively incorporate the factor of goods into the study, considering the possible impact of goods categories and improper storage on public security.

Human factor includes professional skill (H_1), physical condition (H_2), safety awareness (H_3), and personnel quality (H_4). Transportation tools and facilities factor includes transport vehicle (F_1), maintenance and inspection (F_2), and facility and instrument (F_3). Goods factor includes goods category (G_1) and storage issues (G_2). Tables 1 and 2 provide detailed description and value set of 11 factors. Direct factors have binary (yes/no, normal/abnormal) value sets, while indirect factors may have more values in the value set.

We have collected 96 urban express logistics accidents for public safety in China from 2016 to 2019 [37–39], and we can determine each value of 11 parameters. Table 3 summarizes the accident data.

For example, example 1 in Table 3 represents an accident that happened in Beijing on June 1, 2017, due to a complaint about the wrong operation of a courier. Survey found that the transport company management problems ($M = 1$), the weather is sunny ($W = 0$), the courier professional skill level is not high ($H_1 = 1$), the courier is in normal health ($H_2 = 0$), the safety awareness of the courier is normal ($H_3 = 0$), the courier's quality is low ($H_4 = 1$), normal delivery vehicles ($F_1 = 0$), the maintenance and inspection of the vehicle are normal ($F_2 = 0$), the equipment and maintain are normal ($F_3 = 0$), normal delivery goods ($G_1 = 0$), and storage requirements are normal ($G_2 = 0$).

4.1.2. ISM Model Construction. In this paper, ISM is first used to construct an initial hierarchical model, and then causal mapping is adopted to improve the initial model and transform the structure into BN model. The research framework is shown in Figure 1.

Step 1: determine the risk factors and their relationship of urban logistics for public safety. Based on the expert knowledge and accident reports, the relationship between the factors involved in the urban express logistics accidents is determined. Any pair of nodes have a relational value set $\{S_i \longrightarrow S_j,\ S_i \leftarrow S_j,\ S_i \uparrow S_j,\ S_i \text{O} S_j\}$. $S_i \longrightarrow S_j$ indicates that S_i directly leads to S_j, $S_i \uparrow S_j$ indicates the interaction between S_i and S_j, $S_i \text{O} S_j$ indicates that the two factors are irrelevant. The details are shown in Table 4.

Step 2: construct the structural self-interaction matrix (SSIM) and calculate the reachability matrix (M). SSIM is constructed by determining the direct relationship between the two factors in Step 1:

$$A = \begin{array}{c} \\ S_1 \\ S_2 \\ S_3 \\ S_4 \\ S_5 \\ S_6 \\ S_7 \\ S_8 \\ S_9 \\ S_{10} \\ S_{11} \end{array} \begin{array}{c} \begin{array}{ccccccccccc} S_1 & S_2 & S_3 & S_4 & S_5 & S_6 & S_7 & S_8 & S_9 & S_{10} & S_{11} \end{array} \\ \begin{bmatrix} 0 & 1 & 1 & 1 & 1 & 1 & 1 & 1 & 1 & 1 & 1 \\ 0 & 0 & 0 & 0 & 0 & 1 & 1 & 1 & 1 & 1 & 1 \\ 0 & 1 & 0 & 1 & 0 & 1 & 1 & 1 & 1 & 1 & 1 \\ 0 & 0 & 0 & 0 & 0 & 1 & 1 & 1 & 1 & 1 & 1 \\ 0 & 0 & 0 & 1 & 0 & 1 & 1 & 1 & 1 & 1 & 1 \\ 0 & 0 & 0 & 0 & 0 & 0 & 1 & 1 & 1 & 1 & 1 \\ 0 & 0 & 0 & 0 & 0 & 1 & 0 & 1 & 1 & 1 & 1 \\ 0 & 0 & 0 & 0 & 0 & 1 & 1 & 0 & 1 & 1 & 1 \\ 0 & 0 & 0 & 0 & 0 & 1 & 1 & 1 & 0 & 1 & 1 \\ 0 & 0 & 0 & 0 & 0 & 0 & 0 & 0 & 0 & 0 & 1 \\ 0 & 0 & 0 & 0 & 0 & 0 & 0 & 0 & 0 & 1 & 0 \end{bmatrix} \end{array}, \tag{6}$$

Table 1: Direct factors involved in urban express logistics for public safety accidents.

Direct factors	Description	Value set
Human (H)		
Professional skill (H_1)	Skill, experience	Normal (0), Abnormal (1)
Physical condition (H_2)	Sickness, fatigue	Normal (0), Abnormal (1)
Safety awareness (H_3)	Safety awareness	Normal (0), Abnormal (1)
Personnel quality (H_4)	Quality, follow rules	Normal (0), Abnormal (1)
Transportation tools and facilities (F)		
Transport vehicle (F_1)	Transport vehicle meets specified requirements	Normal (0), Abnormal (1)
Maintenance and inspection (F_2)	Transport vehicle is maintained regularly	Normal (0), Abnormal (1)
Facility and instrument (F_3)	Transport vehicle is equipped with the required equipment	Normal (0), Abnormal (1)
Goods factor (G)		
Goods category (G_1)	Goods are inflammable, explosive, poisonous, or other contraband	Normal (0), Abnormal (1)
Storage issues (G_2)	Store as required	Normal (0), Abnormal (1)

Table 2: Indirect factors involved in urban express logistics for public safety accidents.

Indirect factors	Description	Value set
Management (M)	Manage personnel, facilities, storage, etc.	Normal (0), Abnormal (1)
Weather (W)	Weather condition	Sunny (0), high temperature (1), foggy (2)

By means of 4 steps of Boolean operation, M can be calculated. $N \neq N^2 \neq N^3 = N^4 = M$. Table 5 shows the accessible set, the antecedent set, and their intersection set table, and the structural relationship among the factors is established. The factors of accessible set include the elements of matrix M whose corresponding row value is 1, including the factors themselves and the factors that may affect. By contrast, the antecedent set consists of the elements of matrix M corresponding to the column median of 1, including the factors themselves and the factors that may affect them.

Firstly, the hierarchy is extracted according to the condition $R(S_i) \cap Q(S_i) = R(S_i)$. The factors that satisfy the condition are the top layer in the hierarchy. Then the top level factors in the subsequent analysis are removed and the same process is repeated to identify the next level factors. The grading process continues until the level of each factor is found:

$$M = \begin{bmatrix} 1 & 1 & 1 & 1 & 1 & 1 & 1 & 1 & 1 & 1 & 1 \\ 0 & 1 & 0 & 0 & 0 & 1 & 1 & 1 & 1 & 1 & 1 \\ 0 & 1 & 1 & 1 & 0 & 1 & 1 & 1 & 1 & 1 & 1 \\ 0 & 0 & 0 & 1 & 0 & 1 & 1 & 1 & 1 & 1 & 1 \\ 0 & 0 & 0 & 1 & 1 & 1 & 1 & 1 & 1 & 1 & 1 \\ 0 & 0 & 0 & 0 & 0 & 1 & 1 & 1 & 1 & 1 & 1 \\ 0 & 0 & 0 & 0 & 0 & 1 & 1 & 1 & 1 & 1 & 1 \\ 0 & 0 & 0 & 0 & 0 & 1 & 1 & 1 & 1 & 1 & 1 \\ 0 & 0 & 0 & 0 & 0 & 1 & 1 & 1 & 1 & 1 & 1 \\ 0 & 0 & 0 & 0 & 0 & 0 & 0 & 0 & 0 & 1 & 1 \\ 0 & 0 & 0 & 0 & 0 & 0 & 0 & 0 & 0 & 1 & 1 \end{bmatrix}. \quad (7)$$

Step 3: ISM model divides the risk factors of urban express logistics into different hierarchical structures, and the results are as follows:

Table 3: Parameter values of 96 case studies are used to support the Bayesian network analysis of factors of urban logistics express delivery for public safety accidents.

Table 3: Continued.

Sample	M	W	H_1	H_2	H_3	H_4	F_1	F_2	F_3	G_1	G_2
1	1	0	1	0	0	1	0	0	0	0	0
2	0	0	0	0	0	1	0	0	0	0	0
3	1	0	1	0	0	1	0	0	0	0	0
4	1	0	0	0	0	1	0	0	0	0	0
5	1	0	1	0	0	1	0	0	0	0	0
6	1	0	1	0	0	1	0	0	0	0	0
7	0	0	1	0	1	0	0	0	0	0	0
8	0	0	1	0	1	0	0	0	0	0	0
9	0	0	1	0	1	0	0	0	0	0	0
10	1	0	1	0	1	0	0	0	0	0	0
11	1	0	0	0	1	0	0	0	0	0	0
12	1	0	0	0	1	1	0	0	0	0	0
13	1	0	0	0	1	1	0	0	0	0	0
14	1	0	0	0	1	1	0	0	0	0	0
15	1	0	0	0	1	0	0	0	0	1	0
16	1	0	0	0	0	1	0	0	0	0	0
17	0	0	1	0	1	0	0	0	0	0	0
18	1	0	1	0	1	1	0	0	0	0	0
19	1	0	0	0	0	1	0	0	0	0	0
20	1	0	0	0	0	1	0	0	0	0	0
21	1	0	0	0	0	1	0	0	0	0	0
22	1	0	0	0	0	1	0	0	0	0	0
23	1	0	1	0	1	0	0	0	0	0	0
24	0	0	0	1	1	0	0	0	0	0	0
25	0	0	1	0	0	0	0	0	0	0	0
26	0	0	1	0	1	0	0	0	0	0	0
27	1	0	1	0	1	0	0	0	0	0	0
28	0	2	1	0	0	0	0	0	0	0	0
29	1	0	1	0	1	0	0	0	0	0	0
30	1	0	1	0	1	0	1	1	0	0	0
31	1	0	0	0	1	0	1	1	0	0	0
32	1	1	0	0	1	0	1	1	0	1	0
33	0	0	0	1	1	0	0	0	0	0	0
34	0	0	1	0	1	0	0	0	0	0	0
35	1	0	0	1	1	0	0	0	0	0	0
36	0	2	1	0	0	0	0	0	0	0	0
37	0	0	0	0	0	0	0	0	0	1	0
38	0	2	0	0	0	0	0	0	0	1	0
39	0	0	1	0	1	0	0	0	0	0	0
40	0	0	1	0	0	0	0	0	0	1	0
41	2	0	0	0	0	0	1	1	0	0	0
42	0	0	1	0	1	0	0	0	0	0	0
43	1	0	0	0	1	1	0	0	0	0	0
44	1	0	1	0	1	0	0	1	0	0	0
45	1	0	0	0	1	1	1	0	0	0	0
46	0	0	1	0	1	0	0	0	0	0	0
47	1	0	1	0	1	0	0	0	0	0	0
48	1	0	0	0	1	1	0	0	0	1	0
49	1	0	1	0	1	0	0	1	0	0	0
50	0	0	1	0	1	0	0	0	0	0	0
51	1	0	0	0	1	1	0	0	0	0	0
52	1	0	0	0	1	0	0	0	0	0	0
53	0	1	1	0	1	0	0	0	0	0	0
54	1	0	0	0	1	0	0	0	0	0	0
55	0	0	1	0	1	0	0	0	0	0	0
56	0	0	1	0	1	0	0	0	0	0	0
57	0	0	1	0	1	0	0	0	0	0	0
58	1	0	0	1	1	0	0	0	0	0	0
59	1	0	1	0	1	0	0	0	0	0	0
60	1	0	0	0	0	0	1	1	1	0	0
61	1	0	0	0	1	0	0	0	0	1	1
62	1	0	0	0	1	0	1	1	0	0	0
63	1	0	0	0	0	0	0	0	0	1	0
64	1	0	0	0	0	0	0	0	0	1	0
65	1	0	0	0	0	1	0	0	0	1	0
66	1	0	0	0	0	0	0	0	0	1	0
67	1	0	0	0	0	0	0	0	0	1	0
68	1	0	0	0	0	0	0	0	0	1	0
69	1	0	0	0	0	0	0	0	0	1	0
70	1	0	0	0	0	0	0	0	0	1	0
71	1	0	1	0	0	0	0	0	0	1	0
72	1	0	0	0	0	0	0	0	0	1	0
73	1	0	0	0	0	0	0	0	0	1	0
74	1	0	0	0	0	0	0	0	0	1	0
75	1	0	0	0	0	0	0	0	0	1	0
76	1	0	0	0	0	0	0	0	0	1	0
77	1	0	0	0	0	0	0	0	0	1	0
78	1	0	0	0	0	0	0	0	0	1	0
79	1	0	0	0	0	0	0	0	0	1	0
80	1	0	0	0	0	0	0	0	0	1	0
81	1	0	0	0	0	0	0	0	0	1	0
82	1	0	0	0	1	0	0	0	0	0	0
83	1	0	0	0	1	0	0	0	0	0	0
84	1	0	0	0	1	1	0	0	0	0	0
85	1	0	0	0	1	0	0	0	0	1	1
86	1	1	0	0	1	0	0	0	0	1	1
87	1	0	0	0	1	0	0	0	0	1	0
88	1	0	0	0	1	0	0	0	0	0	0
89	1	0	0	0	1	0	0	0	0	0	0
90	1	0	0	0	1	0	0	0	0	0	1
91	1	0	0	0	1	0	0	0	1	0	0
92	1	0	0	0	1	0	0	0	0	0	0
93	1	0	0	0	1	0	0	0	0	0	0
94	1	0	0	0	1	1	0	0	0	0	0
95	1	0	0	0	1	0	0	0	0	0	0
96	1	0	1	0	1	0	0	0	0	0	0

$$
\begin{aligned}
L_1 &= \{S_{10}, S_{11}\},\\
L_2 &= \{S_7, S_8, S_9\},\\
L_3 &= \{S_3, S_5\}, \qquad (8)\\
L_4 &= \{S_4, S_6\},\\
L_5 &= \{S_1, S_2\}.
\end{aligned}
$$

Table 6 shows the structural hierarchy of risk factors, among which management factor and weather factor are first identified as level 5. The first level is the goods factor, including the goods category factor and storage issues factor. The main factors including human factor and transportation tools and facilities factor are in the middle level.

Step 4: according to the hierarchical relationship obtained in Step 3, a multilevel hierarchical directed graph is drawn, and the initial model of BN is established, as shown in Figure 2.

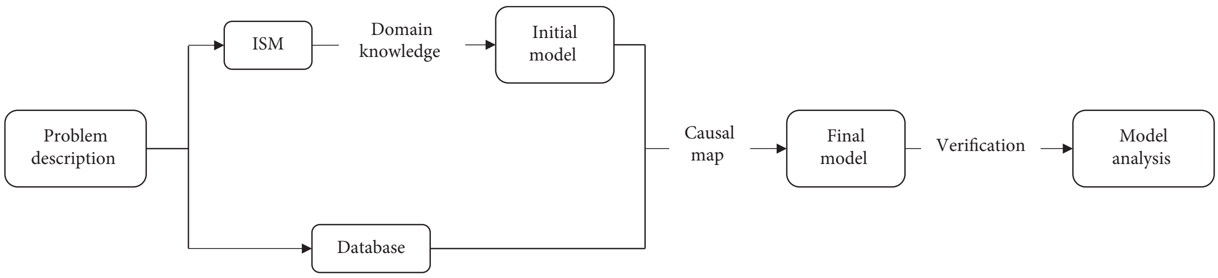

Figure 1: The research framework of combining ISM and causal mapping to construct BN.

Table 4: Structural self-interaction matrix (SSIM).

	M	W	H_1	H_2	H_3	H_4	F_1	F_2	F_3	G_1	G_2
M		○	⟶	⟶	⟶	⟶	⟶	⟶	⟶	⟶	⟶
W			⟶	○	○	○	○	○	○	○	⟶
H_1				○	○	○	⟶	○	○	⟶	⟶
H_2					⟶	○	⟶	○	○	○	○
H_3						⟵	⟶	⟶	○	⟶	⟶
H_4							○	○	○	⟶	○
F_1								↑	↑	○	○
F_2									⟶	○	⟶
F_3										○	⟶
G_1											↑
G_2											

⟶: row has an effect on the column; ⟵: column has an effect on the row; ↑: row and column interact; ○: the two factors are irrelevant.

Table 5: Accessible set and antecedent set and their intersection set table.

I	$R(S_i)$	$Q(S_i)$	$R(S_i) \cap Q(S_i)$
1	1, 3, 4, 5, 6, 7, 8, 9, 10, 11	1	1
2	2, 3, 7, 8, 9, 10, 11	2	2
3	3, 7, 8, 9, 10, 11	1, 2, 3, 4	3
4	3, 4, 5, 7, 8, 9, 10, 11	1, 4	4
5	5, 7, 8, 9, 10, 11	1, 5, 6	5
6	5, 6, 7, 8, 9, 10, 11	1, 6	6
7	7, 8, 9, 10, 11	1, 2, 3, 5, 6, 7, 8, 9	7, 8, 9
8	7, 8, 9, 10, 11	1, 2, 3, 5, 6, 7, 8, 9	7, 8, 9
9	7, 8, 9, 10, 11	1, 2, 3, 5, 6, 7, 8, 9	7, 8, 9
10	10, 11	1, 2, 3, 5, 6, 7, 8, 9, 10, 11	10, 11
11	10, 11	1, 2, 3, 5, 6, 7, 8, 9, 10, 11	10, 11

ISM method is used for risk identification, the hierarchical structure is established, and the initial directed graph of BN is further developed. The network diagram describes the horizontal interdependence among factors and the vertical influence of factors at different levels.

4.2. Improving the Bayesian Network Structure. The initial network diagram is complex and shows circular links that are not allowed in Bayesian network. So we changed the initial network diagram to be BN compatible. The modification of the initial model is based on a causal mapping method proposed by Nadkarni and Shenoy [40]. When modifying network graph, this method generally adopts two principles. The first principle is to reduce the complexity of the network presentation by removing redundant links. This requires the distinction between direct and indirect relationships, and only direct relationships remain. For example, although management factor (M) is related to safety awareness factor (H_3), experts believe that the direct relationship between the two factors is weak. M directly affects physical condition (H_2) and personnel quality (H_4), both of which subsequently affect H_3. Therefore, the link to H_3 was removed from the network.

The second principle is to eliminate any cyclic relationships to satisfy the noncyclic graphic structure of BN. For example, transport vehicle (F_1), maintenance and inspection (F_2), and facility and instrument (F_3) are interrelated, forming a circular connection. F_2 will affect the performance of the vehicle and then cause latent risks, which is directly related to F_1. However, when the availability of vehicle is not a problem, F_1 has no significant influence on F_2, which is the same with F_3. Therefore, the relationship between them can be eliminated. Finally, a directed graph suitable for BN is shown in Figure 3.

The perfect network diagram using causal mapping method specifies the interdependence between the same-level or cross-level factors, which makes the overall structure clear and easy to understand, deals with the relations among factors more effectively, and ensures a deeper understanding of the problem.

4.3. Parameter Learning of Bayesian Network. When the BN structure is established, the values of some variables can be obtained from the case database, and then the parameters of the model (i.e. conditional probability) can be estimated with these cases. This is called parameter estimation or parameter learning. Maximum likelihood estimation algorithm (MLE) is a universal method to find a set of parameters of maximum likelihood θ, provided that a complete dataset is available. Record the sample set as $D = \{x_1, x_2, \ldots, x_N\}$.

The joint probability density function $p(D \mid \theta)$ is called the likelihood function of θ relative to $\{x_1, x_2, \ldots, x_N\}$ and is defined as follows:

$$l(\theta) = p(D \mid \theta) = p\{x_1, x_2, \ldots, x_N \mid \theta\} = \prod_{i=1}^{N} p\left(x_i \mid \theta\right). \tag{9}$$

Table 6: Factor rating table.

Level	Factors	Category
Level 1	Goods category (G_1), Storage issues (G_2)	Goods factor (G)
Layer 2	Transport vehicle (F_1), Maintenance and inspection (F_2), Facility and instrument (F_3)	Transportation tools and facilities (F)
Layer 3	Professional skill (H_1), Safety awareness (H_3)	Human factor (H)
Layer 4	Physical condition (H_2), Personnel quality (H_4)	Human factor (H)
Layer 5	Management (M), Weather (W)	Management (M), weather (W)

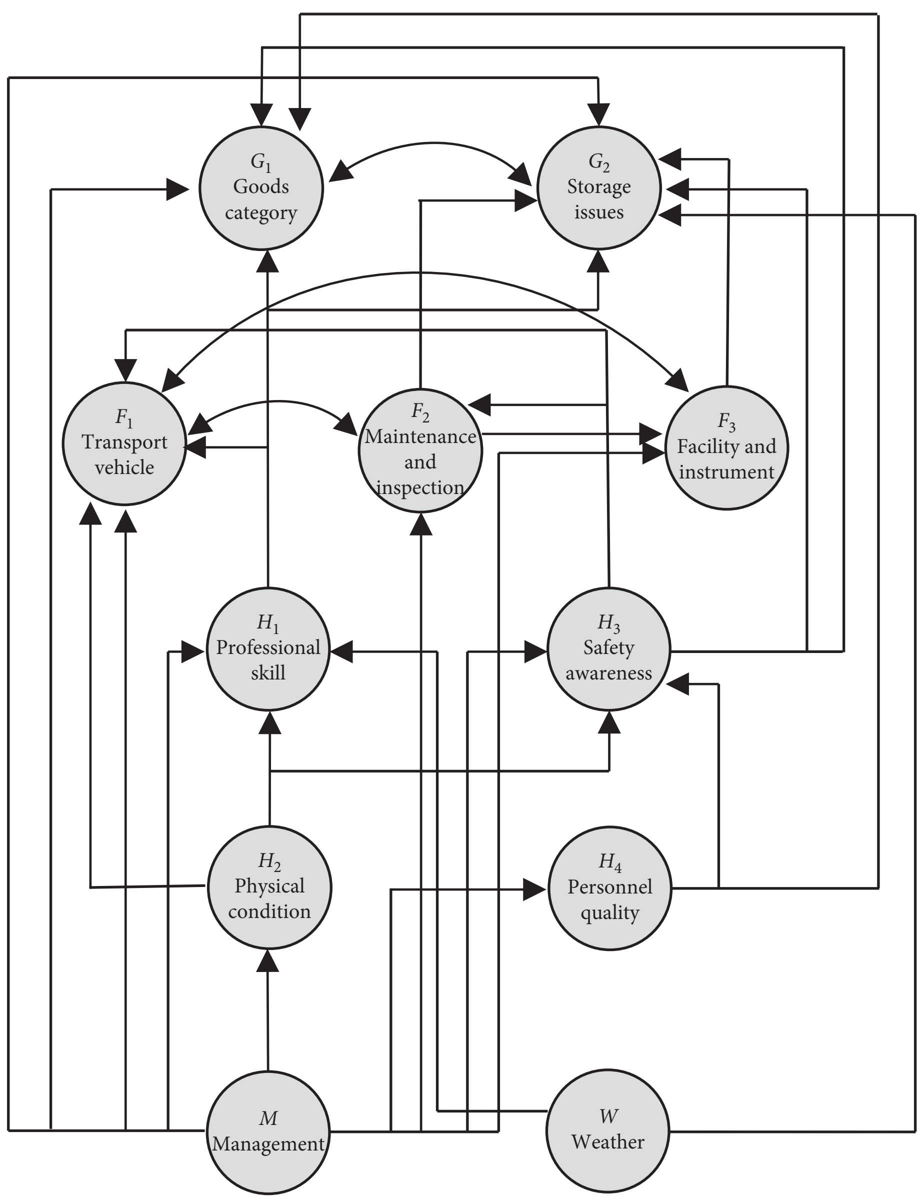

Figure 2: Preliminary digraph from ISM.

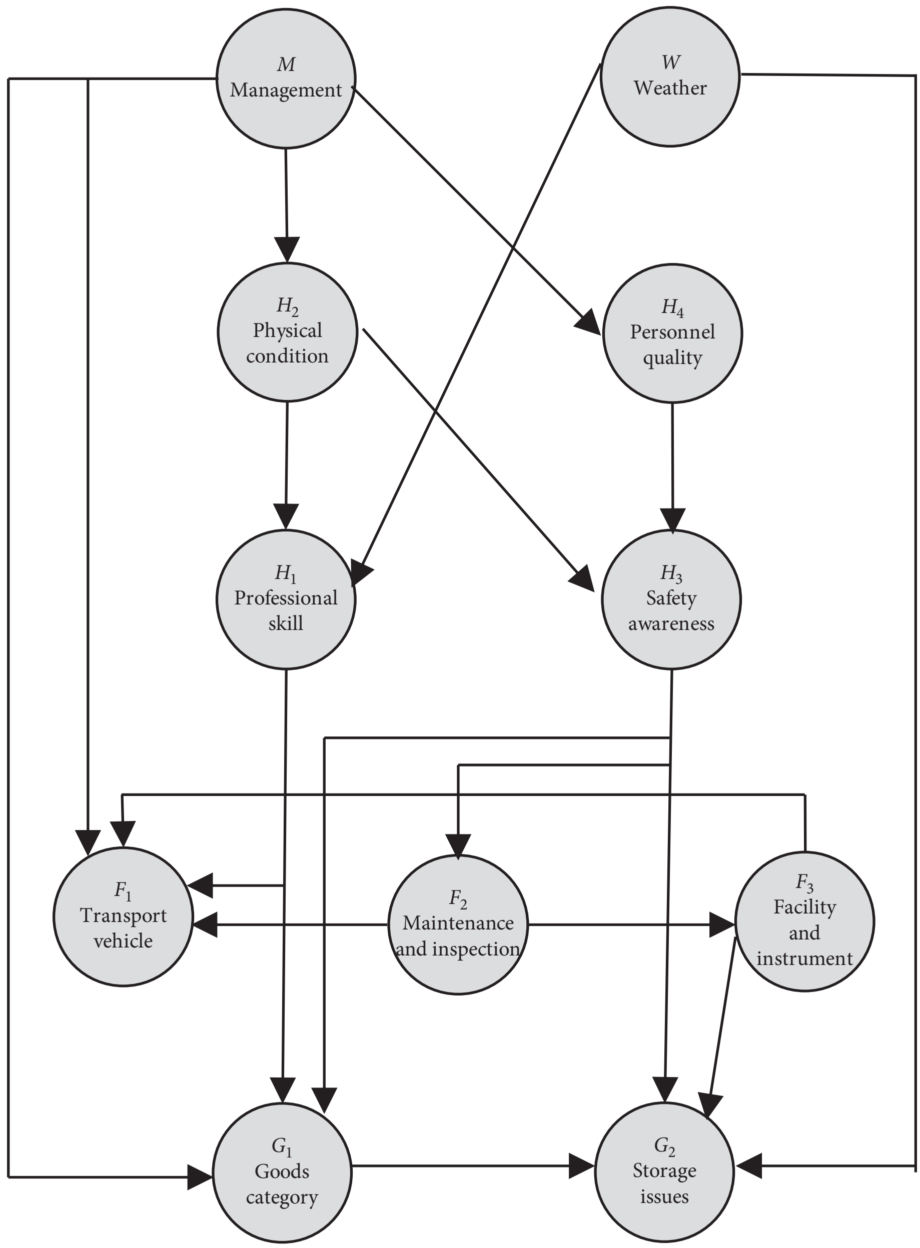

Figure 3: Bayesian network based on ISM digraph.

If $\widehat{\theta}$ is the value θ can make the likelihood function $l(\theta)$ largest in the parameter space, $\widehat{\theta}$ is the maximum likelihood estimator of θ. In order to facilitate analysis, the logarithmic similarity is defined as follows:

$$\widehat{\theta} = d\{x_1, x_2, \ldots, x_N\} = \arg\max_{\theta} \ln l(\theta) = \arg\max_{\theta} \sum_{i=1}^{N} \ln p\left(x_i \mid \theta\right). \quad (10)$$

We use Netica32 software and combined the sample data in Table 3 to complete the parameter learning process. Table 7 shows a CPT example associated with the child factor H_3(safety awareness) and its corresponding parent factors H_2(physical condition) and H_4(personnel quality). Figure 4 shows the established BN model. Assume that F_2 (maintenance and inspection) is taken as the evidence variable and the state value is set to 1, indicating that the evidence variable is known state. The result is shown in Figure 5.

Table 7: An example of a conditional probability table.

H_3		Father node	
0	1	M	F_2
0.375	0.625	0	0
0.166	0.833	0	1
0.541	0.458	1	0
0.5	0.5	1	1

At this time, the abnormal probability of F_1 (vehicle state) changes from 12.6% to 62.1%, the abnormal

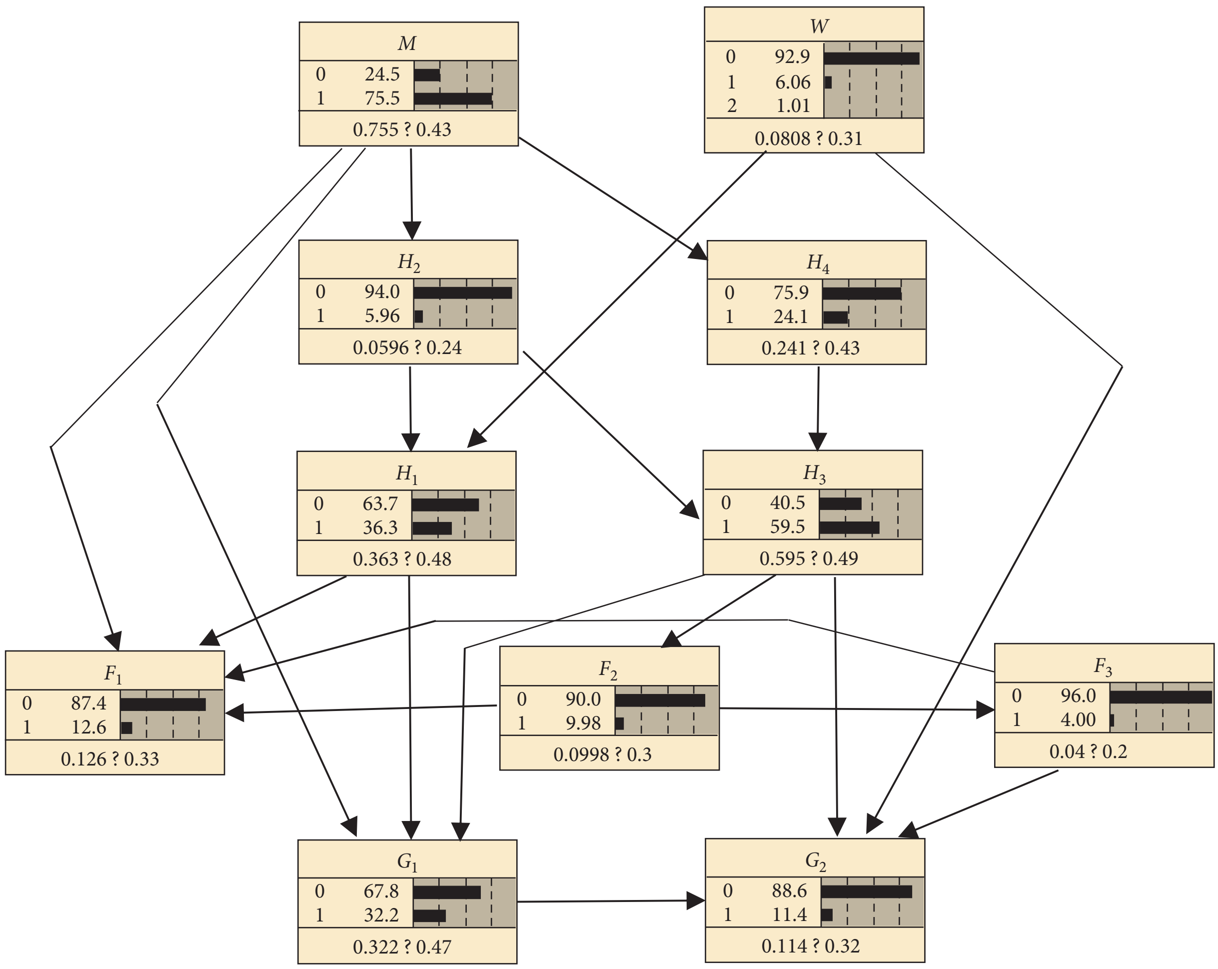

Figure 4: Bayesian network model by Netica.

probability of F_3 (facilities and instrument) changes from 4.0% to 20.0%, and the abnormal probability of G_2 (storage issues) changes from 11.4% to 16.4%. It can be seen that the risk probability of other factors will increase if the maintenance and supervision work is not done properly.

4.4. Sensitivity Analysis. One of the main functions of BN is to analyze the evidence sensitivity of query nodes. Sensitivity analysis can get the sensitivity of query node probability to the probability change of evidence node. In probability system, entropy is a common index to express the degree of uncertainty. The following equation represents the entropy of the distribution of the variable X:

$$H(X) = -\sum_{x\in X} P(x)\log(x). \tag{11}$$

Variance is also an indicator of the degree of uncertainty, as shown in the following equation:

$$\operatorname{Var}(X) = \sum_{x\in X} P(x-\mu)^2 P(x), \tag{12}$$

where μ is the mean, that is, $\sum_{x\in X} xP(x)$.

Table 8 shows the sensitivity analysis of other evidence nodes with F_2 as an example. Details of other nodes are shown in Table 9. The second column represents the mutual information values, the third column represents the percentage of entropy decreased, and the fourth column is variance.

As can be seen from Table 8, the nodes that have the most influence on F_2 are their parents and children. The factors that are most likely to have the greatest influence on the reliability of F_2 are listed in the front.

5. Discussion

This paper presents a new risk factor analysis method based on the combination of domain knowledge and data. Nearly 4 years of China's urban logistics express for public safety accident data are modeled, and the sensitivity to risk factors is evaluated. The advantages and development of this study are further discussed as follows:

(1) As a method of probabilistic reasoning, BN model has some specific advantages over other probabilistic models such as artificial neural network (ANN) and support vector machine (SVM). BN can fuse multiple information sources and infer uncertainty. In the BN model, domain knowledge can be encoded as a prior distribution, which means that it is independent of any sample data. This feature makes it

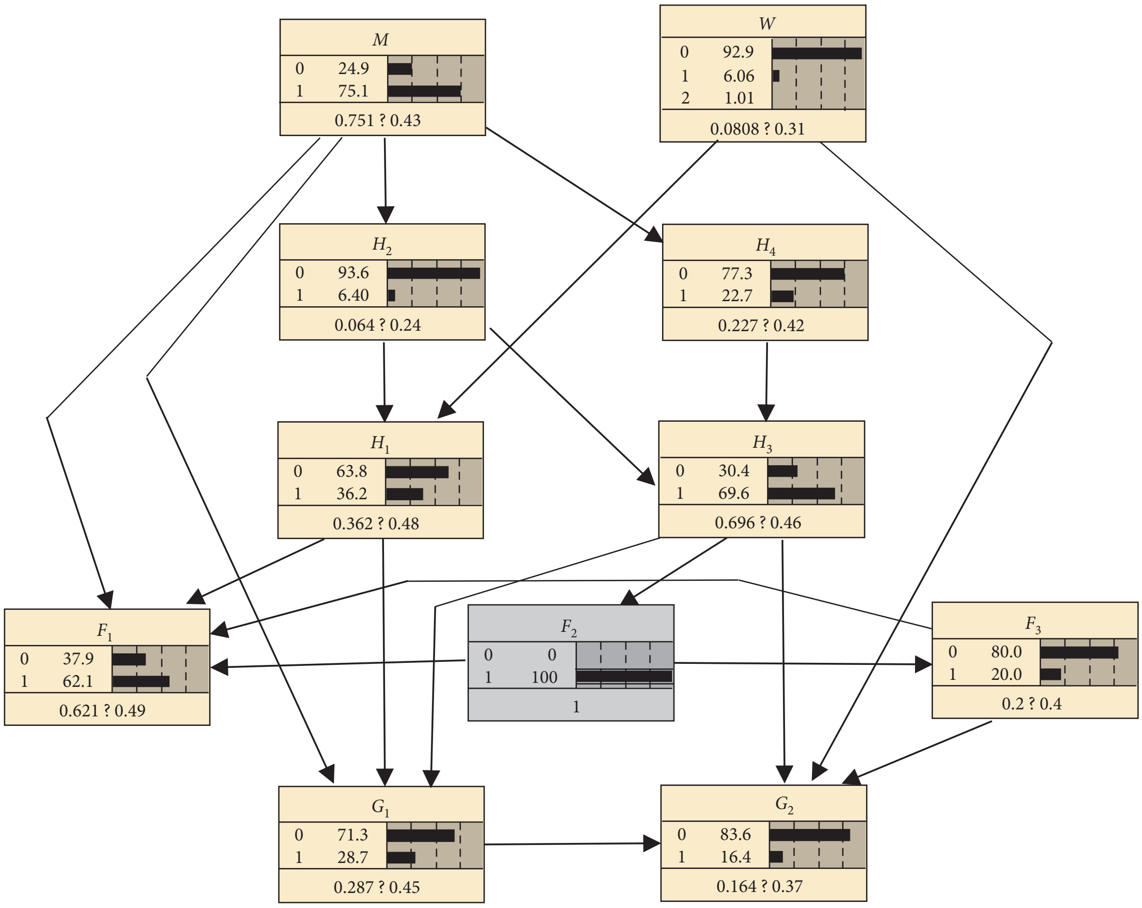

Figure 5: Bayesian network model with perfect F_2.

Table 8: Sensitivity of F_2 to evidence from other nodes.

Node	Mutual info	Percent	Variance of beliefs
F_2	0.46838	100	0.0898455
F_1	0.11740	25.1	0.0220976
F_3	0.03168	6.76	0.0066493
H_3	0.00346	0.74	0.0004182
G_2	0.00180	0.383	0.0002465
G_1	0.00045	0.0953	0.0000546
H_4	0.00008	0.0175	0.0000101
H_2	0.00003	0.00567	0.0000034
M	0.00001	0.00151	0.0000009
H_1	0.00000	0	0.0000000
W	0.00000	0	0.0000000

easy to combine domain knowledge with sample data. ANN, on the other hand, usually needs a lot of parameters to learn for a long time and cannot observe its learning process. In addition, BN can integrate different variable types into a model for processing, such as continuous, discrete, quantitative, and qualitative variables, while ANN and SVM models cannot process. More importantly for BN, the model can be updated according to the new given data. Even incomplete data can be processed to improve the previous BN model. These are not done by other models such as ANN and SVM.

(2) Comprehensive multisource information for decision-making. It is a complex multiattribute decision-making problem to analyze the influencing factors of urban express logistics on public security risk. There are many kinds of information, such as investigation report, detection sensor, and expert opinion. How to integrate objective and subjective data from multiple sources to analyze the risk factors of the system has become an urgent problem. This study combines expert knowledge and accident data and established a comprehensive analysis framework of risk factors of urban express logistics on public safety (Figure 1), including four work links, five risk categories, and 11 influencing factors. According to the results of this study, among all risk factors of urban logistics accident, management error and human factor have the highest prior probability. This result means that most accidents are caused by these factors, which is consistent with previous research results [18, 30]. It can be considered that management (M) and human factor (H) are the key factors to reduce public safety accidents. Enterprises should further strengthen safety supervision, reduce the employee safety violations, strengthen the safety management of employees, provide safety training courses for employees, strict assessment system, and enhance safety awareness.

Table 9: Sensitivity of each node to the others.

Node	Mutual	Percent	Variance of beliefs
M node			
M	0.80309	100	0.184923
H_4	0.03916	4.88	0.008506
H_2	0.01323	1.65	0.003905
F_1	0.00199	0.248	0.000532
H_3	0.00154	0.192	0.000392
G_1	0.00047	0.0581	0.000119
H_1	0.00012	0.0155	$3.19E-05$
G_2	0.00001	0.0018	$3.70E-06$
F_2	0.00001	0.000883	$1.80E-06$
F_3	0	$6.46E-05$	$1.00E-07$
W	0	0	0
H_1 node			
H_1	0.94504	100	0.231196
G_1	0.04975	5.26	0.014953
W	0.00873	0.923	0.002924
H_2	0.00648	0.686	0.001889
F_1	0.00113	0.12	0.000356
G_2	0.00039	0.0412	0.000123
M	0.00012	0.0132	$3.99E-05$
H_3	0.00005	0.00503	$1.53E-05$
H_4	0.00001	0.00061	$1.80E-06$
F_2	0	$2.22E-05$	$1.00E-07$
F_3	0	0	0
W node			
W	0.41039	100	0.068026
G_2	0.02604	6.35	0.002946
H_1	0.00873	2.13	0.000799
G_1	0.00061	0.149	$5.25E-05$
F_1	0.00001	0.00353	$1.30E-06$
F_3	0	0	0
F_2	0	0	0
H_3	0	0	0
H_2	0	0	0
H_4	0	0	0
M	0	0	0
F_3 node			
F_3	0.24213	100	0.038368
F_2	0.03168	13.1	0.00284
F_1	0.02513	10.4	0.00202
G_2	0.01578	6.52	0.001232
H_3	0.00025	0.104	$1.32E-05$
G_1	0.00003	0.0135	$1.70E-06$
H_4	0.00001	0.00252	$3.00E-07$
H_2	0	0.000824	$1.00E-07$
M	0	0.0002	0
H_1	0	0	0
W	0	0	0
H_2 node			
H_2	0.32582	100	0.056041
M	0.01323	4.06	0.001184
H_1	0.00648	1.99	0.000458
H_3	0.00625	1.92	0.000453
H_4	0.00074	0.227	$5.44E-05$
F_1	0.00018	0.0541	$1.43E-05$
G_1	0.00013	0.0403	$1.01E-05$
G_2	0.00011	0.0332	$8.70E-06$
F_2	0.00003	0.00817	$2.10E-06$
F_3	0	0.000608	$2.00E-07$
W	0	0	0

Table 9: Continued.

Node	Mutual	Percent	Variance of beliefs
G_1 node			
G_1	0.90664	100	0.218347
H_3	0.09421	10.4	0.028508
H_1	0.04975	5.49	0.014122
G_2	0.01623	1.79	0.005234
H_4	0.00247	0.272	0.00076
W	0.00061	0.0676	0.00018
M	0.00047	0.0515	0.00014
F_2	0.00045	0.0492	0.000133
H_2	0.00013	0.0145	$3.92E-05$
F_3	0.00003	0.00361	$9.80E-06$
F_1	0.00003	0.0028	$7.70E-06$
H_4 node			
H_4	0.79685	100	0.182965
M	0.03916	4.91	0.008416
H_3	0.01712	2.15	0.004403
G_1	0.00247	0.31	0.000637
H_2	0.00074	0.0927	0.000178
F_1	0.0002	0.0257	$5.11E-05$
G_2	0.0001	0.0126	$2.52E-05$
F_2	0.00008	0.0103	$2.05E-05$
F_3	0.00001	0.000759	$1.50E-06$
H_1	0.00001	0.000719	$1.50E-06$
W	0	0	0
G_2 node			
G_2	0.51192	100	0.101018
W	0.02604	5.09	0.005244
F_3	0.01578	3.08	0.003244
G_1	0.01623	3.17	0.002422
H_3	0.00405	0.79	0.00055
F_2	0.0018	0.351	0.000277
F_1	0.00135	0.264	0.000203
H_1	0.00039	0.0761	$5.39E-05$
H_2	0.00011	0.0211	$1.57E-05$
H_4	0.0001	0.0196	$1.39E-05$
M	0.00001	0.00282	0.000002
F_1 node			
F_1	0.54699	100	0.1103
F_2	0.1174	24.6	0.02713
F_3	0.02513	5.27	0.005807
M	0.00199	0.288	0.000318
G_2	0.00135	0.201	0.000222
H_1	0.00113	0.154	0.00017
H_3	0.00099	0.136	0.00015
H_4	0.0002	0.0279	$3.08E-05$
H_2	0.00018	0.0255	$2.81E-05$
G_1	0.00003	0.00351	$3.87E-06$
W	0.00001	0.00199	$2.20E-06$

(3) The output of sensitivity analysis shows that the low safety awareness of employees (H_3) and management factor (M) are the main reasons of accidents caused by the failure of transportation vehicles. This is consistent with previous research results [41, 42]. Accidents may occur when employees neglect the safety inspection of vehicles and fail to do regular maintenance of vehicles, and the enterprise is poorly supervised. A lack of safety knowledge may be one reason why employees ignore safety issues. In order to reduce these errors,

the company's management must pay attention to these factors, strengthen supervision, clarify safety management policies, implement safety training plan, improve the staff's attention to details, and reduce mistakes.

(4) Although this study proposes a modeling framework using the artificial intelligence methods, the BN model developed is only a prototype, and further studies are needed to improve it. For example, some of the risk factors identified in urban express logistics represent general operational process concepts. In order to be more realistic, some factors must be refined to manage specific express logistics risk factors. In addition, in order to improve the integrity of BN model, more domain experts should be introduced.

6. Conclusion

In this paper, by combining Interpretative Structural Model and causal mapping method, Bayesian network is constructed to analyze the risk factors of urban express logistics on public security, including risk factor identification, relationship analysis between factors, prior probability and likelihood calculation, reasoning, and interpretation. With the help of domain experts, ISM and causal mapping methods can be effectively applied to the BN construction of urban express logistics, extending the application of BN model in the risk factor analysis of urban logistics. The flexibility of this approach allows the integration of multiple types of information sources to quantify the relationship between risk factors, and the model can be constantly updated based on new information. This study considers more important factors (11 factors) of urban logistics accidents from five aspects of management, weather, human, transportation means, and goods and concludes the interrelation and relative importance of risk factors, revealing that human factor and management factor are important direct factors of accidents. Through the sensitivity analysis, it is concluded that the low safety awareness of employees and the poor management of enterprises bring potential risks to vehicles, so as to increase the possibility of accidents. These research results combined with the actual situation of urban logistics in China have certain practical significance and provide guidance for logistics managers to take necessary measures to reduce accidents.

Data Availability

The data used to support the results of this study are provided in Table 3.

Conflicts of Interest

The authors declare that they have no conflicts of interest.

Acknowledgments

The research was supported by grants from the National Key R&D Program of China (2018YFB1601600).

References

[1] E. Taniguchi, R. G. Thompson, T. Yamada, and R. V. Duin, *City Logistics: Network Modelling and Intelligent Transport Systems*, Elsevier, Amsterdam, The Netherlands, 2001.

[2] C. J. Cao, C. D. Li, Y. Wang, W. B. Li, and F. S. Zhang, "Governance mode of urban public safety risk in big data era," *Urban Development Studies*, vol. 24, no. 11, pp. 76–82, 2017.

[3] C. Zheng, C. Jin, X. Zhang, W. Meng, and B. Zhang, "Research of items safe hidden trouble in express transportation process," *Popular Science and Technology*, vol. 14, no. 12, pp. 163–177, 2012.

[4] L. Xuan, D. Y. Wei, and Y. Shi, "A brief analysis of security risks in transportation of logistics enterprises," *Chinese Market*, vol. 41, p. 68, 2015.

[5] S. Ren, "Assessment on logistics warehouse fire risk based on analytic hierarchy process," *Procedia Engineering*, vol. 45, pp. 59–63, 2012.

[6] Q. Su and Y. Zhao, "Study on control of logistics risk from the angle of risk management," *Logistics Sci-Tech*, vol. 30, no. 9, pp. 115–117, 2007.

[7] X. Liu and Z.-y. Tian, "Risk assessment of logistics outsourcing based on BP neural network," in *Proceedings of the International Conference on Photonics and Image in Agriculture Engineering*, vol. 8762, Article ID 87620D, Sanya, China, March 2013.

[8] T. Song, L. Y. Wei, C. L. Zhang, and P. Chen, "Project logistics risk evaluation based on matter-element analysis," *Applied Mechanics and Materials*, vol. 174–177, no. 177, pp. 2820–2824, 2012.

[9] S. Raut and S. Karmore, "Review on: severity estimation unit of automotive accident," in *Proceedings of the Computer Engineering and Applications*, Ghaziabad, India, March 2015.

[10] H. Alyami, Z. Yang, R. Riahi, S. Bonsall, and J. Wang, "Advanced uncertainty modelling for container port risk analysis," *Accident Analysis & Prevention*, vol. 123, pp. 411–421, 2019.

[11] M. Onder, S. Onder, and E. Adiguzel, "Applying hierarchical loglinear models to nonfatal underground coal mine accidents for safety management," *International Journal of Occupational Safety and Ergonomics*, vol. 20, no. 2, pp. 239–248, 2014.

[12] H. Xiao, X. Cheng, and C. Zou, "The risk analysis and evaluation of urban underground logistics system development based on the grey analytic hierarchy process," *The Open Mechanical Engineering Journal*, vol. 8, no. 1, pp. 354–357, 2014.

[13] L. Zhao, X. Wang, and Y. Qian, "Analysis of factors that influence hazardous material transportation accidents based on Bayesian networks: a case study in China," *Safety Science*, vol. 50, no. 4, pp. 1049–1055, 2012.

[14] M. Spada, P. Burgherr, and M. Hohl, "Toward the validation of a National Risk Assessment against historical observations using a Bayesian approach: application to the Swiss case," *Journal of Risk Research*, vol. 22, no. 11, pp. 1323–1342, 2018.

[15] S.-S. Leu and C.-M. Chang, "Bayesian-network-based safety risk assessment for steel construction projects," *Accident Analysis & Prevention*, vol. 54, pp. 122–133, 2013.

[16] N. Batarlienė, "Risk analysis and assessment for transportation of dangerous freight," *Transport*, vol. 23, no. 2, pp. 98–103, 2008.

[17] D. A. Wiegmann and S. A. Shappell, "Human error analysis of commercial aviation accidents using the human factors analysis and classification system (HFACS)," *Aviation Space and Environmental Medicine*, vol. 72, no. 11, pp. 1006–1016, 2001.

[18] C.-d. Chen and Y. Liu, "Analysis on formation reasons and hidden dangers of safety accidents in logistics enterprises' road transport," *Journal of Minjiang University*, vol. 34, no. 6, pp. 53–58, 2013.

[19] A. Kibe, W. Mwangi, and S. Kimani, "Risk management in financial information systems using Bayesian networks," *Journal of Information Engineering and Applications*, vol. 4, no. 3, pp. 42–51, 2014.

[20] C. Contaldi, F. Vafaee, and P. C. Nelson, "Bayesian network hybrid learning using an elite-guided genetic algorithm," *Artificial Intelligence Review*, vol. 52, no. 1, pp. 245–272, 2019.

[21] X. Xie, Y. Liu, V. Perkovic et al., "Renin-angiotensin system inhibitors and kidney and cardiovascular outcomes in patients with ckd: a Bayesian network meta-analysis of randomized clinical trials," *American Journal of Kidney Diseases*, vol. 67, no. 5, pp. 728–741, 2016.

[22] J. Mi, Y. F. Li, W. Peng, and H. Z. Huang, "Reliability analysis of complex multi-state system with common cause failure based on DS evidence theory and Bayesian network," in *Reliability Engineering and System Safety*, vol. 174, pp. 71–81, Springer, Berlin, Germany, 2018.

[23] J. Zhou, X. Zhou, X. Du, and F. Wang, "Research on design of dam-break risks control for cascade reservoirs," *Journal of Hydroelectric Engineering*, vol. 37, no. 1, pp. 1–10, 2018.

[24] C. Liang and M. Ghazel, "A risk assessment study on accidents at French level crossings using Bayesian belief networks," *International Journal of Injury Control and Safety Promotion*, vol. 25, no. 2, pp. 162–172, 2018.

[25] S. Li, T. Tryfonas, R. Gordon, and A. Panagiotis, "Risk assessment for mobile systems through a multilayered hierarchical Bayesian network," *IEEE Transactions on Cybernetics*, vol. 46, no. 8, pp. 1749–1759, 2016.

[26] M. M. Aliabadi, H. Aghaei, O. Kalatpour, A. R. Soltanian, and A. Nikravesh, "Analysis of human and organizational factors that influence mining accidents based on Bayesian network," *International Journal of Occupational Safety and Ergonomics*, Article ID 101080, 2018.

[27] C. Cai and Y. Q. Liu, "Reliability analysis of logistics service supply chain system based on fuzzy Bayesian networks," *China Business and Market*, vol. 32, no. 4, pp. 49–58, 2018.

[28] Y. Yan and B. Suo, "Risks analysis of logistics financial business based on evidential Bayesian network," *Mathematical Problems in Engineering*, vol. 2013, Article ID 785218, 8 pages, 2013.

[29] L. S. Zhu and F. Yang, "Bayesian model for agricultural product logistics safety early warning," *Revista de la Facultad de Agronomia de la Universidad del Zulia*, vol. 36, no. 2, pp. 341–347, 2019.

[30] K. Li, Z.-S. Tan, and X.-Y. Tang, "Research on risk prediction and control of emergency logistics based on Bayesian network," *Logistics Sci-Tech*, vol. 40, no. 2, pp. 98–101, 2017.

[31] Y. Huang and Q. B. Qian, "Analysis and countermeasures of cold chain transportation failures based on Bayesian network," *Logistics Technology*, vol. 37, no. 9, pp. 20–26, 2018.

[32] J.-L. Hu, X.-W. Tang, and J.-N. Qiu, "A Bayesian network approach for predicting seismic liquefaction based on interpretive structural modeling," *Georisk: Assessment and Management of Risk for Engineered Systems and Geohazards*, vol. 9, no. 3, pp. 200–217, 2015.

[33] J. N. Warfield, "On arranging elements of a hierarchy in graphic form," *IEEE Transactions on Systems Man and Cybernetics*, vol. SMC-3, no. 2, pp. 121–132, 1973.

[34] M. D. Singh, R. Shankar, R. Narain, and A. Agarwal, "An interpretive structural modeling of knowledge management in engineering industries," *Journal of Advances in Management Research*, vol. 1, no. 1, pp. 28–40, 2003.

[35] V. Ravi and R. Shankar, "Analysis of interactions among the barriers of reverse logistics," *Technological Forecasting and Social Change*, vol. 72, no. 8, pp. 1011–1029, 2005.

[36] M. Q. Zhang and Y. Zhou, "Study on the alarming and prevention of logistics operation risk," *Logistics Technology*, vol. 27, no. 4, pp. 49–51, 2008.

[37] http://www.safehoo.com/.

[38] http://www.esafety.cn/shiguanli/.

[39] http://www.anquan.com.cn/.

[40] S. Nadkarni and P. P. Shenoy, "A causal mapping approach to constructing Bayesian networks," *Decision Support Systems*, vol. 38, no. 2, pp. 259–281, 2004.

[41] Z. G. Zhu, "Strengthen safety management in logistics and transportation," *Traffic Transportation*, vol. 1, no. 57, p. 53, 2012.

[42] K. Yang, "Discuss about how to make logistics express transport vehicler traffic safety management," *Management Observer*, vol. 607, no. 8, pp. 40-41, 2016.

Hindawi
Mathematical Problems in Engineering
Volume 2020, Article ID 3618424, 11 pages
https://doi.org/10.1155/2020/3618424

Research Article

Research on Industrial Waste Recovery Network Optimization: Opportunities Brought by Artificial Intelligence

Bin Liao and Ting Wang

School of Management, University of Guizhou, Guiyang, China

Correspondence should be addressed to Ting Wang; wting74@163.com

Received 3 November 2019; Revised 26 February 2020; Accepted 23 March 2020; Published 25 April 2020

Guest Editor: Davide Castellano

With the acceleration of industrialization and urbanization in China, a large amount of waste in industrial parks has become the main cause of regional environmental pollution. In order to solve this problem, this paper relied on artificial intelligence's prediction technology and image recognition technology to intelligently upgrade the traditional industrial waste planning management system and designed a waste intelligent classification center with intelligent prediction and intelligent classification capabilities. So, as to realize this new intelligent classification center and explain its value, this paper explains the key implementation technology of this intelligent classification center and validates it by constructing a multitarget location model that considers both economic and environmental benefits.

1. Introduction

With the rapid development of industry and economy, the problem of environmental pollution is becoming more and more serious. In the face of the "three great mountains" of competition proliferation, resource depletion, and environmental degradation, governments have begun to attach great importance to the coordinated balance between economic development and environmental protection issues. As of 2017, China produces about 3.3 billion tons of industrial waste each year, with a total stockpiled over 60 billion tons over the years. Industrial waste that has not been disposed of in a timely manner has not only caused a huge waste of land resources but also caused regional ecosystem disturbances [1–3]. How to safely, economically, environmentally, and efficiently treat these wastes has become one of the important research topics for the development of a sustainable economy in China.

The social demand for recovering and reusing discarded products has stimulated a research boom in product-recycling networks [4]. After years of accumulation, the research on the waste product-recycling network has achieved results, but it mainly focuses on the recovery and reuse of mobile phones, automobiles, washing machines, and other electronic products. Few studies have discussed the issue of industrial waste recycling [5–9]. In the existing research on industrial waste management, most scholars treat industrial waste and domestic waste as urban waste for discussion. Huang and Li discussed the problems of Wuhan municipal waste recycling, treatment, and resource reuse. Finally, they proposed the scientific classification of municipal waste and diversified garbage collection, charging, and treatment management methods to promote Wuhan's waste management related development of the industry [10]; Li et al. proposed an urban waste recycling system based on radio frequency wireless network, including system function description, hardware design, and software design. The system uses sensor technology and radio frequency wireless network technology to realize the information collection of urban garbage bins and the positioning of urban garbage collection systems. This research has realized the dynamic tracking and monitoring of garbage from the source to the disposal terminal and has made some contributions to the intelligent development of garbage recycling management [11]; Wang et al. established a game relationship model for residents, receiving and transporting enterprises, and waste processing enterprises under different classification ratios based on the Stackelberg game theory. The proportion of the responsibility of the waste management of the subject and the simulation analysis of the model show that the waste classification capacity of industrial waste service enterprises is the main factor affecting the interests of the subjects in the recycling network [12].

Importantly, as the process of industrialization and urbanization continues to accelerate, the large concentration of industries and populations has saturated the load of the previous urban waste transportation network, which has led to a sudden decline in the efficiency of the traditional industrial waste. As a result, severe waste accumulation and environmental pollution have occurred in many regions of China. Therefore, the separation of traditional waste recycling systems and the design of a recycling management network dedicated to the treatment of industrial waste to improve the efficiency of waste treatment are becoming research hotspots in the field of industrial waste management and reuse.

In the research of industrial waste recycling management network, scholars mostly discuss the industrial waste network planning and design based on the perspectives of logistics cost, service level, and equipment utilization efficiency [13–15]. Wang et al. constructed a two-objective optimization model when designing the logistics network to analyze the impact of different input costs on the environment in the design of the supply chain while considering the two goals of cost and environmental protection level to analyze the project's return on investment. The rate has a positive enlightening effect on the future green management of the supply chain [16]. Since then, Elhedhli and Ryan further explore the relationship between distance and carbon emissions [17]; Rui et al. considered a logistics network planning model with a hard time window and analyzed the impact of different time windows on the economy and the environment [18]; Zhang and Li-rong others have considered the uncertainty of the quality of the recycled products in the market, set up a multiobjective stochastic programming model with the goal of minimizing logistics network costs and environmental pollution, and solved the stochastic programming model with scenario analysis [19].

This thesis considers the intelligent upgrading of industrial waste recycling management network in an industrial park with multiple factories. First, the artificial intelligence prediction technology and image recognition technology are used to intelligently upgrade the traditional industrial waste planning management system. An intelligent classification center for industrial waste with intelligent prediction and intelligent classification capabilities is designed, and its key implementation technology is discussed. Finally, the value and significance of the intelligent classification center designed in this paper are illustrated by constructing a multiobjective site selection model considering both economic and environmental benefits.

The rest of this article is organized as follows. The next section puts forward the key technologies for the realization of the industrial waste intelligent classification center system architecture, including the industrial waste production and component prediction models based on BP learning algorithms and deep learning-based waste identification and detection implementation technologies. In the fourth section, the site selection model, implementation algorithm, and numerical simulation of the industrial waste intelligent recycling center considering economic and environmental benefits are designed. The last section discusses and summarizes the thesis work.

2. Design of Artificial Intelligent Waste Sorting Center

2.1. System Framework of Artificial Intelligence Recycling Classification Center. The optimization of an industrial waste recycling network system is essentially a multilevel, multiobjective management decision problem. To upgrade the traditional model, it is necessary to redesign a decision model with corresponding functions. In this research, artificial intelligence technology is integrated into the traditional waste logistics recycling system. The system framework of the artificial intelligence recycling classification center that integrates the two core technologies of waste production prediction technology and image recognition is designed, as well as its functional decision model. It can be seen from Figure 1 that this intelligent recycling classification center has basic decision-making functions for industrial waste production forecasting, component forecasting, image recognition, and intelligent location selection. During the operation of the classification center, the quantity and category prediction of the waste to be processed is first based on the preset related parameters. On the one hand, these prediction results can be used as training sets to train and detect the image recognition model. On the other hand, it can be combined with processing power as a parameter source for the location model of the intelligent classification center to verify the economic and environmental benefits of such intelligent classification centers replacing traditional artificial classification centers. It can be seen that the data flow is progressively advanced between different models, forming an organic whole with complex relationships.

2.2. Key Technologies Implemented by Artificial Intelligence Recycling Classification Center. As can be seen from the above, the basis for realizing the artificial intelligence classification center designed in this paper is the design of industrial waste prediction technology and image recognition technology. In this section, we focus on the design ideas and algorithms of these two technologies.

2.2.1. Prediction Model of Industrial Waste Products and Components Based on BP Learning Algorithm. The neural network is a kind of multilayer feedforward neural network trained according to the error backpropagation algorithm. It is the most widely used neural network. The artificial neural network does not need to determine the mathematical equation of the mapping relationship between input and output in advance. It only learns certain rules through its own training and obtains the result closest to the expected output value when given the input value. With the

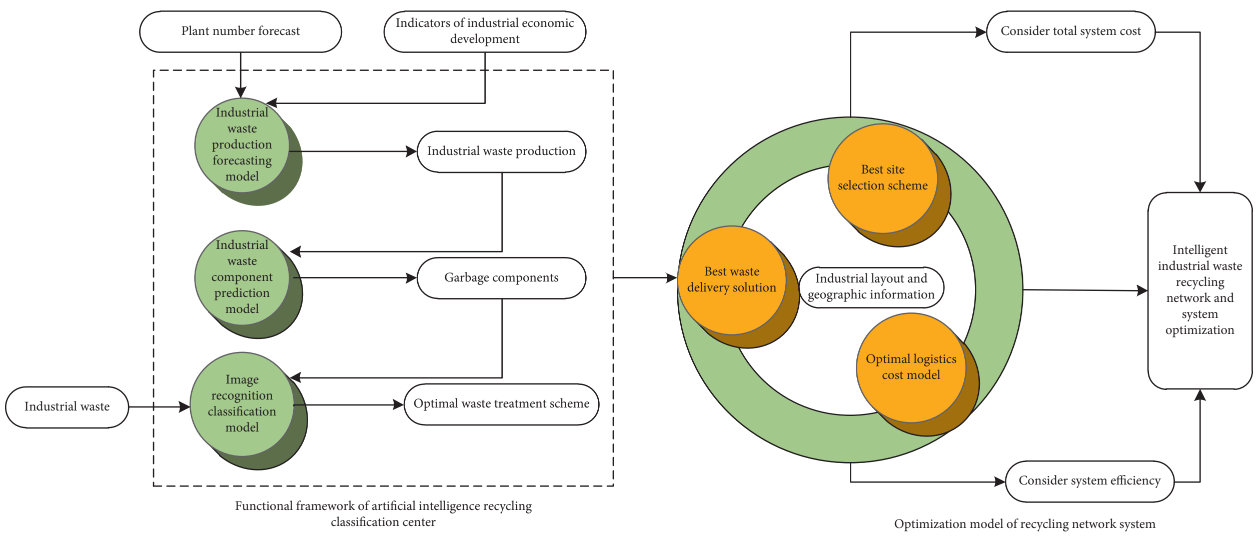

Figure 1: System framework of artificial intelligence recycling classification center and its functional decision-making model.

advantages of high prediction accuracy and robust results, this method is widely used in intelligent prediction, machine learning, and other fields [20]. This paper designs the BP network prediction model of industrial waste products and composition, as shown in Figure 2.

The core of an artificial neural network to realize its function is the algorithm. BP neural network is a multilayer feedforward network trained by error backpropagation. The BP learning algorithm is an error correction method based on this principle. The learning process of the algorithm consists of forwarding and backpropagation (partial composition). When an input mode of a network is given, it is passed from the input layer unit to the hidden layer unit, processed by the hidden layer unit, and then sent to the output layer unit, and an output mode is generated by the output layer unit. Because this is a layer-by-layer effect in the process, each layer of neurons can only affect the state of the next layer of neurons, which is called forward propagation; if the output response is in error with the expected output mode and does not meet the requirements, then the error is transferred to the backpropagation and then transmitted. The value is transmitted layer by layer along the connection path, and the connection weight of each layer is modified. For a set of samples, learning is performed by using different training modes, and the model is continuously repeated in the forward and backward propagation processes. Only when each training mode meets the requirements, the BP network training is completed. Network learning is a process of minimizing the objective function to complete the input-to-output mapping. Generally, the objective function is defined as the sum of the squared error of the output layer unit's desired output and the actual output on all input modes. The prediction algorithm of industrial waste production and composition in this paper is as follows:

Step 1: suppose the input layer has $n$neurons, the input vector is $X(x_1, x_2, \ldots, x_n)$; the hidden layer has m neurons, the hidden layer vector is $H(h_1, h_2, \ldots, h_m)$; the output layer has k neurons, the output vector is $Y(y_1, y_2, \ldots, y)_k$. The weight between the input layer and the output layer is and the threshold is ; the weight between the hidden layer and the output layer is and the threshold is.

Step 2: assign initial values to all connection weights and node thresholds

Step 3: do the following calculations for each input sample:

(a) Forward calculation:

$$\left\{ y_k = \sum_{j=0}^{m} \omega_{jk \cdot h_j}, h_j = \sum_{j=0}^{n} \omega_{ij \cdot x_i}. \right. \tag{1}$$

Let the transfer function be a sigmoid function, that is, $f(x) = (1/1 + \exp(-ax))(a > 0)$.

For the P_i sample in the training set, the network input vector is $X(x_1, x_2, \ldots, x_n)$, the actual output is $Y(y_1, y_2, \ldots, y_k)$, the expected output is $T(t_1, t_2, \ldots, t_n)$, and the error function is defined as follows:

$$E = \frac{1}{2} \sum_{k=1}^{i} (t_k - y_k)^2. \tag{2}$$

Let the total number of samples is N, then the mean of the squared error is

$$E_{AV} = \frac{1}{N} \sum_{N=1}^{N} E. \tag{3}$$

E_{AV} is the mean of the squared error. The purpose of the algorithm learning is to minimize E_{AV}.

(b) Inverse calculation

When the algorithm fails to meet the target expectations, it will calculate backward. The first is to calculate the local gradient δ_k. The first is to calculate

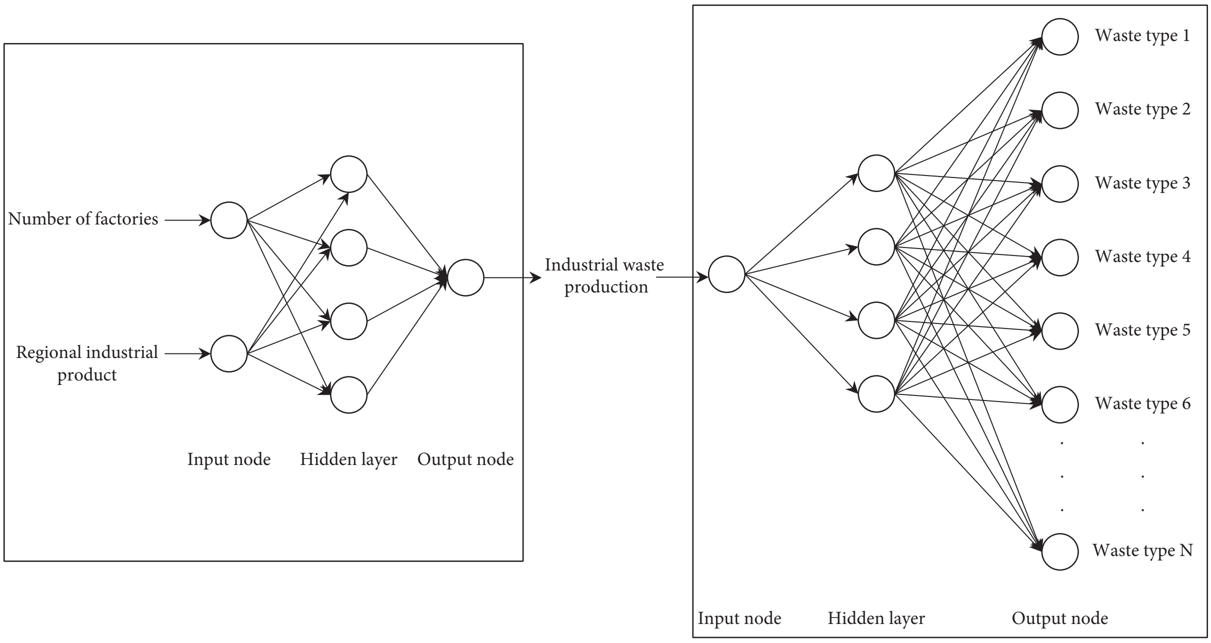

FIGURE 2: BP network prediction model for industrial waste products and components.

the local gradient. It is worth noting that for the output and hidden layers, the algorithms of the local gradient are different, as shown in formulas (4) and (5):

$$\text{Output layer } \delta_k = (t_k - y_k) f(x_k), \tag{4}$$

$$\text{Hidden layer } \delta_k = \frac{\delta E}{\delta y_k} f(x_k). \tag{5}$$

(c) Correction weight:

Using the minimum value of the gradient descent method, the updated amount $\Delta\omega_{ij}$ of ω_{ij} can be expressed by the following formula:

$$\Delta\omega_{ij} = -\eta \frac{\partial E}{\partial \omega_{ij}}. \tag{6}$$

η represents the learning rate of the neural network, and its value is greater than zero.

Step3: enter a new sample until E_{AV} meets the predetermined requirements. Eventually, the model can output the annual industrial waste output and composition of the region. These data will be used as a training sample for image data and site selection for training to implement waste identification and monitoring technology data source for the model.

2.2.2. Realization Technology of Waste Recognition and Detection Based on Deep Learning. Deep learning is an emerging research field of machine learning. Its research content is to automatically extract multilayer features from the data and represent them. In the process, a series of nonlinear transformations can be used to extract features from the original data and finally realize machine vision and intelligent operation such as machine sensing. This research uses the idea of deep learning to design the target detection technology of industrial waste images and uses the type, position, size, and confidence of the target object as the determination parameters to achieve intelligent detection and recognition of the predetermined target object. The basic flow of the target detection technology is shown in Figure 3.

The target detection algorithm is the key to achieve intelligent detection. Considering the complexity of industrial waste detection tasks in different environments, this study improves the Faster RCNN [21] target detection model, which combines the RPN network and Fast-RCNN Unified to identify the location and angle of industrial waste at the same time. Faster RCNN model, which is composed of two subnetworks: Region Proposal Generation (RPN) network and VGG-16 classification network as shown in Figure 4.

The RPN network adopts the design method of the fully convolutional network, in which the convolutional layer uses the VGG-16 model and shares convolutions with subsequent classification networks to reduce double counting. Figure 5 shows the structure of the RPN network. A small network is used to slide the feature image output by the last shared convolution layer to generate the region of interest. The input of this small network comes from the $n \times n$ size window input on the convolutional feature image, and then the features of each sliding window will be mapped to the lower dimensional feature vector. After the mapping, Re LU will perform nonlinear processing. The features, thus, obtained are used as input to two parallel fully connected layers—the bounding box return layer (REG) and the classification layer (CLS). The regression layer is responsible for readjusting the

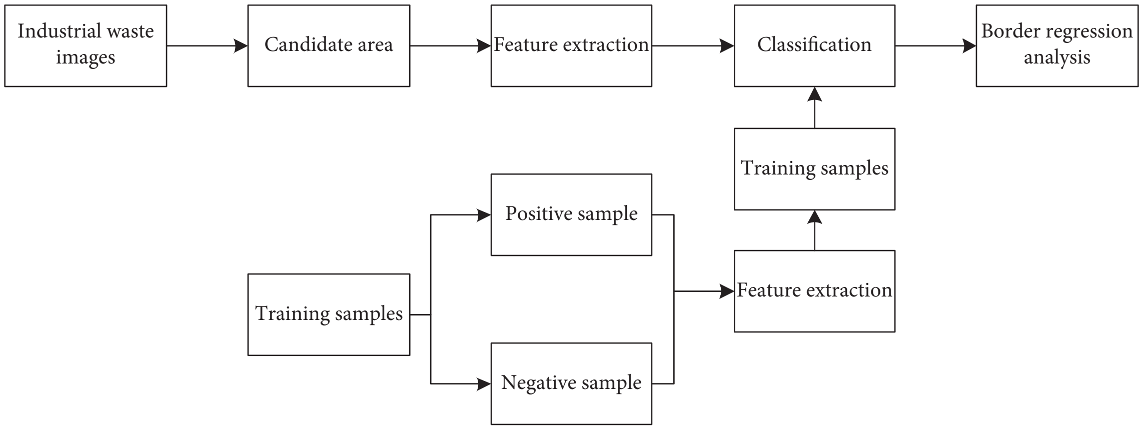

Figure 3: Basic flowchart of industrial waste monitoring technology.

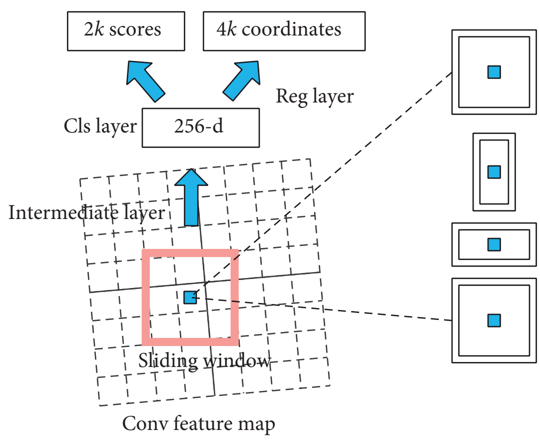

Figure 4: RPN network structure.

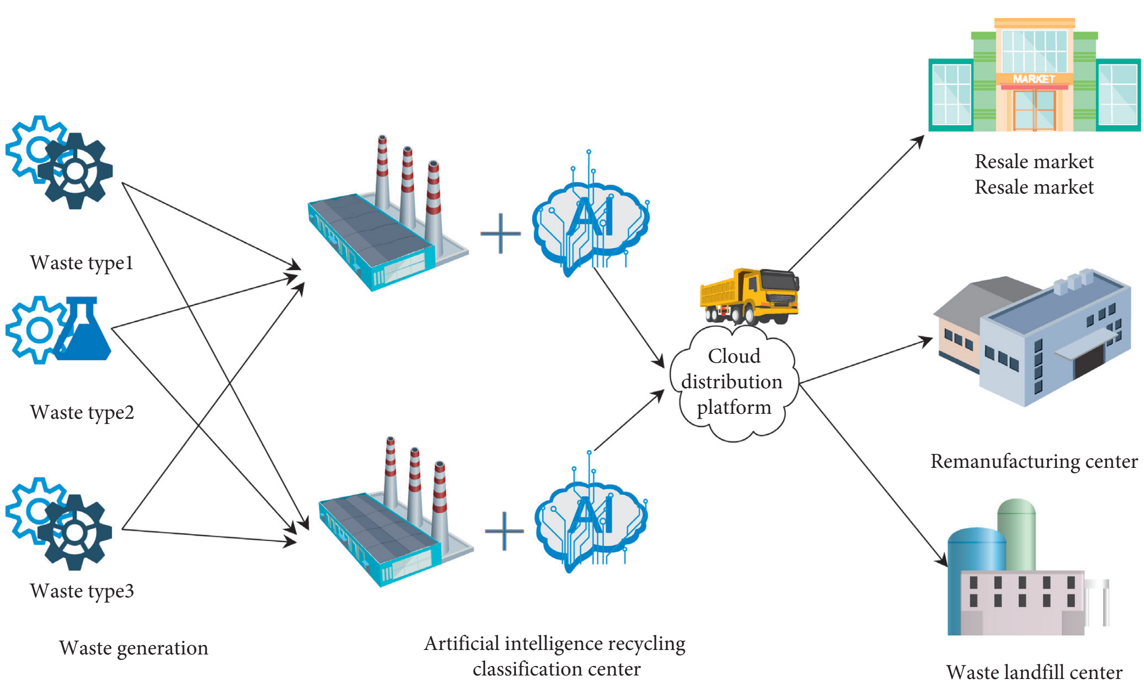

Figure 5: Industrial waste smart recycling model concept illustration.

inaccurate area of interest, and the function of the classification layer is responsible for determining whether the area belongs to a candidate area. This processing method ensures that all features are associated with the REG and CLS layers. At the position of each sliding window, determine whether multiple regions of interest contain objects at the same time. The number of regions predicted simultaneously at each position is recorded as k. Thus, the bounding box regression layer outputs a total of $4k$ coordinates for k regions, and the classification layer outputs a total of $2k$ scores to evaluate whether each region contains an object. In each sliding window position, 3 scales and 3 aspect ratios are used by default, so there are $k = 9$ anchor points in total. So, for a featured image of size $w \times h$, there are "$w * h * k$ anchor points. After obtaining candidate regions of interest through the RPN network, the VGG-16 network pretrained on the ImageNet dataset is used for classification.

The VGG-16 network is a convolutional neural network structure proposed by the VGG group in 2014. The dataset is ImageNet. It uses 16 network layers with parameters, including 13 convolution kernels with a size of 3×3. It consists of 3 fully connected layers [22]. In addition, the same as Fast R-CNN, on the last convolutional layer, the spatial pyramid pooling (SPP) layer is also used to pool the feature layers to the same size. In the original RPN scheme, a decoupling scheme different from the traditional model is adopted, that is, the angle prediction layer is separately connected behind the copied FC layer of the VGG-16 network, so that it is not updated at the same time as the position of the industrial waste and the category layer. The scheme can further reduce the error of the bottle object angle prediction. As with Fast R-CNN, our training model uses a minimizing multitask loss function. The loss function of the RPN and VGG-16 networks is the same. The loss function consists of two terms in the following formula:

$$L(\{P_i\}, \{t_i\}) = \frac{1}{N_{\text{cls}}} \sum_i L_{\text{cls}}(p_i, p_i^*) + \lambda \frac{1}{N_{\text{reg}}} \sum_i p_i^* L_{\text{reg}}(t_i, t_i^*). \tag{7}$$

Among them, i represents the pulling of anchor points in mini-batch and P_i represents the probability that the i anchor point is predicted to be an object. If the anchor point belongs to a positive sample, then p_i^* is 1, otherwise, it is 0. t_i is a 5-dimensional vector and belongs to the parameterized predicted object's bounding box coordinates, and t_i^* is the t_i label associated with the positive anchor. The classification loss function L_{cls} is calculated using a softmax loss strategy and the regression loss calculation is performed using a robust regression loss function (Smooth L1). When $p_i^* = 1$, it means that the regression loss is only activated at the anchor point for processing positive samples. At this time, the outputs of the corresponding CLS and REG layers are $\{P_i\}$ and $\{t_i\}$.

Among them, for the graphs bounding box regression, we adopt the R-CNN parameterization method to unify the regression parameters:

$$\begin{aligned}
t_x &= \left(\frac{(x - x_a)}{w_a}\right), \\
t_y &= \left(\frac{(y - y_a)}{h_a}\right), \\
t_x^* &= \left(\frac{(x^* - x_a)}{w_a}\right), \\
t_y^* &= \left(\frac{(y^* - y_a)}{h_a}\right), \\
t_w &= \log\left(\frac{w}{w_a}\right), \\
t_h &= \log\left(\frac{h}{h_a}\right), \\
t_w^* &= \log\left(\frac{w^*}{w_a}\right), \\
t_h^* &= \log\left(\frac{h^*}{h_a}\right), \\
t_p &= \left(\frac{t}{2\pi}\right), \\
t_p^* &= \left(\frac{t^*}{2\pi}\right).
\end{aligned} \tag{8}$$

Among them, x, y, and w represent the center coordinates of the frame, h represents the length, x_a represents the position of the anchor point, and x^* and y^* represent the position of the callout frame.

3. Study on Site Selection of Intelligent Industrial Waste Recycling Center

3.1. Problem Statement. The key technologies of the artificial intelligence recycling classification center have been explained above. It is not difficult to find that the artificial intelligence recycling classification center with image recognition technology and prediction technology can save a lot of labor costs. In order to verify the economic benefits of the designed artificial intelligence classification and processing center, from the perspective of system integrity, this paper designs a two-level goal of system planning research with system cost minimization and system efficiency maximization. The intelligent processing center will be integrated and sent to the waste data according to the operation process. At the same time, the optimal number and location of intelligent processing centers in the industrial waste processing network will be determined based on the geographical location of the various end-of-waste processing nodes. Finally, the economic benefits are judged by comparing the difference between the construction cost and the saved human resources.

Before this, it is necessary to briefly explain the operation mode of the entire waste system. This research integrates artificial intelligence technology into the traditional waste logistics recycling network and connects the various recycling nodes of industrial waste through the artificial intelligence classification center. The goal is to achieve the intelligence of the full recycling network, minimize costs, and maximize efficiency. The waste in the city is classified and processed (e.g., landfill, remanufacturing, and resale). Simplifying the problem can be summarized as the main point of industrial waste generation, artificial intelligence processing center, remanufacturing center, and landfill center, and for the small-cap market, the relationship is shown in Figure 5.

3.2. Mathematical Formula

3.2.1. Model Assumptions. In order to facilitate the analysis and description of the problem, this article makes some assumptions:

(1) All activities included in the recycling model proposed in this article are carried out in this model
(2) The system relies on existing secondary market, remanufacturing plant, no longer considers their construction costs, and only considers their operating costs
(3) The transportation costs of industrial waste are linearly related to the distance
(4) The waste output predicted by the trained neural network is equal to the real output

3.2.2. Model Parameter Setting and Description. The parameters involved in the model built in this paper mainly include node parameters, other parameters, general parameters, and decision variables, as shown in Table 1.

3.2.3. Objective Function and Constraints. The objective function considered in this paper is mainly the economic and environmental benefits of building an artificial intelligence classification center, so the following two objective functions are constructed:

$$\max F_1 = \left(\frac{\left(\sum_k Z_{mL}^{ER} + \sum_k Z_{kl}^{WR} \right)}{\sum_j Z_{jk}^{QW}} \right), \tag{9}$$

$$\begin{aligned} \min F_2 = {} & \left[\sum_k b_k^n + \lambda \left(Z_{kl}^{WR} + Z_{ml}^{ET} \right) \right] \\ & - \left[\sum_k p_k^W + \alpha \sum_k Z_{jk}^{QW} + \beta \sum_k Z_{km}^{WE} + \gamma \left(Z_{mn}^{WT} + Z_{mn}^{ET} \right) \right] \\ & - \left[\sum_k dZ_{jk}^{QW} g + \sum_k dZ_{km}^{WE} g + \left(\sum_k dZ_{mn}^{WT} g + \sum_k dZ_{mn}^{ET} g \right) \right. \\ & \left. + \left(\sum_k dZ_{kl}^{WR} g + \sum_k dZ_{ml}^{ER} g \right) \right]. \end{aligned} \tag{10}$$

Among them, equation (9) indicates that the maximum reuse rate of waste is the reflection of the environmental protection benefits of the recycling network, and equation (10) indicates that the overall revenue of the entire recycling network system is maximized, which is a reflection of economic benefits

$$\overset{\text{s.t.}}{\sum_j} Z_{jk}^{QW} = \sum_k Z_{km}^{WE} + \sum_k Z_{kl}^{WR} + \sum_k Z_{kn}^{WT}, \quad \forall k, j, \tag{11}$$

$$\sum_k Z_{km}^{WE} = Z_{ml}^{ET} + Z_{mn}^{ER}, \quad \forall k, \tag{12}$$

$$X_k^{WE} \cdot \sum_j Z_{jk}^{QW} = \sum_k Z_{km}^{WE}, \quad \forall k, \tag{13}$$

$$X_k^{WR} \cdot \sum_j Z_{jk}^{QW} = \sum_k Z_{kl}^{WR}, \quad \forall k, \tag{14}$$

$$X_k^{WT} \cdot \sum_j Z_{jk}^{QW} = \sum_k Z_{kn}^{WT}, \quad \forall k, \tag{15}$$

$$Z_{jk}^{QW} = Y_c, \tag{16}$$

$$\sum_j Z_{jk}^{QW} \le \sum_k W_k, \tag{17}$$

$$D \in (0, 1). \tag{18}$$

Constraints (11) and (12) indicate the conservation of material quality at each logistics node, that is, the amount of industrial waste input at each waste generation point, artificial intelligence recycling classification center, remanufacturing center, resales center, and waste landfill center equal to the output amount; constraints (13) to (15) restrict the amount of waste transported by the classification center to each secondary node through a proportional limit; constraint (16) indicates that the predicted value in the artificial intelligence center is the waste input entered in the model; constraint (17) indicates the processing limit of each waste treatment center; and constraint (17) indicates the range of decision variables.

3.2.4. Multiobjective Function Solution Design. The above model belongs to a multiobjective mixed-integer programming model. Multiobjective programming generally belongs to the Pareto optimization problem. Because of the mathematical optimization problem involving multiple objective functions, it can only be as close as possible to the ideal solution based on the coordination of the objective functions. Based on the literature [23], this paper uses the fuzzy membership function in fuzzy theory to fuzzify the objective function and converts the multiobjective problem into a single-objective problem for solving. Specific steps are as follows:

Step 1: First, disassemble the dual objective function into two single-objective functions and use Lingo software to obtain the value interval of each objective function. First, the value range $[F_{1\min}, F_{1\max}]$ of the first objective function is calculated by programming when only the

TABLE 1: List of model parameters and descriptions.

Node parameters	Description	Subscript	Operating cost
Q	Industrial waste generation point	$:j$	—
W	AI recycling classification center	$:k$	α
E	Remanufacturing center	m	β
R	Resale market	l	λ
T	Landfill center	n	γ
Other parameters	**Description**		
W_k	Maximum processing capacity per cycle of artificial intelligence recycling classification center		
$Q_j(x, y)$	j industrial waste generation point		
d	Distance between the two places (circle/km/ton)		
p_k^w	Cost of constructing the kth artificial intelligence classification processing center		
b_k^w	Reduced employee commissions for the construction of the kth artificial intelligence classification processing center		
Y_c	Artificial waste recycling center's forecasted garbage reception volume (tons)		
g	Average transportation cost (m/yuan)		
General parameters	**Description**		
Z_{jk}^{QW}	Amount of industrial waste transported from factories to artificial intelligence recycling sorting centers over a period of time (tons)		
Z_{km}^{WE}	Amount of industrial waste transported from the intelligent sorting center to the remanufacturing center over a period of time (tons)		
Z_{kl}^{WR}	Amount of industrial waste transported from the intelligent sorting center to the resale market over a period of time (tons)		
Z_{mn}^{WT}	Amount of industrial waste transported from the intelligent sorting center to the landfill center over a period of time		
Z_{ml}^{ER}	Amount of industrial waste from remanufacturing center to resale market over time (tons)		
Z_{mn}^{ET}	Amount of industrial waste from remanufacturing center to landfill center over time (tons)		
X_k^{WE}	Proportion of waste in AI recycling sorting centers shipped to remanufacturing centers		
X_k^{WR}	Proportion of waste shipped to resale markets in artificial intelligence recycling sorting centers		
X_k^{WT}	Proportion of wastes sent to landfill centers in artificial intelligence recycling sorting centers		
Decision variables	**Description**		
D	0-1 variable, indicating whether to choose to set up a recycling point at k; if selected, take 1, otherwise take 0		

environmental benefit target is considered; similarly, when only the economic benefits are considered, the value range of the second objective function can be obtained by programming calculation as $[F_{2\min}, F_{2\max}]$.

Step 2: the membership degree fuzzy function method is used to assign a fuzzy wish value to each objective function, and the membership degree of the fuzzy wish is used to indicate the degree of satisfaction of the decision-maker team in responding to the target level. This model belongs to the maximization optimization problem, and the membership function of its fuzzy desire is as follows:

$$\mu_1 = \begin{cases} 1, & F_1 > F_{1\min}, \\ \dfrac{F_1 - F_{1\min}}{F_{1\max} - F_{1\min}}, & F_{1\min} \le F_1 \le F_{1\max}, \\ 0, & F_1 < F_{1\min}, \end{cases}$$
$$\mu_2 = \begin{cases} 1, & F_2 > F_{\min}, \\ \dfrac{F_2 - F_{2\min}}{F_{2\max} - F_{2\min}}, & F_{2\min} \le F_2 \le F_{2\max}, \\ 0, & F_2 < F_{2\min}. \end{cases} \tag{19}$$

Step 3: Assign different weight coefficients to target satisfaction, unify the satisfaction of each target to form the overall satisfaction, so as to realize the conversion of multiple targets into a single target. That is, $\max F = \omega_1\mu_1 + \omega_2\mu_2$, where ω_1 and ω_2 are the weight coefficients of the two membership fuzzy functions, which indicate the relative importance of the objective function and can be given by the industrial waste recycling network design planner based on the comprehensive analysis of the regional environmental and industrial policies.

Step 4: Use Lingo10 to solve the new objective function.

3.2.5. Analysis of Examples. A waste recycling company plans to deploy an artificial intelligence waste recycling and processing network in the industrial agglomeration area of City G. It is known that there are 20 existing waste-generating points in this area, a waste remanufacturing center, a waste resale center, and a waste landfill One for each center. The coordinates and related costs of each existing facility and those to be selected are shown in Table 2. Among them, Table 2 shows the coordinates of the existing remanufacturing center, sales center, and landfill center. Table 3 shows the coordinates and cost of the alternative artificial intelligence classification processing center, which is the maximum classification processing capacity in the period

Table 2: Remanufacturing center, resale market, and landfill center.

	X-axis	Y-axis
Remanufacturing center	35	85
Resale market	70	38
Landfill center	20	37

Table 3: Coordinates of alternative points, construction cost, and cycle capacity.

Recycling classification center	X-axis	Y-axis	Construction cost (yuan)	Cycle capacity (tons)
1	76	12	200000	1200
2	71	16	200000	1200
3	68	25	200000	1200
4	65	66	200000	1200
5	55	47	200000	1200
6	45	68	200000	1200
7	35	41	200000	1200
8	49	27	200000	1200

Table 4: Coordinates of waste generation points, predicted value, and original classification costs.

Waste generation point	X-axis	Y-axis	Cycle production (tons)
1	92	19	328
2	22	47	235
3	51	59	224
4	89	92	166
5	55	76	205
6	14	76	362
7	26	57	400
8	84	7	280
9	82	53	191
10	93	94	161
11	24	35	346
12	57	45	263
13	42	22	460
14	1	79	135
15	67	15	265
16	98	48	158
17	65	76	410
18	37	85	260
19	88	54	372
20	29	67	340

Table 4 shows the data use formulas (1)–(6) to predict the waste products in the next cycle of G city. Table 5 shows the transportation ratio of each node. Table 6 shows the operating costs of processing waste per ton of waste at each node. In addition, according to the basic local conditions, the transportation cost is 4 yuan/ton/km, the cost of traditional manual waste treatment is 200 yuan/ton, and the reuse rate of traditional industrial waste is 74.6%.

Using Lingo software, the objective functions under different weights are solved, and the logistics network facilities location schemes under three weights and the corresponding objective function values of environmental and economic benefits of the network system are obtained (as shown in Table 7).

Table 5: Transportation proportion of each node after classification.

	Transportation ratio (%)
X_k^{WE}	50
X_k^{WR}	30
X_k^{WT}	20

Table 6: Operating costs of each node.

	Unit processing cost (yuan/ton/km)
Z_{jk}^{QW}	4
Z_{km}^{WE}	3
Z_{kl}^{WR}	3
Z_{kn}^{WT}	3
Z_{ml}^{ER}	3
Z_{mn}^{ET}	3

It can be known from the example that when only environmental protection benefits are used as the objective function, alternative points 1, 2, 4, 5, 6, 7, and 8 need to be selected intelligence to build an artificial classification center. The economic benefits generated at this time are 174,206 yuan per unit cycle. The environmental protection benefit is to achieve 84.6% of the reuse rate of waste; when only economic benefits are considered and when only economic benefits are used as the objective function, alternative points 2, 3, 4, 5, 6, and 8 need to be selected. During the construction of artificial intelligence classification center, the economic benefit generated at this time is 288,014 yuan per cycle, and the environmental protection benefit is to achieve 82.7% of the reuse rate of waste; when considering both economic and environmental benefits, at this time, alternative points 2, 4, 5, 6, 7, and 8 are selected. At this time, the economic benefit is 246,137 yuan per cycle, and the environmental protection benefit is to achieve 83.5% of the reuse rate of the waste. This plan takes into account both economic and environmental benefits. Therefore, the solution of the model in this paper is shown in Figure 6 at this time.

Table 7: Logistics network facility location plan.

Weight coefficient (ω_1, ω_2)	Total network cost (yuan)	Landfill rate (%)	AI recycling classification center alternative point
(1, 0)	174206	84.6	1, 2, 4, 5, 6, 7, 8
(0, 1)	288014	82.7	2, 3, 4, 5, 6, 8
(1, 1)	246137	83.5	2.4, 5, 6, 7, 8

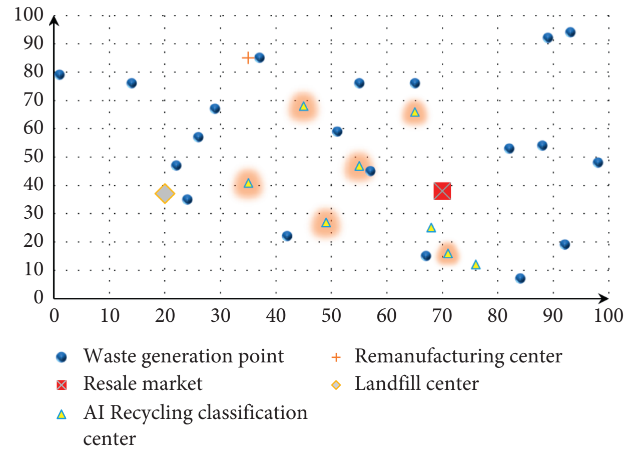

Figure 6: Distribution of site selection schemes.

4. Conclusion and Discussion

With the acceleration of China's industrialization and urbanization process, the traditional urban waste treatment and logistics network has been unable to meet the rapidly expanding population and production capacity, and the large accumulation of waste in industrial parks has become a major cause of environmental pollution. One of the main challenges of the sustainable development strategy is to solve the problem of upgrading and designing waste network systems in industrial parks.

Based on artificial intelligence's prediction technology and image recognition technology, this article intelligently upgrades the traditional industrial waste planning and management system, designs an industrial waste intelligent classification center with intelligent prediction and intelligent classification capabilities, and implements its key implementation. The technology was explored. Finally, the value and significance of the intelligent classification center designed in this paper are illustrated by constructing a multiobjective site selection model considering both economic and environmental benefits.

It can be seen from the different weighted results of economic and environmental benefits of fuzzy mathematical methods that regardless of focusing on economic benefits or environmental benefits, huge economic benefits can be obtained by reducing the dependence on human resources after building a new intelligent classification center. Therefore, relevant departments and responding companies can be advised to fully apply such artificial intelligence technology to the existing industrial waste recycling network, thereby enhancing the global benefits of the existing industrial waste recycling network, improving system efficiency and robustness, and ultimately achieve green sustainable development.

In previous research, [11] proposed an urban waste recycling system based on radio frequency wireless networks. Using sensor technology and radio frequency wireless network technology, the information collection of urban waste bins and the apex and positioning of urban trash cans were achieved. This has a certain enlightening effect on us. Big data technology and artificial intelligence technology are gradually changing our way of life. Therefore, this article uses new artificial intelligence technology to optimize the existing industrial waste recycling network and realize the idea of intelligent, economical, and sustainable recycling systems. It can promote academic innovation and disciplinary intersection in the field of waste management. In [16], while considering the cost, and taking into account the benefits of investment in environmental protection, a green supply chain network design model was proposed, and the optimization method was used to study the supply network construction cost and the minimum environmental pollution of the entire supply chain system. Their research found that the main way to reduce carbon dioxide emissions and total costs is to increase network capacity and enhance the service capabilities of facilities, which coincides with our research conclusions. To some extent, this shows that the only way for the supply chain network to achieve greening and maximize economic benefits is to improve service capabilities and response capabilities through technological improvements. References [17, 19], etc., proposed or applied classic multiobjective function tools such as particle swarm optimization and genetic algorithms when solving multiobjective function problems. The multiobjective function algorithm designed in this paper uses the fuzzy membership function in the fuzzy theory to obfuscate the objective function and converts the multiobjective problem into a single-objective problem for solving. On the one hand, the solution process and results can be more clearly explained and analyzed. For example, the effect of the objective function on the overall system optimization under different preferences can be further analyzed. On the other hand, only 0 and 1 were the two extreme weights. Researchers can also design new solving algorithms based on different weight preferences.

Our further research direction is to consider more factors in the supply chain, such as transportation mode, demand uncertainty, artificial intelligence learning ability, image recognition fault tolerance rate, etc., in order to enhance its applicability to real-world scenarios. On the contrary, we can also extend our research by designing new solutions to solve this multiobjective model.

Data Availability

The data used to support the findings of this study are available from the corresponding author upon request.

Conflicts of Interest

The authors declare that there are no conflicts of interest regarding the publication of this paper.

Acknowledgments

This work was supported by the Construction Project for Domestic 2017 First-Class-Discipline in Guizhou Province (GNYL[2017]005), Guizhou Provincial Philosophy and Social Science Planning Joint Fund (18GZLH03), and Major project fund for social science & humanities of Guizhou University (GDZT201702).

References

[1] Z. Lu, J. Zhang, S. Lu et al., "Pollution characteristics and evaluation of heavy metal elements in the soil around the municipal solid waste incineration power plant and in the plant area," *Environmental Science*, vol. 40, no. 5, pp. 483–2492, 2019.

[2] Y. Peng, L. Lei, X. Peng, P. Yang, X. Zhao, and W. Ma, "The development of domestic waste classification in China? Obstacles and countermeasures," *China Environmental Science*, vol. 38, no. 10, pp. 3874–3879, 2018.

[3] L. Dan, G. Chen, W. Ma, and N. Duan, "Characteristics and treatment status of domestic garbage in villages and towns in China," *China Environmental Science*, vol. 38, no. 11, pp. 4187–4197, 2018.

[4] T. Lindhqvist, *Extended Producer in Cleaner Production: Policy Principle to Promote Environmental Improvements of Product Systems*, IIIEE, Lund, Sweden, 2000.

[5] J. Li, D. Li, and M. Lu, "Research on the design of C2B waste mobile phone reverse logistics recycling network based on carbon emission," *Manufacturing Automation*, vol. 40, no. 9, pp. 95–101, 2018.

[6] Y. Chen, Y. Yang, and Q. Zhang, "Design of reverse logistics network for waste household appliances based on third party recycling," *Mathematics in Practice and Theory*, vol. 46, no. 17, pp. 81–89, 2016.

[7] D. Wang, H. Du, and W. Yang, "A two-stage fourth-party reverse logistics network design model based on CVaR," *Industrial Engineering and Management*, vol. 20, no. 1, pp. 22–27, 2015.

[8] H. Prajapati, R. Kant, and R. Shankar, "Bequeath life to death: state-of-art review on reverse logistics," *Journal of Cleaner Production*, vol. 211, pp. 503–520, 2019.

[9] S. Agrawal, R. K. Singh, and Q. Murtaza, "A literature review and perspectives in reverse logistics," *Resources, Conservation and Recycling*, vol. 97, pp. 76–92, 2015.

[10] D. Huang and Y. Li, "Problems in urban domestic waste treatment in Wuhan and suggestions for improvement," *Resources and Industries*, vol. 14, no. 3, pp. 167–173, 2012.

[11] L. I. Yan, G. Yang, and A. Ren, "Research on urban garbage recycling system based on radio frequency wireless network," *Modern Electronic Technology*, vol. 38, no. 16, pp. 48–50, 2015.

[12] W. Wang, X. Ge, and Y. Xu, "Analysis of multi-agent interest game and differential responsibility in urban waste separation and recycling," *China Population, Resources and Environment*, vol. 27, no. S2, pp. 41–44, 2017.

[13] Q. Wang, Li Xia, and C. Tong, "Selection and evaluation of reverse logistics suppliers based on program satisfaction," *Logistics Technology*, vol. 37, no. 11, pp. 50–55, 2018.

[14] Q. Zhang and X. Lu, "Research on e-commerce return vehicle routing problem and ant colony algorithm," *Computer Engineering and Applications*, vol. 54, no. 22, pp. 239–245, 2018.

[15] M. Lu, Z. Ye, J. Tian, and F. Wang, "Optimization design of reverse logistics network considering random reproducibility ratio," *System Engineering*, vol. 35, no. 6, pp. 113–120, 2017.

[16] F. Wang, X. Lai, and N. Shi, "A multi-objective optimization for green supply chain network design," *Decision Support Systems*, vol. 51, no. 2, pp. 262–269, 2011.

[17] S. Elhedhli and M. Ryan, "Green supply chain network design to reduce carbon emissions," *Transportation Research Part D: Transport and Environment*, vol. 17, no. 5, pp. 370–379, 2012.

[18] Li Rui, M. Huang, and F. Sun, "Multi-to-multiple network design of fourth-party logistics with hard time windows," *Control Engineering*, vol. 25, no. 10, pp. 1927–1933, 2018.

[19] Q. Zhang and W. Li-rong, "Multi-objective stochastic programming model for reverse logistics network design," *Soft Science*, vol. 29, no. 10, pp. 120–124, 2015.

[20] S. Yang and L. Huang, "Financial early warning model of listed companies based on BP neural network," *Systems Engineering Theory & Practice*, vol. 25, no. 1, pp. 12–18, 2005.

[21] W. Yang, H. Wang, J. Zhang et al., "An improved vehicle real-time detection algorithm based on Faster-RCNN," *Journal of Nanjing University (Natural Science Edition)*, vol. 55, no. 2, 2019.

[22] K. Simonyan and A. Zisserman, "Very deep convolutional networks for large-scale image recognition," 2014, https://arxiv.org/abs/1409.1556.

[23] X. Xu and J. Li, *Theory and Method of Multi-Objective Decision Making*, Tsinghua University Press, Beijing, China, 2005.

Hindawi
Mathematical Problems in Engineering
Volume 2020, Article ID 9808370, 14 pages
https://doi.org/10.1155/2020/9808370

Research Article

Optimal Strategies for CLSC considering Supply Disruption and Carbon Tax

Lin Tong, Kuan Yang, and Wei-Jin Xu

School of Business Administration, Hunan University, Changsha 410082, China

Correspondence should be addressed to Kuan Yang; yangkuanhnu@163.com

Received 7 November 2019; Revised 2 March 2020; Accepted 16 March 2020; Published 24 April 2020

Academic Editor: Mosè Gallo

Under the background of economic globalization, supply chain is becoming more and more complex, which is manifested in the instability of external environment. On the one hand, with the improvement of global environmental protection awareness, the government's policy tools for environmental impact (carbon tax) on the whole supply chain have become one of the major external problems faced by the supply chain enterprises; on the other hand, the intensification of competition between upstream and downstream in supply chains makes supply disruption an important proposition to be solved urgently. In this paper, the two propositions of green and supply disruption are reduced to two factors affecting the cost. The average total cost function of the manufacturer as a recycler is established. The practicability of the algorithm and the effectiveness of the model are verified by Lingo, Particle Swarm Optimization, and Genetic Algorithm, with the purpose of obtaining the optimal strategies for manufacturers who play the role of the recycler in the closed-loop supply chain.

1. Introduction

In recent years, managing supply chain through remanufacturing is an active research area, closed-loop supply chain management [1]. For the manufacturing industry, remanufacturing mitigating the deterioration of the environment to some extent not only increases resource utilization and promotes the increasing of social economic and the profits of enterprises but also improves the competitiveness of enterprises and shapes the corporate image [2]. At present, reverse logistics management has become the focus of many enterprises. Through recycling and remanufacturing activities, enterprises make themselves more competitive in product prices [3]. In the forward supply chain, the customer is the end of the supply chain. However, products that initially did not meet customer requirements still had residual value. Enterprises can release additional value from reverse logistics and remanufacturing processes to protect the environment. Through the combination of forward and reverse logistics management, the linear noncircular supply chain is transformed into closed-loop recycle.

Guo et al. [4] study the optimal strategies for the CLSC under supply disruption, and the influence of government subsidy mechanism on the business activities of enterprises in case of supply disruption is considered. Their article regards the cost caused by supply disruption as a part of the total cost of manufacturers, which is a great improvement on the total cost function of manufacturers as recyclers. But, with the increasingly prominent environmental problems and the increasing scarcity of natural resources, environmental protection has been deeply rooted among people. Green and sustainability have become an important symbol of enterprise competition, helping them to cope with the growing environmental pressure [5]. Globally, green cycle and low carbon development have become the trend. In the manufacturing industry, manufacturers are also affected by green policies: the existence of carbon tax policy makes manufacturers more inclined to recycle old products for remanufacturing because the cost of carbon tax in the process of remanufacturing products per unit is lower than that in the production process of new products per unit—which means that the cost of carbon tax has become an inevitable part of the total cost of manufacturers in the context of CLSC [6–8].

This article is a further study after the research of Guo et al. [4]. Thus, this article studies the optimal production strategy of the closed-loop supply chain in the context of carbon tax and supply disruption. Based on their research in [4], the cost of carbon tax has taken into consideration the total cost function for manufacturers; this will make the manufacturers as recyclers in the CLSC implement optimal production and recycling strategies according to the advanced cost structure in the current complex environment and get the maximum benefit. In addition, the hypothesis defined in [4] is that the recycling rate will decrease if the required quality level increases, so the quality of returned products is exponential distribution in their paper, $q \sim E(\lambda)$. But, in reality, when the quality level of recycled products q is close to 0, the product's residual value is almost 0, so the product is more likely to be directly discarded rather than being recycled; when q is close to 1, the product's residual value is very high, and the product is more likely to be used by its owner—the quality of returned products is more suitable to be normal distribution. The main contributions and highlights of this study are as follows:

(i) Not only supply disruption but also carbon tax is considered in the CLSC system

(ii) The hypothesis of quality of returned products obeys normal distribution making it more real

2. Literature Review

This paper will next sort out the literature from three aspects: green sustainable closed-loop supply chain, comparison and selection of recycling channels, and closed-loop supply chain considering supply disruption.

2.1. Green and Sustainable Closed-Loop Supply Chain. All over the world, green cycle and low carbon development have become the trend of all walks of life, and closed-loop supply chain is no exception. Many contributions on the sustainable closed-loop supply chain are worked out. Paksoy et al. [9] developed a multiproduct closed-loop supply chain taking environmental impact into consideration. By adding cost factors on the basis of environment, Ma et al. [10] proposed a robust double objective green closed-loop supply chain design problem. Some scholars established a multiobjective green CLSC model to minimize the expected cost of the supply chain network and greenhouse gas emissions [11, 12]. Bazan et al. [6] focused on two levels of CLSC, one for manufacturers and the other for retailers, with facilities for remanufacturing used goods. They considered three key environmental factors: (1) the materials consumed in manufacturing and remanufacturing activities, (2) the greenhouse gas emissions produced in production and transport activities, and (3) the items used for remanufacturing (recycling). Banasik et al. [13] established a multiobjective mixed integer linear programming model to quantify economic and environmental indicators and tried to find the balance between them. A multiobjective optimization mathematical model—developed by the National University of the United States (NU), was tested by Nurjanni et al. [14], in order to find the best balance between economy and environment. Haddadisasakht and Ryan [15] put forward their own model based on carbon tax with uncertain tax rate. Wang and Guo [16] study the optimal operation strategy of multicycle hybrid manufacturing/remanufacturing system considering carbon tax. Considering emissions of greenhouse gases and the overall operational cost, a green urban closed-loop logistics distribution network model is proposed in [7].

2.2. Selection of Recycling Channels. In recent years, many researches on closed-loop supply chain from different recycling channels are worked out. Generally speaking, they mainly study single-channel and multichannel recycling.

The relevant **single-channel** literature [17–24]is summarized in Table 1.

The relevant **multichannel** literatures: Yi and Yuan [25] coordinate and analyse the CLSC model of double-channel recycling that manufacturers and retailers can be recyclers. Hong et al. [26] constructed a model of manufacturer, retailer, and third-party mixed recycling and studied the selection of optimal mixed recycling mode. Giovanni and Zaccour [27] studied the different recycling channels of manufacturers and obtained the conditions for manufacturers to outsource the recycling business to retailers and third parties. Giovanni et al. [28] explored the incentive strategy model for both manufacturers and sellers to recycle waste products.

2.3. CLSC considering Supply Disruption. Supply chain disruption according to its causes can be divided as follows: (1) disruption by major unforeseen events and (2) disruption by operational accidents. The researchers propose corresponding recovery strategies for different disruptions.

Researchers' research achievements on disruption risk: Aryanezhad et al. [29] work out the design of supply chain when the distribution center is disturbed randomly and solve the disruption by developing a version of GA. The concept of P-Robust is applied in the design of reliable network model and measures to reduce disruption risk are implemented [30]. The model can run as normal (no disruption) after failure. Baghalian et al. [31] studied the demand-side uncertainty with probability function and the failure probability at the supply side of each factory in order to design the supply network of the Middle East agricultural food industry. Hernandez et al. [32] used the multiobjective optimization method to provide the decision-maker with the choice of the total weighted distance before and after the disruption. Disruption risk for robust decision-making is studied by Sawik [33]. In addition to the above, Asl-Najafi et al. [34] also researched the inventory design under interruption risk. Ghomi-Avili et al. [35] proposed a fuzzy biobjective bilevel model with a price-dependent demand for the network design in the presence of random disruptions at suppliers. Jabbarzadeh et al. [36] established a flexible CLSC network based on the consideration of lateral transfer as a

Table 1: Single-channel recycling.

Modes	Researcher	Time	Main research contents
Manufacturer	Polotski et al.	2015	Manufacturing and remanufacturing system production plan
	Navin et al.	2017	Considering manufacturing and remanufacturing, the problem of production planning in CLSC is studied
	Hariga et al.	2017	Minimizing the total chain cost
Comparing	Savaskan et al.	2004	The pricing strategies and channel efficiency of different recovery modes in closed-loop supply chain
	Wen and Dong	2016	Concluding that CSR and government incentives will promote producers to undertake recycling of waste products
	Chen and Tian	2017	The optimal recovery mode selection of manufacturer and retailer under price fluctuation is obtained
	Hong et al.	2012	The optimality of retailer recycling by comparing retailer recycling with others
	Wang and Da	2010	The optimal decision-making of CLSC under retailer recycling and third-party recycling is discussed

response strategy aiming at reducing the risk of operation and disruption. In this paper, the disruption of raw material supply generally refers to the failure of suppliers to meet customer needs on time [37]. The reason may be network disruption or infrastructure disruption.

In addition to the three parts in the abovementioned literature review, Saha et al. [38] investigate a reward-driven policy; three different modes of collection are employed. Mathematical models for both noncooperative and centralised scenarios are developed to characterise the pricing decisions and remanufacturing strategies. Nielsen et al. [39] study the different results of the three policy subsidies. The research shows that the results of the subsidy policy can bring benefits to consumers and increase the complexity of CLSC members to some extent. Network design and collective planning issues are also included in closed-loop supply chain planning.

In summary, the existing literature mostly studies the network design of CLSC under supply chain disruption and the recovery strategy after disruption or aimed to find the balance of environmental and economic objectives of green sustainable supply chain. Different from the existing literature, this paper combines the carbon tax and supply disruption to carry out relevant research under the recycling mode of manufacturers: manufacturers as recyclers, how to adjust the level of recycling quality to reduce their costs in the context of sustainable development; changes in government carbon tax policy, how to affect its cost at this time and how to formulate its recovery and production strategy; when considering the risk of supply disruption, how does the risk affect the manufacturer and how does the manufacturer formulate its strategy at this time. In research methods, Lingo, Particle Swarm Optimization, and Genetic Algorithm are used to verify the credibility and validity of the model.

The structure of this paper is as follows. In Section 3, the detailed problem description (assumptions, notations, and mathematical function with nine kinds of cost) is presented. The PSO and GA methodology which will be used in later analysis are introduced in Section 4. The numerical experiment and analyzes of the results are illustrated in Section 5. Finally, Section 6 has conclusions and deficiency.

3. Problem Description

The whole process in CLSC in this paper is shown in Figure 1.

3.1. Assumptions

(1) The quality of recycled products obeys normal distribution [4, 40].

(2) The demand is known (the demand rate remains unchanged).

(3) Remanufactured products and new products are homogeneous (the utility functions of consumers are the same) [41].

(4) In a cycle, raw materials are purchased once from material suppliers

(5) Buyback cost and remanufacturing cost are both functions of quality level of recycled products [42]

(6) All recycled products are not discarded

(7) The delivery time in manufacturing and remanufacturing processes is negligible

(8) The lead time is too difficult to be determined to be considered

(9) Assume that there is no shortage in the whole process

3.2. Notations. Considering a CLSC where the manufacturer is the recycler, the parameters are settled, as shown in Table 2.

3.3. Function. In the assumed closed-loop supply chain system, the total cost function of the manufacturer includes the following parts: (1) buyback cost, (2) remanufacturing cost, (3) raw material cost, (4) manufacturing cost, (5) inventory holding cost, (6) setup cost, (7) ordering cost, (8) carbon tax cost, and (9) supply disruption cost. Buyback cost, remanufacturing cost, inventory holding cost, carbon tax cost, and supply disruption cost will be detailed in Sections 3.3.1~3.3.5, respectively. The remaining costs are described in Section 3.3.6.

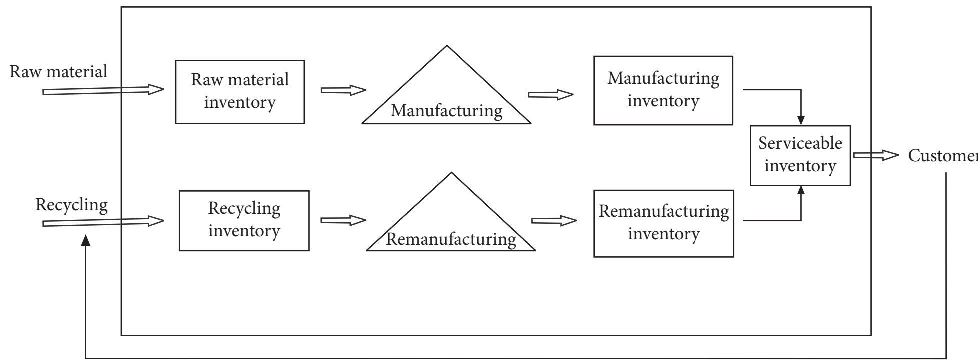

Figure 1: CLSC process.

Table 2: Parameter definition.

Symbol	Meaning
a, θ	Parameters of the buyback cost function
b, ψ	Parameters of the recycling rate function
c, δ	Parameters of the remanufacturing cost function
D	Demand rate
$(1-\beta)\ D$	Manufacturing rate
$(1-\gamma)\ D$	Remanufacturing rate
d_1 (d_2)	Purchasing cost per unit of raw materials charged by major (secondary) suppliers
C_{raw}	Purchasing cost for raw material per unit of one manufactured product
h_s $(h_r$, $h_{\text{raw}})$	Holding cost of serviceable (returned, raw materials) stock
C_n	Manufacturing cost
P	Buyback cost ratio
D	Return rate
Ω	Probability of supply disruption of major raw material suppliers
A	Marginal recycling rate
S_m (S_n)	Installation cost for remanufacturing (manufacturing)
e_m (e_n)	The amount of carbon emissions from unit remanufactured (manufactured) goods
C_1	Cost of carbon tax per unit emission
T_m (T_n)	Time required to produce remanufactured (manufactured) products
C_0	Ordering cost

T, m, n, and q are decision variables in this paper, where T means one cycle time of manufacturing and remanufacturing system; m presents number of remanufactures in a cycle, while n is number of manufactures, and q is the required minimum quality level of returned products.

3.3.1. Buyback Cost. Recycling rate: $d = \alpha D$ is the recycling rate and $\alpha = be^{-\varphi q}$ is the marginal recycling rate, $0 \le b \le 1$, referring to Vörös's paper [40] and a series of the study Guo et al. [4, 43]. In Vörös's paper, the recycling rate is inversely proportional to the quality level of recycled products [40]. Based on the assumptions above, the higher the quality level of recycled products is, the lower the remanufacturing cost is, but the price used to recycle products for companies becomes higher.

In this paper, the quality of returned items is assumed to be normal distribution. For convenience of calculation, we assume that the quality of returned products q obeys the standard normal distribution, $q \sim N(0,1)$, and x is the quality level of returned products $(q \le x \le 1)$ [16]. The probability density function of x is as follows:

$$X(x) = \begin{cases} \dfrac{1}{\sqrt{2\pi}} e^{-x^2/2}, & q < x < 1, \\ 0, & \text{others.} \end{cases} \quad (1)$$

Buyback cost ratio: considering the assumption that remanufactured products and new products are homogeneous to customers, buyback cost ratio p is the ratio of return cost per unit of recycled goods to production cost per unit of new products (production cost includes raw material cost and manufacturing cost, $C_n + C_{\text{raw}}$). p is defined as $p = ae^{-\theta(1-x)}, x \in [q,1]$ [4, 16, 40, 43]. If the required quality level is higher, p will increase, as shown in Figure 2.

The average buyback cost is $V_1 = d(C_n + C_{\text{raw}})E(p)$:

$$\begin{aligned} E(p) &= \int_{-\infty}^{+\infty} \frac{1}{\sqrt{2\pi} e^{-x^2/2}} ae^{-\theta(1-x)} \mathrm{d}x = ae^{\theta^2 - 2\theta/2} \int_q^1 \\ &\quad \cdot \frac{1}{\sqrt{2\pi} e^{-(x-\theta)^2/2}} \mathrm{d}x \\ &= ae^{\theta^2 - 2\theta/2} \int_{q-\theta}^{1-\theta} \frac{1}{\sqrt{2\pi}} e^{-(x-\theta)^2/2} \mathrm{d}(x-\theta) \\ &= ae^{\theta^2 - 2\theta/2} [\phi(1-\theta) - \phi(q-\theta)]. \end{aligned} \quad (2)$$

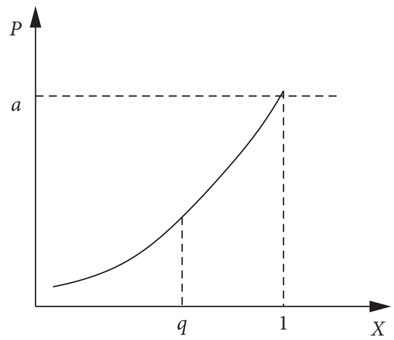

Figure 2: Buyback cost ratio p.

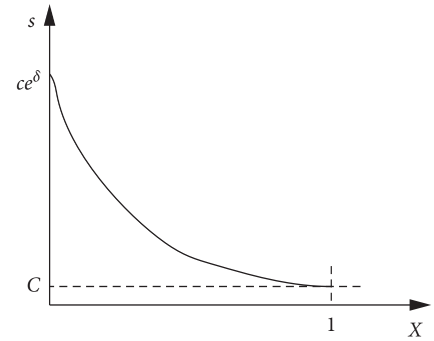

Figure 3: Remanufacturing cost s.

Thus, $V_1 = d(C_n + C_{\text{raw}})E(p) = a\,D(C_n + C_{\text{raw}}) be^{-\varphi q+\theta^2-2\theta/2}[\phi(1-\theta) - \phi(q-\theta)]$.

3.3.2. Remanufacturing Cost. The relationship between remanufacturing cost rate and product recovery quality is shown in Figure 3. Therefore, the remanufacturing cost ratio s is defined as $s = ce^{\delta(1-x)}$, $x \in [q, 1]$ [44].

The average remanufacturing cost is $V_2 = dC_nE(s)$:

$$\begin{aligned}E(s) &= \int_{-\infty}^{+\infty} \frac{1}{\sqrt{2\pi}e^{-x^2/2}} ce^{\delta(1-x)}\mathrm{d}x = ce^{(\delta^2+2\delta)/2}\int_q^1 \\ &\quad\cdot \frac{1}{\sqrt{2\pi}e^{-(x+\delta)^2/2}}\mathrm{d}x \\ &= ce^{(\delta^2+2\delta)/2}\int_{q+\delta}^{1+\delta} \frac{1}{\sqrt{2\pi}e^{-(x+\delta)^2/2}}\mathrm{d}(x+\delta) \\ &= ce^{(\delta^2+2\delta)/2}[\phi(1+\delta) - \phi(q+\delta)].\end{aligned} \tag{3}$$

Thus, $V_2 = dC_nE(s) = c\,DC_nbe^{-\varphi q+\delta^2+2\delta/2}[\phi(1+\delta) - \phi(q+\delta)]$.

3.3.3. Inventory Holding Cost. The raw material inventory, the recycling inventory, and the serviceable inventory—which include manufacturing inventory and remanufacturing inventory—compose the CLSC cycle. That is, one cycle T contains m manufacturing periods and n remanufacturing periods assumed [43, 45].

For recycled goods with short life cycle, the value decreases with shelf time. Therefore, this model considers the first stage of remanufacturing of recycled goods and the second stage of manufacturing of new products. Figure 4 shows in detail the inventory.

Above all, we got the following.

The average inventory holding cost consists of the following four parts: (1) remanufacturing products' inventory cost H_m, (2) manufacturing products' inventory cost H_n, (3) recycling products' inventory cost H_r, and (4) raw materials' inventory cost H_s:

$$\begin{aligned}H_m &= \frac{1}{2}h_sI_mT_m\frac{1}{T} = \frac{1}{2}h_s * \frac{1}{m}(1-\gamma)\alpha\,DT * T_m\frac{1}{T} \\ &= \frac{1}{2m^2}h_s(1-\gamma)\alpha^2DT, \\ H_n &= \frac{1}{2}h_sI_nT_n\frac{1}{T} = \frac{1}{2}h_s * \frac{1}{n}(1-\beta)(1-\alpha)DT * T_n\frac{1}{T} \\ &= \frac{1}{2n^2}h_s(1-\beta)(1-\alpha)^2DT, \\ H_r &= \frac{1}{2}h_rI_rT\frac{1}{T} = \frac{1}{2}h_r\frac{\alpha}{m}DT[m(1-\alpha) + \alpha(1-\gamma)] \\ &= \frac{1}{2}h_r\left[\alpha(1-\alpha) + \frac{\alpha^2}{m}(1-\gamma)\right]DT, \\ H_r &= \frac{1}{2}h_rI_rT\frac{1}{T} = \frac{1}{2}h_r\frac{\alpha}{m}DT[m(1+\alpha) + \alpha((1+\gamma))] \\ &= \frac{1}{2}h_r\left[\alpha(1-\alpha) + \frac{\alpha^2}{m}(1+\gamma)\right]DT, \\ S &= \frac{1}{2}(1-\alpha)^2\frac{\beta+n-1}{n}DT^2, \\ H_{\text{raw}} &= h_{\text{raw}}S\frac{1}{T} \\ &= \frac{1}{2}h_{\text{raw}}(1-\alpha)^2\frac{\beta+n-1}{n}DT.\end{aligned} \tag{4}$$

In summary, the average inventory holding cost V_3 is

$$\begin{aligned}V_3 &= H_m + H_n + H_r + H_{\text{raw}} \\ &= \frac{1}{2m^2}h_s(1-\gamma)\alpha^2DT + \frac{1}{2n^2}h_s(1-\beta)(1-\alpha)^2DT \\ &\quad + \frac{1}{2}h_r\left[\alpha(1-\alpha) + \frac{\alpha^2}{m}(1-\gamma)\right]DT \\ &\quad + \frac{1}{2}h_{\text{raw}}(1-\alpha)^2\frac{\beta+n-1}{n}DT.\end{aligned} \tag{5}$$

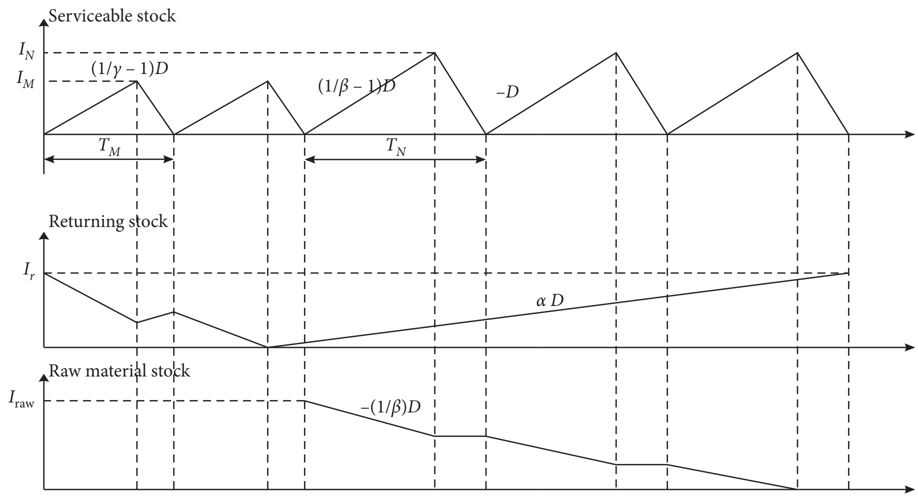

FIGURE 4: Inventory status.

3.3.4. Carbon Tax Cost. Remanufacturing is the implementation of high-tech repair and transformation of recycled old products, so the carbon emissions in remanufacturing process are much less than those in the production of completely new products, which is why remanufacturing has attracted much attention. In this article, we assume that carbon emissions per unit of remanufactured goods are e_x, manufactured ones are e_n, and $e_x < e_n$.

The average carbon tax cost is $V_4 = (C_1/T)[\alpha De_m + (1-\alpha)De_n]$.

3.3.5. Supply Disruption Cost. In a sustainable CLSC system, two levels of raw material suppliers, major suppliers and secondary suppliers, are considered. Because the cost of raw materials per unit charged by major suppliers is low, supply disruption is prone to occur.

Making use of the achievements of Guo and He [4], the average cost of supply disruption is shown as follows:

$$V_5 = (1-\omega)(1-\alpha)Dd_1 + \omega(1-\alpha)Dd_2. \quad (6)$$

The probability of disruption of raw materials supply by major suppliers is ω; d_1 (d_2) is the purchasing cost per unit of raw materials charged by major (secondary) suppliers. Thus the cost for manufacturers to purchase raw materials from major suppliers is $(1-\omega)(1-\alpha)Dd_1$, and it costs manufacturers $\omega(1-\alpha)Dd_2$ from secondary suppliers due to the insufficient supply of the primary supplier.

3.3.6. Average Total Cost Function. Referring to the series of research worker of Guo et al. [4, 6, 43, 46], other costs are as follows.

The total demand is D and the amount of αD is remanufactured by recycling, so the manufacturing quantity should be $(1-\alpha)D$. C_{raw} is the purchasing cost for raw material per unit of a manufactured product.

Therefore,

(1) Manufacturing cost V_6 is $(1-\alpha)DC_n$.

(2) Raw materials' cost (raw materials here refer to the raw materials for manufacturing new products, which need to be purchased from suppliers) V_7 is $(1-\alpha)DC_{raw}$. T means one cycle time of manufacturing and remanufacturing system. Suppose that a cycle includes producing m remanufactured products and n manufactured products; then T can be expressed as $mT_m + nT_n$. S_m represents the installation cost for remanufacturing while S_n represents the manufacturing.

(3) Setup cost V_8 is $(mS_m + nS_n)/T$.

(4) Ordering cost V_9 can be expressed as C_0/T.

In the closed-loop system, in which the manufacturer acts as the recycler, the total cost function of the manufacturer consists of (1) buyback cost V_1, (2) remanufacturing cost V_2, (3) raw material cost V_7, (4) manufacturing cost V_6, (5) inventory holding cost V_3, (6) setup cost V_8, (7) ordering cost V_9, (8) carbon tax cost V_4, and (9) supply disruption cost V_5.

To sum up, the average total cost function is as follows:

$$\begin{aligned}
\text{ATC} &= V_1 + V_2 + V_3 + V_4 + V_5 + V_6 + V_7 + V_8 + V_9 \\
&= aD(C_n + C_{raw})be^{-\varphi q + \theta^2 - 2\theta/2}[\phi(1-\theta) - \phi(q-\theta)] \\
&\quad + cDC_n be^{-\varphi q + \delta^2 + 2\delta/2}[\phi(1+\delta) - \phi(q+\delta)] + (1-\alpha)DC_n \\
&\quad + \frac{1}{2m^2}h_s(1-\gamma)\alpha^2 DT + \frac{1}{2n^2}h_s(1-\beta)(1-\alpha)^2 DT \\
&\quad + \frac{1}{2}h_r\left[\alpha(1-\alpha) + \frac{\alpha^2}{m}(1-\gamma)\right]DT \\
&\quad + \frac{1}{2}h_{raw}(1-\alpha)^2\frac{\beta+n-1}{n}DT + (1-\alpha)DC_{raw} + C_0/T \\
&\quad + (mS_m + nS_n)/T \\
&\quad + \frac{C_1}{T}[\alpha De_m + (1-\alpha)De_n] + (1-\omega)(1-\alpha)Dd_1 \\
&\quad + \omega(1-\alpha)Dd_2.
\end{aligned} \quad (7)$$

4. Optimization Algorithm

PSO and GA are used to calculate the optimal value in this paper, avoiding limitation of each other. Meanwhile to verify that the model is built in green and sustainable CLSC, the computational results achieved by PSO, GA, and Lingo are worked out. This study first uses Lingo11 to find the best solution. Lingo is an "interactive linear and general optimization solver," which is suitable for nonlinear programming or linear programming. Optimal model solutions usually use this method to obtain the best solution. Because the model in this paper is a linear problem, in this case the global optimal solution must be found, rather than the approximate optimal solution. The program is simple, has less code, and is faster. Secondly, in order to prove the feasibility of the model, a more mature Genetic Algorithm was selected, and binary coding was used to find a suitable solution. However, the Genetic Algorithm may have problems such as the cliff of Hamming. So the particle swarm algorithm is used which has an information sharing mechanism; that is to say, it is more enlightening than the Genetic Algorithm. It can avoid the shortcomings of Genetic Algorithm and analyze the calculation examples. The two algorithms have different convergence speeds. When two different calculation methods are used, the model and calculation results are better verified.

4.1. Genetic Algorithm. Genetic Algorithm (GA) is a global parallel search algorithm based on the idea of "survival of the fittest" biological evolution and heredity. The key parameters are population number, replication, crossover, and mutation probability.

Step 1 (*encoding and initial population*). Each chromosome in the algorithm consists of four variables (q, T, m, and n), and a variable is represented by four binary codes. A chromosome is composed of 16 genotypes. The longer the chromosomes are, the higher the accuracy of calculation is. The first generation population was randomly generated, and the population size was 30.

Step . (*fitness function and selection operator*). In fitness, the smaller the objective function value is, the higher the fitness value correspondingly is. Thus, the fitness function is $f(x) = 1000/\text{objvalue}$, where "objvalue" presents the objective function value. In selection, individual chromosomes are selected and duplicated. It is more likely to select the chromosome with higher fitness. Then, the probability of chromosome selection is the roulette strategy which was used to select the population.

Step 3 (*crossing and variation*). Multipoint crossing is used to generate crossover bits randomly, and the crossover probability is used to judge whether the crossover exists or not. Variation of mutation sites is selected randomly according to the determined variation probability.

Step 4 (*the termination rule*). When the algorithm reaches the preset evolutionary algebra, this terminates the algorithm; otherwise, it is transferred to Step 2.

The main calculation process is as shown in Figure 5.

4.2. Particle Swarm Optimization Algorithm. In Particle Swarm Optimization (PSO), every particle in PSO represents the possible solution of a problem. Through the simple behavior of individual particles and the information interaction within the group, the intelligence of problem solving is realized. It has the characteristics of simple operation and fast convergence [47]. Guo and Ya [43] applied PSO to verify the cost model of the manufacturer. Guo et al. [46] applied PSO and GA to verify a logistics network under the environment of low carbon.

Step 1: first, each particle is given a random position and velocity. $X_i = (m, n, T, q)$ and the value of i is 1~30 defined.

Step 2: all particles will get a fitness value according to the objective function (ATC), which is defined as $(\text{ATC}_1 \sim \text{ATC}_{30})$. Then the Pbest is defined as the best position of each particle, and Gbest is defined as the best fitness value and position among the Pbest in all particles.

Step 3: update the position and velocity of 30 particles. If $x_i = r$ and ≥ 0.7 or $v_i = r$ and ≥ 0.7, the position and velocity of particles would be spontaneously updated.

Step 4: the objective function is run. After it all updated particles will get the new fitness value $\text{ATC}_1' \sim \text{ATC}_{30}'$.

Step 5: compare $\text{ATC}_1' \sim \text{ATC}_{30}'$ with $\text{ATC}_1' \sim \text{ATC}_{30}'$ and then select the best as the Pbest value of the particle.

Step 6: update the global best Gbest fitness value. Choose the best one from all the values of Gbest and Pbest.

Step 7: end the algorithm while the Gbest reaches the optimal value; otherwise return to Step 3.

The main calculation process is as shown in Figure 6.

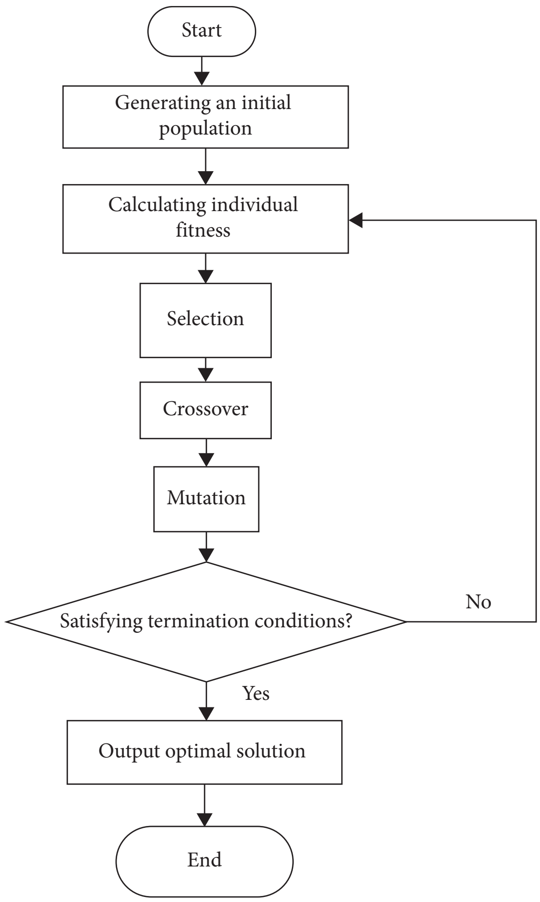

Figure 5: GA flow chart.

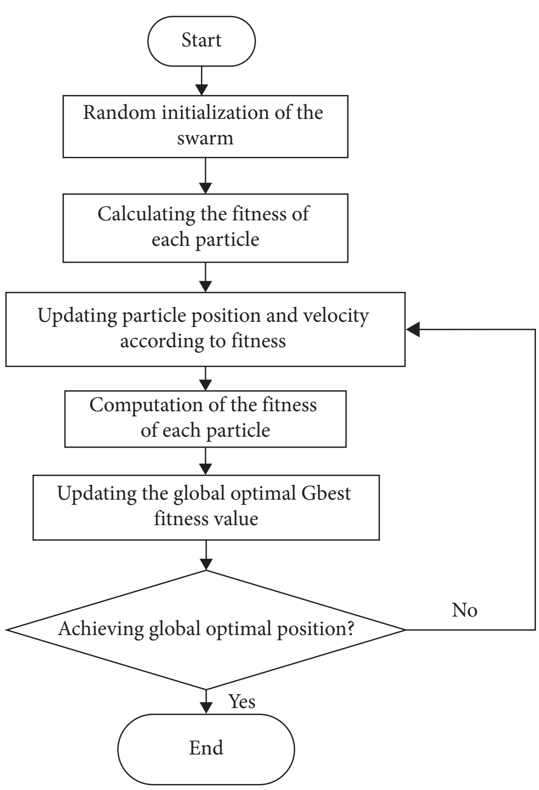

Figure 6: PSO flow chart.

5. Numerical Examples

5.1. Results. The numerical values of the parameters are as follows:

$$\begin{aligned} h_s &= 1, \\ h_r &= 0.2, \\ h_{\text{raw}} &= 0.2, \\ C_n &= 20, \\ C_{raw} &= 10, \\ C_0 &= 1000, \\ S_m &= 1500, \\ S_n &= 1500, \\ D &= 1000, \\ \varphi &= 2, \\ \beta &= 0.9, \\ \gamma &= 0.1, \\ a &= 0.9, \\ b &= 0.1, \\ c &= 0.9, \\ e_n &= 0.5, \\ d_1 &= 20, \\ d_2 &= 28. \end{aligned} \tag{8}$$

For different quality levels of recycled products (0.1~0.9), unit carbon emissions e_m are shown in Table 3. Among them, the data refer to the relevant literature [48] and are sorted out. With various values of θ, δ, C_1, and ω, different cases are studied. MATLAB language is used in the PSO and GA algorithms.

Table 4 shows the average total cost corresponding to different quality levels calculated by Lingo11 ($\theta = 4, \delta = 1, C_1 = 1$, and $\omega = 0.2$).

From Table 5 (GAP = (PSO − GA)/GA), it can be seen that, compared with the optimal value of Genetic Algorithm, Particle Swarm Optimization algorithm has achieved better results. Then, the results of Table 6 are obtained by comparing PSO with Lingo algorithm (GAP = (PSO − Lingo)/Lingo).

The sensitivity analysis results of supply disruption probability ω under the ratio of different remanufacturing and manufacturing times (m: n) with parameters $\theta = 4, \delta = 1, C_1 = 1$, and $q = 0.3$ are shown in Table 7. Table 8 is the total cost change of different carbon taxes under different ratios (m: n) when parameters $\theta = 4, \delta = 1, w = 0.2$ and $q = 3$.

5.2. Analysis. We can draw the following conclusions.

From Table 4, we can see that, with the increase of recycling quality, the ratio of remanufacturing times to manufacturing times (m: n) increases gradually. Furthermore, the higher the recycling quality is, the shorter the

Table 3: Unit carbon emissions of manufactured and remanufactured products.

Quality level x	0.1	0.2	0.3	0.4	0.5	0.6	0.7	0.8	0.9
e_x	0.3	0.3	0.25	0.25	0.2	0.2	0.15	0.1	0.1
e_m	0.5								

Table 4: Different quality levels of recycled products (Lingo).

q	e_m	m	n	T	ATC
0.1	0.3	1	3	8.7697	49984.95
0.2	0.3	1	3	8.7557	50476.73
0.3	0.25	1	3	8.7347	50910.62
0.4	0.25	1	2	7.6090	51144.72
0.5	0.2	1	2	7.5882	51471.58
0.6	0.2	1	2	7.5705	51751.41
0.7	0.15	1	1	5.7485	51965.07
0.8	0.1	1	1	5.7344	52166.07
0.9	0.1	1	1	5.7232	52334.57

manufacturing and remanufacturing cycle is. In this case, the increase of recycling cost is greater than the decrease of remanufacturing cost, so the ATC increases.

According to Tables 5 and 6, from the perspective of algorithm and model, we can get the following: (1) whether it is PSO or GA algorithm, the difference between the two algorithms and Lingo optimal value is very small, which shows the effectiveness of the algorithm; (2) according to the change trend of ATC with parameters, it is found that the change trend of GA algorithm and PSO algorithm is the same, which proves the effectiveness of the model; (3) from the result of gap analysis, the gap between PSO algorithm and Lingo algorithm is smaller than that of GA algorithm, which shows that PSO algorithm is closer to the optimal value.

According to the results from Tables 5 and 6, we can get management conclusions as follows:

(1) With the rise of θ(when δ and m: n are still), q and ATC will decrease and T is longer; when θ is the same, δ increases, the ratio m: n then diminishes, q and ATC will ascend, and T is shorter. In other words, if the remanufacturing cost remains unchanged, the quality level of the recycled product will be reduced and the total average cost too; in the case of constant buyback cost, the increase of remanufacturing cost will increase the total average cost and lead manufacturers to recycle higher quality recycled products. However, because of the recycle of high-quality recycled products, the recycle cost will greatly increase, so manufacturers will increase the number of new products manufactured and reduce the number of remanufactures.

(2) T is related to the proportion of remanufacturing and manufacturing m: n. When the proportion is smaller, this means that the number of remanufacturing times in a cycle is reduced (assuming that the number of manufacturing times is certain), so T is shorter.

In summary, the optimal strategy for manufacturers at this time is to use products that meet the lowest level of remanufacturing quality for remanufacturing, so as to reduce ATC. After meeting the minimum quality level, manufacturers can consider reasonable planning of remanufacturing and manufacturing times to reduce costs (the ratio of optimal remanufacturing to manufacturing times in this example is 3 : 1).

From Tables 7 and 9, we can get some management recommendations.

(1) When the carbon tax remains unchanged and the quality level of recycled products remains unchanged ($C1 = 1$ and $q = 0.3$), the average total cost increases with the increase of the probability of supply disruption (as shown in Table 7). Because the occurrence of supply disruption will affect the normal development of the downstream enterprises of the whole supply chain to a certain extent, the increase of the probability of supply disruption will bring more serious losses to the members of the supply chain (shown in Table 9).

(2) With the increase of ω, we can see that T also increases, which can be explained as follows. The increase in the probability of supply disruption may increase the manufacturing time T_n, so T increases. Combined with Table 6, we can see that the cycle T has a significant correlation with the proportion m: n but has no significant relationship with the probability of supply disruption. This article focuses on the impact of supply disruption and carbon tax on ATC, so the impact of supply disruption and carbon tax on the cycle T is no longer considered in the sensitivity analysis.

(3) Therefore, enterprises need to formulate and implement effective supply disruption risk prevention strategies to avoid the occurrence of supply disruption as far as possible, so as to make the production of enterprises go smoothly.

(4) However, the risk of supply disruption is unavoidable. Once supply disruption occurs, manufacturers should immediately adjust x to the lowest level to meet the recycling requirements and adjust the proportion of remanufacturing and manufacturing times, so as to minimize the average total cost (in this case, when $q = 0.1, m$: $n = 1$: 1, the average total cost can reach the minimum value under supply disruption).

Table 8 examines the impact of different carbon taxes on total average costs when supply disruption risks remain unchanged and the quality level of recycled products is consistent ($\omega = 0.2$ and $q = 0.3$). Table 10 shows the minimum average total cost and the best ratio (m: n) under different recycling quality levels and different carbon taxes.

The managerial implications that can be derived from Tables 8 and 10 are as follows:

Table 5: Comparison with PSO and GA ($C_1 = 1$ and $\omega = 0.2$).

θ	δ	m	n	q	T By PSO	ATC	q	T By GA	ATC	GAP (%)
4	0.5	3	1	0.1462	7.7849	50341.48	0.1491	7.4757	50342.24	−0.0015
	1.0	2	1	0.2380	6.8362	50814.65	0.2281	3.7857	50964.41	−0.2939
	1.5	1	1	0.3527	6.0158	50998.63	0.3538	6.7043	51018.26	−0.0385
5	0.5	3	1	0.1428	7.8051	50268.44	0.1407	7.1054	50269.32	−0.0018
	1.0	2	1	0.2283	6.8513	50649.07	0.2033	4.2545	50712.07	−0.1242
	1.5	1	1	0.3398	6.0643	50918.61	0.3342	6.6400	50930.37	−0.0231
6	0.5	3	1	0.1401	7.8142	50177.39	0.1305	7.2107	50185.33	−0.0158
	1.0	2	1	0.2019	6.8725	50538.28	0.1976	4.9052	50569.56	−0.0619
	1.5	1	1	0.3156	6.1547	50818.52	0.3112	5.8369	50821.60	−0.0061

Table 6: Comparison with PSO and Lingo ($C_1 = 1$ and $\omega = 0.2$).

θ	δ	m	n	q	T By PSO	ATC	q	T By Lingo	ATC	GAP (%)
4	0.5	3	1	0.1462	7.7849	50341.48	0.1490	7.6681	50340.98	0.0010
	1.0	2	1	0.2380	6.8362	50814.65	0.2279	6.8026	50652.63	0.3199
	1.5	1	1	0.3527	6.0158	50998.63	0.3521	5.8209	50996.85	0.0035
5	0.5	3	1	0.1428	7.8051	50268.44	0.1430	7.6724	50267.02	0.0028
	1.0	2	1	0.2283	6.8513	50649.07	0.2176	6.8079	50581.30	0.1340
	1.5	1	1	0.3398	6.0643	50918.61	0.3311	5.8263	50906.37	0.0240
6	0.5	3	1	0.1401	7.8142	50177.39	0.1395	7.6749	50156.28	0.0421
	1.0	2	1	0.2019	6.8725	50538.28	0.2033	6.8153	50513.62	0.0488
	1.5	1	1	0.3156	6.1547	50818.52	0.3188	5.8295	50812.12	0.0126

Table 7: Result of sensitivity test on different supply disruption probability ω ($\theta = 4, \delta = 1, C_1 = 1$, and $q = 0.3$).

ω	m	n	T	ATC
0	3	1	6.8874	49660.97
	2	1	6.4235	49453.46
	1	1	6.0123	49222.59
	1	2	6.7939	49253.50
	1	3	7.6967	49398.43
0.2	3	1	6.9025	51173.16
	2	1	6.4356	50965.65
	1	1	6.0258	50734.78
	1	2	6.8342	50765.69
	1	3	7.7014	50910.62
0.4	3	1	7.0134	52685.35
	2	1	6.4922	52477.84
	1	1	6.0305	52246.97
	1	2	6.8901	52277.88
	1	3	7.7233	52422.81
0.6	3	1	7.0279	54197.54
	2	1	6.5138	53990.03
	1	1	6.0366	53759.16
	1	2	6.9280	53790.07
	1	3	7.7614	53935.00
0.8	3	1	7.0401	55709.73
	2	1	6.5313	55502.22
	1	1	6.0419	55271.35
	1	2	6.9847	55302.26
	1	3	7.8432	55447.19
1.0	3	1	7.0496	57221.92
	2	1	6.6003	57014.41
	1	1	6.0485	56783.54
	1	2	7.2360	56814.45
	1	3	7.9659	56959.38

Table 8: Result of sensitivity test on different carbon tax C_1 ($\omega = 0.2$ and $q = 0.3$).

C_1	m	n	ATC
1	3	1	51173.16
	2	1	50965.65
	1	1	50734.78
	1	2	50765.69
	1	3	50910.62
2	3	1	51236.35
	2	1	51036.11
	1	1	50816.00
	1	2	50828.18
	1	3	50965.42
3	3	1	51297.64
	2	1	51003.96
	1	1	50893.34
	1	2	50888.37
	1	3	51018.56
4	3	1	51357.19
	2	1	51169.48
	1	1	50967.31
	1	2	50946.48
	1	3	51070.21
5	3	1	51415.15
	2	1	51232.90
	1	1	51038.31
	1	2	51002.73
	1	3	51120.46

(1) With the increase of carbon tax, the average total cost rises gradually. Therefore, the total carbon emissions should be considered as much as possible in the

Table 9: Optimal operational strategies (different supply disruption probability when $C_1 = 3$).

q	ω	m	n	ATC
0.1	0	1	1	48487.33
	0.5	1	1	52159.83
	1	1	1	55832.34
0.2	0	1	2	48961.05
	0.5	1	2	52692.92
	1	1	2	56424.79
0.3	0	1	2	49376.18
	0.5	1	2	53156.65
	1	1	2	56937.13
0.4	0	1	2	49740.23
	0.5	1	2	53560.56
	1	1	2	57380.77
0.5	0	1	2	50054.45
	0.5	1	2	53907.29
	1	1	2	57760.14
0.6	0	1	2	50324.39
	0.5	1	2	54203.91
	1	1	2	58083.43
0.7	0	1	2	50553.36
	0.5	1	2	54454.72
	1	1	2	58356.08
0.8	0	1	2	50746.65
	0.5	1	2	54665.89
	1	1	2	58585.13
0.9	0	1	2	50909.08
	0.5	1	2	54842.96
	1	1	2	58776.84

production operation of enterprises, and the total cost should be reduced by adjusting the ratio of remanufacturing times to manufacturing times in the production process. (In this case, when carbon tax is 1 or 2, the best ratio of remanufacturing times to manufacturing times is 1 : 1 making the average total cost reach the optimum state; when carbon tax is greater than 2 and less than or equal to 5, the best ratio of remanufacturing times to manufacturing times is 1 : 2, shown in Table 10 and Figure 7.)

(2) If the government wants to promote remanufacturing, it can consider decreasing carbon tax reasonably, to encourage manufacturers to increase the ratio of remanufacturing times to manufacturing times.

(3) For the carbon tax value set by the government, enterprises can choose the optimal production strategy to minimize the average total cost according to the recycling quality level (in this case, when $C_1 = 3$, enterprises can choose the best ratio $m: n = 1: 1$ under the quality level $q = 0.1$ or choose the best ratio $m: n = 1: 2$ under the quality level $q \geq 0.2$, shown in Table 10).

(4) The optimal strategy of enterprises is to control the proportion of remanufacturing times and manufacturing times reasonably according to the quality level of recycled products in the model and the relevant policies of the government, so as to minimize the average total cost. The setting of carbon tax value needs to take into account the interests of enterprises. Only by pursuing the balance point of economic interests and environmental protection

Table 10: Optimal operational strategies (different carbon taxes $\omega = 0.2$).

q	C_1	m	n	ATC
0.1	1	1	1	49800.18
	3	1	1	49956.33
	5	1	2	50073.48
0.2	1	1	1	50297.21
	3	1	2	50453.80
	5	1	2	50567.90
0.3	1	1	1	50734.78
	3	1	2	50888.37
	5	1	2	51002.73
0.4	1	1	1	51116.41
	3	1	2	51268.34
	5	1	2	51383.55
0.5	1	1	1	51445.18
	3	1	2	51595.58
	5	1	2	51711.15
0.6	1	1	1	51726.57
	3	1	2	51876.20
	5	1	2	51992.46
0.7	1	1	1	51965.07
	3	1	2	52113.90
	5	1	2	52230.51
0.8	1	1	1	52166.24
	3	1	2	52314.72
	5	1	2	52431.88
0.9	1	1	1	52334.57
	3	1	2	52482.63
	5	1	2	52600.08

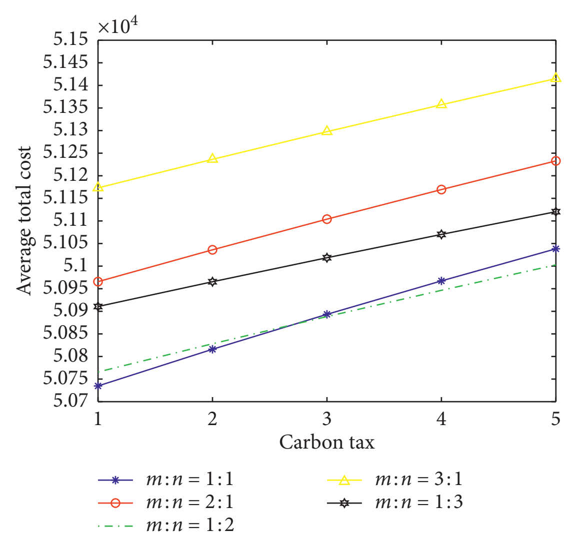

Figure 7: Average total cost fluctuation chart with different carbon taxes.

interests can the government and enterprises achieve a win-win situation.

(5) What is interesting is that we get a result that seems to be contrary to our expectation: with the increase of carbon tax, the ratio m: n should also increase (the increase of carbon tax means that remanufactured products is more advantageous than new products in the cost of carbon tax, so theoretically enterprises will increase the number of remanufacturing times only considering the carbon tax), but in fact we get that the value of m: n corresponding to the minimum total average cost decreases with the increase of carbon tax. The reason may be that, in our numerical example, the carbon tax cost per unit of remanufactured goods and its average inventory holding cost increase more than the carbon tax cost of manufactured goods and the average inventory holding cost of manufactured goods increase, so the carbon tax increases and the remanufacturing and manufacturing ratio decreases.

6. Conclusions and Recommendations

The optimal recovery and production strategy of manufacturers as recyclers in a sustainable CLSC considering carbon tax and supply disruption are studied. We assume that the recovery quality level obeys the standard normal distribution. The average total cost function of the manufacturer is established and the cost model considering environment and supply disruption and its corresponding algorithm are proved by Lingo, PSO, and GA. Through numerical examples, we analyze the effects of supply disruption risk and carbon tax policy on the optimal production and recycling strategies for manufacturers; then, the optimal strategies are given.

With the rise of supply interruption probability, ATC of the system will increase. Once supply interruption occurs, it will bring serious losses to the operation of the enterprise. In the process of recovery and production, enterprises can adjust the quality level of recycled products according to carbon tax, rationally arrange remanufacturing and manufacturing batches to reduce their ATC, and actively deal with the problem of supply disruption.

Further research direction is to reduce the constraints of hypothetical conditions (random market demand, considering the discarding and shortage of recycled goods, etc.).

Data Availability

The data used to support the findings of this study are included within the article.

Conflicts of Interest

The authors declare that they have no conflicts of interest.

Acknowledgments

This work was supported by the Ministry of Education's Humanities and Social Sciences Project (17YJA630119).

References

[1] C. T. Zhang and M. L. Ren, "Closed-loop supply chain coordination strategy for the remanufacture of patented products under competitive demand," *Applied Mathematical Modelling*, vol. 40, no. 13-14, pp. 6243–6255, 2016.

[2] A. Shakourloo, A. Kazemi, and M. O. M. Javad, "A new model for more effective supplier selection and remanufacturing process in a closed-loop supply chain," *Applied Mathematical Modelling*, vol. 40, no. 23-24, pp. 9914–9931, 2016.

[3] A. Yenipazarli, "Managing new and remanufactured products to mitigate environmental damage under emissions regulation," *European Journal of Operational Research*, vol. 249, no. 1, pp. 117–130, 2016.

[4] J. Guo, H. Lu, and M. Gen, "Optimal strategies for the closed-loop supply chain with the consideration of supply disruption and subsidy policy," *Computers & Industrial Engineering*, vol. 128, pp. 886–893, 2018.

[5] P. C. Sauer and S. Stefan, "Extending the reach of multi-tier sustainable supply chain management—insights from mineral supply chains," *International Journal of Production Economics*, vol. 217, pp. 31–43, 2018.

[6] E. Bazan, M. Y. Jaber, and S. Zanoni, "Carbon emissions and energy effects on a two-level manufacturer-retailer closed-loop supply chain model with remanufacturing subject to different coordination mechanisms," *International Journal of Production Economics*, vol. 183, pp. 394–408, 2017.

[7] J. Wang, M. K. Lim, M.-L. Tseng, and Y. Yang, "Promoting low carbon agenda in the urban logistics network distribution system," *Journal of Cleaner Production*, vol. 211, pp. 146–160, 2019.

[8] L. Zhen, L. Huang, and W. Wang, "Green and sustainable closed-loop supply chain network design under uncertainty," *Journal of Cleaner Production*, vol. 227, pp. 1195–1209, 2019.

[9] T. Paksoy, N. Y. Pehlivan, and E. Özceylan, "Fuzzy multi-objective optimization of a green supply chain network with risk management that includes environmental hazards," *Human and Ecological Risk Assessment: An International Journal*, vol. 18, no. 5, pp. 1120–1151, 2012.

[10] R. Ma, L. Yao, M. Jin, P. Ren, and Z. Lv, "Robust environmental closed-loop supply chain design under uncertainty," *Chaos, Solitons & Fractals*, vol. 89, pp. 195–202, 2016.

[11] L. Ameknassi, D. Aït-Kadi, and N. Rezg, "Integration of logistics outsourcing decisions in a green supply chain design: a stochastic multi-objective multi-period multi-product programming model," *International Journal of Production Economics*, vol. 182, pp. 165–184, 2016.

[12] M. Fazli-Khalaf, A. Mirzazadeh, and M. S. Pishvaee, "A robust fuzzy stochastic programming model for the design of a reliable green closed-loop supply chain network," *Human and Ecological Risk Assessment: An International Journal*, vol. 23, no. 8, pp. 2119–2149, 2017.

[13] A. Banasik, A. Kanellopoulos, G. D. H. Claassen, J. M. Bloemhof-Ruwaard, and J. G. A. J. van der Vorst, "Closing loops in agricultural supply chains using multi-objective optimization: a case study of an industrial mushroom supply chain," *International Journal of Production Economics*, vol. 183, pp. 409–420, 2017.

[14] K. P. Nurjanni, M. S. Carvalho, and L. Costa, "Green supply chain design: a mathematical modeling approach based on a multi-objective optimization model," *International Journal of Production Economics*, vol. 183, no. B, pp. 421–432, 2017.

[15] A. Haddadsisakht and S. M. Ryan, "Closed-loop supply chain network design with multiple transportation modes under stochastic demand and uncertain carbon tax," *International Journal of Production Economics*, vol. 195, pp. 118–131, 2018.

[16] X. Y. Wang and J. Q. Guo, "Subsidy strategy model of multi-period closed-loop hybrid system under carbon tax," *Computer Engineering and Applications*, vol. 54, no. 14, pp. 236–240, 2018.

[17] V. Polotski, A. Kenne, and A. Gharbi, "Optimal production scheduling for hybrid manufacturing-remanufacturing systems with setups," *Journal of Manufacturing Systems*, vol. 37, no. 3, pp. 703–714, 2015.

[18] K. D. Navin, R. Shankar, and A. Choudhary, "Strategic design for inventory and production planning in closed-loop hybrid systems," *International Journal of Production Economics*, vol. 183, pp. 345–353, 2017.

[19] M. Hariga, Z. R. As'ad, and Z. Khan, "Manufacturing-remanufacturing policies for a centralized two stage supply chain under consignment stock partnership," *International Journal of Production Economics*, vol. 183, pp. 362–374, 2017.

[20] R. C. Savaskan, S. Bhattacharya, and L. N. Van Wassenhove, "Closed-loop supply chain models with product remanufacturing," *Management Science*, vol. 50, no. 2, pp. 239–252, 2004.

[21] W. Xiao-qin and Y.-R. Dong, "A study on recycling mode selection in the reverse logistics with consideration of corporate social responsibility," *Operations Research and Management Science*, vol. 25, no. 1, pp. 275–281, 2016.

[22] J. Chen and D.-G. Tian, "Selection of the recycling mode based on closed-loop supply chain model," *Chinese Journal of Management Science*, vol. 25, no. 1, pp. 88–97, 2017.

[23] I.-H. Hong and J.-S. Yeh, "Modeling closed-loop supply chains in the electronics industry: a retailer collection application," *Transportation Research Part E: Logistics and Transportation Review*, vol. 48, no. 4, pp. 817–829, 2012.

[24] W. B. Wang and Q. L. Da, "The study on collection and pricing for closed-loop supply chain with retailer and the third party collecting," *Journal of Industrial Engineering and Engineering Management*, vol. 24, no. 2, pp. 130–134, 2010.

[25] Y. X. Yi and J. Yuan, "Pricing coordination in closed-loop supply chain with hybrid recovery channel," *Business Review*, vol. 23, no. 11, pp. 169–176, 2011.

[26] X. Hong, Z. Wang, D. Wang, and H. Zhang, "Decision models of closed-loop supply chain with remanufacturing under hybrid dual-channel collection," *The International Journal of Advanced Manufacturing Technology*, vol. 68, no. 5–8, pp. 1851–1865, 2013.

[27] P. D Giovanni and G. Zaccour, "A two-period game of a closed-loop supply chain," *European Journal of Operational Research*, vol. 232, no. 1, pp. 22–40, 2014.

[28] P. D. Giovanni, P. V. Reddy, and G. Zaccour, "Incentive strategies for an optimal recovery program in a closed-loop supply chain," *European Journal of Operational Research*, vol. 249, no. 2, pp. 605–617, 2016.

[29] M.-B. Aryanezhad, S. G. Jalali, and A. Jabbarzadeh, "An integrated supply chain design model with random disruptions consideration," *African Journal of Business Management*, vol. 4, no. 12, pp. 2393–2401, 2010.

[30] P. Peng, A. Snyder, and Z. Liu, "Reliable logistics networks design with facility disruptions," *Transportation Research Part B: Methodological*, vol. 45, no. 8, pp. 1190–1211, 2011.

[31] A. Baghalian, S. Rezapour, and R. Z. Farahani, "Robust supply chain network design with service level against disruptions and demand uncertainties: a real-life case," *European Journal of Operational Research*, vol. 227, no. 1, pp. 199–215, 2013.

[32] I. Hernandez, J. Emmanuel Ramirez-Marquez, C. Rainwater, E. Pohl, and H. Medal, "Robust facility location: hedging against failures," *Reliability Engineering & System Safety*, vol. 123, pp. 73–80, 2014.

[33] T. Sawik, "On the robust decision-making in a supply chain under disruption risks," *International Journal of Production Research*, vol. 52, no. 22, pp. 6760–6781, 2014.

[34] J. Asl-Najafi, B. Zahiri, A. Bozorgi-Amiri, and A. Taheri-Moghaddam, "A dynamic closed-loop location-inventory problem under disruption risk," *Computers & Industrial Engineering*, vol. 90, pp. 414–428, 2015.

[35] M. Ghomi-Avili, S. G. Jalali Naeini, R. Tavakkoli-Moghaddam, and A. Jabbarzadeh, "A fuzzy pricing model for a green competitive closed-loop supply chain network design in the presence of disruptions," *Journal of Cleaner Production*, vol. 188, pp. 425–442, 2018.

[36] A. Jabbarzadeh, M. Haughton, and A. Khosrojerdi, "Closed-loop supply chain network design under disruption risks: a robust approach with real world application," *Computers & Industrial Engineering*, vol. 116, pp. 178–191, 2018.

[37] M. J. Braunscheidel and N. C. Suresh, "The organizational antecedents of a firm's supply chain agility for risk mitigation and response," *Journal of Operations Management*, vol. 27, no. 2, pp. 119–140, 2009.

[38] S. Saha, S. P. Sarmah, and I. Moon, "Dual channel closed-loop supply chain coordination with a reward-driven remanufacturing policy," *International Journal of Production Research*, vol. 54, no. 5, pp. 1503–1517, 2016.

[39] I. E. Nielsen, S. Majumder, and S. Saha, "Game-theoretic analysis to examine how government subsidy policies affect a closed-loop supply chain decision," *Applied Sciences*, vol. 10, no. 1, p. 145, 2020.

[40] J. Vörös, "Product balancing under conditions of quality inflation, cost pressures and growth strategies," *European Journal of Operational Research*, vol. 141, no. 1, pp. 153–166, 2002.

[41] N. Hamta, S. M. T. Fatemi Ghomi, F. Jolai, and M. Akbarpour Shirazi, "A hybrid pso algorithm for a multi-objective assembly line balancing problem with flexible operation times, sequence-dependent setup times and learning effect," *International Journal of Production Economics*, vol. 141, no. 1, pp. 99–111, 2013.

[42] J. Wang, J. Zhao, and X. Wang, "Optimum policy in hybrid manufacturing/remanufacturing system," *Computers & Industrial Engineering*, vol. 60, no. 3, pp. 411–419, 2011.

[43] J. Guo and G. Ya, "Optimal strategies for manufacturing/remanufacturing system with the consideration of recycled products," *Computers & Industrial Engineering*, vol. 89, pp. 226–234, 2015.

[44] L. I. Xin-jun, "Monopoly production optimization model for remanufacturing cost with stochastic distribution and market segmentation," *Chinese Management Science*, vol. 15, no. 5, pp. 72–77, 2007.

[45] I. Dobos and K. Richter, "An extended production/recycling model with stationary demand and return rates," *International Journal of Production Economics*, vol. 90, no. 3, pp. 311–323, 2004.

[46] J. Guo, X. Wang, and M. S. Gen, "Forward and reverse logistics network and route planning under the environment of low-carbon emissions: a case study of Shanghai fresh food e-commerce enterprises," *Computers & Industrial Engineering*, vol. 106, pp. 351–360, 2017.

[47] M. A. Mohandes, "Modeling global solar radiation using Particle Swarm Optimization (PSO)," *Solar Energy*, vol. 86, no. 11, pp. 3137–3145, 2012.

[48] C. H. Yang, H. Liu, P. Ji et al., "Optimal acquisition and remanufacturing policies for multi-product remanufacturing systems," *Journal of Cleaner Production*, vol. 135, pp. 1571–1579, 2015.

Hindawi
Mathematical Problems in Engineering
Volume 2020, Article ID 7989386, 18 pages
https://doi.org/10.1155/2020/7989386

Research Article

An Evolutionary Game Model to Study Manufacturers and Logistics Companies' Behavior Strategies for Information Transparency in Cold Chains

Xiao-Hu Xing,[1] Zhi-Hua Hu ,[1] Shu-Wen Wang,[1] and Wen-Ping Luo[2]

[1]*Logistics Research Center, Shanghai Maritime University, Shanghai 201306, China*
[2]*School of Economical and Management, Shanghai Maritime University, Shanghai 201306, China*

Correspondence should be addressed to Zhi-Hua Hu; zhhu@shmtu.edu.cn

Received 9 December 2019; Revised 23 March 2020; Accepted 30 March 2020; Published 21 April 2020

Academic Editor: Dongping Song

Cold goods manufacturers and logistics service providers are two essential groups of players in the goods safety issue in cold chains under the administration or inspection of governments and various stakeholders, including customers and final consumers. In this research, we applied the evolutionary game theory to examine the behavioral strategies of manufacturers and logistics service providers, while we formulated the governments and various other stakeholders' impacts by contracted subsidy and penalty. First, we developed an evolutionary game theory model of the interaction between manufacturers and logistics service providers. Then, we examined the evolutionary stable strategy (ESS) of the manufacturers and logistics service providers under various constraints. Finally, we used simulation to demonstrate the impact of combinations of various parameters on the ESS and evolutionary paths. The results showed that the behavior strategies of the manufacturers and logistics service providers are interleaved and affected by the parameters in the developed model. We analyzed the ESSs and evolutionary paths by considering profits of the cold goods, the cold chain logistics costs, mainly the additional profits and costs of sharing information, and the subsidy and penalty regulated by contracts and governments. By tuning the parameters for numerical studies, we can find that the subsidy and penalty are essential for the cold chain manufactures and logistics service providers to adopt the information-sharing strategy, while the cost of the strategy and the profit of them constrains the positivity. Although, besides instant costs and profits, the information-sharing strategy can add values to cold chains in the long run, the administrators must consider the two populations of players and advocate them to adopt the information-sharing strategy consistently by using optimal policies.

1. Introduction

In cold chains, safety problems of fresh goods frequently happen because of the temperature out of control, especially in the logistics processes [1]. Economically, the temperature is not well controlled due to technology investment and cost reasons. In the context of food quality and safety, the stakeholders in cold chains believe that it is beneficial to visualize the cold chains based on the information transparency technologies and mechanisms [2]. Besides, the increasing degree of information transparency helps the administration of the cold chain by the stakeholders and the related governmental departments.

In cold chains, the manufacturers, as cold food suppliers and specialized logistics service providers, are two relevant stakeholders. The logistics service providers usually undertake the transportation and warehousing processes from the manufacturers to the customers (typically retailers or final consumers). Generally, the manufacturers will make contracts with the logistics service providers to maintain the temperature during the whole logistics process so that they can control the food quality. The logistics service providers should share the information in the logistics processes to the manufacturers and related government departments, even the related customers and final consumers. So, various sensors, wireless sensor networks, and even the Internet of things should be applicable in the logistics facilities and devices [1, 3]. By these technologies and devices, the temperature and other quality-related information can be sensed, transported, and shared. However, different logistics operators may use different technologies, and the information transparency degree is affected by various factors. Notably, the manufacturers usually outsource the logistics processes to various local companies, which makes the information less transparent. Besides, some companies may hesitate to share information due to distrust and competition. On the manufacturer's and customer's sides, information transparency is a crucial way to inspect the temperature status and administrate the distributive logistics processes.

To study this dilemma and the mutual interactions between the manufacturers and logistics service providers in cold chains, an evolutionary game [4, 5] is used to formulate the information transparency mechanisms. We consider the manufacturers and logistics service providers as two populations with dynamic interactions, while the evolutionary game models are capable of studying the dynamics between populations. The manufacturers and logistics service providers adjust the strategies according to the feedbacks in the cold chain markets. We studied the penalty and various interference costs and returns in the context of contracts between manufacturers and logistics service providers without considering the third-party coordination organizations. However, the related government departments and industrial organizations can regulate the business in the cold chain, primarily due to food safety issues.

This study contributes to the literature in the following aspects. First, although some studies have examined information transparency or information sharing issues in logistics [6], cold chain logistics is not studied. However, the temperature control features the cold chain, especially for safety problems [1], and so the information transparency incurs additional investment and administration. Meanwhile, the evolutionary game is an essential tool to examine the behavior strategy of information transparency [7] in the context of cold chains. Second, some pioneering studies have examined the technologies, devices, operations, and even information systems for cold chain logistics [8], while they did not investigate the dynamics among the main stakeholders (here manufacturers and logistics service providers). An evolutionary game model contributes to analyzing such dynamics. Third, although many pioneering studies using evolutionary games in supply chains provide useful references for this study, the administrators must consider the costs and benefits induced by temperature control technologies and processes and governments' different roles to extend these existing studies to cold chains.

In the following sections, we firstly review the studies related to information transparency, cold chain logistics, and evolutionary games in supply chains. Then, we elucidate the research problem with the assumptions in Section 3. Section 4 developed formulations and model analysis. In Section 5, we conduct numerical studies. Section 6 concludes the study.

2. Related Studies

2.1. Information Transparency in Logistics. To inspect and manage the temperature-controlled cold chains, the stakeholders must provide the relation information interfaces connected with the logistics facilities and devices. Information transparency is a concept to represent the easiness of accessing the information shared among the stakeholders in the cold chain. However, we can seldom find the researches in the context of cold chain logistics, while the communities of logistics and supply chains have published some pioneering studies.

In Table 1, we reviewed the pioneering studies on logistics information transparency in three dimensions. First, information transparency coincides with information sharing. In the "Issue" column, "RFID" is a hot topic, especially from several years ago. The Internet of Things (IoTs) plays an essential role in information transparency in logistics and supply chains, including cold chains. Investments and risks have been identified and studied because investments in technologies and devices must pay the value information transparency. The "Stakeholders" mainly include the members in supply chains and the governments. In Table 1, two studies examine the logistics service providers [6, 19] in the context of supply chains.

2.2. Cold Chain Logistics. A cold chain is a temperature-controlled supply chain, where the technologies, devices, and management systems play essential roles in the processes of the cold chain. Logistics makes the cold chain temperature control much complicate because the facilities and processes are usually distributive and undertaken by various stakeholders and even outsourcing. The industry has developed the technology aspect of the cold chain well, notably including refrigerators and power technologies. The information and system aspects are highly related to this study. In Table 2, we reviewed the studies to present the typical issues examined in the literature and the methods used. We classify the issues into three categories: operations research, operations management, and systems. In cold chain systems, sustainability and safety issues are increasingly concerned. Furthermore, we classify the issues into logistics problems and supply chain problems. The research methods include assessment, optimization algorithms, empirical and case studies, and review.

2.3. Evolutionary Games in Supply Chain Studies. Evolutionary game is a tool to study the dynamic evolutionary strategies between two interacted populations by establishing and analyzing the replicator dynamic systems. The pioneering studies have developed evolutionary games for policymaking problems and the behavior strategies of interreacted stakeholders. Although the evolutionary game is also widely used to study the supply chain, the cold chain is seldom examined by it. Therefore, in Table 3, 12 studies in supply chain management (SCM) are reviewed. Mainly the issues and the interacted populations are summarized. In the studied issues, most papers studied sustainability (also including green, low carbon, and remanufacturing behavior strategies), while these papers also examined the risk and knowledge-sharing issues. The populations involved mainly include production supply chain members (typically

Table 1: Studies in logistics information transparency.

Study	Issue	Stakeholders	Method
[9]	Information integration and profitability	Manufacturers, retailers	Conceptual model
[10]	Information sharing, supply uncertainty, and demand volatility	Manufacturer, retailers	Simulation
[11]	Role of information sharing in SCE	Vendors, retailers	Case study
[12]	Information flows in SCEs	Buyers, suppliers	Data analysis
[13]	RFID investment	SCE	Survey
[14]	RFID-enabled business intelligence	Manufacturers, distributors	IS
[15]	Information sharing and investment in procurement	Suppliers, buyers	Game model
[8]	RFID information sharing and exchanging	Governments, enterprises	IS
[16]	RFID investment risk and gain reallocation	SCE	Risk assessment
[17]	Information sharing, environmental and economic benefits	Manufacturers, suppliers	Inventory model
[18]	Information linkages with retailers	Multinational companies and retailers	Case study
[19]	Information sharing of VMI	TPL, its customer	Inventory model
[20]	Information sharing and safety traceability	Producers, distributors, and ordinary users	IS
[6]	Blockchain and information sharing	Manufacturer, supplier, and logistics service integrator	Stackelberg game
[21]	Food traceability	Farmers, traders, and consumers	Case study

Note. IS = information system; RFID = radio frequency identification; SCE = supply chain enterprises; TPL = third-party logistics.

Table 2: Studies in cold chain logistics.

Study	Issues	Methods
[22]	Performance evaluation	Assessment
[23]	Logistics competence	AHP, FCE
[24]	Distribution network	GA
[25]	VRPTW	GA
[26]	Sustainable distribution	MILP
[27]	Disruption management	Partial least squares
[28]	Perishable product	Empirical study
[29]	Data-driven decision-making	Review
[30]	Recommender systems	Heuristics algorithm
[31]	Value-added service	Case study
[32]	Distribution optimization	PSO
[33]	Integrated IRP	GSAA
[34]	Sustainability	Graph theory
[35]	Distribution optimization	GA
[36]	Vehicle routing problem	Heuristics algorithm

Notes. AHP = analytic hierarchy process; FCE = fuzzy comprehensive evaluation; GA = genetic algorithm; GSAA = genetic simulated annealing algorithm; IRP = inventory routing problem; MILP = mixed-integer linear program; PSO = particle swarm optimization; VRPTW = vehicle routing problem with time windows.

manufacturers, suppliers, and retailers) and governments. These studies do not study logistics service providers or other entities related to logistics.

3. Problem Description and Assumptions

3.1. Problem Description. As estimated by [52], the global cold chain market will probably reach approximately USD 269.61 billion by 2024, growing at a CAGR of around 7.5% between 2018 and 2024. The cold chain is a system for the management and transportation of temperature-sensitive products through refrigerated and thermal methods of packaging. A cold chain is a temperature-controlled supply chain from the manufacturers of the cold goods to final customers. Unlike other goods, cold chain goods are perishable and sensitive to temperature changes. So, cold chain logistics is not just a process of warehousing and transportation. Its validity involves innovative technologies, devices, and managerial systems to ensure temperature control and maintenance in the whole logistics process. Simultaneously, the natures of the cold chain goods are different and demand different temperature control technologies, methods, and devices, which involve knowledge transfer from the manufacturers to the logistics service providers.

In a cold chain, various stakeholders are involved. The manufacturers and logistics service providers are two roles strictly related to ensuring the cold chain goods quality and the key players in temperature control. In the logistics scenarios, from the manufacturers to the final customers, the cold goods are stored and transported through various warehouses and containers by trucks, trains, ships, and other means. Therefore, it is challenging to manage the time-varying status of cold goods when the cold chain is not transparent. In the cold chain, the individual logistics service suppliers can apply various technologies and devices to control the temperature, while these devices are not well connected. So, it is beneficial for the logistics service provider to connect the logistics processes (even devices) when the information acquired by these processes is shared, at least in the cold chain. Although the devices and their collected data may even be not credible and traceable, the information transparency degree deduced by information sharing in the cold chain is a way to manage the cold goods' temperature. As analyzed above, technology and devise investments contribute to the additional costs of logistics. When the investment costs still restrict the whole industry, the tradeoff and evolutionary games between the manufacturers and logistics service providers may determine the development tendency of the cold chain ecosystem. In the

Table 3: Studies of evolutionary games in supply chain management.

Study	Issues	Populations
[37]	Behavior strategies triggering green practices	Producers, retailers
[38]	Remanufacturing closed-loop supply chain	Manufacturers, retailers
[39]	Green SCM diffusion	Governors, enterprises
[40]	Long-term green purchasing relationships	Suppliers, manufacturers
[41]	Energy source selection	Government, power plants
[42]	Low-carbon investment strategies	Suppliers, manufacturers
[43]	Financial risk cooperation behaviors	Suppliers, manufacturers
[44]	Sustainability and government intervention	Governors, producers
[45]	Wholesale-retail pricing strategies	Manufacturer, retailers
[46]	Cooperation relationships and tendency	Constructors, suppliers
[47]	Remanufacturers competing for leadership	Manufacturers, retailers
[48]	Green investment strategies with subsidy	Manufacturers, suppliers
[49]	Low-carbon behaviors, strategies, and policies	Retailers, manufacturers
[50]	Knowledge-sharing behavior and alliance	Construction enterprises
[51]	Green production and financial intervention	Suppliers, manufacturers, and governments

following study, we employ an evolutionary game to study the information transparency mechanisms between these two key stakeholders (manufacturers and logistics service providers) in a cold chain.

On the side of logistics service providers, to organize the temperature-controlled cold chain logistics processes, the following information is beneficial: the food status (original temperature and quality), the refrigerator technologies suitable for the food, and the restrict time and temperature standards allowed for food package handlings for warehousing and transsshipment [3]. The stakeholders can negotiate possible other demands in the contracts for ensuring food quality in logistics. These information aspects affect the costs and efficiencies of logistics, and so the risks and profits are different from the logistics service providers. Well-controlled information transparency in cold chains incurs increasing costs and responsibilities to the manufacturers and logistics service providers.

As analyzed above, in cold chains, information transparency incurs two-sided effects. On the one side, information transparency can increase food safety and satisfaction degrees by propelling companies to share their information related to temperature control by using various advanced refrigerator and information technologies. On the other side, information sharing for increasing information transparency incurs technology investment and management costs, operations risks, and possible competitions [53]. Therefore, it is a dilemma for companies to increase information transparency in the whole cold chain industry. Various food safety events frequently happen, while the cold chain technologies and markets are developing very fast at the same time [27].

3.2. Model Assumption. In the context of evolutionary games, cold chain manufacturers and logistics service providers are two distinct groups of companies as two populations of players. The individual player in a population behaves under the affection of other players in the same population. They will stimulate each other. The mutual interactions between the players from the two populations will directly affect the behaviors of the two players and, thus, as a whole affect the populations' behaviors [54]. The individuals in the same population can share behavior information in a manner of cooperation.

In cold chains, as for information transparency, manufacturers and logistics service providers may cooperate and not cooperate in propelling information sharing. The possibilities of adopting the cooperation strategy are denoted by x and y ($x, y \in [0, 1]$) for the two populations; inversely, the possibilities of not adopting the cooperation strategy are $(1 - x)$ and $(1 - y)$. In an evolutionary game, these possibilities evolve and present dynamics.

In cold chain logistics, advocating information transparency incurs an additional cost (denoted by C) for the infrastructures of sensors, communication networks, and application systems. The logistics service provider may obtain the additional profit (denoted by P) due to market acceptance. When a manufacturer does not share information, the unit profit of cold goods production is π_A, while the logistics service provider can just manage the cold chain by general cold chain practices. The logistics service provider can obtain the profit (π_B), when the company does not choose the strategy of cooperation. When the manufacturer and the logistics service provider cooperate closely, they can obtain profit P from the market, and they can undertake the cost C cooperatively. In the cooperation (information sharing for information transparency) strategy in the evolutionary game, when one player shares information while another does, a penalty (denoted by F) will incur to the one that does not choose cooperation; simultaneously, the one choosing to share information will obtain a subsidy V. The penalty and subsidy mechanisms can be contracted and administrated by the governments.

Information transparency will benefit the stakeholders in the cold chains, including customers and administration departments. So, the improvement of food safety due to information transparency may result in the readjusting of the market. The administrators should reallocate the induced surplus of the additional profit between the manufacturer and the logistics service provider. The amount allocated to the manufacturer is denoted by a proportion, α ($\alpha \in [0, 1]$); thus, the logistics service provider can obtain $(1 - \alpha)$. Simultaneously, the cost also will be allocated to the manufacturer (β) and the logistics service provider $(1-\beta)$, $\beta \in [0,1]$. The values of (α, β) will affect the evolutionary tendencies of the game and should be negotiated in practice.

4. Formulations and Model Analysis

4.1. Payoff Matrix. Considering the assumptions and notations elucidated in Section 3.2, the payoff matrix between the cold chain manufacturer and logistics service provider is presented in Table 4. The additional cost and profit are reallocated to the players when at least one player chooses the cooperation for information sharing in the information transparency mechanisms.

4.2. Replicator Dynamic System. Based on the payoff matrix (Table 1), the average profit obtained by the cold chain manufacturers when the cooperation strategy (denoted by F_{co}) is dominant is computed as (1). Similarly, the average profit of the manufacturers when cooperation is adopted (F_{noco}) is formulated by (2). Synthesizing (1) and (2), the average profit obtained by the manufacturer ($\overline{F}$) is formulated by (3). Then, the replicator dynamic equation of the manufacturers adopting the cooperation strategy is formulated by (4):

$$F_{co} = y(\pi_A + \alpha P - \beta C) + (1-y)(\pi_A - \beta C + V), \tag{1}$$

$$F_{noco} = y(\pi_A - F) + (1-y)(\pi_A), \tag{2}$$

$$\overline{F} = xF_{co} + (1-x)F_{noco}, \tag{3}$$

$$\begin{aligned} F(x) &= \frac{dx}{dt} = x(F_{co} - \overline{F}) = x(1-x)[F_{co} - F_{noco}] \\ &= x(1-x)[(\alpha P - V + F)y - \beta C + V]. \end{aligned} \tag{4}$$

Like (1)–(4), the logistics service provider's average profits when it adopts cooperation and non-cooperation strategies (E_{co} and E_{noco}) are formulated by (5) and (6). So, the overall average profit ($\overline{E}$) is computed by (7). Thus, the replicator dynamic equation ($E(y)$) is given in (8):

$$\begin{aligned} E_{co} = {} & x(\pi_B + (1-\alpha)P - (1-\beta)C) \\ & + (1-x)(\pi_B - (1-\beta)C + V), \end{aligned} \tag{5}$$

$$E_{noco} = x(\pi_B - F) + (1-x)(E_B), \tag{6}$$

$$\overline{E} = yE_{co} + (1-y)E_{noco}, \tag{7}$$

$$\begin{aligned} E(y) = \frac{dy}{dt} = y(E_{co} - \overline{E}) = y(1-y)[x((1-\alpha)P - V + F) \\ - (1-\beta)C + V]. \end{aligned} \tag{8}$$

4.3. Evolutionary Equilibrium Point. Combining (4) and (5), we developed a replicator dynamic system in (9). The values of x and y of an evolutionary stable strategy (ESS) should meet $F(x) = F(y) = 0$ in (9). Under these two equations, we can obtain two groups of ESS as (10) and (11). We then can derive five equilibrium points (EPs) from the dynamic system (9) in the domain $s = \{(x, y) \mid 0 \le x, y \le 1\}$. These EPs are denoted by $E_1(0,0)$, $E_2(0,1)$, $E_3(1,0)$, $E_4(1,1)$, $E_5(x_*, y_*)$, $x_* \in [0,1]$, and $y_* \in [0,1]$:

$$\begin{cases} F(x) = x(1-x)[(\alpha P - V + F)y - \beta C + V], \\ E(y) = y(1-y)[x((1-\alpha)P - V + F) - (1-\beta)C + V], \end{cases} \tag{9}$$

$$\begin{aligned} x_1 &= 0, \\ x_2 &= 1, \\ y_* &= \frac{\beta C - V}{\alpha P - V + F}, \end{aligned} \tag{10}$$

$$\begin{aligned} y_1 &= 0, \\ y_2 &= 1, \\ x_* &= \frac{(1-\beta)C - V}{(1-\alpha)P - V + F}. \end{aligned} \tag{11}$$

4.4. ESS Analysis. We analyze the equilibrium points' stability by using the stability of the Jacobian matrix of the replicator dynamic system. Firstly, we derive the Jacobian matrix (denoted by J) in (12). The determinant ($\det J$) and trace ($\operatorname{tr} J$) of J are then computed in (13) and (14) individually. The equilibrium points satisfying $\{\det J > 0, \operatorname{tr} J < 0\}$ are stable points of the replicator dynamic system. The $\det J$ and $\operatorname{tr} J$ of the five equilibrium points are computed as Table 5 by using (13) and (14):

$$J = \begin{bmatrix} \dfrac{\partial F(x)}{\partial x} & \dfrac{\partial F(x)}{\partial y} \\ \dfrac{\partial E(y)}{\partial x} & \dfrac{\partial E(y)}{\partial y} \end{bmatrix},$$

$$\begin{cases} \dfrac{\partial F(x)}{\partial x} = (1-2x)[(\alpha P - V + F)y - \beta C + V], \\ \dfrac{\partial F(x)}{\partial y} = (\alpha P - V + F)x(1-x), \\ \dfrac{\partial E(y)}{\partial x} = ((1-\alpha)P - V + F)y(1-y), \\ \dfrac{\partial E(y)}{\partial y} = (1-2y)[x((1-\alpha)P - V + F) - (1-\beta)C + V], \end{cases} \tag{12}$$

$$\begin{aligned} \det J = {} & (1-2x)[(\alpha P - V + F)y - \beta C + V] \\ & \cdot (1-2y)[x((1-\alpha)P - V + F) - (1-\beta)C + V] \\ & - (\alpha P - V + F)x(1-x)((1-\alpha)P - V + F)y(1-y), \end{aligned} \tag{13}$$

Table 4: Payoff matrix.

		Logistics service provider	
		Cooperation (y)	Non-cooperation $(1-y)$
Manufacturer	Cooperation (x)	$\pi_A + \alpha P - \beta C$ $\pi_B + (1-\alpha)P - (1-\beta)C$	$\pi_A - \beta C + V$ $\pi_B - F$
	Non-cooperation $(1-x)$	$\pi_A - F$ $\pi_B - (1-\beta)C + V$	π_A π_B

Table 5: The det$J$ and tr J of the five equilibrium points.

EP	det$J$	tr J
$E_1(0,0)$	$(-\beta C + V)[-(1-\beta)C + V]$	$2V - C$
$E_2(1,0)$	$-(-\beta C + V)((1-\alpha)P - (1-\beta)C + F)$	$(1-\alpha)P + \beta C + F - (1-\beta)C - V$
$E_3(0,1)$	$(\alpha P + F - \beta C)(-)(-(1-\beta)C + F)$	$-\alpha P + \beta C - (1-\beta)C$
$E_4(1,1)$	$-(\alpha P + F - \beta C) - ((1-\alpha)P + F - (1-\beta)C)$	$C - 2F - P$
$E_5(x_*, y_*)$	Δ	0

Note. $\Delta = -[(1-\beta)C - V](((1-\alpha)P + F - (1-\beta)C)/((1-\alpha)P - V + F))[\beta C - V]((\alpha P + F - \beta C)/(\alpha P - V + F))$.

$$\operatorname{tr} J = (1-2x)[(\alpha P - V + F)y - \beta C + V] + (1-2y) \cdot [x((1-\alpha)P - V + F) - (1-\beta)C + V]. \quad (14)$$

(1) $E_1(0,0)$ is an ESS when $\{(-\beta C + V)[-(1-\beta)C + V] > 0; 2V - C < 0\}$ is met. Because of $-\beta C + V \leq 0$ and $-(1-\beta)C + V \leq 0$, we can obtain $V < \beta C$ and $V < (1-\beta)C$. It indicates that when the subsidy cannot compensate for the cooperation cost, the cold chain manufacturer and the logistics service provider will give up the cooperation by sharing information.

(2) $E_2(1,0)$ is an ESS when $\{-(-\beta C + V)\ ((1-\alpha)P - (1-\beta)C + F) > 0;\ (1-\alpha)P + \beta C + F - (1-\beta)C - V < 0\}$, we can deduce that $\{\beta C - V \leq 0; (1-\alpha) P - (1-\beta)C + F \leq 0\}$. So, $V > \beta C$ and $(1-\beta)C > (1-\alpha)P + F$. Under this ESS, the cold chain manufacturer undertakes less cost; the logistics service provider obtains minor profit. Comparatively, α is big, while β is small.

(3) $E_3(0,1)$ is an ESS when $\{-(\alpha P + F - \beta C)\ (-(1-\beta)C + F) > 0; \alpha P - V + F < 0\}$ is met. Setting $\{-\alpha P - F + \beta C \leq 0; -(-(1-\beta)C + F) \leq 0\}$, we can get $\{\beta C > \alpha P + F; F > (1-\beta)C\}$. Under this ESS, β is small and α is big, while the subsidy V should be big comparatively.

(4) $E_4(1,1)$ is an ESS when $\{-(\alpha P + F - \beta C) - ((1-\alpha) P + F - (1-\beta)C) > 0; C - 2F - P < 0\}$ is met. When $-(\alpha P + F - \beta C) < 0$ and $-((1-\alpha)P + F - (1-\beta)C) < 0$, we can get $\beta C < \alpha P + F$ and $(1-\beta)C < (1-\alpha)P + F$. In this ESS, β is big. So, the cold chain manufacturer undertakes more cost than the additional profit and the penalty paid by the logistics service providers; the cost undertaken by the logistics service provider is also beyond the profit and the penalty paid by the logistics service providers. Two times of additional profit and subsidy are more significant than the cost of information sharing.

We classify the studies on the ESSs into four parts in Tables 6–9 considering the inequalities between V and βC and the inequalities between V and $(1-\beta)C$.

(1) Category 1: $V < \beta C$ and $V < (1-\beta)C$

(1) In Category 1.1, $(1-\beta)C > (1-\alpha)P + F$, $\beta C < \alpha P + F$, and $F < (1-\beta)C$. The subsidy cannot compensate for the cost of information sharing to the manufacturers and logistics service providers. The information-sharing cost of the logistics service providers is higher than the additional profit and penalty (obtained from the manufacturers when they do not adopt the cooperation strategy). In summary, the subsidy is low, the profit is low, the information-sharing cost is high, and the penalty to the non-cooperation strategy is low. An ESS exists, $E_2(0,0)$, and both players will give up the cooperation of sharing information.

(2) In Category 1.2, $(1-\beta)C > (1-\alpha)P + F$, $\beta C > \alpha P + F$, and $F < (1-\beta)C$. For the manufacturers and logistics service providers, the cost of sharing information is high, while the subsidy, the additional profit deduced by information sharing, and the penalty cost deduced by non-cooperation are low. Here, the ESS is $E_2(0,0)$. Thus, both players will give up the cooperation strategy.

(3) In Category 1.3, $(1-\beta)C < (1-\alpha)P + F$, $\beta C < \alpha P + F$, and $F < (1-\beta)C$. For both players, the cost of sharing information, the subsidy, and the penalty cost of non-cooperation strategy are all low. Affected by the additional profit P, two ESSs will occur: $E_2(0,0)$ and $E_4(1,1)$. The players will choose cooperation or non-cooperation strategies according to the additional profit.

(4) In Category 1.4, $(1-\beta)C < (1-\alpha)P + F$, $\beta C < \alpha P + F$, and $F > (1-\beta)C$. For both players, the cost of sharing information and the subsidy is

Table 6: Local stability analysis ($V < \beta C$ and $V < (1-\beta)C$).

No.	Figure	Constraints	EP	det J	tr J	State
1	Figure 1(a)	$V < \beta C$, $V < (1-\beta)C$	$E_1(0,0)$	+	−	ESS
		$(1-\beta)C > (1-\alpha)P + F$	$E_2(1,0)$	−		Saddle point
		$\beta C < \alpha P + F$, $F < (1-\beta)C$	$E_3(0,1)$	+	+	Instability point
			$E_4(1,1)$	−		Saddle point
			$E_5(x_*, y_*)$	Δ	0	
2#		$V < \beta C$, $V < (1-\beta)C$	$E_1(0,0)$	+	−	ESS
		$(1-\beta)C > (1-\alpha)P + F$	$E_2(1,0)$	−		Saddle point
		$\beta C < \alpha P + F$, $F > (1-\beta)C$	$E_3(0,1)$	−		Saddle point
			$E_4(1,1)$	−		Saddle point
			$E_5(x_*, y_*)$	Δ		
3	Figure 1(b)	$V < \beta C$, $V < (1-\beta)C$	$E_1(0,0)$	+	−	ESS
		$(1-\beta)C > (1-\alpha)P + F$	$E_2(1,0)$	−		Saddle point
		$\beta C > \alpha P + F$, $F < (1-\beta)C$	$E_3(0,1)$	−		Saddle point
			$E_4(1,1)$	+	+	Instability point
			$E_5(x_*, y_*)$	Δ		
4#		$V < \beta C$, $V < (1-\beta)C$	$E_1(0,0)$	+	−	ESS
		$(1-\beta)C > (1-\alpha)P + F$	$E_2(1,0)$	−		Saddle point
		$\beta C > \alpha P + F$, $F > (1-\beta)C$	$E_3(0,1)$	+	−	ESS
			$E_4(1,1)$	+	+	Instability point
			$E_5(x_*, y_*)$	Δ		
5	Figure 1(c)	$V < \beta C$, $V < (1-\beta)C$	$E_1(0,0)$	+	−	ESS
		$(1-\beta)C < (1-\alpha)P + F$	$E_2(1,0)$	+	+	Instability point
		$\beta C < \alpha P + F$, $F < (1-\beta)C$	$E_3(0,1)$	+	+	Instability point
			$E_4(1,1)$	+	−	ESS
			$E_5(x_*, y_*)$	Δ		
6	Figure 1(d)	$V < \beta C$, $V < (1-\beta)C$	$E_1(0,0)$	+	−	ESS
		$(1-\beta)C < (1-\alpha)P + F$	$E_2(1,0)$	+	+	Instability point
		$\beta C < \alpha P + F$, $F > (1-\beta)C$	$E_3(0,1)$	−		Saddle point
			$E_4(1,1)$	+	−	ESS
			$E_5(x_*, y_*)$	Δ		
7	Figure 1(e)	$V < \beta C$, $V < (1-\beta)C$	$E_1(0,0)$	+	−	ESS
		$(1-\beta)C < (1-\alpha)P + F$	$E_2(1,0)$	+	+	Instability point
		$\beta C > \alpha P + F$, $F < (1-\beta)C$	$E_3(0,1)$	−		Saddle point
			$E_4(1,1)$	−		Saddle point
			$E_5(x_*, y_*)$	Δ		ESS
8	Figure 1(f)	$V < \beta C$, $V < (1-\beta)C$	$E_1(0,0)$	+	−	ESS
		$(1-\beta)C < (1-\alpha)P + F$	$E_2(1,0)$	+	+	Instability point
		$\beta C > \alpha P + F$, $F > (1-\beta)C$	$E_3(0,1)$	+	−	ESS
			$E_4(1,1)$	−		Saddle point
			$E_5(x_*, y_*)$	Δ		

Note. # = the constraints conflict with each other.

low. Affected by the additional profit P, two ESSs emerge, $E_2(0,0)$ and $E_4(1,1)$. So, the players will choose cooperation or non-cooperation strategies according to the additional profit.

(5) In Category 1.5, $(1-\beta)C < (1-\alpha)P + F$, $\beta C > \alpha P + F$, and $F < (1-\beta)C$. For the manufacturers, the cost of sharing information is high; however, for the logistics service providers, this cost, the subsidy, and the penalty of adopting the non-cooperation strategy are low. An ESS exists, $E_2(0,1)$.

(6) In Category 1.6, $(1-\beta)C < (1-\alpha)P + F$, $\beta C > \alpha P + F$, and $F > (1-\beta)C$. Comparing with (5), the penalty cost increases, resulting in two ESSs, $E_1(0,0)$ and $E_3(0,1)$.

(2) Category 2: $V < \beta C$ and $V > (1-\beta)C$

(1) In Category 2.1, $(1-\beta)C > (1-\alpha)P + F$, $\beta C < \alpha P + F$, and $F < (1-\beta)C$. Here, the subsidy to the manufacturers is low, and the cost of sharing information is also low. However, the subsidy to the logistics service providers is high as well as the cost of sharing information. When the penalty of non-cooperation is also low, both players behave by waiting and following the other ones. So, no ESS exists.

(2) In Category 2.2, $(1-\beta)C > (1-\alpha)P + F$, $\beta C > \alpha P + F$, and $F < (1-\beta)C$. The logistics service providers can get a high subsidy that is higher than the cost of sharing information. So, they will choose the cooperation strategy.

Table 7: Local stability analysis $V < \beta C$ and $V > (1-\beta)C$.

No.	Figure	Constraints	EP	det$J$	tr J	State
1	Figure 2(a)	$V < \beta C$, $V > (1-\beta)C$	$E_1(0,0)$	−		Saddle point
		$(1-\beta)C > (1-\alpha)P + F$	$E_2(1,0)$	−		Saddle point
		$\beta C < \alpha P + F$, $F < (1-\beta)C$	$E_3(0,1)$	+	+	Instability point
			$E_4(1,1)$	−		Saddle point
			$E_5(x_*, y_*)$	Δ	0	
2#		$V < \beta C$, $V > (1-\beta)C$	$E_1(0,0)$	−		Saddle point
		$(1-\beta)C > (1-\alpha)P + F$	$E_2(1,0)$	−		Saddle point
		$\beta C < \alpha P + F$, $F > (1-\beta)C$	$E_3(0,1)$	−		Saddle point
			$E_4(1,1)$	−		Saddle point
			$E_5(x_*, y_*)$	Δ	0	
3	Figure 2(b)	$V < \beta C$, $V > (1-\beta)C$	$E_1(0,0)$	−		Saddle point
		$(1-\beta)C > (1-\alpha)P + F$	$E_2(1,0)$	−		Saddle point
		$\beta C > \alpha P + F$, $F < (1-\beta)C$	$E_3(0,1)$	−		Saddle point
			$E_4(1,1)$	+	+	Instability point
			$E_5(x_*, y_*)$	Δ	0	
4#		$V < \beta C$, $V > (1-\beta)C$	$E_1(0,0)$	−		Saddle point
		$(1-\beta)C > (1-\alpha)P + F$	$E_2(1,0)$	−		Saddle point
		$\beta C > \alpha P + F$, $F > (1-\beta)C$	$E_3(0,1)$	+	−	ESS
			$E_4(1,1)$	+	+	Instability point
			$E_5(x_*, y_*)$	Δ	0	
5	Figure 2(c)	$V < \beta C$, $V > (1-\beta)C$	$E_1(0,0)$	−		Saddle point
		$(1-\beta)C < (1-\alpha)P + F$	$E_2(1,0)$	+	+	Instability point
		$\beta C < \alpha P + F$, $F < (1-\beta)C$	$E_3(0,1)$	+	+	Instability point
			$E_4(1,1)$	+	−	ESS
			$E_5(x_*, y_*)$	Δ	0	
6	Figure 2(d)	$V < \beta C$, $V > (1-\beta)C$	$E_1(0,0)$	−		Saddle point
		$(1-\beta)C < (1-\alpha)P + F$	$E_2(1,0)$	+	+	Instability point
		$\beta C < \alpha P + F$, $F > (1-\beta)C$	$E_3(0,1)$	−		Saddle point
			$E_4(1,1)$	+	−	ESS
			$E_5(x_*, y_*)$	Δ	0	
7	Figure 2(e)	$V < \beta C$, $V > (1-\beta)C$	$E_1(0,0)$	−		Saddle point
		$(1-\beta)C < (1-\alpha)P + F$	$E_2(1,0)$	+	+	Instability point
		$\beta C > \alpha P + F$, $F < (1-\beta)C$	$E_3(0,1)$	−		Saddle point
			$E_4(1,1)$	−		Saddle point
			$E_5(x_*, y_*)$	Δ	0	
8	Figure 2(f)	$V < \beta C$, $V > (1-\beta)C$	$E_1(0,0)$	−		Saddle point
		$(1-\beta)C < (1-\alpha)P + F$	$E_2(1,0)$	+	+	Instability point
		$\beta C > \alpha P + F$, $F > (1-\beta)C$	$E_3(0,1)$	+	−	ESS
			$E_4(1,1)$	−		Saddle point
			$E_5(x_*, y_*)$	Δ	0	

Note. # = the constraints conflict with each other.

However, to the manufacturers, the subsidy is lower than the cost of sharing information; the cost of sharing information is even less than the sum of the additional profit of sharing information and the penalty paid by the logistics service providers. So, the manufacturers will not choose the cooperation strategy.

(3) In Category 2.3, $(1-\beta)C < (1-\alpha)P + F$, $\beta C < \alpha P + F$, and $F < (1-\beta)C$. The cost of sharing information to the manufacturers is low; the additional profits of sharing information are all high for the two players. So, the manufacturers and logistics service providers will both choose the cooperation strategy. An ESS exists, $E_4(1,1)$.

(4) In Category 2.4, $(1-\beta)C < (1-\alpha)P + F$, $\beta C < \alpha P + F$, and $F > (1-\beta)C$. The penalty cost of the non-cooperation strategy is at a high level. If both players do not adopt the cooperation strategy, the penalty costs will decrease their profit. So, they will choose to adopt the cooperation strategy.

(5) In Category 2.5, $(1-\beta)C < (1-\alpha)P + F$, $\beta C > \alpha P + F$, and $F < (1-\beta)C$. The subsidy to the logistics service providers is higher and more significant than the penalty of non-cooperation strategy; the cost of sharing information and the additional profit of sharing information are both low. Therefore, they both will not adopt the cooperation strategy, and so no ESS exists.

Table 8: Local stability analysis $V > \beta C$ and $V > (1-\beta)C$.

No.	Figure	Constraints	EP	det$J$	tr J	State
1	Figure 3(a)	$V > \beta C$, $V > (1-\beta)C$	$E_1(0,0)$	+	+	Instability point
		$(1-\beta)C > (1-\alpha)P + F$	$E_2(1,0)$	+	−	ESS
		$\beta C < \alpha P + F$, $F < (1-\beta)C$	$E_3(0,1)$	+	+	Instability point
			$E_4(1,1)$	−		Saddle point
			$E_5(x_*, y_*)$	Δ	0	
2#		$V > \beta C$, $V > (1-\beta)C$	$E_1(0,0)$	+	+	Instability point
		$(1-\beta)C > (1-\alpha)P + F$	$E_2(1,0)$	+	−	ESS
		$\beta C < \alpha P + \mathrm{F}$, $F > (1-\beta)C$	$E_3(0,1)$	−		Saddle point
			$E_4(1,1)$	−		Saddle point
			$E_5(x_*, y_*)$	Δ	0	
3	Figure 3(b)	$V > \beta C$, $V > (1-\beta)C$	$E_1(0,0)$	+	+	Instability point
		$(1-\beta)C > (1-\alpha)P + F$	$E_2(1,0)$	+	−	ESS
		$\beta C > \alpha P + F$, $F < (1-\beta)C$	$E_3(0,1)$	−		Saddle point
			$E_4(1,1)$	+	+	Instability point
			$E_5(x_*, y_*)$	Δ	0	
4#		$V > \beta C$, $V > (1-\beta)C$	$E_1(0,0)$	+	+	Instability point
		$(1-\beta)C > (1-\alpha)P + F$	$E_2(1,0)$	+	−	ESS
		$\beta C > \alpha P + F$, $F > (1-\beta)C$	$E_3(0,1)$	+	−	ESS
			$E_4(1,1)$	+	+	Instability point
			$E_5(x_*, y_*)$	Δ	0	
5	Figure 3(c)	$V > \beta C$, $V > (1-\beta)C$	$E_1(0,0)$	+	+	Instability point
		$(1-\beta)C < (1-\alpha)P + F$	$E_2(1,0)$	−		Saddle point
		$\beta C < \alpha P + F$, $F < (1-\beta)C$	$E_3(0,1)$	+	+	Instability point
			$E_4(1,1)$	+	−	ESS
			$E_5(x_*, y_*)$	Δ	0	
6	Figure 3(d)	$V > \beta C$, $V > (1-\beta)C$	$E_1(0,0)$	+	+	Instability point
		$(1-\beta)C < (1-\alpha)P + F$	$E_2(1,0)$	−		Saddle point
		$\beta C < \alpha P + F$, $F > (1-\beta)C$	$E_3(0,1)$	−		Saddle point
			$E_4(1,1)$	+	−	ESS
			$E_5(x_*, y_*)$	Δ	0	
7	Figure 3(e)	$V > \beta C$, $V > (1-\beta)C$	$E_1(0,0)$	+	+	Instability point
		$(1-\beta)C < (1-\alpha)P + F$	$E_2(1,0)$	−		Saddle point
		$\beta C > \alpha P + F$, $F < (1-\beta)C$	$E_3(0,1)$	−		Saddle point
			$E_4(1,1)$	−		Saddle point
			$E_5(x_*, y_*)$	Δ	0	
8	Figure 3(f)	$V > \beta C$, $V > (1-\beta)C$	$E_1(0,0)$	+	+	Instability point
		$(1-\beta)C < (1-\alpha)P + F$	$E_2(1,0)$	−		Saddle point
		$\beta C > \alpha P + F$, $F > (1-\beta)C$	$E_3(0,1)$	+	−	ESS
			$E_4(1,1)$	−		Saddle point
			$E_5(x_*, y_*)$	Δ	0	

Note. # = the constraints conflict with each other.

(6) In Category 2.6, $(1-\beta)C < (1-\alpha)P + F$, $\beta C > \alpha P + F$, and $F > (1-\beta)C$. The penalty of non-cooperation strategy increases. So, the logistics service providers adopting the cooperation strategy will obtain higher profit from the penalty when the manufacturers adopt the non-cooperation strategy. To the manufacturers, the subsidy cannot compensate for the cost of sharing information. So, an ESS exists, $E_2(0,1)$.

(3) Category 3: $V > \beta C$ and $V > (1-\beta)C$

(1) In Category 3.1, $(1-\beta)C > (1-\alpha)P + F$, $\beta C < \alpha P + F$, and $F < (1-\beta)C$. To the logistics service providers, the subsidy of sharing information is high and even higher than the cost of sharing information. The evolutionary tendency depends on the additional profit of sharing information. There exists an ESS, $E_2(1,0)$.

(2) In Category 3.2, $(1-\beta)C > (1-\alpha)P + F$, $\beta C > \alpha P + F$, and $F < (1-\beta)C$. Similarly, an ESS, $E_2(1,0)$ exists.

(3) In Category 3.3, $(1-\beta)C < (1-\alpha)P + F$, $\beta C < \alpha P + F$, and $F < (1-\beta)C$. The subsidy is higher than the cost of sharing information; this cost of sharing information is low; simultaneously, the subsidy and additional profit of sharing information are high; and the penalty cost of the non-cooperation strategy is low. So, for the manufacturers and logistics service providers, adopting the cooperation strategy will increase the total profit. So, the ESS is $E_4(1,1)$.

TABLE 9: Local stability analysis $V > \beta C$ and $V < (1-\beta)C$.

No.	Figure	Constraints	EP	det$J$	tr J	State
1	Figure 4(a)	$V > \beta C$, $V < (1-\beta)C$ $(1-\beta)C > (1-\alpha)P + F$ $\beta C < \alpha P + F$, $F < (1-\beta)C$	$E_1(0,0)$ $E_2(1,0)$ $E_3(0,1)$ $E_4(1,1)$ $E_5(x_*, y_*)$	− + + − Δ	 − + 0	Saddle point ESS Instability point Saddle point
2#		$V > \beta C$, $V < (1-\beta)C$ $(1-\beta)C > (1-\alpha)P + F$ $\beta C < \alpha P + F$, $F > (1-\beta)C$	$E_1(0,0)$ $E_2(1,0)$ $E_3(0,1)$ $E_4(1,1)$ $E_5(x_*, y_*)$	− + − − Δ	 − 0	Saddle point ESS Saddle point Saddle point
3	Figure 4(b)	$V > \beta C$, $V < (1-\beta)C$ $(1-\beta)C > (1-\alpha)P + F$ $\beta C > \alpha P + F$, $F < (1-\beta)C$	$E_1(0,0)$ $E_2(1,0)$ $E_3(0,1)$ $E_4(1,1)$ $E_5(x_*, y_*)$	− + − + Δ	 − + 0	Saddle point ESS Saddle point Instability point
4#		$V > \beta C$, $V < (1-\beta)C$ $(1-\beta)C > (1-\alpha)P + F$ $\beta C > \alpha P + F$, $F > (1-\beta)C$	$E_1(0,0)$ $E_2(1,0)$ $E_3(0,1)$ $E_4(1,1)$ $E_5(x_*, y_*)$	− + + + Δ	 − − + 0	Saddle point ESS ESS Instability point
5	Figure 4(c)	$V > \beta C$, $V < (1-\beta)C$ $(1-\beta)C < (1-\alpha)P + F$ $\beta C < \alpha P + F$, $F < (1-\beta)C$	$E_1(0,0)$ $E_2(1,0)$ $E_3(0,1)$ $E_4(1,1)$ $E_5(x_*, y_*)$	− − + + Δ	 + − 0	Saddle point Saddle point Instability point ESS
6	Figure 4(d)	$V > \beta C$, $V < (1-\beta)C$ $(1-\beta)C < (1-\alpha)P + F$ $\beta C < \alpha P + F$, $F > (1-\beta)C$	$E_1(0,0)$ $E_2(1,0)$ $E_3(0,1)$ $E_4(1,1)$ $E_5(x_*, y_*)$	− − − + Δ	 − 0	Saddle point Saddle point Saddle point ESS
7	Figure 4(e)	$V > \beta C$, $V < (1-\beta)C$ $(1-\beta)C < (1-\alpha)P + F$ $\beta C > \alpha P + F$, $F < (1-\beta)C$	$E_1(0,0)$ $E_2(1,0)$ $E_3(0,1)$ $E_4(1,1)$ $E_5(x_*, y_*)$	− − − − Δ	 0	Saddle point Saddle point Saddle point Saddle point
8#		$V > \beta C$, $V < (1-\beta)C$ $(1-\beta)C < (1-\alpha)P + F$ $\beta C > \alpha P + F$, $F > (1-\beta)C$	$E_1(0,0)$ $E_2(1,0)$ $E_3(0,1)$ $E_4(1,1)$ $E_5(x_*, y_*)$	− − + − Δ	 − 0	Saddle point Saddle point ESS Saddle point

Note. # = the constraints conflict with each other.

(4) In Category 3.4, $(1-\beta)C < (1-\alpha)P + F$, $\beta C < \alpha P + F$, and $F > (1-\beta)C$. Comparing with (3), the penalty of the non-cooperation strategy increases. So, for the manufacturers, adopting the cooperation strategy can avoid the penalty and obtain a high subsidy and additional profit of sharing information. The ESS is to adopt the cooperation strategy, namely, $E_4(1,1)$.

(5) In Category 3.5, $(1-\beta)C < (1-\alpha)P + F$, $\beta C > \alpha P + F$, and $F < (1-\beta)C$. The subsidy is high, while the additional profit of sharing information is low. No ESS exists.

(6) In Category 3.6, $(1-\beta)C < (1-\alpha)P + F$, $\beta C > \alpha P + F$, and $F > (1-\beta)C$. The additional profit of cooperation strategy drops, while the logistics service providers' additional profit increases. So, an ESS exists, $E_3(0,1)$.

(4) Category 4: $V > \beta C$ and $V < (1-\beta)C$

(1) In Category 4.1, $(1-\beta)C > (1-\alpha)P + F$, $\beta C < \alpha P + F$, and $F < (1-\beta)C$. To the logistics service providers, the cost of sharing information is high, while the additional profit is low. Additionally, to the manufacturers, the additional profit of sharing information is high, and the subsidy is higher than the cost of sharing information. So, to maximize the total profit, an ESS exists, $E_2(1,0)$.

(2) In Category 4.2, $(1-\beta)C > (1-\alpha)P + F$, $\beta C > \alpha P + F$, and $F < (1-\beta)C$. The subsidy to

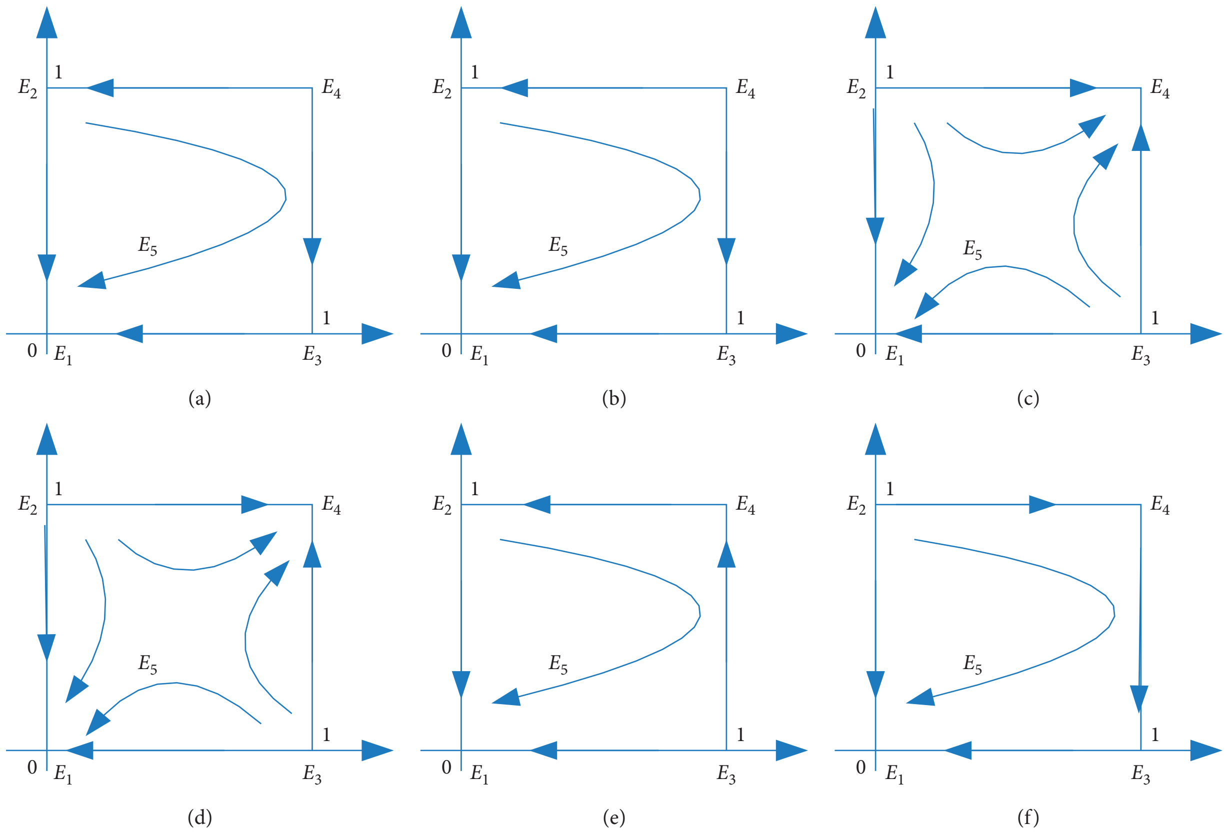

Figure 1: The local stability of the evolutionary game $V < \beta C$ and $V < (1 - \beta)C$.

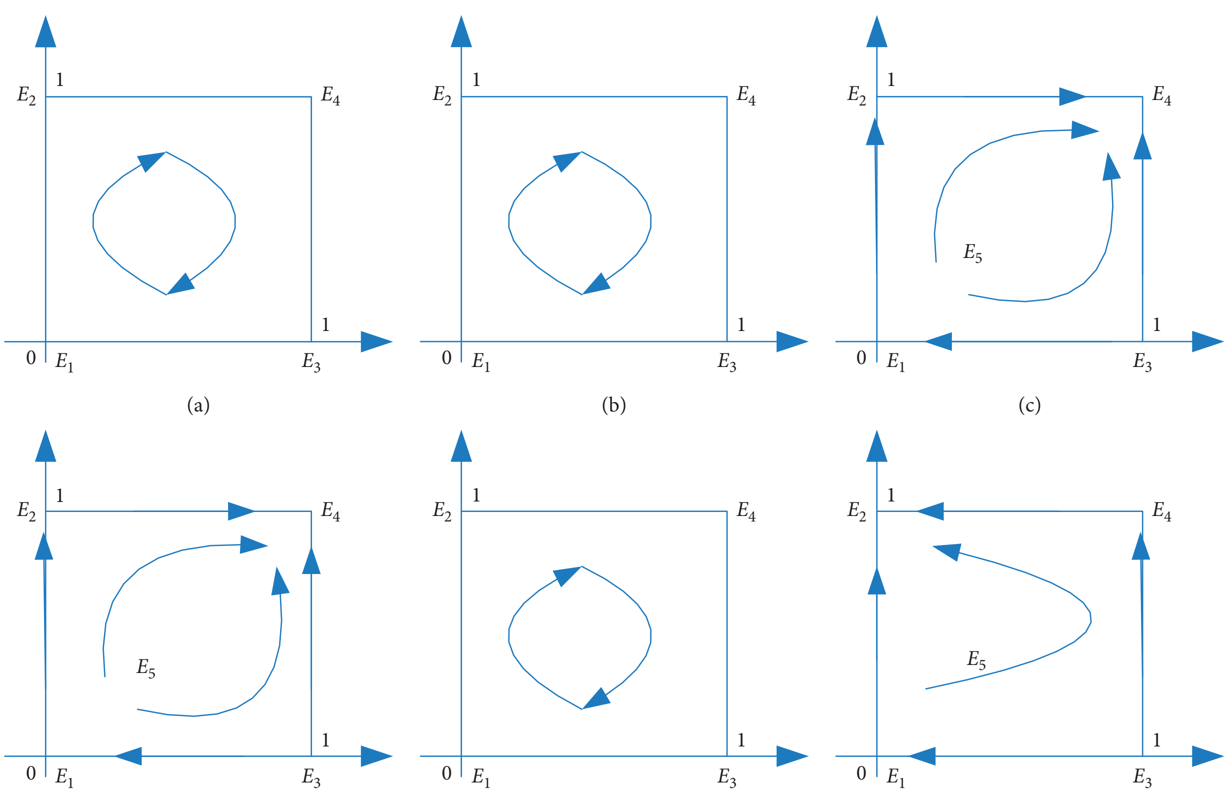

Figure 2: The local stability of the evolutionary game $V < \beta C$ and $V > (1 - \beta)C$.

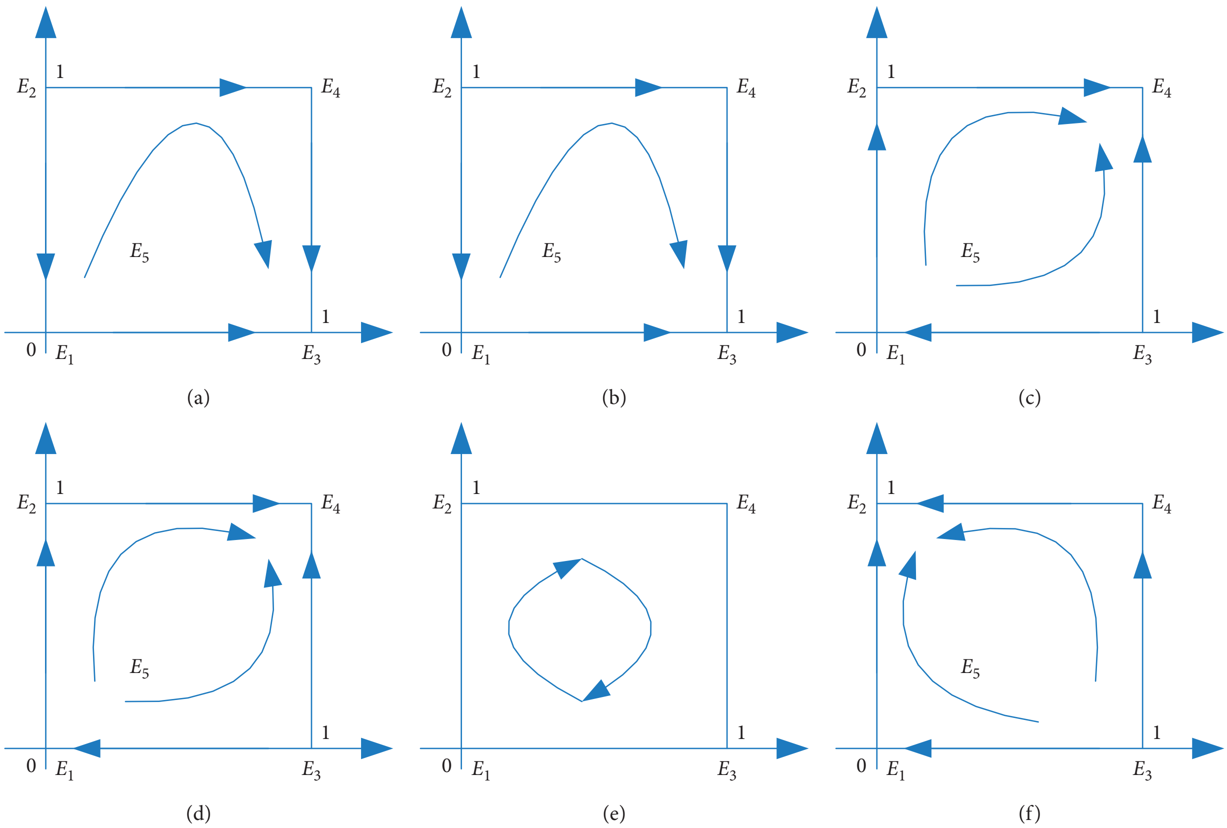

Figure 3: The local stability of the evolutionary game $V > \beta C$ and $V > (1-\beta)C$.

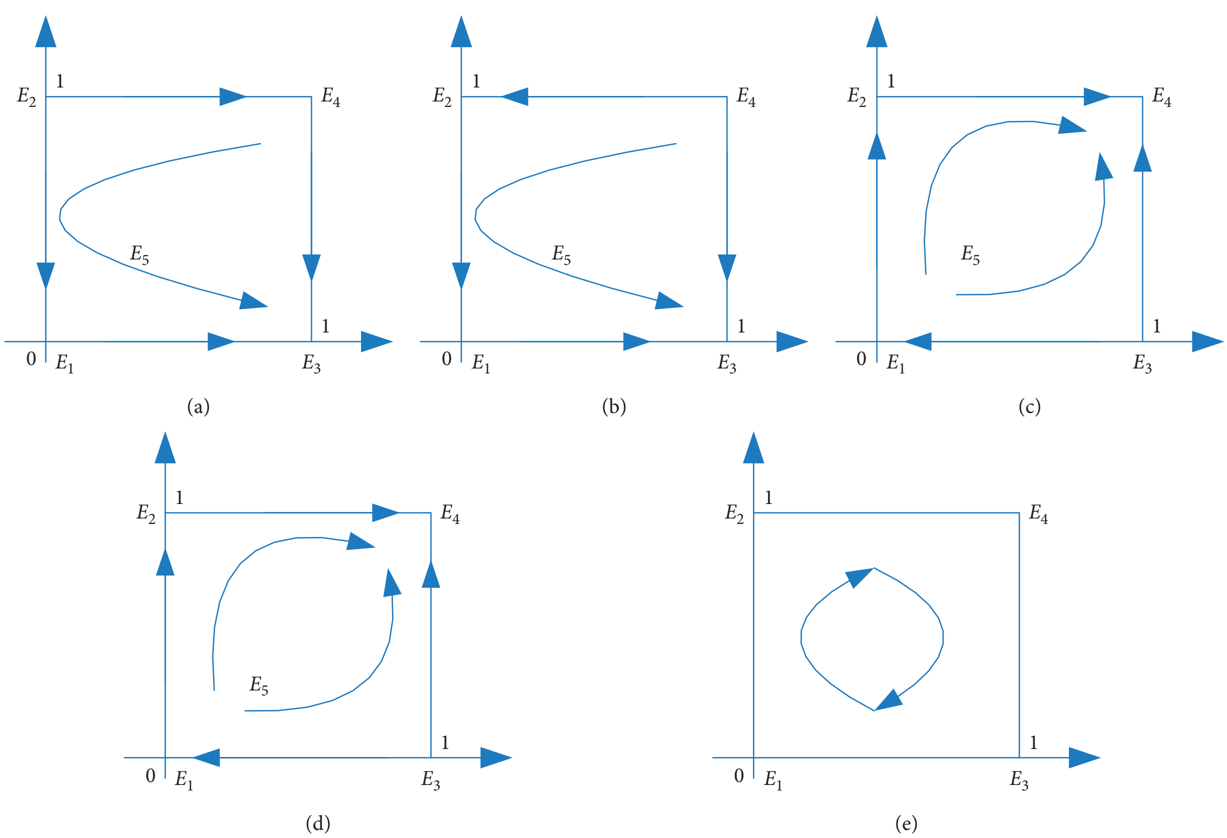

Figure 4: The local stability of the evolutionary game $V > \beta C$ and $V < (1-\beta)C$.

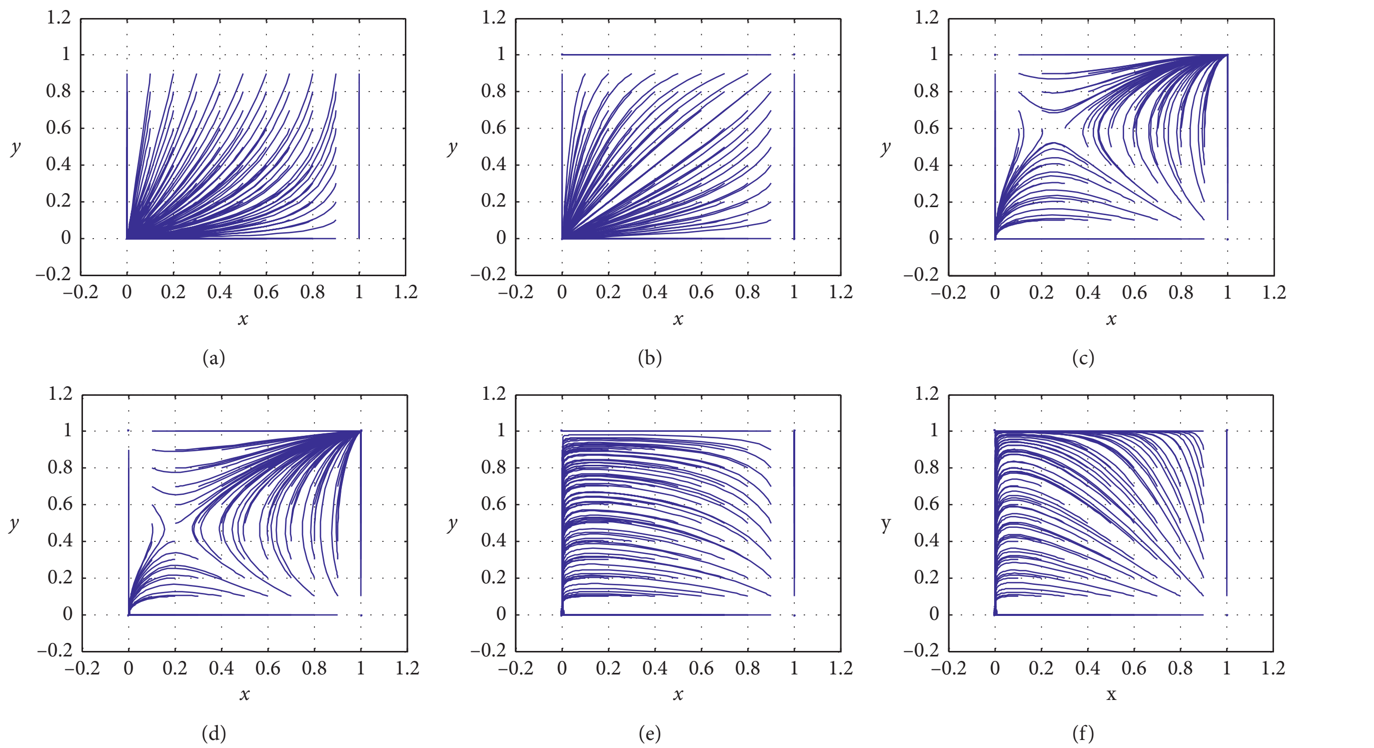

Figure 5: Evolutionary paths $V < \beta C$ and $V < (1-\beta)C$.

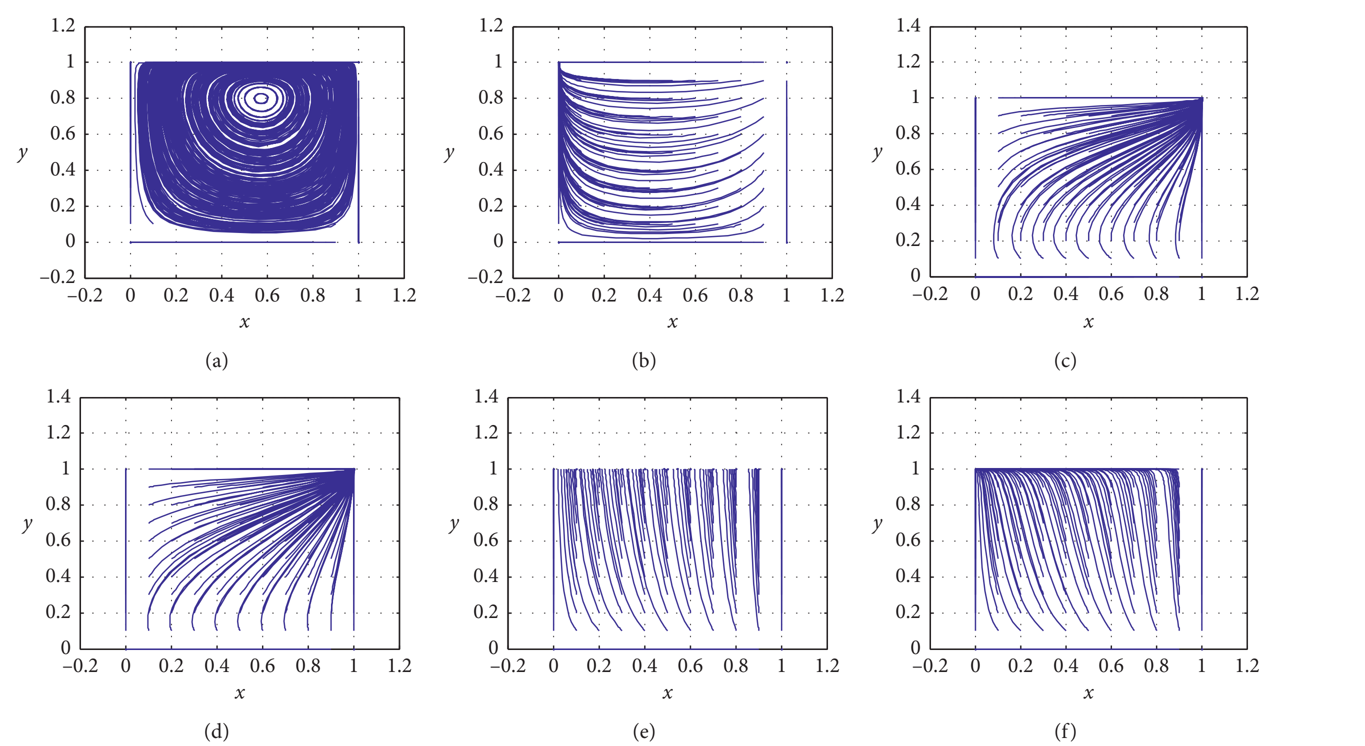

Figure 6: Evolutionary paths $V < \beta C$ and $V > (1-\beta)C$.

the manufacturers is higher than the cost of sharing information. However, for the logistics service providers, the subsidy is lower than the cost of sharing information, and the additional profit is also low. So, an ESS exists, $E_2(1,0)$.

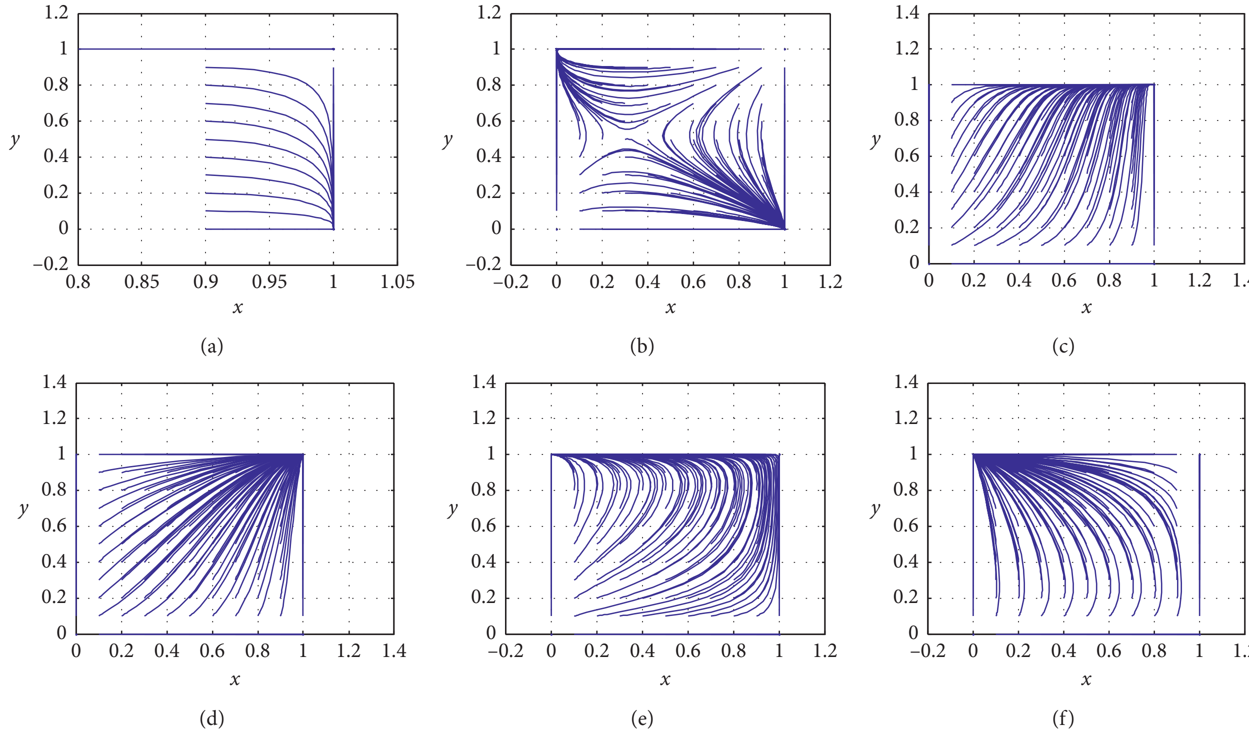

Figure 7: Evolutionary paths $V > \beta C$ and $V > (1 - \beta)C$.

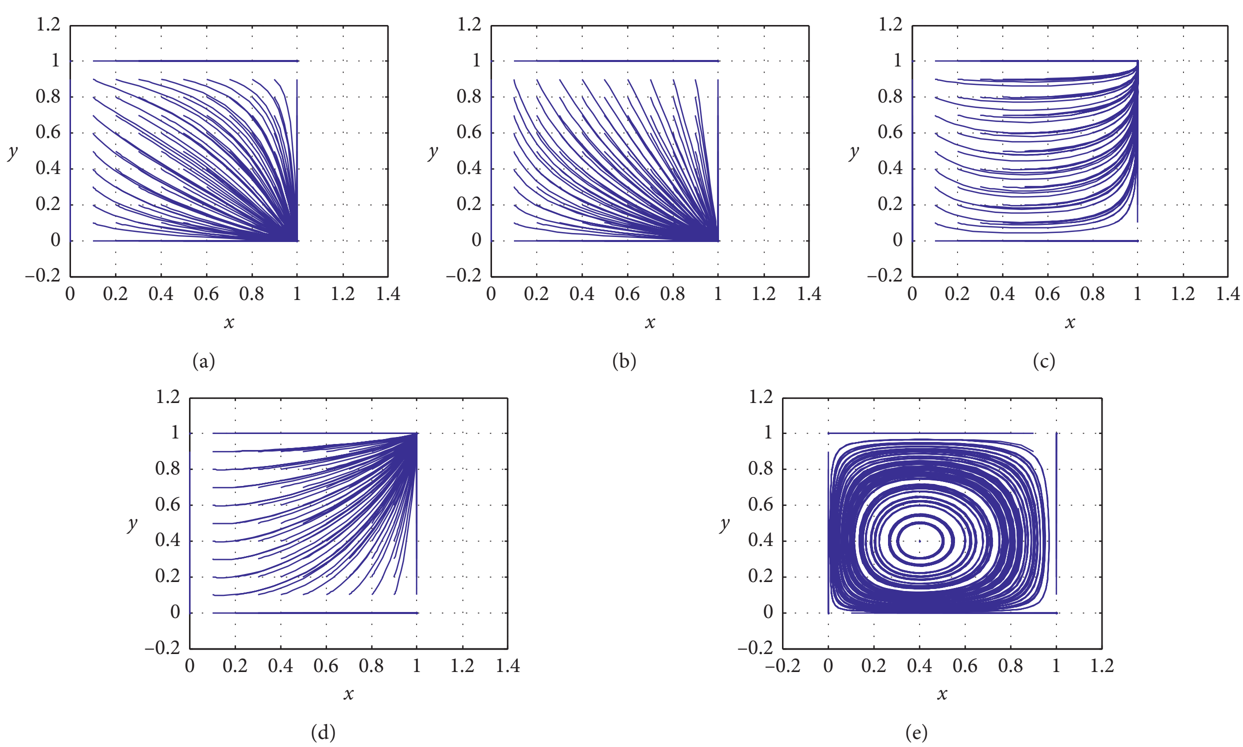

Figure 8: Evolutionary paths $V > \beta C$ and $V < (1 - \beta)C$.

(3) In Category 4.3, $(1-\beta)C < (1-\alpha)P + F$, $\beta C < \alpha P + F$, and $F < (1-\beta)C$. The additional profit of sharing information increases, which benefits both players. An ESS exists, $E_4(1, 1)$.

(4) In Category 4.4, $(1-\beta)C < (1-\alpha)P + F$, $\beta C < \alpha P + F$, and $F > (1-\beta)C$. The additional profit of sharing information and the penalty cost of non-cooperation both increase, which

propels the manufacturers and logistics service providers to adopt the cooperation strategy. Therefore, an ESS exists, $E_4(1,1)$.

(5) In Category 5.5, $(1-\beta)C < (1-\alpha)P + F$, $\beta C > \alpha P + F$, and $F < (1-\beta)C$. The subsidy to the logistics service providers is low, while the subsidy to the manufacturers is high, but the additional profit of sharing information is low. Under these conditions, no ESS exists.

5. Numerical Study

In the developed evolutionary game model (see (1)–(14)), eight parameters are involved $[\pi_A, \pi_B, P, F, V, C, \alpha, \beta]$. In Table 10, corresponding to the ESS analysis in Section 4.4, we use four groups of settings to present different combinations of these parameters. In this study, we use Matlab 2018 to implement the models and depict the results.

6. Discussion and Conclusion

6.1. Discussion. In Section 4, we constructed an evolutionary game model between the cold chain manufactures and logistics service providers for studying the impacts of information transparency on safety. To demonstrate and examine the model, we devised four categories with 23 groups of parameters to represent various scenarios for numerical experiments.

Figures 5(c), 5(d), 6(c), 6(d), 7(c), 7(d), 8(c), and 8(d) depict the impacts of the constraints $(1-\beta)C < (1-\alpha)P + F$ and $\beta C < \alpha P + F$ on the ESS and simulations. The cold chain manufacturers and logistics service providers will adopt the information-sharing strategy with high probabilities. When the right parts of the two constraints increase, the profits deduced by information sharing are high, and so the stakeholders can obtain much from the strategy. The penalty to the cold chain companies plays an important role in pushing them to adopt the information-sharing strategy.

We consider the constraints $V < \beta C$ and $V < (1-\beta)C$ in the evolutionary game model. The low subsidy will result that the stakeholders give up the information sharing strategy. We produced the numerical simulation results, as presented in Figures 5(a)–5(e). The probability of giving up the information sharing strategy is high. When the governments increase the subsidies, the stakeholders will be active in adopting the information-sharing strategy. So, in the developed model, the subsidy is an essential instrument for advocating the information-sharing strategy.

The costs undertaken by the cold chain companies are harmful to them to adopt the information-sharing strategy. When the governments can subsidize these costs, the penalties are severe enough, and the companies have no choice and will adopt the information-sharing strategy. We depict the simulation results in Figures 7(a)–7(f) when considering the constraints $V > \beta C$ and $V > (1-\beta)C$ in the evolutionary game model. It is beneficial for the cold chains to find effective ways to reduce the costs for information sharing technology and systems. The governments should support the companies to reduce these costs by policy-making, technology innovation, and administration.

The cold chain manufacturers and logistics service providers may present different attitudes to the information sharing strategy. The cost of sharing information may be beyond the subsidy and the penalty for some stakeholders. If the stakeholders can not adopt the information-sharing strategy consistently, they will reduce the positive effects of information sharing on cold chain safety significantly. So, the policymakers should carefully consider the profit and cost allocation ratios and the subsidy amounts according to the practical situations. These considerations should contribute to the simultaneous adoption of the information sharing strategy. Alternatively, the policy may damage the positivity of sharing information. We illustrate these analysis in Figures 6(b), 6(e), 6(f), 7(b), 7(f), and Figures 8(a)–8(d). When the manufactures and logistics service providers adopt a different strategy, the evolutionary game cannot be stable with ESSs.

Besides instant costs and profits, the information-sharing strategy can add values to cold chains. Consumers can buy cold chain products when product safety is trustful. Information sharing and transparency provide a way for the public to inspect the cold chains and so contribute to increasing purchases and profits. Therefore, when the governments devote much to administrate the cold chain transparency, the cold chain industry may be productive and effective.

6.2. Conclusion. To guard the cold chain safety, the governments should advocate information transparency as a premise for the temperature-controlled cold goods supply chains. While information transparency incurs additional costs for cold chain infrastructure, communication, and information management systems, due to its contribution to cold chain safety, the contracts between the main stakeholders and the related government departments can supervise and administrate the cooperation of sharing information by subsidies and penalties. In this study, at the industrial level, the interactions between the main cold chain stakeholders (cold goods manufacturers and cold chain logistics service providers) under administration are formulated by an evolutionary game model. The ESS analysis is conducted theoretically and numerically by considering the relations among the parameters (including the additional profits of sharing information, the penalty of adopting non-cooperation strategy, the subsidies paid to the players adopting the cooperation strategy, and the ratio of reallocating costs and profits between the two populations). By using different combinations of parameters, the ESS emerges or disappears. Therefore, well-developed strategies and combinations of technical parameters contribute to safe and efficient cold chains. However, in this study, the evolutionary model is static because the parameters are given and not affected by each other. In more practical conditions, the behaviors of manufacturers, logistics service providers, and governments may interact with each other, and the static parameters will present dynamics. Besides, we will try to use

Table 10: Parameter settings for the simulation study.

Category	No.	π_A	π_B	P	F	V	C	α	β	Evo-path
1	1	1000	800	100	30	50	200	0.7	0.5	Figure 5
$V < \beta C$	2	1000	800	100	30	50	200	0.5	0.5	
$V < (1-\beta)C$	3	1000	800	200	70	50	200	0.5	0.6	
Table 6	4	1000	800	100	150	50	200	0.5	0.6	
	5	1000	800	100	50	50	200	0.25	0.7	
	6	1000	800	100	100	50	200	0.25	0.7	
2	7	1000	800	100	45	100	200	0.8	0.6	Figure 6
$V < \beta C$	8	1000	800	50	50	100	200	0.5	0.55	
$V > (1-\beta)C$	9	1000	800	200	50	100	200	0.7	0.6	
Table 7	10	1000	800	200	90	100	200	0.7	0.6	
	11	1000	800	200	60	100	200	0.3	0.6	
	12	1000	800	100	100	100	200	0.15	0.6	
3	13	1000	800	100	50	150	200	0.8	0.6	Figure 7
$V > \beta C$	14	1000	800	50	50	120	200	0.25	0.45	
$V > (1-\beta)C$	15	1000	800	200	50	120	200	0.25	0.45	
Table 8	16	1000	800	200	150	120	200	0.25	0.45	
	17	1000	800	70	70	120	200	0.2	0.45	
	18	1000	800	50	70	120	200	0.25	0.55	
4	19	1000	800	100	40	120	200	0.75	0.25	Figure 8
$V > \beta C$	20	1000	800	50	40	120	200	0.25	0.25	
$V < (1-\beta)C$	21	1000	800	100	70	100	200	0.5	0.45	
Table 9	22	1000	800	100	120	100	200	0.5	0.45	
	23	1000	800	100	50	100	200	0.25	0.45	

Note. evo-path = evolutionary path.

dynamic, differential, and Bayesian game models to examine the dynamics between the manufacturers and logistics service providers. Different models may reveal different features of the problem. Moreover, a cold chain involves various stakeholders in the supply chain, other than just manufacturers and logistics service providers. A complicate supply chain may revise the proposed evolutionary game models and generate new research opportunities in the future. We conduct theoretical analysis in this study, while we can further improve the study by using real-world cases.

Data Availability

The data used to support the findings of this study are included within the article.

Conflicts of Interest

The authors declare that they have no conflicts of interest.

Acknowledgments

The National Natural Science Foundation of China (no. 71871136) and the Science and Technology Commission of Shanghai Municipality (no. 17DZ2280200) partially support this study financially.

References

[1] Y. Bouzembrak, M. Klüche, A. Gavai, and H. J. P. Marvin, "Internet of things in food safety: literature review and a bibliometric analysis," *Trends in Food Science & Technology*, vol. 94, pp. 54–64, 2019.

[2] H.-I. Hsiao and K.-L. Huang, "Time-temperature transparency in the cold chain," *Food Control*, vol. 64, pp. 181–188, 2016.

[3] H. Luo, M. Zhu, S. Ye, H. Hou, Y. Chen, and L. Bulysheva, "An intelligent tracking system based on internet of things for the cold chain," *Internet Research*, vol. 26, no. 2, pp. 435–445, 2016.

[4] W. Chen and Z.-H. Hu, "Analysis of multi-stakeholders' behavioral strategies considering public participation under carbon taxes and subsidies: an evolutionary game approach," *Sustainability*, vol. 12, no. 3, p. 1023, 2020.

[5] W. Chen and Z.-H. Hu, "Using evolutionary game theory to study governments and manufacturers' behavioral strategies under various carbon taxes and subsidies," *Journal of Cleaner Production*, vol. 201, pp. 123–141, 2018.

[6] K. Zheng, Z. Zhang, Y. Chen, and J. Wu, "Blockchain adoption for information sharing: risk decision-making in spacecraft supply chain," *Enterprise Information Systems*, pp. 1–22, 2019.

[7] Z. Min, X. Mikai, and D. Debao, "Research on game strategy of information sharing in cross-border e-commerce supply chain between manufacturers and retailers," in *Advances in Intelligent Systems and Computing*, pp. 399–406, Springer, Berlin, Germany, 2020.

[8] H. Deng and X. Liang, "RFID public logistics information sharing and exchanging solution," *International Journal of Manufacturing Technology and Management*, vol. 21, no. 3-4, pp. 254–268, 2010.

[9] S. C. Kulp, H. L. Lee, and E. Ofek, "Manufacturer benefits from information integration with retail customers," *Management Science*, vol. 50, no. 4, pp. 431–444, 2004.

[10] W. K. Chiang and Y. Feng, "The value of information sharing in the presence of supply uncertainty and demand volatility,"

International Journal of Production Research, vol. 45, no. 6, pp. 1429–1447, 2007.

[11] H. S. Hsu, C. A. Alexander, and Z. Zhu, "Understanding the reverse logistics operations of a retailer: a pilot study," *Industrial Management and Data Systems*, vol. 109, no. 4, pp. 515–531, 2009.

[12] R. Klein and A. Rai, "Interfirm strategic information flows in logistics supply chain relationships," *MIS Quarterly*, vol. 33, no. 4, pp. 735–762, 2009.

[13] R. Angeles, "Anticipated IT infrastructure and supply chain integration capabilities for RFID and their associated deployment outcomes," *International Journal of Information Management*, vol. 29, no. 3, pp. 219–231, 2009.

[14] E. Bottani, M. Bertolini, R. Montanari, and A. Volpi, "RFID-enabled business intelligence modules for supply chain optimisation," *International Journal of RF Technologies: Research and Applications*, vol. 1, no. 4, pp. 253–278, 2009.

[15] R. J. Kauffman and H. Mohtadi, "Information sharing and strategic signaling in supply chains," *Journal of Systems Science and Systems Engineering*, vol. 18, no. 2, pp. 129–158, 2009.

[16] D. Hellstrom, C. Johnsson, and A. Norrman, "Risk and gain sharing challenges in interorganisational implementation of RFID technology," *International Journal of Procurement Management*, vol. 4, no. 5, pp. 513–534, 2011.

[17] J. J. Nativi and S. Lee, "Impact of RFID information-sharing strategies on a decentralized supply chain with reverse logistics operations," *International Journal of Production Economics*, vol. 136, no. 2, pp. 366–377, 2012.

[18] A. Khare and A. Khare, "Harnessing supply chain efficiency through information linkages: case of multi national companies and small retail sector in India," *International Journal of Information Systems and Supply Chain Management*, vol. 5, no. 4, pp. 86–104, 2012.

[19] B. Jiang and L. Teng, "Vendor managed inventory integration on pharmaceutical third-party logistics," *International Journal of Multimedia and Ubiquitous Engineering*, vol. 11, no. 6, pp. 397–410, 2016.

[20] Z. Li, "A study of agricultural products distribution using the internet of things," *International Journal of Simulation: Systems, Science and Technology*, vol. 17, no. 19, pp. 13.11–13.15, 2016.

[21] Y. C. Liu and H. M. Gao, "An empirical case study for the application of agricultural product traceability system," in *Advances in Intelligent Systems and Computing*, pp. 210–217, Springer, Berlin, Germany, 2020.

[22] W. Wu, Y. Deng, M. Zhang, and Y. Zhang, "Performance evaluation on aquatic product cold-chain logistics," *Journal of Industrial Engineering and Management*, vol. 8, no. 5, pp. 1746–1768, 2015.

[23] S. Jian and Z. Jing, "Evaluation of core competence of cold-chain logistics enterprises based on FCE model," *The Open Cybernetics & Systemics Journal*, vol. 9, no. 1, pp. 2605–2613, 2015.

[24] W. Jiang, Z. Hu, Y. Liang, and Y. Chen, "Modeling and optimization of food cold-chain intelligent logistics distribution network," *Advance Journal of Food Science and Technology*, vol. 7, no. 8, pp. 573–578, 2015.

[25] S. Wang, F. Tao, Y. Shi, and H. Wen, "Optimization of vehicle routing problem with time windows for cold chain logistics based on carbon tax," *Sustainability (Switzerland)*, vol. 9, no. 5, p. 694, 2017.

[26] A. Gallo, R. Accorsi, G. Baruffaldi, and R. Manzini, "Designing sustainable cold chains for long-range food distribution: energy-effective corridors on the silk road belt," *Sustainability (Switzerland)*, vol. 9, no. 11, 2017.

[27] A. E. Osorio, M. G. Corradini, and G. Dewi, "In-store cold chain failures: food safety considerations," *Journal of Marketing Channels*, vol. 24, no. 3-4, pp. 153–170, 2017.

[28] I. Ali, S. Nagalingam, and B. Gurd, "A resilience model for cold chain logistics of perishable products," *The International Journal of Logistics Management*, vol. 29, no. 3, pp. 922–941, 2018.

[29] A. Chaudhuri, I. Dukovska-Popovska, N. Subramanian, H. K. Chan, and R. Bai, "Decision-making in cold chain logistics using data analytics: a literature review," *The International Journal of Logistics Management*, vol. 29, no. 3, pp. 839–861, 2018.

[30] X. Li and Z. Wang, "Multidimensional context-aware recommendation algorithm towards intelligent distribution of cold chain logistics," *Journal of Intelligent & Fuzzy Systems*, vol. 35, no. 1, pp. 171–185, 2018.

[31] S. Wang, "Developing value added service of cold chain logistics between China and Korea," *Journal of Korea Trade*, vol. 22, no. 3, pp. 247–264, 2018.

[32] L. Chen, M. Ma, and L. Sun, "Heuristic swarm intelligent optimization algorithm for path planning of agricultural product logistics distribution," *Journal of Intelligent & Fuzzy Systems*, vol. 37, no. 4, pp. 4697–4703, 2019.

[33] L. Li, Y. Yang, and G. Qin, "Optimization of integrated inventory routing problem for cold chain logistics considering carbon footprint and carbon regulations," *Sustainability (Switzerland)*, vol. 11, no. 17, 2019.

[34] S. K. Mangla, Y. K. Sharma, P. P. Patil, G. Yadav, and J. Xu, "Logistics and distribution challenges to managing operations for corporate sustainability: study on leading Indian diary organizations," *Journal of Cleaner Production*, vol. 238, 2019.

[35] C. Wei, W.-W. Gao, Z.-H. Hu, Y.-Q. Yin, and S.-D. Pan, "Assigning customer-dependent travel time limits to routes in a cold-chain inventory routing problem," *Computers & Industrial Engineering*, vol. 133, pp. 275–291, 2019.

[36] N. Al Theeb, H. J. Smadi, T. H. Al-Hawari, and M. H. Aljarrah, "Optimization of vehicle routing with inventory allocation problems in cold supply chain logistics," *Computers and Industrial Engineering*, vol. 142, 2020.

[37] S. Barari, G. Agarwal, W. J. Zhang, B. Mahanty, and M. K. Tiwari, "A decision framework for the analysis of green supply chain contracts: an evolutionary game approach," *Expert Systems with Applications*, vol. 39, no. 3, pp. 2965–2976, 2012.

[38] J. Li, W. Du, F. Yang, and G. Hua, "Evolutionary game analysis of remanufacturing closed-loop supply chain with asymmetric information," *Sustainability*, vol. 6, no. 9, pp. 6312–6324, 2014.

[39] Y. Tian, K. Govindan, and Q. Zhu, "A system dynamics model based on evolutionary game theory for green supply chain management diffusion among Chinese manufacturers," *Journal of Cleaner Production*, vol. 80, pp. 96–105, 2014.

[40] P. Ji, X. Ma, and G. Li, "Developing green purchasing relationships for the manufacturing industry: an evolutionary game theory perspective," *International Journal of Production Economics*, vol. 166, pp. 155–162, 2015.

[41] A. Hafezalkotob and R. Mahmoudi, "Selection of energy source and evolutionary stable strategies for power plants under financial intervention of government," *Journal of Industrial Engineering International*, vol. 13, no. 3, pp. 357–367, 2017.

[42] G. Zhu, G. Pan, and W. Zhang, "Evolutionary game theoretic analysis of low carbon investment in supply chains under governmental subsidies," *International Journal of Environmental Research and Public Health*, vol. 15, no. 11, 2018.

[43] Z. Li, G. Jin, and S. Duan, "Evolutionary game dynamics for financial risk decision-making in global supply chain," *Complexity*, vol. 2018, Article ID 9034658, 10 pages, 2018.

[44] R. Mahmoudi and M. Rasti-Barzoki, "Sustainable supply chains under government intervention with a real-world case study: an evolutionary game theoretic approach," *Computers & Industrial Engineering*, vol. 116, pp. 130–143, 2018.

[45] A. Hafezalkotob, R. Mahmoudi, E. Hajisami, and H. M. Wee, "Wholesale-retail pricing strategies under market risk and uncertain demand in supply chain using evolutionary game theory," *Kybernetes*, vol. 47, no. 6, pp. 1178–1201, 2018.

[46] Q. Shi, J. Zhu, and Q. Li, "Cooperative evolutionary game and applications in construction supplier tendency," *Complexity*, vol. 2018, Article ID 8401813, 13 pages, 2018.

[47] T. Shu, Y. Wang, S. Chen, S. Wang, K. K. Lai, and Y. Yang, "Analysis of evolutionary game in structural formation of market power in remanufacturing supply chains," *Applied Economics*, vol. 51, no. 20, pp. 2195–2220, 2019.

[48] H. Sun, Y. Wan, L. Zhang, and Z. Zhou, "Evolutionary game of the green investment in a two-echelon supply chain under a government subsidy mechanism," *Journal of Cleaner Production*, vol. 235, pp. 1315–1326, 2019.

[49] K. Kang, Y. Zhao, J. Zhang, and C. Qiang, "Evolutionary game theoretic analysis on low-carbon strategy for supply chain enterprises," *Journal of Cleaner Production*, vol. 230, pp. 981–994, 2019.

[50] C. Hao, Q. Du, Y. Huang, L. Shao, and Y. Yan, "Evolutionary game analysis on knowledge-sharing behavior in the construction supply chain," *Sustainability (Switzerland)*, vol. 11, no. 19, 2019.

[51] J. Xu, J. Cao, Y. Wang, X. Shi, and J. Zeng, "Evolutionary game on government regulation and green supply chain decision-making," *Energies*, vol. 13, no. 3, 2020.

[52] Zion Market Research, Cold Chain Market by Type (Refrigerated Storage and Transport), by Temperature Type (Chilled and Frozen), and by Application (Dairy & Frozen Desserts; Meat, Fish, and Seafood, Fruits & Vegetables, Bakery & Confectionery, Pharmaceuticals, and Others)—Global Industry Perspective, Comprehensive Analysis and Forecast, 2017–2024, 2017, https://www.zionmarketresearch.com/report/cold-chain-market.

[53] K. Cai, S. He, and Z. He, "Information sharing under different warranty policies with cost sharing in supply chains," *International Transactions in Operational Research*, vol. 27, no. 3, pp. 1550–1572, 2020.

[54] M. A. Abd, S. F. Al Rubeaai, S. Salimpour, and A. Azab, "Evolutionary game theoretical approach for equilibrium of cross-border traffic," *Transportmetrica B: Transport Dynamics*, vol. 7, no. 1, pp. 1611–1626, 2019.